

Mast cell migration in allergy

Maria Dawson

**Thesis submitted to University College London for the degree of
Doctor of Philosophy**

**Institute of Ophthalmology
University College London
May 2012**

Declaration

I, Maria Dawson confirm that the work presented in this thesis is my own. Where information has been derived from other sources, I confirm that this has been indicated in the thesis.

May 2012

Acknowledgements

The work presented in this thesis would not have been possible without the help of many people. I would like to express my sincere gratitude to:

-Dr. Maryse Bailly, Professor John Greenwood and Dr. Virginia Calder. I could not have completed this thesis without you all, and I feel privileged to have you as my mentors.

-My primary supervisor, Dr. Maryse Bailly (Cell Biology, UCL) for her guidance and advice over the past few years, being so patient and understanding with me in learning new techniques (argghh chemotaxis pippete assays☺!), for always being available to help me better understand the nature of my research, and for giving me the opportunity to work in this excellent group...but moreover providing a supportive and new 'scientific home' when my initial supervisor Professor Ono left UCL...

-My secondary supervisor Professor John Greenwood (Cell Biology, UCL), for teaching me how to question even the most fundamental ideas in order to truly become an investigative scientist, for his continuing guidance and words of encouragement, especially when I traveled between the States and UCL to complete experiments, and during my writing up period...

-Dr. Virginia Calder (Immunology, UCL), who is not only an outstanding immunologist, but also made time to read through and correct the immunology presented in this thesis.

-GSK and UCL Graduate School, for funding my PhD.

-All former and present friends, colleagues and P.I's for exciting discussions, productive collaborations, and teaching me the importance of working in a group and sticking with your goals, even when the research seems overwhelming...

-Professor Santa Ono for giving me the opportunity to initiate a PhD in his laboratory during his tenure at UCL.

-at UCL (U.K): Adam, Rushee, Becca, Vicky, Jenny, Karen, Belen, Matt, Amanda, Mark, Golnaz, Maria and James, Dr. Tim Levine, Dr. Astrid Limb, Peggy Khaw; what was then Professor Ono's Lab..Tom, Bitu, Takao, Yoshi, Colleen, Steve, Dr. Masako Toda (now in Germany)- my very first post-doc who was always patient and provided a wealth of expertise; Harvard (U.S.A): Dr. Rick Stevens and lab members; Emory Eye Center (U.S.A): Kei, Grace, Ken, Lane, Mark, Nimi

-Professor Avron Mitchison (UCL), Professor Mary Ritter (Imperial College), for being an 'immunological compass', and for wonderful scientific banter and guidance.

- My scientific family and dear friends who have traveled my journey of science and life with support and encouragement, scientific banter and everything in between..Sasha, Stevee, Mythili, Rich, Olga, Ambreen, Shweta, Bhairavi, Ify, Nadine, Natasha, Ash and Jim...thank you

-Mary B and Des B, members of my family who have been there through smiles and tears. I am truly blessed to have you in my life and I thank you for always making time and being a pillar of strength and support over the years..

-Cadbury's, Lindt and peach-iced tea that kept me alive at night during those long experiments.

-Last but not least, This PhD would not have been possible were it not for one incredible person, my father, who raised me with devotion, who gave me strength, sacrificed everything willingly with love and smiles. This PhD is dedicated to you dad...I thank you with all my heart, I am truly blessed.

For everything there is a season, and a time for every purpose

Ecclesiastes 3: 1-2

Abstract

The symptomology associated with allergic diseases are a direct consequence of the release of pro-inflammatory mediators from mast cells following bi- or multi-valent antigen cross-linking with the high affinity immunoglobulin (Ig) E receptor, FcεR1. Chemokines, small 8-15 kDa polypeptides, control the activation and recruitment of immune cells during the allergic response.

Previous studies have demonstrated that co-stimulation by the chemokine, macrophage inflammatory protein-1α (Mip-1α) and cross-linking by IgE with antigen result in four phenomenon 1) enhanced degranulation in *ex vivo* conjunctival mast cells and rat basophilic leukemia (RBL-2H3) cell line via its chemokine receptor (CCR) 1, cell line also referred to as RBL-CCR1; 2) arrested Mip-1α-induced chemotaxis of RBL-CCR1 cells; 3) enhanced production of pro-inflammatory mediators from RBL-CCR1 cells and 4) enhanced gene expression in RBL-CCR1 cells of regulatory molecules downstream of CCR1 and FcεR1 signaling pathways, Regulator of G-protein Signaling (RGS)-1 and Tribbles (TRB)-3. It has therefore been proposed that co-engagement of CCR1 and FcεR1 affects other mast cell processes such as chemotaxis, and moreover these data indicate cross-talk between CCR1 and FcεR1 signaling pathways. Chemotaxis of mast cells to sites of inflammation and the subsequent release of pro-inflammatory mediators are key to eliciting allergic response. Although there is a vast amount of information pertaining to the molecular mechanisms of chemotaxis in several cell types, there is very little evidence to understand mast cell chemotaxis at this level. Based on current knowledge, the main objective of this thesis was to investigate 1) the effect of CCR1 and FcεR1 co-engagement on mast cell motility and 2) the role of RGS1 and TRB3 on mast degranulation, mediator release and chemotaxis.

The data obtained from this thesis is the first to demonstrate the role of WASP, CCR1 and actin polymerisation as mechanisms underlying Mip-1α induced RBL-CCR1 chemotaxis, using real time microscopy. Moreover, CCR1 and FcεR1 engagement inhibits RBL-CCR1 actin cytoskeletal re-organisation and significantly increases other cell motility parameters such as directionality and Euclidean distances which are required for efficient Mip-1α-induced chemotaxis. Also, by using a murine model of allergic conjunctivitis, conjunctival mast cells accumulate in the forniceal area of an inflamed conjunctiva in comparison to non-diseased

mice. In addition, by using siRNA the present study is also the first to show that RGS1 and TRB3 serve as negative regulators of RBL-CCR1 degranulation, mediator release and chemotaxis upon CCR1 and Fc ϵ R1 engagement. In conclusion, the data presented in this thesis could advance our understanding of the mechanisms responsible for mast cell migration and arrest during an allergic response, and hence provide new targets for anti-allergic drugs.

Table of contents

Declarations	ii
Acknowledgements	iii
Abstract	v
Table of contents	vii
List of figures	xii
List of tables	xv
Abbreviations	xvi
Chapter 1. General introduction and hypothesis	1
1. Introduction	2
1.1 Mast Cell Biology	3
1.1.1 Mast cell origins and development	3
1.1.2 Mast cell activation and mediator release	6
1.1.3 Roles of mast cells in physiology, disease and immunity	10
1.1.3.1 Mast cells in physiology	10
1.1.3.2 Mast cells in disease: allergy and the allergic cascade	11
1.1.3.3 Mast cells in innate and acquired immunity	17
1.1.4 Experimental models for studying mast cell function and signaling	19
1.1.4.1 FcεR1 -mediated signaling in mast cells	20
1.1.4.2 The FcεR1 receptor and IgE binding	20
1.1.4.3 General outline of mast cell FcεR1 signaling	22
1.1.4.4 TRB3: a regulator of cell signaling	25
1.2. Chemokines, signaling and regulation	29
1.2.1 Chemokine and chemokine receptors	29
1.2.2 Chemokine signaling through GPCR	32
1.2.3 Regulation of GPCR signaling pathways: RGS family	35
1.3. Regulation of Actin cytoskeleton and chemotaxis	38
1.3.1 Actin cytoskeleton and Rho GTPases	38
1.3.2 WASP: a component of actin assembly	42
1.3.3 Cell migration, chemotaxis and cell polarity	43
1.3.4 Imaging cell migration	46
1.4 Hypothesis and aims of this thesis	48

2. Materials and methods	49
2.1 Induction of murine allergic conjunctivitis	50
2.1.1 Mice	50
2.1.2 Murine models of allergic conjunctivitis	50
2.1.2.1 Induction of murine allergic conjunctivitis model 1-A/J mice	50
2.1.2.2 Induction of murine allergic conjunctivitis model 2- BALB/c mice	52
2.2 Cell line and cell culture	54
2.2.1 RBL-CCR1 cell line	54
2.2.2 RBL-CCR1 cell culture	54
2.2.3 GFP-AKT-RBL-CCR1 cell culture	55
2.3. Transfection of RBL-CCR1 cells with either Rgs1 or TRB3 using Oligofectamine	55
2.4 Degranulation assay	56
2.5 Mediator release Assay	57
2.6 Chemotaxis assay using transwell system	57
2.7 Real time microscopy	60
2.7.1 Chemotaxis pipette assay analysed by real time microscopy	60
2.7.2 Analysis of PI(3,4,5)P3 localisation in RBL-CCR1 cells in response to a Mip-1 α gradient using real time microscopy	60
2.8 Staining	61
2.8.1 Phallotoxin	61
2.8.1.1 Localisation of actin filaments in RBL-CCR1 cells	61
2.8.2 Dyes	62
2.8.2.1 Identification of mast cells by Toluidine blue staining	62
2.9. Immunocytochemistry	62
2.9.1 Localisation of of WASP and CCR1 in RBL-CCR1 cells in response to a Mip-1α gradient	62
2.10 Immunohistochemistry	63
2.10.1 Staining of murine conjunctival paraffin sections: Detection of mMCP-5 and CCR1	63
2.10.2 Staining of conjunctival frozen sections: Detection of WASP and actin	64
2.11 Analysis of Microscopy	65
2.11.1 Quantification of Migration	65

2.11.2 Quantification of Toluidine Blue positive murine conjunctival mast cells	69
2.11.3 Quantification of mMCP5 and CCR1 positive murine conjunctival mast cells	69
2.12 RT-PCR	71
2.12.1 RNA isolation	71
2.12.2 Reverse Transcription (RT)	71
2.12.3 Real Time Quantitative PCR (qPCR)	71
2.12.4 Analysis of qPCR	72
2.13 Western Blotting	72
2.13.1 Protein Isolation	72
2.13.2 Protein Gel Electrophoresis and transfer	73
2.13.3 Immunoblotting	74
2.14 Statistical analysis of results	74
Chapter 3. The effect of FcεRI and CCR1 co-engagement on RBL-CCR1 cell motility	76
3. The effect of FcεRI and CCR1 co-engagement on RBL-CCR1 cell motility	76
3.1 Introduction and hypothesis	77
3.2 Results	79
3.2.1 Actin reorganization in RBL-CCR1 cells induced by homogeneous co-stimulation by Mip-1α and IgE/antigen	79
3.2.2 Behavioral responses of RBL-CCR1 Cells to gradients of Mip-1α and IgE/antigen co-stimulation using real time microscopy	82
3.2.3 Localisation of PI(3,4,5) P3 in RBL-CCR1 cells in response to a Mip-1α gradient	98
3.2.4 Localisation of CCR1, actin and WASP in RBL-CCR1 cells in response to a Mip-1α gradient	101
3.3 Discussion	109
Chapter 4. The effect of FcεRI and chemokine co-engagement on mast cell motility in murine allergic conjunctivitis	114
4. The effect of FcεRI and chemokine co-engagement on mast cell motility in murine allergic conjunctivitis	115
4.1 Introduction and hypothesis	115
4.2 Results	117

4.2.1 Murine models of allergic conjunctivitis	117
4.2.2 Behavioural and morphological responses of murine conjunctival mast cells in inflamed conjunctiva.	120
4.2.3 Kinetic analysis of murine conjunctival mast cells accumulation within an inflamed conjunctiva.	122
4.2.4 Localisation of CCR1, actin and WASP in conjunctival mast cells within an inflamed murine conjunctiva.	126
4.3 Discussion	132
Chapter 5. The role RGS1 in mast cell degranulation, mediator release and chemotaxis	138
5. The role RGS1 in mast cell degranulation, mediator release and chemotaxis	139
5.1 Introduction and hypothesis	139
5.2 Results	141
5.2.1 Depletion of endogenous RGS1 in RBL-CCR1 cells by RNA interference.	141
5.2.2. Effect of RGS1 on RBL-CCR1 degranulation	142
5.2.3 Effect of RGS1 on RBL-CCR1 mediator release of cytokines and chemokines	144
5.2.4 Gene expression of inflammatory mediators IL-6, IL-13 and CCL7 in RBL-CCR1 cells	146
5.2.5 Effect of RGS1 on the gene expression of inflammatory mediators IL-6, IL-13 and CCL7 in RBL-CCR1 cells	148
5.2.6 Effect of RGS1 on RBL-CCR1 chemotaxis	150
5.3 Discussion	152
Chapter 6. The role of TRB 3 in mast cell degranulation, mediator release and chemotaxis	155
6. The role of TRB 3 in mast cell degranulation, mediator release and chemotaxis	156
6.1 Introduction and hypothesis	156
6.2 Results	157
6.2.1 Depletion of endogenous TRB3 in RBL-CCR1 cells by RNA interference.	157
6.2.2 Effect of TRB3 on RBL-CCR1 degranulation	158
6.2.3 Effect of TRB3 on RBL-CCR1 mediator release of cytokines and chemokines	160

6.2.4 Effect of TRB3 on RBL-CCR1 chemotaxis	162
6.3 Discussion	164
Chapter 7. General discussion and future work	167
Chapter 8 References	176
Chapter 9 Publications	222
Supplementary data. CD ROM 1 – Real time movies for PhD thesis.	Attached to back cover of this thesis

List of figures

Chapter 1:

Figure 1. Mast cell development and tissue distribution.

Figure 2. Differentiation of naïve T cells into Th 2 cells, production of IgE by B cells and sensitisation of mast cells.

Figure 3. The Fc ϵ R1 receptor.

Figure 4. Simplified model of Fc ϵ R1-mediated signaling events.

Figure 5. Simplified model of GPCR-mediated signaling events.

Figure 6. RGS proteins accelerate GTPase activity of the α -subunit, thereby inhibiting downstream events.

Figure 7. The formation of lamellipodia and filopodia by RAC and Cdc42 signaling pathways.

Chapter 2:

Figure 8. Induction of murine allergic conjunctivitis model 1 using A/J mice.

Figure 9. Induction of murine allergic conjunctivitis model 2 using BALB/c mice.

Figure 10. A diagram depicting the transwell chemotaxis assay

Figure 11. Open Lab snapshots showing the outline of each cell at timepoints t1 (A) and t2 (B) with its corresponding centroid x.

Figure 12. Image J snapshots showing a migration plot with its corresponding parameters. Cell traces were arranged to show their origins at x=y=0.

Figure 13. Accumulated and Euclidean distance, where t_i represents initial time and t_f, final time.

Figure 14. Schematic representation of the conjunctivia showing the location of the chemokine gradient, G, and the location away from the chemokine gradient, AG, the areas in which mast cells were counted.

Figure 15. Schematic representation of the conjunctivia showing the location of the chemokine gradient, G, the area in which mast cells were counted.

Chapter 3:

Figure 16. Rhodamine phalloidin-stained RBL-CCR1 cells showing F-actin distribution (red) and decreased membrane ruffling following stimulation with Mip-1 α and co-stimulation with Mip-1 α + IgE/Antigen

Figure 17. RBL-CCR1 cells do not migrate towards PBS/DMEM.

Figure 18. RBL-CCR1 cells chemotax towards Mip-1 α .

Figure 19. RBL-CCR1 cells pre-sensitised with IgE do not chemotax towards Mip-1 α and antigen.

Figure 20. RBL-CCR1 cells do not migrate towards antigen.

Figure 21. RBL-CCR1 chemotax towards Mip-1 α and antigen.

Figure 22. RBL-CCR1 sensitised with IgE chemotax towards Mip-1 α .

Figure 23. Motility parameters of RBL-CCR1 cells.

Figure 24. Localisation of PI(3,4,5)P3 at the leading edge of RBL-CCR1 cells in response to a Mip-1 α gradient.

Figure 25. In response to a pipette of PBS/DMEM for 20 minutes CCR1 localises at the cell membrane, whilst actin and WASP remain throughout the cytoplasm of RBL-CCR1 cells.

Figure 26. In response to a pipette of Mip-1 α for 5 minutes. CCR1, actin and WASP localise in the polarised membrane ruffles and lamellipodia of RBL-CCR1 cells.

Figure 27. In response to a pipette of Mip-1 α for 10 minutes, CCR1 begins to internalise. Actin remains localised in the polarised membrane ruffles and lamellipodia, whilst WASP now re locates from the polarised membrane ruffles to the cytoplasm and nucleus of RBL-CCR1 cells.

Figure 28. In response to a pipette of Mip-1 α for 20 minutes. CCR1 localises at the cell membrane. Actin begins to re-localise from the polarised membranes to the cytoplasm, whilst WASP localises throughout the cytoplasm and nucleus of RBL-CCR1 cells.

Chapter 4:

Figure 29. Symptoms of murine allergic conjunctivitis.

Figure 30. Morphology of murine conjunctival mast cells in naïve and post allergen challenged conjunctiva.

Figure 31. Kinetic analysis of mast cell accumulation within the inflamed mouse conjunctiva induced by allergic conjunctivitis model 1-using A/J mice.

Figure 32. Kinetic analysis of mast cell accumulation within the inflamed mouse conjunctiva induced by allergic conjunctivitis model 2- using BALB/c mice.

Figure 33. Conjunctival mast cells (purple) 1 and 2 (pink arrows) in the vicinity of a chemokine gradient, G, in SRW sensitised-challenged mice.

34. (A) Actin (red) and (B) WASP (green) localisation in murine conjunctival mast cells 1 and 2 (indicated by purple arrows) in the vicinity of a chemokine gradient, from a serial section of tissue shown in figure 33 in SRW sensitised-challenged mice. (C) Co-localisation (yellow) of actin (red) and WASP (green) in murine conjunctival mast cells in SRW sensitised-challenged mice.

Figure 35. (A) CCR1 (green) and (B) positive mast cell (red) expression in the vicinity of a chemokine gradient (forniceal region), in non-sensitised non-challenged murine conjunctiva. (E) co-localisation (yellow/orange) of CCR1 (green) positive mast cells (red) in the vicinity of a chemokine gradient (forniceal region), in non-sensitised non-challenged murine conjunctiva. This figure is representative of five separate experiments with at least 3-5 eyes analysed in each.

Figure 36. (A) CCR1 (green) and (B) positive mast cell (red) expression in the vicinity of a chemokine gradient (forniceal region), in sensitised-challenged murine conjunctiva. (C) co-localisation (yellow/orange) of CCR1 (green) positive mast cells (red) in the vicinity of a chemokine gradient (forniceal region), in sensitised-challenged murine conjunctiva. This figure is representative of five separate experiments with at least 3-5 eyes analysed in each.

Chapter 5:

Figure 37. Reduction of endogenous RGS1 in RBL-CCR1 cells by RNA interference.

Figure 38. Co-stimulation by Mip1- α and IgE/antigen enhanced degranulation of RGS1 siRNA treated RBL-CCR1 cells.

Figure 39. Co-stimulation by Mip-1 α and IgE/antigen enhanced mediator release of IL-4, IL-6 and MCP-1 from RGS1 siRNA treated RBL-CCR1 cells.

Figure 40. Gene expression of inflammatory mediators following IgE/Antigen stimulation of RBL-CCR1 cells.

Figure 41. Effect of RGS1 on gene expression of inflammatory mediators following IgE/Antigen stimulation of RBL-CCR1 cells.

Figure 42. Co-stimulation by Mip1- α and IgE/antigen enhanced chemotaxis of RGS1 siRNA treated RBL-CCR1 cells.

Chapter 6

Figure 43. Reduction of endogenous TRB3 in RBL-CCR1 cells by RNA interference

Figure 44. Co-stimulation by Mip1- α and IgE/antigen enhanced degranulation of TRB3 siRNA treated RBL-CCR1 cells.

Figure 45. Co-stimulation with Mip-1 α and IgE/antigen enhanced mediator release of IL-10, and MCP-1 from TRB 3 siRNA treated RBL-CCR1 cells.

Figure 46. Co-stimulation by Mip1- α and IgE/antigen enhanced chemotaxis of TRB3 siRNA treated RBL-CCR1 cells.

List of tables

Chapter 1:

Table 1. The function of mediators released by activated mast cells

Chapter 2:

Table 2. A table to show concentrations of stains, primary and secondary antibodies for each target antigen used in this study.

Chapter 3:

Table 3. Summary of cellular effects (motility parameters) from the pipette assays of RBL-CCR1 cells

Abbreviations

Alum	Aluminum hydroxide
AP-2	Adaptin 2
AP1	Activator protein
Arp	Actin related proteins
ATF	Activating transcription factor
BCA	Bicinchoninic acid
BMMC	Bone marrow mast cells
BSA	Bovine serum albumin
Btk	Bruton's tyrosine kinase
CCD	Charged-couple device
CCR	Chemokine receptor
CD	Cluster of differentiation
cdk1	Cyclin-dependent kinase
cDNA	Complimentary DNA
CHOP	C-homologous protein
CR	Complement receptor
CSF	Colony stimulating factor
DMEM	Dulbecco's modified Eagle's medium
DMSO	Dimethyl Sulfoxide
DNA	Deoxyribonucleic acid
DNP	Anti-dinitrophenyl
DNP-HSA	Dinitrophenyl human serum albumin
ds RNA	Double stranded ribonucleic acid
DTT	Dithiothreitol
ECL	Enhanced luminol-based chemiluminescent
ER	Endoplasmic reticulum
ERK	Extracellular-signal-regulated kinase
ET-1	Endothelin-1
F-actin	Filamentous actin
FBS	Fetal bovine serum
FGF	Fibroblast growth factor
FITC	Fluorescein isothiocyanate

fMLP	N-formyl-methionyl peptide
Foxp3	Forkhead box P3
Gab2	Grb2-associated binder 2
GAPDH	Glyceraldehyde 3-phosphate dehydrogenase
GAPs	GTPase activating proteins
GATA3	GATA binding protein 3
GBD	GTPase binding domain
GDP	Guanosine diphosphate
GEFs	Guanine exchange factors
GFP	Green fluorescent protein
GM-CSF	Granulocyte-macrophage colony-stimulating factor
GPCRs	G- protein couple receptors
GRKs	G protein-coupled receptor kinases
GTP	Guanosine triphosphate
HIV	Human immunodeficiency virus
HMC	Human mast cell
HO-1	Heme oxygenase-1
hPa	Hectopascal
HRP	Horseradish peroxidase
IFN	Interferon
Ig	Immunoglobulin
IL	Interleukin
iNKT cells	Invariant NK T cells
IP3	Inositol -1,4,5 triphosphate
ITAMS	Immunoreceptor tyrosine-based activation motifs
IRSp53	Insulin-receptor substrate p53
JNK	JUN amino-terminal kinase
kDa	Kilo daltons
L15	Leibovitz-15
LAD	Laboratory of allergic disease
LAT	Linker for activation of T cells
LIMK	LIM kinase.

LPS	Lipopolysaccharide
LT	Leukotriene
M	Molar
M-PER	Mammalian Protein Extraction Reagent
MAb	Monoclonal antibody
MAPK	Mitogen-activated protein kinase
MAPKK	MAPK kinases
MCP	Monocyte chemotactic protein
mdia2	Mammalian diaphanous-2
MHC	Major Histocompatibility Complex
Mip	Macrophage inflammatory protein
mMCP	Mouse Mast Cell Protease
N-WASP	Neural WASP
NF- κ B	Nuclear factor of kappa light chain gene enhancer in B cells
NFAT	Nuclear factor of activated T cells
nm	Nanometres
OCT	Optimal cutting temperature
PAF	Platelet- activating factor
PAK	p21-activated kinase
PAMPs	Pathogen associated molecular patterns
PBS	Phosphate Buffer Saline
PDGF	Platelet-derived growth factor
PDK1	Phosphoinositide-dependent kinase 1
PFA	Paraformaldehyde
PGD2	Prostaglandin D2
PGN	Proteoglycans
PH	Pleckstrin homology
PI(3,4,5)P3	Phosphatidylinositol 3,4,5-triphosphate
PI(4,5)P2	Phosphatidylinositol 4,5-bisphosphate
PI3K	Phosphoinositide 3-kinase
PKC	protein kinase C
PLC	Phospholipase C
PMSF	Phenyl Methyl Sulfonyl Fluoride

PPAR- α	Peroxisome proliferator-activated receptor alpha
PRR	Pattern recognition receptors
PTK	Protein tyrosine kinases
PVDF	Poly Vinylidene Fluoride
R	Receptor
RANTES	Regulated upon Activation, Normal T-cell Expressed, and Secreted
RBL-2H3	Rat basophilic leukemia
RGS	Regulator of G-protein Signaling
Rho-GDIs	Rho guanine-nucleotide-dissociation
RNAi	RNA interference
rpm	Revolutions per minute
S1P	Sphingosine-1-phosphate
SCF	Stem cell factor
SDF-1	Stromal cell-derived factor-1
SEM	Standard error mean
SH2 domains	SRC-homology-2-domains
SHIP	SH2 domain-containing inositol phosphatase
siRNA	Short interference RNA
Sos	Son of sevenless
SRW	Short ragweed pollen
STAT	Signal transducer and activator of transcription
STIM-1	Stromal interaction molecule 1
Syk	Spleen tyrosine kinase
Tapp-1	Tandem PH domain-containing protein 1
TBS	Tris-buffered saline
TCR	T cell receptor
tf	Final time point
TGF	Transforming growth factor
Th	T helper
ti	Initial time point

TLRs	Toll-like receptors
TNF	Tumor necrosis factor
TRB	Tribbles
Tregs	Regulatory T cells
ug	Microgram
ul	Microlitre
um	Micrometre
WASP	Wiskott–Aldrich syndrome protein
WAVES	WASP family verprolin homologous protein
WH1	WASP homology domain 1
WHAMM	WASP homolog associated with <i>actin</i> , membranes, and microtubules
ZAP70	ζ-chain-associated protein kinase of 70kDa
°C	Degrees centigrade

Chapter 1.
General introduction and hypothesis

1. Introduction

The immune system is a complex highly orchestrated network of cells, receptors, and chemical mediators, which collectively maintain the homeostasis of an organism. Over the past century scientists have identified and elucidated how various immune cells and their mediators protect us from disease. The protective role of the immune system is highly regulated, and is designed to be self-limiting once the pathologic condition is resolved. However, there are instances when this regulation breaks down causing the immune system to initiate diseases such as allergy, autoimmunity and cancer.

The immune system consists of two components, the innate (non-specific) and adaptive (specific). The innate immune response responds rapidly as the first line of defence against viral and bacterial infections, responding to foreign agents by phagocytosis and by releasing reactive chemicals, which non-specifically destroy at the site of inflammation. In contrast, the adaptive immune response is slower to respond. It relies on cells of the innate system to capture, internalize and present foreign agents, which it utilises to prepare a highly specific response upon secondary exposure.

Recently it has been realized that some immune cells, including the mast cell can cross the boundaries between innate and adaptive immunity exhibiting roles in both components of the immune system.

Mast cells are tissue-resident cells of hematopoietic origin, which are located at strategic sites such as the skin and vascular and mucosal barriers enabling them to respond to invading pathogens, allergens and environmental agents. Since their discovery in 1878, mast cells have been long implicated as the key effector cells of allergic disorders by virtue of their ability to be activated through antigen that binds antigen-specific immunoglobulin E (IgE) via FcεRI receptor expressed on the mast cell surface (Mota and Vugman, 1956; Ishizaka et al., 1970; Eiseman and Bolen, 1992; Parravicini et al., 2002; Gould and Sutton, 2008). However, mast cells have been recognised for their critical role during innate immunity to bacteria (Echtenacher et al., 1996; Malaviya et al., 1996, Wang et al., 2012), adaptive immunity to parasites (Ruitenbergh et al., 1976, Han et al., 2012; Hepworth et al., 2012), tissue remodeling during wound healing (Garbuzenko et al., 2002), immune suppression, angiogenesis and cancer (Littlepage et al., 2005).

Allergic conditions range from the annoying hay fever to the more fatal anaphylaxis and costs associated with them dominate public health budgets. As current treatments are not completely effective and in the eye can give rise to adverse side effects such as glaucoma and cataracts there is a continuing effort to better understand the allergic cascade. In light of this the focus of this study has been to further characterise the molecular basis of mast cell degranulation, mediator release and chemotaxis during the allergic response and thereby identify alternative anti-inflammatory therapies.

1.1 Mast cell biology

1.1.1 Mast cell origins and development

The tissue-resident mast cell is a 10-20µm in diameter with an *in situ* appearance ranging from elongated to ovoid (Schulman et al., 1983; Metcalfe et al., 1997). Defined by the presence of dense cytoplasmic granules which, when stained with toluidine blue, cause metachromasia.

Mast cells are hematopoietic in origin and differentiate from cluster of differentiation (CD)-34⁺ bone marrow progenitor cells. Progenitor mast cells migrate from the bone marrow into the circulation, migrating through blood vessel endothelium and localise into vascularised mucosal and connective tissue, where they undergo final maturation expressing the FcεRI receptor (R) capable of binding immunoglobulin (Ig) E and hence effector function (Kitumura et al., 1977; Metcalfe, 1997; Kawakami et al., 2002; Galli et al., 2008) (Figure1). Subsequent studies have validated that the development of mast cell progenitors requires constitutive signals from cytokines such as interleukin (IL)-3, IL-4, IL-5 and IL-9 (Metcalfe, 1997) and growth factors such as stem cell factor (SCF) (Huang et al., 1990), that dictate their trafficking from circulation, survival and maturation.

The most crucial viability and differentiation signal for mast cells is provided from the interaction between the membrane-associated c-kit receptor and its ligand SCF (Huang et al., 1990), a growth factor that is expressed constitutively by endothelial cells and fibroblasts. Studies have demonstrated membrane bound SCF, its soluble isoform or a combination are chemotactic for mast cells and their progenitors

(Nillson et al., 1994), elicit their adhesion (Lorentz et al., 2002), facilitate their proliferation (Yee et al., 1994) and sustain their survival, differentiation and maturation (Irani et al., 1992).

Mouse bone marrow cultured in IL-3 gives rise to a population of 85% or more of mast cells by 4-5 weeks (Rottem et al., 1993). It has been reported that after one week of culture in IL-3, a third of mouse bone marrow mast cells (BMMC) express IgE receptors (Metcalf, 1997), however these cells contain sparse granules and hence lack characteristics of mature mast cells. The expression of FcεRI⁺ mast cells increases over 3 weeks of culture and in parallel a progressively large number of cells become increasingly granulated which is accompanied by an increase in histamine content (Rottem et al., 1993). Moreover, IL-4 in the presence of IL-3 enhances proliferation and maturation in vitro of both bone marrow derived and peritoneal mast cells (Metcalf, 1997). In addition IL-4, along with IL-6, can induce apoptosis in mast cells. IL-9 alone has no proliferative effects on BMMC, although, in combination with IL-3, growth of BMMC can be observed (Hultner et al., 1990). Development of the reactive mast cell requires additional cytokines such as IL-3, IL-4, IL-5 and IL-9 from activated T cells.

Variation in the phenotype of mast cells during the course of individual biological responses or at different anatomical sites has been called mast cell 'heterogeneity' (Galli et al., 2008; Beaven, 2009). The capacity of the mast cell lineage to generate individual populations that exhibit various functional properties, mediator content and/or other aspects of phenotype may contribute to their multifunctional capability in immunological and pathological responses.

In mouse, there are two main mast cell subtypes, connective tissue mast cells that are found in the intestinal submucosa, peritoneum, eye and skin and mucosal mast cells that are associated with the epithelium of the lung and gastrointestinal tract. Intestinal mucosal mast cells express the chymases, mouse Mast Cell Protease (mMCP)-1 and mMCP-2, while, connective tissue mast cells are characterised by expression of chymase, mMCP-4, an elastinolytic enzyme, mMCP-5, and two tryptases, mMCP-6 and mMCP-7 (Miller et al., 2002). Whilst in humans there are two main mast cell subtypes, those containing tryptase alone and those containing chymase and tryptase (Pejler et al., 2010).

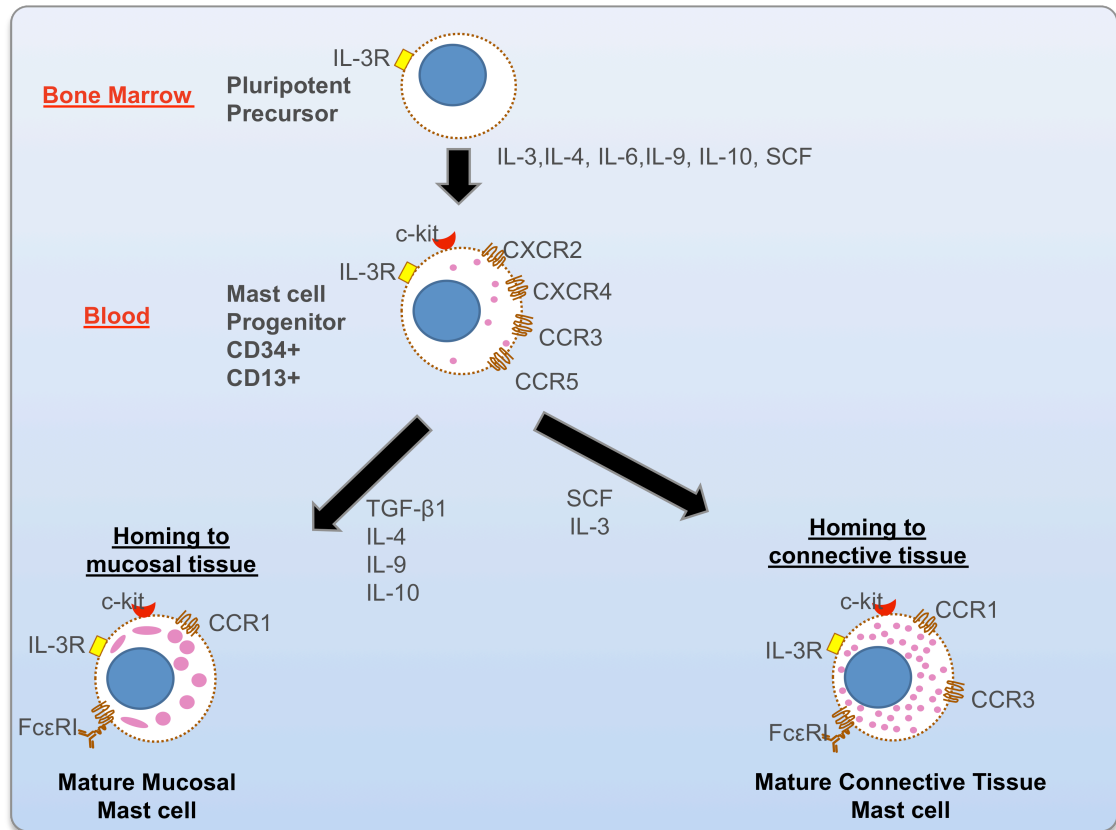


Figure 1. Mast cell development and tissue distribution. Changes in chemokine receptor expression and cytokines involved during mast cell development, from bone-marrow derived mast cell progenitors to tissue resident mature mast cells. This figure was adapted from Ono et al., 2003.

1.1.2 Mast cell activation and mediator release

Mast cell activation in response to both exogenous and endogenous stimuli occurs through distinct receptors. The kinetics, amounts and/or profile of mediators released is determined by the nature of the activating stimulus and is under the influence of the local environment in which activation takes place.

The most studied mechanism of mast cell activation is through the high affinity IgE receptor, FcεRI. The binding of multivalent allergen to IgE-FcεRI complex triggers mast cell activation, and initiates classic mast cell-mediated allergic reactions, which will be further discussed in section 1.1.3.2. IgE-dependent activation of mast cells results in their release of 1) preformed mediators that are stored in the cells cytoplasmic granules, including histamine, proteases chymase and tryptase, cytokines and proteoglycans (PGN) and 2) growth factors, cytokines and chemokines (Segal et al., 1977; Gordon et al., 1991; Okayama et al., 2001). In contrast, mast cells also secrete newly synthesised lipid mediators that are the products of endogenous arachidonic acid metabolism, such as prostaglandin D2 (PGD2), leukotriene (LT)-B4, platelet-activating factor (PAF), LTC4 (Roberts et al., 1979; Lewis et al., 1982) and a diverse range of cytokines and chemokines (Bissonnette et al., 1997; Okayama et al., 2003). In 1989 Wodnar-Filipowicz and Plaut along with co-workers demonstrated that stimulated mast cells synthesized and released IL-3, IL-4, IL-5, IL-6 and granulocyte-macrophage colony-stimulating factor, (GM-CSF) (Plaut et al., 1989; Wodnar-Filipowicz et al., 1989). Thereafter in 1990, Gordon and Galli reported that mast cells were a biologically significant source of both pre-formed and antigen-inducible tumor necrosis factor (TNF)-α (Gordon and Galli, 1990).

The diversity of these biologically active mediators allows the mast cell to participate in a wide variety of biological functions, thereby mediating pro-inflammatory, anti-inflammatory and immunoregulatory effects (Table 1). Preformed mediators including histamine and serotonin, increase vascular permeability and smooth muscle contraction, while proteases such as tryptase and/or chymase induce bronchial mucus secretion, degradation of blood vessel basement membrane, degradation of microbial structures and generation of complement pathway products. Newly synthesised lipid mediators induce vasodilation, increase vascular permeability, bronchoconstriction of the lungs and mucus secretion. In addition, newly synthesized cytokines and chemokines

promote proliferation of mast cells, recruitment of other immune cells and hence promotion of inflammation.

Although FcεRI-IgE dependent mast cell activation is well characterized, it is only one of several potential mechanisms that can initiate mast cell effector function. Mast cells can be activated by: complement components (Wojta et al., 2002) through complement receptors, microbes (Supajatura et al., 2001) through Toll-like receptors (TLRs), IgG, and chemokines through chemokine receptors.

The initial recognition of pathogens is mediated by pattern recognition receptors (PRR), which include TLRs. TLRs are present on many immune cells, including mast cells (Haidl et al., 2010; Franchi et al., 2008), and are a family of cytosolic and cell-surface receptors that collectively recognize pathogen associated molecular patterns (PAMPs) (Appelquist et al., 2002), and provide a critical link between innate and adaptive immunity. Human and mouse mast cells have been shown to express TLR 1-7 and TLR9 under defined conditions (Supajatura et al., 2002; Varadaradjalou et al., 2003), and specific TLR stimulation by various pathogens induces different mast cell responses. Each of these recognition receptors recognize a distinct category of microbial products such as PGN via TLR2 (Kochan et al., 2012), double stranded ribonucleic acid (dsRNA) by TLR3 (Kulka et al., 2004), lipopolysaccharide (LPS) by TLR4 (Tsukamoto et al., 2012), and bacterial deoxyribonucleic acid (DNA) by TLR9 (Matsushima et al., 2004). Expression of TLR varies among different subsets of mast cells and conditions, for example reports suggest mast cells derived from human cord blood lack TLR4 under certain culture conditions but then express functional TLR4 after stimulation with interferon (IFN)-γ or IL-4 (Varadaradjalou et al., 2003; Okumura et al., 2003). The interaction between mast cells and TLR's during innate immunity will be further discussed in section 1.1.3.3.

The complement pathway constitutes a significant component of innate immunity to various infections, comprising of more than 30 serum proteins and cell-surface receptors that co-ordinate host defense through opsonization, leukocyte activation, cell lysis, and chemotaxis. Mast cells express receptors for several complement products, which include complement receptor (CR) 3, CR4, and CR5, and split products of complement activation such as C3aR and C5aR (Metz et al., 2008). Complement peptides induce histamine release from mast cells and a wheal and flare reaction in the skin. C3a induces degranulation and production of the

chemokines, Regulated upon Activation, Normal T cell Expressed, and Secreted (RANTES) and monocyte chemotactic protein (MCP)-1 (Venkatesha et al., 2005; Woolhiser et al., 2004). In addition, C3a and C5a have been reported as potent chemoattractants for mast cells (Nilsson et al., 1996).

Mast cells can be positively or negatively regulated through IgG receptors, of these Fc γ RI and Fc γ RIII are activating receptors and are inducible (Kirshenbaum et al., 2003; Katz et al., 1992).

Exogenous components such as wasp venom (associated with pathogens) can also activate mast cells. Although the mechanisms are not completely elucidated, certain venom components may directly activate trimeric G proteins and other signalling molecules (Ferry et al., 2002; Chahdi et al., 2004).

Parasitic infections are often associated with elevated levels of IgE (parasite-specific or non-specific), mast cell activation and increased mast cell numbers, strongly indicating mast cell participation in host response to parasite infection (Anthony et al., 2007). Mast cell activation upon subsequent exposure to the parasite itself or parasite antigen leads to the release of an array of pro-inflammatory mediators as well as cytokines, which augment the adaptive response (Knight et al., 2000; Gurish et al., 2004; Watanabe et al., 2009; Hepworth et al., 2012).

Mediator		Function
Stored preformed in cytoplasmic granules	Histamine	Promotes smooth muscle contraction. Increases vascular permeability
	Enzymes- tryptase, chymase, cathepsin G, carboxypeptidase	Degrade microbial structures. Tissue remodelling and damage
Lipid mediators synthesized on activation	Prostaglandin D2	Vasodilation, bronchoconstriction
	Leukotriene C4,	Prolonged bronchoconstriction, mucus secretion, increased vascular permeability
	Platelet-activating factor	Bronchoconstriction, chemotaxis and activation of leukocytes. Increased vascular permeability
Cytokines, chemokines and growth factors produced on activation	IL-3, SCF	Promotes mast cell proliferation
	TNF- α , Mip-1 α	Promotes inflammation.
	IL-4 and IL-13	Promotes Th2 differentiation
	IL-5	Promotes eosinophil activation

Table 1. The effects of mediators released by activated mast cells

1.1.3 Roles of mast cells in physiology, disease and immunity

The constitutive development of mast cells and their diverse effector functions likely evolved to serve significant homeostatic and protective functions. It is now evident that mast cells can enhance initiation of both innate and adaptive immune response to allergens as well as to foreign pathogens. Whilst for allergens these immune responses are pro-inflammatory, in contrast for pathogens these immune responses are protective. The following sections discuss the multi-faceted roles of mast cells.

1.1.3.1 Mast cells in physiology

Mast cells exist in many different tissues not only to act as immune surveillance cells to detect and respond to pathogens but also to maintain physiological homeostasis.

Mast cells are important in the homeostasis of organs that undergo remodeling and continuous growth such as bones and hair follicles. Mast cell-derived $\text{TNF-}\alpha$ is implicated in deterioration of hair follicles and regulating growth between periods of hair growth and rest (Maurer et al., 2003). In addition, mast cells also contribute to bone remodeling. It has been suggested that mast cell mediators, transforming growth factor (TGF)- β , IL-6, IL-1 and histamine could manipulate osteoclast development and recruitment (Silberstein et al., 1991; Nagasaka et al., 2008). Homeostasis can also be maintained by mast cells by degrading toxins such as endothelin-1 (ET-1), a potent vasoconstrictor. Mast cells are activated by ET-1, releasing proteases, which degrade this protein, therefore promoting survival in mice during bacterial peritonitis (Maurer, et al., 2004). In the gut, mast cells and neurons work co-operatively to maintain homeostasis by regulating secretory activity of mucus, vascular permeability ion transport, epithelial cells, and intestinal motility (Van et al., 2007).

Mast cells are thought to be critical for the maintenance of tissue integrity and function. Mast cells synthesise several different growth factors including vascular endothelial growth factor (VEGF), platelet-derived growth factor (PDGF), fibroblast growth factor (FGF)-2, which are involved in proliferation of fibroblasts and epithelial cells (Abe et al., 2000).

Mast cells localise near nerve endings in many different tissues, such the central nervous system, skin, lungs and intestinal mucosa. Mediators released from mast cells, for example histamine, tryptase and serotonin can regulate neuronal activity (Welle, 1997). The interaction between mast cells and neurons may also lead to immunosuppression demonstrated by the observation that upon UV irradiation mast cells migrate to lymph nodes and secrete increased levels of IL-10, a potent anti-inflammatory cytokine, avoidance of which abrogates the induction of immunosuppression (Byrne et al., 2008).

1.1.3.2 Mast cells in disease: allergy and the allergic cascade

Although mast cells have been implicated in several disease types such as: autoimmune diseases, heart disease, cancer and allograft rejection, for the purpose of this thesis the following sections will discuss allergy, the allergic cascade and the role of mast cells during the allergic response.

In 1906, Clemens von Pirquet coined the term 'allergy'. It has been suggested that allergies are the result of a hypersensitive immune system reacting inappropriately to normal innocuous substances (allergens), which the immune system misidentifies as harmful. For an adaptive immune response, a normal host response to antigen presentation brings forth a mixed humoral and cellular response. In general intracellular pathogens including viruses, fungi and mycobacteria incite a cell-mediated response while extracellular pathogens like bacteria elicit primarily a humoral response. The equilibrium between humoral versus cellular responses to antigen challenge is maintained by a specific cytokine profile derived from T cells, which will be discussed in further detail later in this section.

There are two types of allergen: the first being any non-infectious, environmental substance that can generate IgE production, thereby sensitizing the individual, so that subsequent re-exposure to that specific substance induces an allergic response; these include: grass, tree pollen, sheddings from animal skin and fur and certain foods; the second type is a non-infectious environmental substance that can generate an adaptive immune response, but occurs independently of IgE, for example allergic dermatitis.

The allergic response consists of two components, the early phase and late phase. The early phase, in which a single allergen exposure produces an acute reaction often known as type 1 immediate hypersensitivity reaction contributes to the development of the late phase. This typically occurs within minutes of allergen exposure. A further six to 24 hours later, a second round of symptoms, known as the late phase response, develops from the recruitment and activation of eosinophils, basophils and persistent mediator production by resident mast cells and resident or recruited T cells that recognise allergen derived peptides. The clinical symptoms, which manifest as consequence of mast cell activation range from itching, oedema and wheezing to more severe or fatal consequences associated with vascular collapse and systemic anaphylaxis.

The mechanisms driving allergic disease, involve both innate and adaptive responses. Allergens are processed and presented in *Major Histocompatibility Complex* (MHC) class II peptide complexes to naïve CD4⁺ T helper (Th) cells by activated and mature dendritic cells. In 1986, Mosmann and co-workers showed the existence of two subtypes of mouse Th cells, Th1 and Th2, differing in cytokine secretion patterns and functions. However, in contrast to murine studies, polarised Th cytokine patterns are seldom apparent in human tissues. Studies have demonstrated that human Th1 cells produce IFN- γ and TNF- β , but not IL-4 and IL-5, whilst Th2 cells do not produce IFN- γ , but primarily produce IL-4, IL-5, IL-9 and IL-13, and more recently, several new subtypes of Th cells have been identified, namely: Th9 cells, predominantly secreting IL-9; Th17 cells, predominantly secreting IL-17; Th22 cells predominantly secreting IL-22 and regulatory T cells (Tregs) predominantly secreting IL-10 (Manetti et al., 1993; Park et al., 2005; Veldhoen et al., 2008; Rubtsov et al., 2008; Dardalhon et al., 2008; Eyerich et al., 2009).

The development of allergic immunity is largely mediated by Th2 cells and their associated cytokine profiles. However, recent investigations have identified other Th subtypes namely Th9, Th17, Th22 and Tregs each with their own distinct cytokine profile involved in Th2 responses.

Although IFN- γ is the signature cytokine produced by Th1 cells, Th1 polarization and IFN- γ production were initially considered protective responses to allergic disorders, based on IFN- γ suppression of many Th2/IL-4 mediated effects.

However, this paradigm in allergic disorders has been challenged by data showing that immune responses to allergen include mixed Th1 and Th2 cells (Dahl et al., 2004; Woodfolk et al., 2006; Yang et al., 2010).

IL-4, the most established determinant driving Th2 differentiation (Seder et al., 1992) induces class switching of B cell Ig production towards IgE. Antigen-specific IgE subsequently primes effector cells, basophils and mast cells, which rapidly degranulate upon re-encounter with the allergen. IL-4 activates signal transducer and activator of transcription (STAT)-6, which in turn promotes expression of GATA binding protein 3 (GATA3), the master regulator of Th2 cells. In addition, mast cells, basophils, nuocytes and invariant natural killer (iNKT) cells are capable of robust IL-4 secretion (Bilenki et al., 2004; Akbari et al., 2006; Neill et al., 2010). Th2 cells produce IL-5, which stimulates the differentiation of eosinophils, which play important roles in killing helminths and other parasites, whereas IL-13 and IL-4 together stimulate excessive production of mucus and contraction of smooth muscle, which helps in expulsion of helminths from the lung and gut (Kool et al., 2012).

Th9 T cells, a proposed subfamily of Th2 cells, are characterized by the major production of IL-9 and relatively little IL-4, which result from the concomitant presence of TGF- β and IL-4 (Veldhoen et al., 2008; Dardalhon et al., 2008). IL-9 supports Th2 cell differentiation, survival, and cytokine production. It promotes recruitment of Th2 cells in part through enhancing their expression of chemokine receptor (CCR)-4. The transgenic IL-9 lung model is also associated with elevated Th2 cytokine expression, bronchial hyper-reactivity, and hyper-secretion of mucus (Temann et al., 2002). IL-9 was initially described as a mast cell growth factor (Hultner et al., 1990), contributing to mast cell-mediated allergic responses through its ability to stimulate Fc ϵ RI expression, protease production and mast cell recruitment (Temann et al., 2002). In addition, IL-9 co-operates with IL-4 to enhance the production of IgE and increases expression of IL-5 receptors and thereby interacts with IL-5 to enhance the production of eosinophils (McLane et al., 1998).

Another CD4⁺ T cell subset, Th17 cells secrete IL-17, which induces expression of a variety of cytokines and chemokines including IL-6, IL-8, IL-11 and TGF- β , all of which are important to both fibroblast activation and neutrophil recruitment. IL-17

family members are expressed in asthma (Molet et al., 2001). In asthma the tendency to induce neutrophil migration, and not eosinophil migration suggests that IL-17 plays a role in asthma, in which the accumulation of neutrophils is characteristic of this phenotype. Hyper-IgE syndrome in humans is characterized by a genetically determined deficiency in Th17 cell differentiation (Milner et al., 2008). The mechanisms underlying Th17 differentiation in humans are not fully elucidated. However, in mice, IL-6 in the presence of TGF- β , is the most important cytokine responsible for Th17 cell differentiation (Iwakura et al., 2006).

Th22 cells are characterized by their major production of IL-22. Th22 polarisation is determined by IL-6 and TNF- α , typically being produced by epithelial cells or keratinocytes (Duhon et al., 2009). Notably, Crohn's disease, psoriasis and rheumatoid arthritis all demonstrate elevated levels of IL-22 that correlate with disease severity (Ikeuchi et al., 2005; Wolk et al., 2007; Duhon et al., 2009).

Unlike other Th cell subsets in which T cell receptor (TCR) engagement under appropriate co-stimulation conditions leads to activation and proliferation, Treg cells proliferate poorly in response to TCR stimulation; instead, they suppress the proliferation of other T cells (orchestrated by forkhead box P3 (Foxp3) expression) or by IL-10 secretion (Itoh et al., 1999; Baecher-Allan et al., 2001; Campbell et al., 2007). In this light, Tregs are therefore regarded as essential players for modulating allergic inflammation (Woodfolk et al., 2006; Xystrakis et al., 2006), preventing autoimmune disease (Sakaguchi et al., 1995) and controlling chronic inflammatory disease (Coombes et al., 2005). The proposed mechanisms of Treg-mediated suppression have been studied and include cell contact and TGF- β , IL-10 and IL-35 dependent mechanisms (Shevach, 2009; Apostolou et al., 2008).

The allergic response consists of sensitization of mast cells and the generation of a specific immune response towards the allergen. The following events occur during sensitization: 1) priming of allergen-specific CD4⁺ Th2 cells and 2) production of IL-4 and IL-13 (Th2 cytokines) and hence induction of IgE (Figure 2). In brief, in the presence of IL-4, CD4⁺ Th cells differentiate into Th2 cells producing IL-4 and IL-13. Thereafter, these cytokines cause B cells (in the presence of co-stimulatory molecules) to undergo Ig class switch recombination, whereby the gene segments, which encode the heavy chain are reorganized so as to produce IgE. Thereafter, IgE diffuses locally entering the lymphatic vessels and subsequently enters the

blood circulation binding to mast cells. Binding of IgE to FcεRI on the mast cell surface sensitizes the cell, hence, upon subsequent exposure to antigen the mast cell is activated, promoting release of pro-inflammatory mediators, which cause the acute symptoms of an allergic response, previously discussed in section 1.1.2 and Table 1 (Roitt et al., 2011).

Reports have demonstrated the potential role for mast cells in allergen sensitisation. Using a mouse model of asthma, intranasal administration of low doses of antigen and LPS resulted in increased eosinophil numbers in the lung upon antigen re-challenge, compared to mice that were sensitised with antigen alone or sensitised with antigen and increased doses of LPS (Eisenbarth et al., 2002; Nigo et al., 2006). In addition, once allergen sensitisation has taken place, it is possible that mast cells expressing allergen-specific IgE may further promote the allergic response by acting as antigen presenting cells, to further amplify allergen-specific Th2 proliferation.

As previously described, mast cells synthesise and secrete a diverse range of pro-inflammatory cytokines, including IL-4, IL-5 and IL-13, which regulate both the development of eosinophilic inflammation and IgE synthesis, and profibrogenic cytokines, including TGF-β and FGF-2 (Yu et al., 2006). In addition, activated mast cell products may also inhibit the pathology of allergic inflammation as demonstrated in MCP-4 deficient mice that displayed increased airway inflammation and airway hyper-responsiveness in response to methacholine (Waern et al., 2009).

Mast cells express the IL-33 receptor (Moritz et al., 1998), and secrete IL-33 following IgE/antigen activation (Hsu et al., 2010). Pushparaj and co-workers (2009) demonstrated that systemic administration of the IL-33 increases IgE-mediated anaphylactic shock in a mast cell dependent manner. These findings indicate that the IL-33 signalling pathway may be important for the regulation of IgE-dependent inflammation in mast cells.

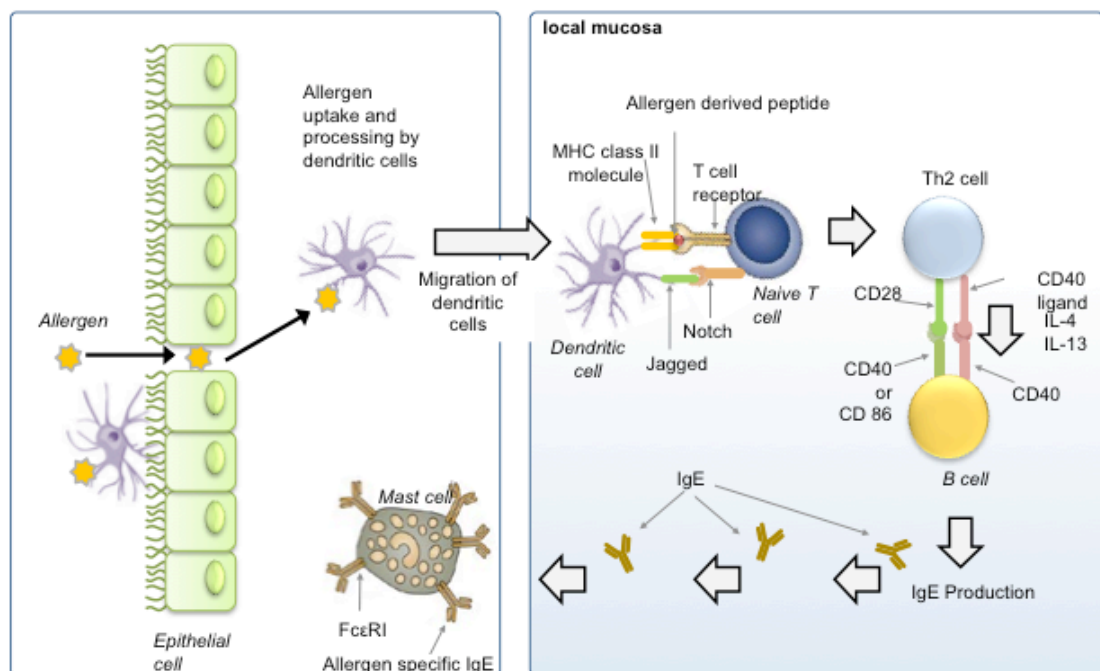


Figure 2. Differentiation of naïve CD4⁺ T cells into Th 2 cells, IgE production and sensitisation of mast cells. Allergens can be sampled by dendritic cells (DC) and can enter tissues through disrupted epithelium. DC then present peptides in the context of the major histocompatibility complex (MHC) to naïve T cells. Naïve T cells, in the presence of IL-4 acquire the characteristics of T helper 2 cells, producing IL-4 and IL-13. In the presence of these cytokines and ligation of co-stimulatory molecules, B cells produce IgE, which diffuses locally and enters the lymphatic system. IgE enters the blood and is then distributed systemically. After gaining access to the interstitial fluid IgE binds to FcεR1 on tissue resident mast cells, thereby sensitising them to respond when the host is re-exposed to the allergen. This figure was adapted from Galli et al, 2008.

1.1.3.3 Mast cells in innate and acquired immunity

Although the role of mast cells in orchestrating many of the pathological sequelae of allergy is well established, it is also recognised that mast cells can enhance initiation of both innate and adaptive immune responses to foreign pathogens as well as to allergens, during coexposure to bacteria or its products.

Mast cells have come to the forefront as activators of innate immune defenses against pathogens. As mast cells are strategically located at many sites of initial antigen entry such as the skin, eye, lung, and gastrointestinal tract, they are ideally positioned to be first responder cells during microbial attack, making them capable immune surveillance cells of innate immunity, thereby participating in protective immune responses. To function as immune surveillance cells during innate immunity, mast cells have developed three mechanisms of pathogen recognition: 1) direct binding of pathogens or their components by PAMP receptors located on the mast cell surface. As previously discussed, one class of PAMP receptors are TLRs, 2) binding of complement coated bacteria or antibody, by complement receptors or immunoglobulin receptors respectively, or 3) recognition of endogenous peptides produced by injured host cells.

Activated human mast cells expressing TLR2 or TLR4 release TNF- α , IL-5, IL-6 IL-10 and IL-13, which mediate the recruitment of phagocytic as well as other immune cells such as neutrophils and eosinophils to sites of infection (Varadaradjalou et al., 2003). The influx of these immune cells are crucial to eliminate and control invading pathogens, as displayed by mast cell deficient mice which have decreased survival due to impaired innate host immune responses (Echtenacher et al., 1996; Malaviya et al., 1996; Thakurdas et al., 2007; Ketavarapu et al., 2008; Piliponsky et al., 2010).

In addition, mast cells can also directly destroy opsonised bacteria, those which have been coated with complement proteins or IgG antibody. Thereafter, bacteria is endocytosed through an endosome lysosome pathway and killed via oxidative and non-oxidative pathways (von Kockritz-Blickwede et al., 2009). Mast cells can also contribute to host defence against bacteria by proteolytic degradation of endogenous mediators such as endothelin-1 (Maurer et al., 2004) and neurotensin (Piliponsky et al., 2008), which would otherwise be upregulated to toxic levels.

The role of mast cells and TLRs in viral infections is still being elucidated. One study has shown TLR3 activation by dsRNA from viruses in human cultured mast cells induces production of type I IFNs (Kulka et al., 2004). Any synergistic effect of TLR3 activation by viruses in the presence of FcεRI activation by allergens on mast cell cytokine production remains to be examined.

In addition to activating the innate immune system during infection, mast cells can have profound effects on two central cells of adaptive immunity, T cells and dendritic cells.

Immature dendritic cells can process antigens but due to low expression of MHC II and costimulatory molecules, such as CD80 and CD86 are unable to act as antigen presenting cells. In addition, they are unable to migrate to peripheral lymph nodes where significant interactions with T cells occur (Galli et al., 2005). Studies have shown that mast cells degranulate at sites of infection releasing prestored TNF-α, which has been demonstrated to increase dendritic cell expression of CCR7, which responds to chemokines, macrophage inflammatory protein (Mip)-3-β and 6Ckine, which are critical for dendritic cell homing to lymph nodes (Sozanni et al., 1998; Yamazaki et al., 1998; McLachlan et al., 2003). In addition, TNFα also induces maturation of dendritic cells, allowing dendritic cells to express antigen in association with MHC II and costimulatory molecules, thereby becoming an antigen presenting cell for T cells (Ritter et al., 2003).

Under certain conditions mast cells have been shown to express MHC class I and II, and along with co-stimulatory molecules are capable of directly activating T cells by functioning as antigen presenting cells (Malaviya et al., 1996; Kambayashi et al., 2009). Expression of bacterial antigens in association with MHC Class I by murine BMMCs is a likely basis for the induction of CD8 T cell responses to pathogens endocytosed by mast cells (Malaviya et al., 1996). One group recently demonstrated that MHC class II expressing murine BMMCs were poor stimulators of naïve CD4 T cells, however, they were able to restimulate previously activated CD4 T cells (Kambayashi et al., 2009). Nakano and co-workers (2009) demonstrated on the surface of murine BMMCs that Notch signaling induced expression of MHC class II and OX40L, a key costimulatory molecule. These BMMCs were able to promote proliferation of naïve CD4⁺ T cells into Th2 cells *in vitro*. Further studies are needed to validate if human mast cells are able to express

MHC II and how MHC class II expressing mast cells influence T cell activation *in vivo*.

Mast cells greatly influence the type of adaptive immune response made to a pathogen through their modulation of T cell responses. Activated mast cells release Th2 polarizing cytokines such as IL4, IL10, and IL13, which can induce stimulated naïve CD4⁺ T cells to differentiate into Th2 cells when activated in the lymph node. These Th2 cells induce humoral immune responses to pathogens by producing cytokines that stimulate B cell production of antibody (McLachlan et al., 2008; Stelekati et al 2009).

In addition, mast cells can also increase proliferation of suboptimally activated T cells, in which T cells are already exposed to antigen but at suboptimal concentrations through FcεRI dependent and independent pathways (Nakae et al., 2005).

1.1.4 Experimental models for studying mast cell function and signaling

The study of mast cell signaling events, which is fundamental for understanding their role in disease processes such as allergy, is also vital for the generation of effective novel therapies for immune-mediated diseases. Techniques for generating primary cultures of murine mast cells from bone marrow progenitor cells are available, whilst similar approaches have been established for humans using peripheral blood or cord blood as a progenitor source (Jamur et al, 2010; McAlpine et al., 2012; Hoffmann et al., 2012). However, all of these tools to study mast cell function are limited by the fact that mast cell maturation cannot be fully achieved by the various mast cell culture protocols, as indicated by functional studies. To overcome such limitations, primary cultures of human tissue mast cells are desirable, in which human mast cells can be isolated from tissue (skin, lung or intestine) and purified by complicated selection means; however, a disadvantage of this method is the availability of fresh human tissue and the limited yield of purified mast cells. In addition to primary cultures of mast cells, transformed mast cell lines have also been used to study mast function, these are: human mast cell (HMC)-1, rat basophilic leukemia (RBL-2H3) and laboratory of allergic disease (LAD)-1 and 2 (Alexandrakis et al., 2003; Castellani et al., 2009; Hewson et al., 2011). LAD mast cells require SCF for survival and hence might be more appropriate as a human mast cell model. Despite the fact that the RBL- 2H3 cell line is derived from

basophils, it is widely used in allergy research since it is a histamine releasing cell line. Although, it has been acknowledged that signaling events in these RBL-2H3 cells may not accurately reflect the signaling events of mature human mast cells, a vast amount of information has been acquired about signaling processes and mediator release with these cells (Anfossi et al., 2003; Naveen et al., 2005; Sanderson et al., 2010; Chung et al., 2012).

1.1.4.1 Fc ϵ R1 -mediated signaling in mast cells

Rapid advances over the past several years reveal antigen – dependent mast cell activation is orchestrated by a series of complex intracellular signaling processes, which are continually evolving. Moreover, these findings also reveal new areas of investigation for therapeutic strategy in disease.

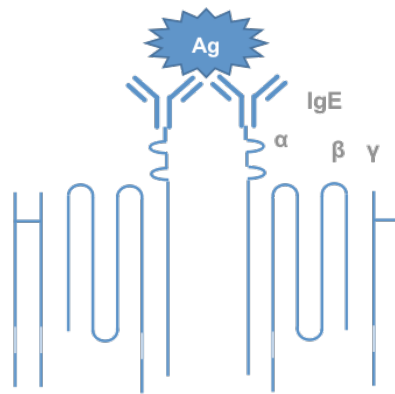
1.1.4.2 The Fc ϵ R1 receptor and IgE binding

The high affinity IgE receptor, Fc ϵ R1, exists in two forms and can be expressed as a trimer or tetramer consisting of an IgE-binding α -chain, a membrane tetraspanning β -chain that is absent in the trimeric receptor and a di-sulphide-linked homodimer of γ -chains (Nadler et al., 2000) (Figure 3). While the trimeric form can be expressed on a variety of immune cells such as eosinophils, monocytes and Langerhan cells, the tetramer is primarily expressed on mast cells and basophils, suggesting that the absence of the β -chain in the trimeric receptor is not required for efficient Fc ϵ R1 signaling and function.

The β and γ chains each contain immunoreceptor tyrosine-based activation motifs (ITAMS). ITAMS, a structural motif that contain tyrosine residues and is found in the cytoplasmic tail of several signalling molecules. The tyrosine residues are a target for phosphorylation by protein tyrosine kinases (PTK) of the Src family and subsequently, for the binding of proteins that contain Src-homology-2-domains (SH2 domains).

Figure 3. The Fc ϵ R1 receptor.

The Fc ϵ R1 receptor is expressed on resident mature mast cells and consists of a single extracellular α chain, a single β chain which passes through the membrane four times and a homodimer of two disulphide linked γ chains.



The FcεR1 receptor can bind to IgE in the absence of antigen with very high affinity (affinity constant of 10^{10} M (Kulczycki and Metzger, 1974) compared to FcγR for IgG binding (affinity constant of 10^8 M (Unkeless and Eisen, 1975). It has been considered that IgE binding therefore provides a form of passive sensitisation prior to subsequent antigen cross-linking. Interestingly, studies have shown that IgE alone can actively promote cytokine production, increased expression of cell surface FcεR1 and mast cell survival (Asai et al., 2001; Kalensnikoff et al., 2001; Matsuda et al., 2005).

IgE-FcεR1 receptor complexes are distributed in a random order, however in the first 30-60 seconds after exposure to multi-valent antigen the complexes redistribute into chain-like aggregates, as demonstrated by electron microscopy (Menon et al., 1986; Seagrave et al., 1991), that are eventually internalised within 6-10 minutes. Ishizaka and co-workers demonstrated that bivalent antibodies to FcεR1 caused degranulation in the absence of IgE implicating the aggregation of FcεR1 as the exocytotic trigger. Maximal histamine release is obtained when 10% of the receptors are aggregated.

1.1.4.3 General outline of mast cell FcεR1 signaling

Stimulation of FcεR1 by IgE with antigen results in aggregation of the receptor on the mast cell membrane, which initiates a series of phosphorylation and dephosphorylation events that are required for early transduction events (Figure 4). It is important to bear in mind that variations of mast cell FcεR1 signaling are likely to exist, and this can be further complicated by the existence of mast cell heterogeneity.

The following section describes a general outline of FcεR1 mediated signaling in mast cells. FcεR1 receptor lacks intrinsic tyrosine kinase activity, and must therefore associate with the PTK, Lyn (Eiseman and Bolen, 1992). FcεR1 engagement activates Lyn and Fyn, by an undefined mechanism (Colgan et al., 2010). Lyn is key for the subsequent phosphorylation of the tyrosine residues in the β and γ subunits of FcεR1. The phosphorylated tyrosine residues within FcεR1 subsequently act as docking sites for another PTK, spleen tyrosine kinase (Syk), which binds via its SH2 domains to the γ subunit of FcεR1. Once activated, Syk is able to phosphorylate and activate several cytosolic adapter molecules, which

include linker for activation of T cells (LAT) and Grb2-associated binder 2 (Gab2) (Rivera, 2002; Iwaki et al., 2005). Adapter molecules are those that have one or more binding motifs and/or tyrosine residues that can be phosphorylated by Syk and ζ -chain-associated protein kinase of 70kDa (ZAP70). They function as components of a molecular scaffold that organize activated receptor signaling complexes. Adapter molecules bind a variety of signaling proteins such as lipases which include phospholipase C (PLC)- γ ; phosphatases, SH2 domain-containing inositol phosphatase (SHIP)-1 and -2 and protein and lipid kinases, Lyn, Fyn, Bruton's tyrosine kinase (Btk); phosphoinositide 3-kinase (PI3K); and mitogen-activated protein kinase (MAPK) which result in the activation of signaling pathways which eventually lead to mast cell degranulation and *de novo* synthesis of inflammatory mediators, chemokines and cytokines (Kawakami and Galli, 2002).

A significant signaling enzyme recruited to phosphorylated LAT is PLC γ . PLC γ activation is essential for inducing the calcium signal required for antigen – mediated mast cell activation. PLC γ hydrolyses phosphatidylinositol 4,5-bisphosphate (PI(4,5)P₂) to generate diacylglycerol (DAG) and inositol -1,4,5 triphosphate (IP₃). DAG, which activates various protein kinase C (PKC) isoforms, which play major roles in the regulation of mast cell activation. The binding of IP₃ to its receptor, IP₃R, in the endoplasmic reticulum (ER) rapidly induces calcium release from the ER stores into the cytosol. This release of intracellular calcium stores leads to an influx through store-operated calcium channels, resulting in a prolongation of the calcium signal (Hoth et al., 1992). Recent studies have identified the molecular sensor for store emptying on the ER membrane as stromal interaction molecule 1 (STIM-1)(Roos et al., 2005). Collectively, these signals lead to mast cell degranulation and eicosanoid generation and contribute to the activation of transcription factors required for cytokine and chemokine production (Metcalf et al., 2009). As described above, the sequence of events that leads from LAT to mast cell degranulation has been clearly defined, although, the sequence of events leading from LAT to cytokine production still remains unclear. The signaling pathways that lead to cytokine gene expression require guanine exchange factors (GEFs), Vav (Manetz et al., 2001) and *son of sevenless* (Sos) (Jabril-Cuenod et al., 1996) to convert RAS from the inactive state to the active state. Activated RAS positively regulates the RAF-dependent pathway that leads to phosphorylation and activation of MAPKs, extracellular-signal-regulated kinase (ERK)-1 and ERK2. Other MAPKs, p38 and JUN amino-terminal kinase (JNK) are similarly activated in

a LAT-dependent manner, but the mechanisms responsible are yet to be elucidated. Together, ERK1, ERK2, JNK and p38 activate transcription factors which include activator protein 1(AP1), nuclear factor of kappa light chain gene enhancer in B cells (NF- κ B) and nuclear factor of activated T cells (NFAT) (Marquardt and Walker, 2000; Pelletier et al., 1998) which ultimately result in cytokine generation.

In addition to Lyn, another Src-family kinase Fyn, was also required for degranulation and cytokine production in mast cells (Parravicini et al., 2002). The Fyn-dependent pathway did not require LAT and did not lead to PLC γ activation, but instead, led to the activation of PI3K. PI3Ks are a family of enzymes which regulate multiple processes within mast cells, which include, the maintenance of LAT/PLC γ -regulated degranulation, chemokine production, mast cell proliferation, differentiation and survival (Kim et al., 2008). PI3K is activated after binding the adaptor protein Gab2, on phosphorylation by Fyn, Syk, or both. Class 1 PI3Ks can phosphorylate PI(4,5)P₂ in the plasma membrane to generate phosphatidylinositol 3,4,5-triphosphate (PI(3,4,5)P₃).

PI(3,4,5)P₃ is a well recognised regulator of mast cell effector functions (Rivera et al., 2008) and moreover, controls the activity and subcellular localisation of a diverse range of signal transduction molecules namely AKT, Btk and phosphoinositide-dependent kinase 1 (PDK1) (Cantrel, 2001; Fruman and Cantley, 2002). Once Btk has been membrane targeted by PI(3,4,5)P₃, it phosphorylates and activates PLC γ . Initial release of calcium from the ER and a Btk sustained calcium influx promotes degranulation, and the release of granule-associated products. Recent studies have suggested that increased or decreased PI(3,4,5)P₃ levels in mast cells is associated with upregulated or downregulated mast cell responsiveness (Ali et al., 2004; Furumoto et al., 2006; Odom et al., 2004), which, in most cases, similarly affects calcium responses. The mechanisms by which PI(3,4,5)P₃ levels might affect calcium responses are not fully understood but it is known that proteins such as PLC γ that regulate calcium also require PI(3,4,5)P₃ for their translocation and function.

1.1.4.4 TRB3: a regulator of cell signaling

Tribbles (TRB) have been described as a family of proteins with potent signaling regulatory functions (Figure 4). The tribbles homolog 3 (TRB3) was originally discovered in *Drosophila* as a novel regulator of *string* in morphogenesis. *String* plays a key role in regulating cell cycle regression beyond G2 by activating the cyclin-dependent kinase (cdk1). However, during morphogenesis high levels of *string* are expressed in the gastrulating mesoderm yet the migrating cells do not divide. An inhibitor to *string* was found and tribbles was identified as a gene that fits this function. Grosshans and Wieschaus showed that overexpression of TRB inhibits mitosis (Grosshans et al., 2000). *Drosophila* tribbles have been shown to regulate embryonic development at several stages either by regulating protein levels by mediating their degradation or by acting as part of a larger protein complex that regulates development.

In humans, the homolog to the TRB3 gene is located on chromosome 20 at p13-p12.2. In 1999, Mayumi-Matsuda and co-workers first described TRB3 as a gene that is upregulated in a neuronal cell line undergoing nerve growth factor withdrawal induced apoptosis. Through various investigations, TRB3 has been identified to affect several protein regulation pathways. TRB3 interacts with several transcription factors, activating transcription factor (ATF)- 4, C-homologous protein (CHOP) and NF- κ B, has been shown to be an important regulator of glucose metabolism during fasting (Kiss-Toth et al., 2004; Bowers et al., 2003; Ord et al., 2003; Ohoka et al., 2005; Du et al., 2003; Kiss-Toth et al., 2006).

TRB3 is able to bind to various MAPK kinases (MAPKK), specifically ERK1 and MAPKK7, and the concentration of these protein complexes regulates preferential activation of the various MAPK pathways, presumably leading to different cellular responses (Hegedus et al., 2007). It has been demonstrated that activation of MAPK cascades occurs in response to a wide range of stimuli, including pro-inflammatory cytokines, growth factors, mechanical stimuli, stress and integrin-dependent cell/matrix interactions (Li et al., 2000; Goldschmidt et al., 2001; Jones et al., 2001). This suggests that TRB3 may also stimulate pro-inflammatory cytokines to activate a MAPK response when gene expression levels are high as well as play an important role in the allergic response.

ATF4 has been shown to have several important regulatory effects including osteoblast differentiation in development and targeting genes such as CHOP and *Heme oxygenase-1* (HO-1), which are involved in the regulation of apoptosis. TRB3 has a negative regulatory effect on ATF4-mediated gene activation, and because of ATF4's relation to CHOP, it is reasonable to link the modulation of TRB3 expression in apoptotic cells to the co-ordination of programmed cell death (Hegedus et al., 2006). It has been hypothesized that the ATF4-CHOP pathway regulates TRB3 expression as well. Ohoka *et al.* found that increasing TRB3 levels inhibited CHOP-mediated transcription, but also showed that the promoter sequence of TRB3 is regulated in an ATF4 and CHOP-mediated manner (Ohoka et al., 2005). This means that interactions between TRB3, CHOP, and ATF4 create a self-regulatory network to fine tune TRB3 expression, and in turn TRB3 mediated cell death. These results corroborate another report that TRB3 expression is up-regulated in stressful conditions through the ATF4/CHOP pathway (Ord et al., 2005). Other studies using fibrates are in concurrence with previous data regarding CHOP and TRB3 expression. Fibrates have been used in the clinical setting as a treatment for hyperlipidemia and atherosclerosis. In lymphocytes, fibrates augment TRB3 and CHOP expression which act as mediators of cell growth, differentiation, proliferation, and inflammation (Selim et al., 2007; Ramji et al., 2002).

NF- κ B plays a key role in immune regulation and inflammation through induction of a large set of chemokines, cytokines, adhesion molecules, and effectors (Karin et al., 2002; Ghosh et al., 2002; Baldwin et al., 2001). Some studies also suggest that NF- κ B is involved with the transcriptional activation of genes important for apoptosis and cell proliferation (Wang et al., 1998; Zong et al., 1999; Micheau et al., 2001; Locksley et al., 2001). TNF- α is a major pro-inflammatory cytokine whose effects are mediated through the activation of NF- κ B. The signaling pathway that is responsible for TNF-induced NF- κ B activation has been well studied and for the most part resolved. In a study by Wu et al., the protein SINK, a protein identical to that produced by the gene TRB3, was found to be an NF- κ B-inducible protein (Wu et al., 2003). Over-expression of this protein inhibited NF- κ B-dependent transcription induced by TNF- α stimulation. *In vitro* assay studies indicated that the TRB3 protein interacted with the NF- κ B transactivator p65 and inhibited phosphorylation of p65, which has been shown to regulate NF- κ B activation. The TRB3 protein has also been associated with the sensitisation of cells to apoptosis induced by TNF- α and its related apoptosis inducing ligand. This mechanism

occurs through inhibited expression of NF- κ B activated anti-apoptotic genes. Therefore, it is suggested that TRB3 is involved in a negative feedback control pathway. However, this same study suggested that while TRB3 inhibits NF- κ B-dependent transcription, it does not inhibit translocation of NF- κ B and its DNA binding ability. These findings illustrate the first human genetic clue for TRB3 and its relevance to chronic inflammatory diseases.

TRB3 is involved with the binding of the kinase domain of AKT, a kinase which plays a key role in a range of cellular functions including cell division, apoptosis, and cellular activation. The physiological relevance of this interaction is supported by findings that TRB3 expression is induced in a normal liver following fasting, and that TRB3 levels are significantly higher in the liver of diabetic mice than in the liver of wild-type mice. TRB3 may serve as a molecular target for peroxisome proliferator-activated receptor alpha (PPAR- α), a protein which is activated by fasting (Koo et al., 2004). However, the findings of these results have conflicted with other experiments and these discrepancies may be based on over expression of either TRB3 messenger RNA or proteins (Lynedjian et al., 2004). These inconsistencies provide evidence that the relative level of TRB3 expression compared with its binding partners is critical in the metabolism of glucose. It is also significant to note that TRB3, in amounts comparable to those of diabetic mice, induced glucose intolerance and hyperglycemia (Du et al., 2003). Ethanol has also been found as an inducer of plasma TRB3 protein levels in other studies (He Ling et al., 2006). Based on data from the same investigation, ethanol-fed rats show decreased levels of membrane associated AKT, increased plasma AKT levels, and elevated TRB3 in the plasma. When RNA interference (RNAi) suppressed TRB3 expression, more than half of insulin stimulation was restored in the presence of ethanol. This suggests that over expression of TRB3 in liver increases glucose production and that knockdown of TRB3 by RNAi improves glucose tolerance. Schwarzer and colleagues showed that glucose or amino acid starvation induces TRB3 expression that is not dependent on AKT activity (Schwarzer et al., 2005). This study also exemplifies that overexpressed TRB3 protects cells from starvation-mediated apoptosis in HeLa cells. In a separate study, a polymorphism in the human TRB3 was shown to impact on AKT activation in HepG2 cells that are associated with insulin resistance and cardiovascular risk (Prudente et al., 2005).

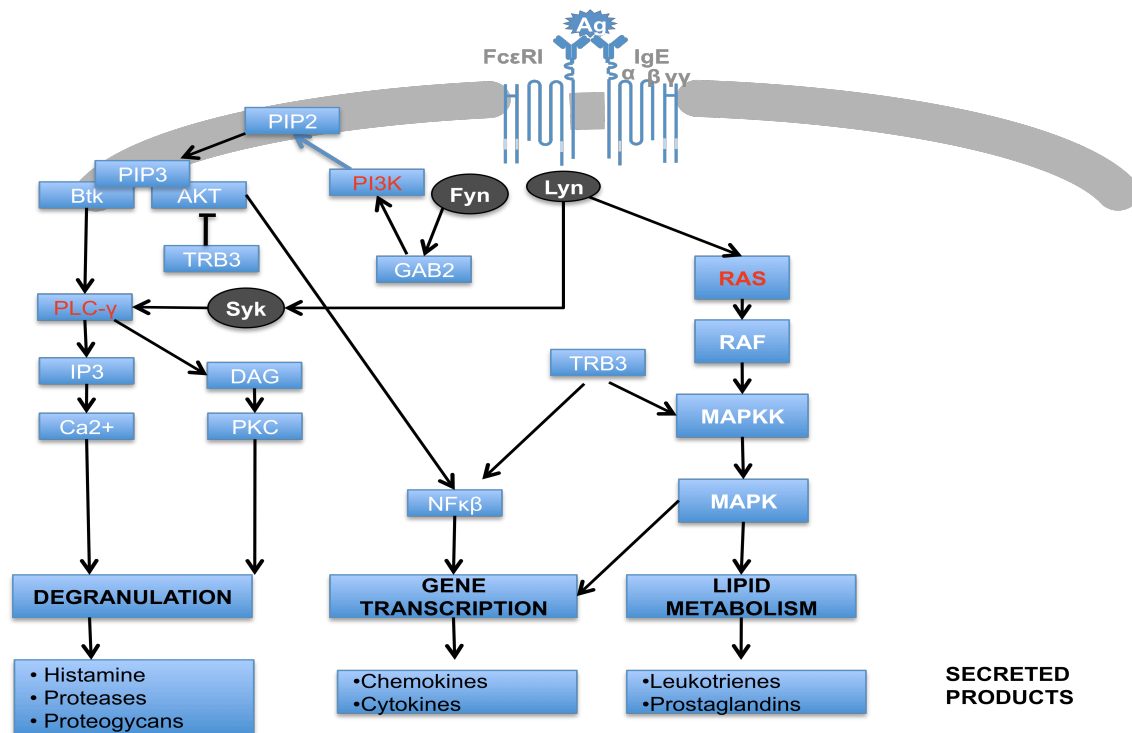


Figure 4. Simplified model of FcεR1-mediated signaling events.

Cross-linking of FcεR1 -bound IgE with bi- or multivalent antigen activates Lyn and Fyn. Lyn in turn phosphorylates the ITAMS in FcεR1 and activates Syk. Lyn, Fyn and Syk phosphorylate many adaptor molecules and enzymes, thereby regulating the activation of the Ras-MAPK, PLC-γ and PI3K pathways leading to degranulation, lipid metabolism and gene transcription of protein mediators.

1.2. Chemokines, signaling and regulation

Numerous studies have demonstrated that chemokines control the activation and recruitment of many immune cells, including mast cells, during an allergic response. Mast cells are able to migrate towards a diverse range of chemokines through chemokine receptors expressed on the mast cell surface. The following sections discuss chemokines, signaling events and regulation of these events.

1.2.1 Chemokine and chemokine receptors

In the 1990's chemokine research groups raced to discover novel chemokines and chemokine receptors. However, two fundamental observations about T cells suddenly made chemokines attractive to immunologists and virologists. The first observation showed that several chemokines inhibit the infection of CD4⁺ T cells by human immunodeficiency virus (HIV)-1 (Cocchi et al., 1995); the second profound observation was that T cells can express multiple chemokine receptors and their expression and responsiveness is regulated after differentiation or activation (Loetscher et al., 1996; Sallusto et al., 1997; Sallusto et al., 1998). Thereafter, the chemokine field expanded immensely, and fundamental questions about the trafficking of leukocytes that induce inflammation were answered in very rapid succession.

Chemokines are a super family of low molecular weight (8-17 kilo Daltons (kDa)), secreted proteins (Borish et al., 2003; Alcamì, 2003). Accumulating evidence now suggests that chemokines act as more than simple chemoattractant molecules in inflammation, and are important regulators in development, homeostasis and pathophysiological processes associated with viral infections, immune responses (Ono et al., 2003) and the mobilization of progenitors to the bone marrow (Pitchford et al., 2009). Chemokines are expressed in a range of cells including resident tissue cells, resident and recruited leukocytes, which include mast cells, macrophages, monocytes and endothelial cells.

Chemokines are thought to have derived from 3 ancestral genes, and members of the chemokine superfamily are divided into four major groups based on the number and spacing of conserved N-terminal cysteine residues. The CC chemokines (or β

chemokines) and CXC chemokines (also known as α chemokines) have four cysteine residues located in closely homologous positions within their amino acid sequence, and are the two most extensively characterised chemokine groups. In the CC chemokines the first two cysteine residues are adjacent, whereas for the CXC chemokines the first two cysteines are separated by a single amino acid (designated X). A third family, the C chemokines has only two cysteine residues and lacks the first and third cysteine residue and contains only one chemokine, lymphotactin. The final chemokine family, CX3C has three amino acids separating the first two cysteine residues and a lectin domain, which attaches it to the cell, and consists of the only chemokine Fractalkine. Over 50 different chemokines have been discovered to date and they carry out their functions via 19 chemokine receptors. Although there is a limited overall sequence homology between the chemokines they are grouped within a family because they have a similar 3-dimensional structure, which is composed of a monomeric fold generated by a floppy N-terminus, which is essential for receptor activation, a C-terminal α helix and 3 internal β strands (Alexander et al., 2002).

Chemokines are recognised by G- protein couple receptors (GPCRs), a large group of receptors that bind a diverse range of molecules, including chemokines, complement components, neurotransmitters and bioactive amines. GPCRs are seven transmembrane spanning receptors, which are coupled to heterotrimeric G-proteins. These 40 kDa receptors approximately 350 amino acids in length possess an extracellular domain consisting of three extracellular loops and a short N-terminus that act together to bind the chemokine ligand. The intracellular domain of the receptor is composed of three loops and a short C-terminus, which act together to transduce the chemokine signal via a conserved DRYLAV motif in the second intracellular loop. The C-terminus possesses several serine and threonine residues, which are phosphorylated during receptor occupancy. The lack of movement within the lipid bilayer is provided by the presence of a disulphide bridge between extracellular loops one and two, and a pocket generated between the N-terminal tail and extracellular loop 3 allows for the formation of a ligand-binding domain.

Each chemokine family associates with a reciprocal family of receptors such that to date there are 11 CCR, 5 CXC receptors (CXCR), 1C receptor and 1 CX3CR receptor. The chemokine receptor family exhibits a high degree of redundancy, with

ten of the chemokine receptors being able to bind two or more chemokines, thereby conferring an enormous versatility on the chemokine system. An example of this redundancy is shown by CCR1, which can bind chemokines Mip-1 α , RANTES, MCP-2 and MCP-3. Several chemokines are also able to activate more than one chemokine receptor, such as RANTES, which can bind CCR1, CCR3 and CCR5.

Chemokine receptor expression is unique to each leukocyte subtype and can vary according to the stage of differentiation and activation of the cell. Mast cells have the potential to express several chemokine receptors which include CCR1, CCR3, CCR4, CCR5, CXCR2 and CXCR4, but their precise receptor profiles can vary in response to their state of differentiation and which tissue they home and reside in (Ono et al., 2003). For example in BMMCs, CCR1, CCR2, CCR3, CCR4 and CCR5 transcripts have been detected in SCF-treated cells, while mast cells isolated from various mouse strains suggest that CCR1, CCR2, CCR3 and CCR6 are expressed on activation of mast cells (Oliveira and Lukacs, 2001; Ono et al., 2003).

The involvement of chemokine receptors in disease makes them ideal candidates for therapeutic intervention. The internalization and intracellular trafficking of chemokine receptors have important implications for the cellular responses elicited by chemokine receptors. In the absence of ligand chemokine receptors undergo a basal level of internalization, degradation or recycling. Ligand binding to GPCR can greatly enhance the internalization and hence trafficking of GPCR. Clathrin-mediated pathway is the major pathway by which chemokine receptors are internalized, but some receptors may utilize caveolae-dependent internalization and lipid rafts routes.

A major mechanism by which GPCR undergo ligand-induced internalization is through clathrin-mediated endocytosis (Vila-Coro et al., 1999; Venkatesan et al., 2003). Ligand binding induces phosphorylation of Serine and Threonine residues in the intracellular loops and carboxyl-terminus of the chemokine receptor by G protein-coupled receptor kinases (GRKs) (Ferguson et al., 1998; Krupnick et al., 1998). Phosphorylation results in 1) the uncoupling of the G protein subunits from the receptor and 2) receptor desensitisation in some cases. In addition, the phosphorylation of these residues are important for the recruitment of adaptor molecules that link the receptor to a lattice of clathrin that mediates receptor internalization. Two adaptor molecules that play important roles in chemokine

receptor internalization are adaptin 2 (AP-2) and β -arrestin. The involvement of receptors with these adaptor molecules results in recruitment of clathrin and formation of clathrin-coated pits which cleave off from the membrane via dynamin and become clathrin-coated vesicles (Barlic et al., 1999; Droese et al., 2004; Orsini et al., 1999). Thereafter, the clathrin-coated vesicle is uncoated and the receptor-ligand complex enters the early endosomal compartment. The chemokine receptor can then 1) enter the perinuclear recycling compartment and traffic back to the plasma membrane to be re-exposed to its corresponding ligand 2) or it can enter the late endosomal compartment where it will be organised to the lysosomal compartment for degradation.

1.2.2 Chemokine signaling through GPCR

Chemokine receptor signaling constitutes a highly complex interplay of intracellular signaling events triggered by dimerisation of the chemokine receptor and the subsequent recruitment of Gi proteins, which upon dissociation act on a number of key effectors.

Chemokine signal transduction was first studied using human neutrophils. The data suggested that IL-8 exhibited the same pattern of responses as other attractants such as the complement fragment C5a and N-formyl-methionyl peptides (fMLP). *Bordetella pertussis* toxin, which inactivates Gi proteins, 17-hydroxywortmannin (wortmannin), later found to block PI3K, and the PKC inhibitor staurosporin inhibited responses to IL-8 (Thelen, et al., 1988). Subsequent studies using such inhibitors showed that all chemokines act on the same class of receptors and induce a common signal transduction cascade.

The effects of chemokines are mediated by GPCR, one of the largest families in the human genome, of which more than 800 sequences have been identified (Fredriksson et al., 2003). In the immune system GPCRs play a fundamental role in innate, adaptive and pathological responses, for example, in allergic diseases such as asthma characterised by chronic inflammation, chemokines secreted by lung resident cells e.g. bronchial epithelial cells and, maybe mast cells, recruit eosinophils and neutrophils (Gonzalo et al., 2007; Thomas et al., 2007). Over 60% of all pharmaceutical agents currently in use target GPCRs for the treatment of several diseases including allergic diseases such as asthma (Pierce et al., 2002).

The primary signal transducer used by GPCRs is the heterotrimeric G protein, which consists of α , β and γ subunits (Gilman 1987). In the absence of receptor ligand, these subunits co-exist as one complex in which the α subunit is bound to GDP. The α subunit consists of 4 major subfamilies, α_i , α_s , α_q and $\alpha_{12/13}$, which are encoded by 20 α genes (Gutkind et al., 1998). Activation of the chemokine receptor by its ligand results in the dissociation of the receptor-bound heterotrimeric G protein into guanosine triphosphate (GTP)-bound α_i subunit and $\beta\gamma$ subunit. Each of these free activated subunits can now independently interact with distinct downstream effector molecules, inducing a diverse range of cellular responses (Figure 5), which include actin cytoskeletal rearrangements, cell movement and gene transcription (Marinissen et al., 2001; Marinissen and Gutkind, 2001). In addition, chemokine receptor signaling can also induce events such as mast cell degranulation.

$G\beta\gamma$ is particularly important, as it activates two signaling pathways. One of these involves PLC and the other involves PI3K. PLC results in the generation of two messengers IP3 and DAG. As previously described IP3 further mobilises calcium from intracellular stores, which along with adenylyl cyclase inhibition results in the calcium fluxes required for degranulation. DAG activates various isoforms of PKC, which activate a series of signal transduction events within the cell. PI3K is the other key effector activated by $G\beta\gamma$ (Curnock and Ward, 2003). Its activation results in the generation of lipid mediators which act as crucial secondary messengers for various downstream effectors including PKC, Rho GTPase and Ras pathways (Weiner et al., 2002). Chemokine ligand binding also activates the MAPK cascade, which activates various cytoskeletal elements.

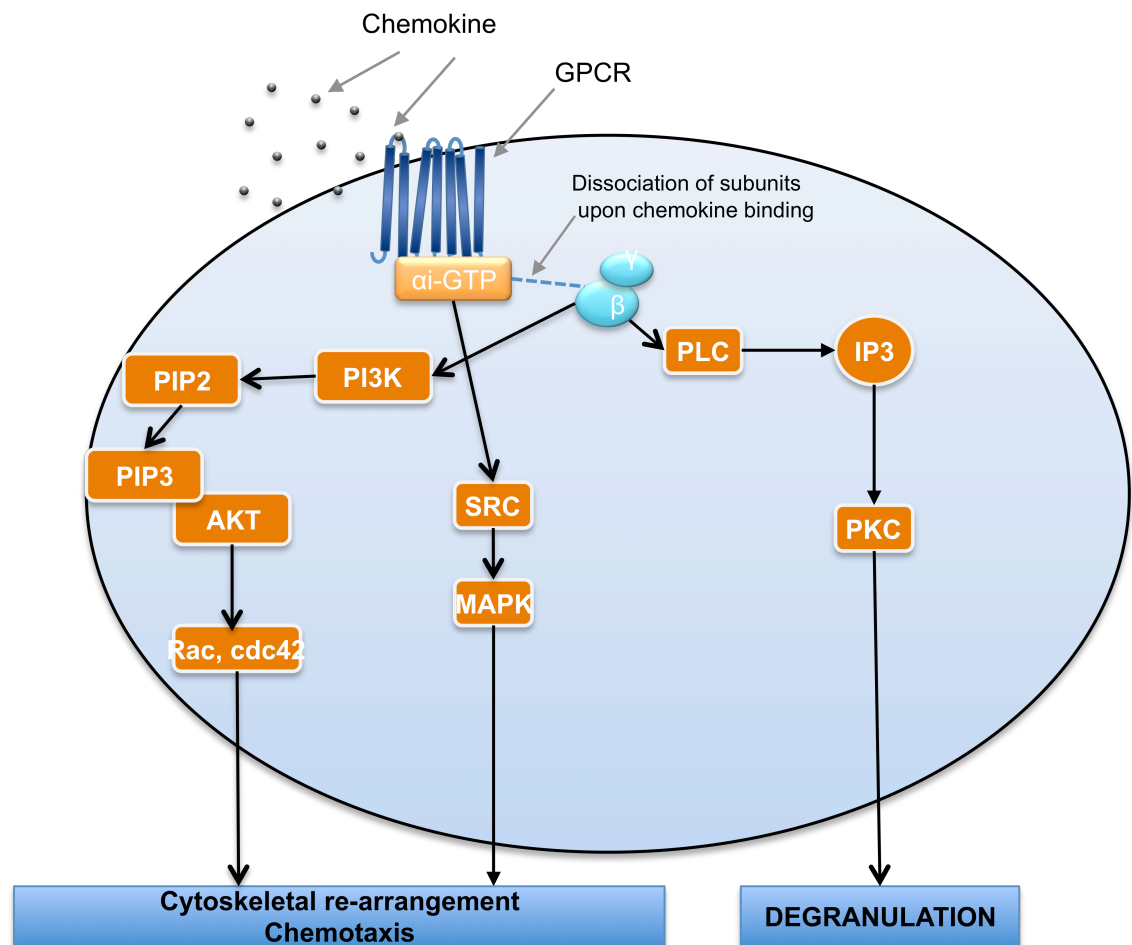


Figure 5. Simplified model of GPCR-mediated signaling events.

Chemokine binding to GPCR induces dissociation of $G\beta\gamma$ complex into $G\alpha$ and $G\beta\gamma$ subunits. These subunits are then free to activate various downstream effector molecules leading to cytoskeletal re-arrangements, chemotaxis and degranulation.

Cross talk between GPCR signaling pathways, such as those for chemokine receptors, has been widely demonstrated (Hur and Kim, 2002). Several studies, which have focused on the regulation of leukocyte trafficking, have shown that cross talk between chemokine receptors and non-GPCRs alters chemotaxis by modulating chemokine expression. An example of this is described by Fan and Malik (2003) who describe receptor cross-talk between TLR4 and CXCR2 in polymorphonuclear leukocytes. Co-stimulation of TLR4 and CXCR2 receptors with MCP-1 and LPS, significantly reduced chemokine receptor internalisation resulting in the augmentation of a migratory response. Parker et al. (2004) found that stimulation of TLR2 and TLR4 in human monocytes resulted in down regulation of CCR1 and CCR2, with CCR1 being down regulated in an autocrine manner through the enhanced production of Mip-1 α . In mast cells, CCR3 has been shown to rapidly locate to the cell surface from intracellular granules upon stimulation of Fc ϵ R1 by IgE/antigen (Price et al., 2003). In a study on RBL-2H3 cells similar stimulation of Fc ϵ R1 resulted in the up-regulation of the GPCR, Sphingosine-1-phosphate (S1P), which is required for enhanced mast cell degranulation. Hence, the activation of non GPCRs, such as Fc ϵ R1 and the TLRs, have clearly been shown to have profound effects on chemokine receptor expression, and there is evidence to suggest that changes in receptor expression may potentially play a role in the co-stimulatory effect of Mip-1 α on Fc ϵ R1 -mediated degranulation in mast cells.

1.2.3 Regulation of GPCR signaling pathways: RGS family

As previously mentioned GPCRs and G-proteins orchestrate a wide variety of signals and their activity is finely tuned by multiple regulatory systems. A crucial regulatory step in the G-protein cycle is the deactivation of G-proteins by GTP hydrolysis, a process that is enhanced by GTPase activating proteins (GAPs). A family of proteins, which function as heterotrimeric G-protein GAPs were identified over 10 years ago in worms and mammals and termed Regulator of G-protein Signaling (RGS) proteins. RGS proteins function to accelerate the GTPase activity of the α subunit, accelerating the return of G α to its inactive guanosine diphosphate (GDP)-bound form thereby inhibiting downstream activity (Figure 6).

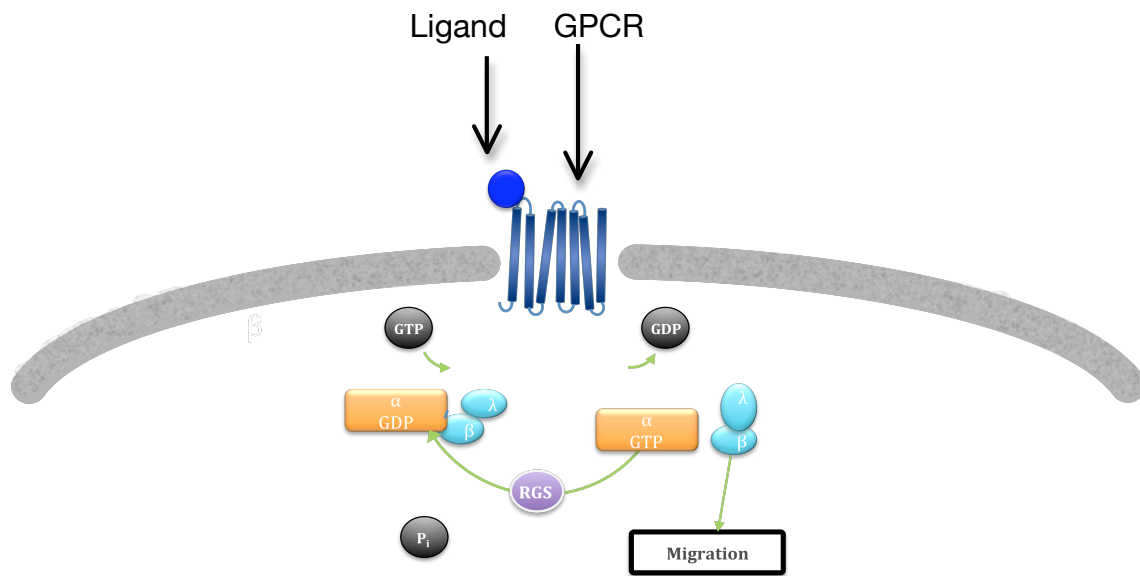


Figure 6. RGS proteins accelerate GTPase activity of the α -subunit, thereby inhibiting downstream events.

In its inactive state the α -subunit is bound to GDP. Upon stimulation (e.g. chemokine) conformational changes in the receptor induce the α subunit to release GDP and bind GTP. The binding of GTP causes the α -subunit to detach from the $\beta\gamma$ -sub unit, thereby allowing them to independently interact with effector molecules associated with cell processes such as migration. G-protein signaling is terminated when the α -subunit hydrolyzes GTP to GDP, which causes re-association to the $\beta\gamma$ -subunit. RGS proteins accelerate GTPase activity of the α -subunit, thereby inhibiting down stream signaling.

Each RGS protein contains a RGS box, which consists of a 120 amino acid domain that is responsible for GAP activity. Based on RGS domain homology and accessory domains, these genes can be divided into eight sub-families: A or RZ; B or R4; C or R7; D or R12; E; RA: F or GEF; G or GRK and H or SNX. The combination of these domains ultimately creates highly regulated multi-functional proteins, capable of conducting complex signaling tasks. RGS proteins can up-regulate GTPase activity up to 1000-fold (Posner et al., 1999). Moreover, RGS domains also serve as scaffolds by promoting rapid cycling of G α subunits between active and inactive states (Willard et al., 2007; Zhong et al., 2003) or effector antagonists by competitively binding activated G α subunits or effector enzymes (Roy et al., 2006; Schoeber et al., 2006).

As previously mentioned Fc ϵ R1 mediated signaling in mast cells induces Syk activation, which in turn recruits and activates PI3K, PLC γ and MAPK. Accumulating evidence indicates PI3K plays an essential role in mast cell homeostasis and allergic responses (Fukao et al., 2002). Mast cells from mice expressing the inactive PI3K subunit p110 δ have profoundly less antigen-induced degranulation (Ali et al., 2004). GPCRs may increase IgE mediated responses or induce mast cell activation alone. Moreover, a study by Laffargue et al. (2002) demonstrated that PI3K γ -deficient mast cells disrupt GPCR- mediated amplification of Fc ϵ R1-mediated degranulation, indicating that PI3K γ is a requirement for GPCR signaling and is a modulator of the allergic signaling pathway. The ability of wortmannin, a non-specific PI3K inhibitor, to block C3a-induced expression of the chemokine, CCL2 in human mast cells suggests a role for PI3K in GPCR-mediated responses in mast cells (Venkatesha et al., 2005). For these reasons it is therefore not surprising that researchers have now started to investigate RGS proteins as regulators of mast cell- driven inflammation induced by GPCRs.

Recent studies have unveiled RGS13 as a new signaling molecule, which may affect the intrinsic reactivity of mast cells to allergens. Bansal and co-workers (2008) established RGS13-deficient mice with Lac Z knock-in. Both immuno-fluorescent and β -galactosidase staining of cultured BMMCs and tissues showed that RGS13 is expressed in murine mast cells. In addition they found that RGS13 deficient mice had significantly increased IgE-mediated anaphylactic responses due to increased mast cell degranulation. Further experiments reconstituting RGS13-deficient BMMCs with RGS13 or over expression of RGS13 in wild type

BMMCs inhibited antigen-induced degranulation. This data suggests that the abnormality observed in RGS13 deficient mast cells was due to the absence of RGS13.

In addition, Bansal and co-workers (2008) characterized how RGS13 affects GPCR-mediated functions of human mast cells *in vitro*. They examined human mast cell lines, HMC-1 and LAD2, depleted of RGS13 by siRNA or short hairpin RNA and HMC-1 cells over-expressing RGS13. The results demonstrated that RGS13 knockdown in LAD2 cells induced increased degranulation in response to S1P, but not to IgE-Ag or C3a. Compared to wild-type cells, cells stably expressing RGS13 short hairpin RNA had enhanced Ca^{2+} mobilization in response to adenosine, C5a, S1P (GPCR ligands), and stromal cell-derived factor-1 (SDF-1). In addition compared with control cells, AKT phosphorylation, chemotaxis, and IL-8 secretion induced by CXCL12 were also up-regulated in short hairpin RGS13-HMC-1 cells.

1.3. Regulation of actin cytoskeleton and chemotaxis

Mast cells play a central and well-established role in mediating allergic disease, whilst chemokines control the activation and recruitment of immune cells during inflammation. The chemotaxis of mast cells to sites of inflammation and the subsequent release of pro-inflammatory mediators are crucial to eliciting allergic response. Over the years, by using several cell types including neutrophils and *Dictyostelium discoideum*, a large amount of evidence has contributed to the molecular basis of chemotaxis. However, to date there is limited evidence to understand the molecular mechanisms underlying mast cell chemotaxis. A continuing effort to better understand the molecular basis of mast cell migration during the allergic response will help identify alternative therapies. The following sections describe what is known about the actin cytoskeleton, chemotaxis and the vital components which regulate it.

1.3.1 Actin cytoskeleton and Rho GTPases

The actin cytoskeleton is a highly dynamic network, playing an essential role in numerous biological processes such as cell surface remodelling and motility. Actin filaments (composed of actin monomers), intermediate filaments and microtubules (composed of α and β tubulin) collectively known as the cytoskeleton, are

responsible for the mechanical properties and shapes of cells, which are often critical to their functions. Actin assembly provides a major force in cell motility, in particular by initiating protrusions such as filopodia (spiky protrusions) and lamellipodia (sheet-like protrusions) that propel the leading edge of the cell forward. Accumulating evidence over the past decade has provided a coherent model of how polymerisation of actin filaments can allow cells to migrate. While researchers have identified some of the major players in the formation of structures such as lamellipodia and filopodia, much remains to be elucidated about the mechanism of assembly and dynamics of these structures in actual physiological settings.

Actin powers protrusions of a cell by polymerizing just under the plasma membrane. A cell has two options of actin filament geometry: bundled filaments leading to filopodial spikes or branched filaments leading lamellipodial sheet-like protrusions. Actin filaments are polar because the monomers in the filament all point in the same direction; the positive end (or 'barbed' end) grows more quickly than the negative end (or 'pointed' end). Capping proteins bind to the barbed ends to terminate elongation of the actin filaments. Once the actin filaments are established, they can elongate without help, but there is a strong barrier to initiating or 'nucleating' new filaments. Branched filaments found in lamellipodia are assembled by the actin related proteins (Arp) 2/3 complex. Arp 2/3 complex is a major nucleator of actin polymerisation. Arp 2/3 performs two actions 1) nucleates actin filaments from monomers and 2) binds pointed ends and caps them. This 220kDa assembly consists of seven subunits: Arp2 and Arp3, being similar in structure and sequences to actin and the remaining five subunits, Arp C1-5, being unique and highly conserved in evolution (Machesky and Gould, 1999). Further studies also identified the ability of the Arp2/3 complex to direct formation of 70° branches on the side of pre-existing filaments generating a dendritic array of filaments (Welch et al., 1997; Mullins et al., 1998, Pollard, 2007). These branches are identical to those observed in electron micrographs of the leading edge of rapidly motile cells (Svitkina and Borisy, 1998).

Rho GTPases, Rac, Cdc42 and Rho are members of the Ras superfamily of GTP binding proteins which are pivotal and well characterised regulators of the actin cytoskeleton. However, they also contribute to diverse cellular functions, including vesicular trafficking and cell cycle. In mammals, at present there are 20 Rho GTPases, all of which bind GTP and most of which exhibit GTPase activity. Each of these Rho GTPases acts as a binary switch, cycling between an active GTP-bound

form and an inactive GDP-bound state. In the GTP-active form they are able to interact with effector molecules to initiate a downstream signaling response, which mediates actin reorganization. Nucleotide binding status, which determines downstream signaling activity, is tightly controlled by the actions of three groups of proteins: GEFs; GAPs and Rho guanine-nucleotide-dissociation (Rho-GDIs). GEFs increase the active GTP-bound conformation by stimulating release of GDP (Schmidt and Hall, 2002), while GAPs stimulate intrinsic GTPase activity, thereby promoting the inactive GDP-bound conformation (Bernards, 2003) and finally Rho-GDIs, which prevent membrane targeting and interaction with downstream effectors by binding to the C-terminal prenyl group of many Rho GTPases (DerMardirossian and Bokoch, 2005). Rac, Rho and Cdc42 control signal transduction through distinct pathways that link membrane receptors to coordination of the cytoskeleton and adhesion complexes (Figure 7). Signal integration and crosstalk exist between Rho GTPases and PI3K mediated signaling pathways, whereby both Rac and Rho are activated downstream of phosphoinositide signaling, and the activity of several GAPs and GEFs are regulated by PI(3,4,5)P₃ binding (Bishop and Hall, 2000; Etienne-Manneville and Hall, 2002; Ridley, 2006).

Rac 1 mediates the formation of lamellipodia (Ridley et al., 1992). These thin protrusive sheets can lift up and fold backwards at the leading edge, giving rise to membrane ruffles. Activation of Cdc42 produces microspikes including filopodia. These are finger-like projections consisting of actin filament bundles (Bishop and Hall, 2000), which act as sensors to explore the microenvironment of the cell, but are not considered essential for chemotaxis. Rho A regulates the generation of stress fibers and focal adhesions (Ridley and Hall, 1992).

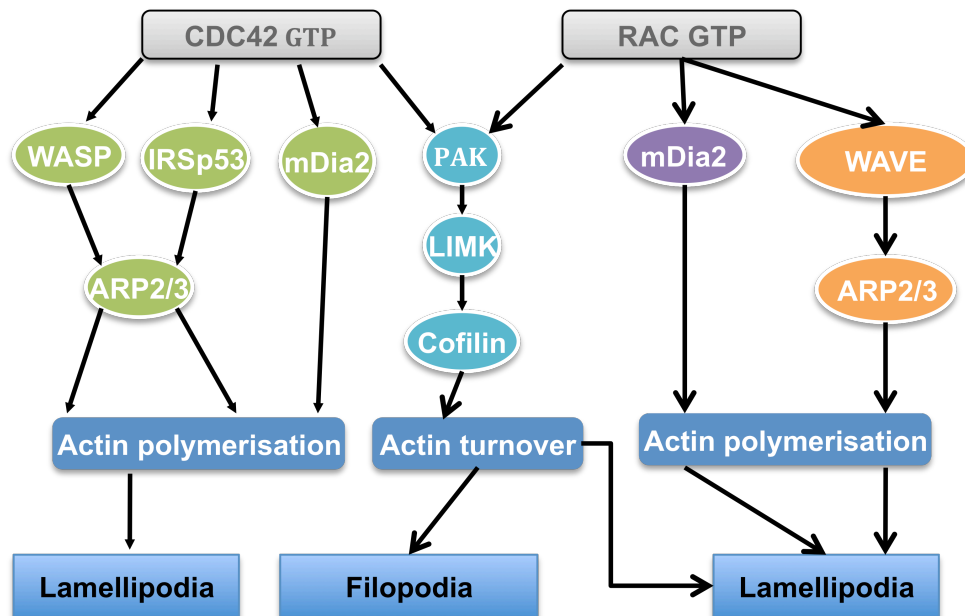


Figure 7. The formation of lamellipodia and filopodia by RAC and Cdc42 signaling pathways.

The highly dynamic lamellipodium, at the leading edge of the cell is extended by ARP2/3. Rac activates actin polymerisation during lamellipodium formation through the WAVE complex, which in turn activates ARP2/3, and mDia2, which nucleates unbranched actin filaments. Filopodia are thin protrusions that contain parallel bundles of actin filaments that extend from the leading edge of the cell, which probably function as sensory probes. CDC42 induces actin polymerization by binding to WASP, IRSp53 to Induce branched actin filaments using the ARP2/3 complex. CDC42 and Rac also induce actin polymerization by activation of mDia2. CDC42-mediated or Rac-mediated activation of the PAK phosphorylates LIMK, which phosphorylates and inhibits cofilin, thereby regulating actin-filament turnover.

KEY: ARP2/3= actin-related protein-2/3. WASP= Wiskott–Aldrich syndrome protein. WAVE=WASP-family verprolin-homologous protein. mdia2= mammalian diaphanous-2. IRSp53= insulin-receptor substrate p53. PAK= p21-activated kinase. LIMK= LIM kinase.

1.3.2 WASP: a component of actin assembly

Wiskott–Aldrich syndrome protein (WASP) was the first identified member of a family of actin regulators, a key adaptor protein that connects multiple signaling pathways to filamentous actin (F-actin) polymerization, a process essential for chemotaxis. The WASP family consists of two principal subfamilies: WASP and WASP family verprolin homologous protein (WAVES). Although WASP expression is confined to haematopoietic cell lineages, neural WASP (N-WASP) and WAVE1, WAVE2 and WAVE3 are more widely expressed. The importance of WASP-mediated cytoskeletal regulation in haematopoietic cells is shown by the human disease, Wiskott–Aldrich syndrome (WAS). These defects are caused by mutations in the *WAS* gene encoding WASP. Classical WAS is an X-linked primary immunodeficiency that is characterized by easy bruising and prolonged bleeding, eczema, low numbers of small platelets, and recurrent infections (Sullivan et al., 1994).

WASP and WAVES are the main activators of Arp2/3 complex (Millard et al., 2004). Upon activation these proteins induce numerous actin based structures, such as lamellipodia and filopodia. In addition to these structural roles, emerging data implicate other roles, which include cell-substrate adhesion (Ibarra et al., 2006) and cytokinesis (Pollitt and Insall, 2008). WASP is present throughout evolutionary history, and homologues have been identified in many eukaryotes from yeast to mammals. Mammals typically possess two WASPs, WASP and N-WASP, and three other WAVE proteins. Other members of the WASP family which have been identified are WASH (Linardopoulou et al., 2007), WASP homolog associated with *actin*, membranes, and microtubules (WHAMM) (Campellone et al., 2008) and JMY (Zuchero et al., 2009), however, at present very little is known about their physiological roles.

The closest homologue to WASP is N-WASP. Both are structurally and functionally very similar, and in many *in vitro* assays one protein can be substituted for the other. WASP is hematopoietic-specific (Derry et al., 1994), whereas N-WASP is ubiquitously expressed (Miki et al., 1996). Both WASP and N-WASP are characterised by a conserved domain arrangement: Ena-Vasp homology domain (EVH1), also known as the WASP homology domain-1 (WH1), a proline-rich domain, a Cdc42/Rac GTPase binding domain (GBD), a G-actin binding verprolin

homology (V) domain, a cofilin homology(C) domain and a C-terminal acidic (A) segment.

In resting cells, WASP and N-WASP exist in an auto-inhibited inactive conformation; this auto inhibition is released by the binding of Cdc42 and PI(4,5)P2 (Kim et al., 2000). The C-terminus is responsible for binding to and activating the Arp 2/3 complex, it consists of one or two WH2 domains, which bind monomeric actin, followed by a short central region and acidic region which interacts with the Arp2/3 complex, resulting in actin nucleation (Higgs and Pollard, 1999). G-actin binds to the V domain (Higgs and Pollard, 2000). Binding of N-WASP to Cdc42 induces a conformational change allowing its VCA domain to interact with the Arp2/3 complex resulting in actin assembly, and this is further enhanced by PI(4,5)P2 (Higgs and Pollard, 2000; Rohatgi et al., 1999). A proline-rich region provides potential sites for the binding of various SH3 domain containing proteins. Tyrosine phosphorylation of WASP increases its capacity to activate Arp 2/3 complex without the need of Cdc42 or PI(4,5)P2. Moreover serine/threonine phosphorylation can induce actin polymerisation *in vitro* (Cory et al., 2003). Interaction between the WH1 domain with the WASP-interacting protein (WIP) is thought to suppress the activity of WASP or N-WASP (Ramesh et al., 1997).

1.3.3 Cell migration, chemotaxis and cell polarity

Cell migration is a highly complex orchestrated process that is crucial for a range of biological processes in animals, which include immune surveillance, wound healing and embryonic morphogenesis (Raja et al., 2007). Cell migration can be divided into distinct stages. Firstly, a cell must adhere to its surrounding environment and establish directionality. In the presence of a chemotactic agent, this requires that cells sense the direction of the chemical gradient in order to establish polarity. In the absence of chemoattractant, polarization maybe induced through changes in receptor occupancy (Lauffenburger and Horwitz, 1996). Once directionality is achieved, the leading edge of the cell composed of lamellipodia (and maybe filopodia) propels the cell forward. Adhesive contacts are formed at the front of the cell, along with simultaneous cell retraction, actin disassembly and detachment of adhesions at the rear of the cell.

Researchers have extensively studied the underlying mechanisms of migration *in vitro* and *in vivo*, using a diverse range of cell types and model systems. These

include leukocytes which migrate during immune surveillance and accumulate at sites of inflammation, slower moving fibroblasts which migrate during wound healing, the body of a mouse, in which the development of an immune response and interactions of T and B cells can be monitored in real time and, more recently, following recruitment of lymphocytes to lymph nodes or movement of tumor cells in the whole animal using fluorescence imaging techniques (Miller et al., 2002; Sahai 2007; Zinselmeyer et al., 2008).

Chemotaxis, the directed movement of cells along an external gradient, is a critical cell biological response. These responses include the aggregation of *Dictyostelium discoideum* to form a multi-cellular organism, neurons finding their way in the developing nervous system and when leukocytes traffic between the vascular and lymphatic systems, and migrate from the blood toward sites of infection. In addition to these roles in normal physiology, inappropriate cell migration is the basis for many pathological conditions including cancer metastasis and chronic inflammatory diseases such as asthma and arthritis.

Chemotaxis involves production and degradation of PI(3,4,5)P₃ at the plasma membrane, generating a net accumulation at the leading edge of the cell. This ultimately drives actin polymerisation and directional cell movement, hence when cells undergo chemotaxis they must first acquire spatial asymmetry in order that generated forces within can be turned into productive forward movement. Abundant data indicate that both PI3Ks, their lipid products PI(3,4,5)P₃ and Rho GTPases affect cell polarization, although their contributions appear to be highly dependent on cell type (Parent and Devreotes, 1999; Rickert et al., 2000; Chung et al., 2001; Ward, 2004). Interestingly, studies indicate cell polarization, and therefore chemotaxis is not a consequence of preferential localization of chemoattractant receptors at the leading edge, instead receptor localization remains uniformly distributed around the plasma membrane as demonstrated in neutrophils and *Dictyostelium discoideum* cells (Servant et al., 1999; Xiao et al., 1997).

The generation of PI(3,4,5)P₃ at the plasma membrane, provides docking sites for the recruitment of many pleckstrin homology (PH) domain containing signal transduction molecules involved in cytoskeletal organisation and cell survival. PH domains are protein modules of approximately 120 amino acids found in more than 150 proteins, which bind phospholipids with high affinity and specificity (Lemmon

et al., 2002). Tandem PH domain-containing protein 1 (Tapp-1) is specific for PI(4,5)P₂, whereas other PH domains from AKT, Btk and Gab-2 have been shown to be highly specific for PI(3,4,5)P₃ (Harriague and Bismuth G, 2002; Costello et al., 2002). Mutant PH domains are unable to bind PI(4,5)P₂ or PI(3,4,5)P₃ and do not translocate to the plasma membrane in response to PI3K activation (Funamoto et al., 2001). In unstimulated cells levels of PI(4,5)P₂ and PI(3,4,5)P₃ are almost undetectable, however levels rise rapidly within 10 seconds of stimulation with chemoattractant (Stephens et al., 1991).

When *Dictyostelium discoideum* cells are exposed to a chemoattractant gradient PI3Ks bind to the membrane at the front, PI(3,4,5)P₃ selectively accumulates at the leading edge, and new F-actin-filled pseudopodia are extended at corresponding sites (Chen et al., 2003). This role for PI(3,4,5)P₃ in polarity and directional sensing has been demonstrated in other cell types such as *Drosophila melanogaster* hemocytes, human neutrophils and fibroblasts, neurons, and a variety of embryonic cells (Wang et al., 2002; Chadborn et al., 2006). An invaluable tool in investigating the involvement of PI(3,4,5)P₃ signaling in gradient sensing and polarity has been the use of green fluorescent protein (GFP) fused to the PH domains of proteins such as AKT, which bind preferentially to PI(3,4,5)P₃ over PI(4,5)P₂. As PI(3,4,5)P₃ represents the major lipid products of class I PI3Ks, these probes have been utilised to investigate sites of cellular PI3K activity (Costello et al., 2002). The GFP-AKT-PH domain probe is uniformly distributed throughout un-stimulated *Dictyostelium discoideum* and fibroblasts, however after exposure to different chemoattractant stimuli the probe is recruited selectively to the membrane at the leading edge (Merlot and Firtel, 2003). In human neutrophils, the translocation of the probe from the cytoplasm to the plasma membrane when exposed to a uniform concentration of chemoattractant was rapid and transient, reaching a maximum accumulation by 30 seconds and decreasing over the ensuing two minutes (Servant et al., 2000), indicating that PI3K functions at the leading edge of the cell to mediate chemotaxis by using PI(3,4,5)P₃ as a crucial secondary messenger.

In leukocytes, both PI3K γ and PI3K δ isoforms have been implicated in asymmetric PI(3,4,5)P₃ accumulation at the leading edge, for example, p110 δ kinase-dead knock-in-macrophages or p110 γ knockout neutrophils do not demonstrate PI(3,4,5)P₃ accumulation and moreover are defective in polarization in response to colony stimulating factor (CSF)-1 and fMLP respectively (Sadhu et al., 2003;

Papakonstanti et al., 2007). Recent work indicates that the importance of PI3K in leukocyte chemotaxis is also dependent on the substrate on which cells are migrating. Ferguson et al., (2007) demonstrated that although accumulation of PI(3,4,5)P3 and F-actin at the leading edge of chemotactically stimulated p110 γ ^{-/-} mouse neutrophils was perturbed, interestingly cells were able to chemotax normally on selected surfaces.

1.3.4 Imaging cell migration

When analysing cell migration, the major starting point is to characterise the behavior of cells, by taking images of shape change, persistence of movement and direction and the dynamics of actin structures such as the extension and retraction of lamellipodia, pseudopods, filopodia and membrane ruffling. These investigations have been conducted by making use of light microscopy methods, especially wide-field microscopy in either Nomarski Interference Contrast or phase contrast settings. Images are recorded and collected by charge-coupled device (CCD) cameras as simple sections or Z-stacks. These time series images then have to be analysed using appropriate software. Alternatively, a vast amount of knowledge of the internal structure and organisation of cells comes from the investigation of fixed cells or tissue specimens, followed by detailed imaging using a combination of light, confocal and electron microscopic techniques. These studies have provided a thorough understanding of the fundamental cytoskeletal components and their architecture during cell migration. Moreover, in order to acquire a detailed understanding of the spatio-temporal control of the cytoskeleton, researchers have made use of GFP tagged cytoskeletal components possessing different spectral properties. The methods described above work well for investigating cell migration provided that there is high enough contrast in the images and that the data is such that the cells do not move out of the area of interest between data points.

In 1888, Leber made the first observation of leukocyte chemotaxis in excised corneal tissues or rabbits; however, it was not until 30 years later that the first *in vitro* assays of chemotaxis were developed. These early assays assessed migration on coverslips or in capillary tubes. Although these systems established whether a substance was chemotactic, it was not possible to provide quantifiable data. In 1962, a quantitative method was developed by Boyden, who developed what is now known to most researchers as the Boyden chamber, a milestone in the study of chemotaxis, and moreover the basis of many chemotaxis assays.

In the Boyden system, a porous membrane separates 2 chambers. Cells are placed in one chamber, whilst the chemotactic agent is placed in another, allowing chemotaxis of the cells across the membrane. Various techniques can then be implemented to quantify the number of migrating cells, including microscopy and enzymatic techniques. This system offers many advantages, including ease of use, the ability to examine chemotaxis and the ability to quickly screen various compounds at many concentrations. However, the design of this system is limiting in that the speed of cell migration and the paths the cells adopt cannot be determined, real-time observations are not possible, and very sharp chemoattractant gradients are formed.

1.4 Hypothesis and aims of this thesis

Former studies by Ono and co-workers (Toda et al., 2004; Miyazaki et al., 2005; Nifidra et al., 2010) found that co-engagement of FcεR1 and CCR1 resulted in 1) synergistically enhanced degranulation in *ex vivo* mast cells and RBL-CCR1 cells, 2) inhibited Mip-1α induced chemotaxis of RBL-CCR1 cells, and 3) enhanced production of pro-inflammatory molecules, indicating that this response was facilitated by cross-talk between FcεR1 and CCR1-mediated signaling pathways. In addition, subsequent studies (Ono and Aye unpublished data) found that the gene expression of regulatory molecules RGS1 and TRB3 downstream of FcεR1 and CCR1 signaling, were significantly increased in RBL-CCR1 cells following FcεR1 and CCR1 co-engagement. It has therefore been proposed that co-engagement of FcεR1 and CCR1 affects mast events other than degranulation and these data indicate cross-talk between CCR1 and FcεR1 signaling pathways.

Based on current knowledge, the hypothesis of this thesis is that mast cell functions can be differentially regulated in response to co-stimulation by IgE/allergen and chemokine.

To address this hypothesis, the specific aims of this thesis were as follows: -

1. To further analyse whether and how simultaneous engagement of FcεR1 and CCR1 may affect mast cell migration and elucidate the molecular mechanisms involved
2. To analyse the roles of regulatory signaling molecules, RGS1 and TRB3 in mast cell degranulation, chemotaxis and mediator release.

The data obtained from this thesis may contribute to our understanding of mast cell migration and arrest during an allergic response, which is key to effectively treating allergic diseases.

Chapter 2
Materials and methods

2. Materials and Methods

2.1 Induction of murine allergic conjunctivitis

2.1.1 Mice

For the present study eight-week-old female A/J mice (Harlan, United Kingdom (U.K)) or BALB C mice (Jackson Laboratory, United States of America (US)) were used for allergic conjunctivitis models 1 and 2 respectively. These preferred atopic strains of mice are routinely used to induce allergic models, including allergic conjunctivitis due to their preferential Th2 cell responsiveness to allergen (Gronberg et al., 2003).

2.1.2 Murine models of allergic conjunctivitis

2.1.2.1 Induction of murine allergic conjunctivitis model 1-A/J mice

All procedures were conducted by myself with the aid of ophthalmologist Mr. Tom Flynn, in accordance with the UK government regulations for the care of experimental animals and with the ARVO Statement on the use of animals in ophthalmic and vision research.

Allergic conjunctivitis was induced using the following protocol based on modification of a previously described method by Ohbayashi et al., 2007. A/J mice were sensitized by intraperitoneal injection with 200µg of short ragweed pollen (SRW) (Greer Laboratories, Inc.) and 2mg of aluminum hydroxide (Alum) (Sigma, St. Louis, MO) in 400µl Phosphate Buffer Saline (PBS) (Invitrogen) on days 0, 7 and 14, and by treatment of eye drops containing 500µg SRW with 25µg Alum in 5µl PBS on days 8 and 15. On day 27, the experimental challenge of 500µg SRW in PBS or PBS alone was administered topically to both eyes (Figure 8). Sensitisation over a 15-day period is required for the generation of systemic T-helper 2 responses, and subsequent challenge with topical SRW induces severe allergic conjunctivitis.

Mice were divided into three groups as follows. 1) Naïve mice which were neither sensitized nor challenged, 2) sensitized/challenged mice, these were sensitized and challenged with SRW on day 27 and 3) sensitized/non-challenged mice, which were sensitized and challenged with PBS alone on day 27. Each group contained at least 5 eyes. 3, 6 and 24 hours after the experimental challenge and on diagnosis of allergic conjunctivitis (conducted by ophthalmologist, Mr. Tom Flynn) mice were sacrificed and whole eyes were enucleated from each group. Each eye was embedded in optimal cutting temperature (OCT) compound (Sakura Finetek Europe) and was frozen on a liquid nitrogen-cooled duralumin plate. Specimens were stored at -70°C until for future use. Cryostat serial sections 10µm thick were cut and air-dried for 30 minutes. The sections were fixed by 30% methanol in 100% acetone for 10 minutes at 4°C. Toluidine Blue staining was conducted on conjunctival sections to identify mast cells and their location. In addition, enucleated eyes from each treatment (at least 5 eyes per group) were also processed by Dr. Peter Munro (UCL) for electron microscopy analysis.

2.1.2.2 Induction of murine allergic conjunctivitis model 2- BALB/c mice

All procedures were undertaken by Dr. Ohbayashi at Emory University, Atlanta, U.S. The protocol conformed to all regulations for laboratory animal research outlined by the Animal Welfare Act, NIH guidelines and the ARVO statement regarding the experimental use of animals.

Briefly, BALB/c mice were sensitized by footpad injections with 50µg SRW and 1mg Alum in 25µl PBS into both hind-footpads on day 0, 14 and 28, and by treatment of eye drops containing 1000ug SRW in 5ul PBS into each eye from days 35-39. On day 42, the experimental challenge of 1000 µg SRW in 5ul PBS or PBS alone was administered topically to both eyes (Figure 9).

Mice were divided into 2 groups as follows: 1) Naïve mice which were neither sensitized nor challenged and 2) sensitized/challenged mice, these were sensitized and challenged with SRW on day 42. Each group contained at least 5 eyes.

30 minutes and 24 hours after the experimental challenge, and on diagnosis of allergic conjunctivitis mice were sacrificed and perfused transcardially with 4% paraformaldehyde (PFA). Whole eyes were enucleated from each group and fixed with 4% PFA for 24 hours at 4°C. The tissue was dehydrated in graded ethanols and embedded in paraffin resin. Cryostat serial sections 5µm thick were cut and sections stored at room temperature until further use. Thereafter, antigen retrieval procedure and immunohistochemical analysis was carried out by my-self as described in section 2.10.1 -staining of murine conjunctival paraffin sections: Detection of mMCP-5 and CCR1.

2.2 Cell line and cell culture

2.2.1 RBL-CCR1 cell line

For the present study a RBL cell line stably expressing the human chemokine receptor CCR1 (RBL-CCR1) was used. These adherent cells express high affinity IgE receptors known as FcεR1, and have been used extensively to study FcεR1 and the biochemical pathways for secretion in mast cells. RBL-CCR1 cells were kindly provided by Professor R. Richardson, JLC-Biomedical/Biotechnology Research Institute, North Carolina Central University, Durham, NC, USA. For plasmid map details please refer to Toda et al., 2004.

2.2.2 RBL-CCR1 cell culture

RBL-CCR1 cells were maintained as a monolayer in Dulbecco's modified Eagle's medium (DMEM) (Invitrogen) supplemented with 15% fetal bovine serum (FBS)(Sigma), 2 mM glutamine (Invitrogen) and 1 mg/ml G418 (Invitrogen). Cells were maintained in a humidified cell incubator with 5% CO₂ in air at 37°C. Cells were passaged once or twice weekly as required under standard sterile conditions as follows.

Media was removed and cell monolayers were washed three times with sterile PBS at room temperature. Pre-warmed Trypsin (Invitrogen) was added to the flask and

incubated at 37°C with 5% CO₂ for 5 minutes. Thereafter the flask was gently tapped in order to release the adherent cells and fresh DMEM containing 15% FBS was added to inactivate Trypsin. The resulting cell suspension was centrifuged for 5 minutes at 1200 *revolutions per minute* (rpm). The supernatant was discarded (thereby removing any residual Trypsin), and re-suspended in fresh DMEM containing 15% FBS and 1mg/ml of G418, as a selection marker for CCR1 positive cells.

Cyropreservation was carried out by re-suspending the cell pellet in 1.5mls of freezing mix containing 90% FBS and 10% Dimethyl Sulfoxide (DMSO) (Sigma). The cells were transferred to a cryovial and allowed to undergo freezing at -80°C for 24 hours. After which point, the frozen cells were transferred to liquid nitrogen at -150°C for long-term storage.

2.2.3 GFP-AKT-RBL-CCR1 cell culture

For the present study RBL cell line stably expressing the human chemokine receptor CCR1 and the PH domain of AKT tagged to GFP (GFP-AKT-RBL-CCR1) were kindly provided by Professor R. Richardson, JLC-Biomedical/Biotechnology Research Institute, North Carolina Central University, Durham, NC, USA. Professor Richardson has stated that the specific plasmid map details will be provided in the case of publications. This cell line was cultured and cryopreserved in the same manner as RBL-CCR1 cells using 1mg/ml of G418, as a selection marker as previously described.

2.3. Transfection of RBL-CCR1 cells with either Rgs1 or TRB3 using Oligofectamine- RNA interference

RBL-CCR1 cells for transfection were plated into 6-well plates with DMEM media (Invitrogen) and 15%FBS (Sigma) and allowed to grow until a confluency of approximately 90% was reached. Thereafter DMEM media (Invitrogen) was replaced with DMEM media without serum.

To achieve transient knockdown of RGS1, antibiotic/serum free DMEM media (Invitrogen) and Oligofectamine (Invitrogen) was mixed with RGS1 Ambion Silencer Select Pre-designed siRNA ID number s132558 (Ambion) at a final concentration of 250nM. The mix was incubated at room temperature for 30 minutes and then

added to the cells. After 3 hours FBS was added to each well to reach a concentration of 10%). After 24 hours cells were validated for transfection efficiency by western blot (See section 2.13). Transient knockdown of TRB3 was achieved following the same protocol as RGS1 transient knockdown, with the exception that a final concentration of 150nM TRB3 siRNA, Ambion Silencer Select Pre-designed short interference RNA (siRNA) ID number s140931 (Ambion) was used. In addition RBL-CCR1 cells were also transfected with control siRNA, Ambion Silencer Select Pre-designed siRNA ID number 4390843 (Ambion) in the same manner as RGS1 and TRB3 transient knockdown.

2.4 Degranulation assay

Degranulation results in the release of chemical mediators, which include β -hexosaminidase (Schwartz et al., 1979). The β -hexosaminidase assay has been widely used to monitor RBL degranulation. Current methods to quantify β -hexosaminidase activity use colorimetric enzyme substrates. The present study used the substrate, *p*-nitrophenyl *N*-acetyl-beta-D-glucosamide, which generates 4-*p*-nitrophenol when hydrolysed by β -hexosaminidase.

RBL-CCR1 cells which had been transfected with Rgs1, TRB3 or control siRNA (Ambion) were sensitised with or without 25 ng/ml anti-dinitrophenyl (DNP) IgE SPE 7 monoclonal antibody (MAb) overnight at 37°C with 5% CO₂. After washing three times with x1 PBS, the cells were stimulated with 10 ng/ml dinitrophenyl human serum albumin (DNP-HSA) and/or 10ng/ml of recombinant human Mip-1 α in DMEM containing 0.1% bovine serum albumin (BSA) for 30 minutes in a total volume of 200ul at 37°C with 5% CO₂. Following stimulation, 50ul of each condition supernatant was collected and added to the substrate *p*-nitrophenyl *N*-acetyl-beta-D-glucosamide (Sigma) in 0.1M sodium citrate buffer (pH 4.5). After 60 minutes at 37°C with 5% CO₂, the reaction was quenched with 1M sodium carbonate (pH 10). Beta-hexaminidase activity was measured by the release of 4-*p*-nitrophenol. This was determined using a spectrophotometer at an absorbance of 405nm. Total beta-hexosaminidase activity was determined as previously described, with the exception that the cells were lysed with DMEM containing 0.1% Triton before addition of with *p*-nitrophenyl *N*-acetyl-beta-D-glucosamide in 0.1 M sodium citrate buffer (pH 4.5). Please note the remaining 150ul supernatant from each condition was left for 24 hours at 37°C with 5% CO₂, and thereafter collected for mediator release analysis, which is described in section 2.5.

2.5 Mediator release assay

Following the 24 hour degranulation assay (section 2.4), 100ul of each condition supernatant was placed in a sterile tube and centrifuged at 13,000 rpm at 4°C for 5 minutes to pellet out any debris. The supernatant was carefully removed, taking care not to disturb the pellet and transferred to into a new sterile tube. Thereafter, the supernatant was centrifuged as before. Finally, the supernatant was carefully transferred into a cryovial, which was frozen at -80°C, and then later transferred into liquid nitrogen. Thereafter these samples were couriered on dry ice to Aushon Biosystems (US), where the Supernatants were assayed simultaneously for the presence of IL-4, IL-6, IL-10 MCP-1 and Mip-1 α by using a multiplexing sandwich-ELISA system.

In brief, to quantitate cytokine and chemokine secretion, wells from a 96-well plate were spotted with capture antibodies specific for IL-4, IL-6, IL-10 MCP-1 and Mip-1 α , therefore allowing detection of multiple proteins in the same well. A volume of 50 μ l culture supernatant was added and incubated with the addition of a cocktail of specific biotinylated detection antibodies. After this time a streptavidin- horseradish peroxidase (HRP) conjugate was added and the plate incubated. Detection of each analyte was achieved by using a chemiluminescent substrate solution and quantitated by using Search Light Array analysis software.

2.6 Chemotaxis assay using transwell system

This assay was performed using 24-well Transwell cell culture chambers with 8.0 μ m pore size (Corning). RBL-CCR1 cells which had been transfected with Rgs1, TRB3 or negative control siRNA (Ambion), were sensitized with 25ng/ml anti-DNP IgE for 6 hours at 37°C with 5% CO₂. After washing three times with x1 PBS, the sensitized cells (2x10⁴ cells) in 100 μ l of DMEM containing 0.5% BSA were seeded in the upper compartment, and the lower compartment was filled with 600 μ l of the same medium containing 1ng/ml recombinant human Mip-1 α and/or 10ng/ml DNP-HSA. The cells were incubated for 100 minutes at 37°C with 5% CO₂ followed by quantitation by hemocytometry. In brief, prior to the chemotaxis assay each transwell membrane (containing pores) was scratched to create a grid. Following the 100 minutes incubation period, the transwell membrane was fixed with 3.7%

PFA and then stained with Geimsa (Sigma) to identify mast cells. Mast cells attached to the bottom of each membrane and in the lower chamber of the transwell were counted using a hemocytometer. Figure 10 shows the setup of the transwell chemotaxis assay.

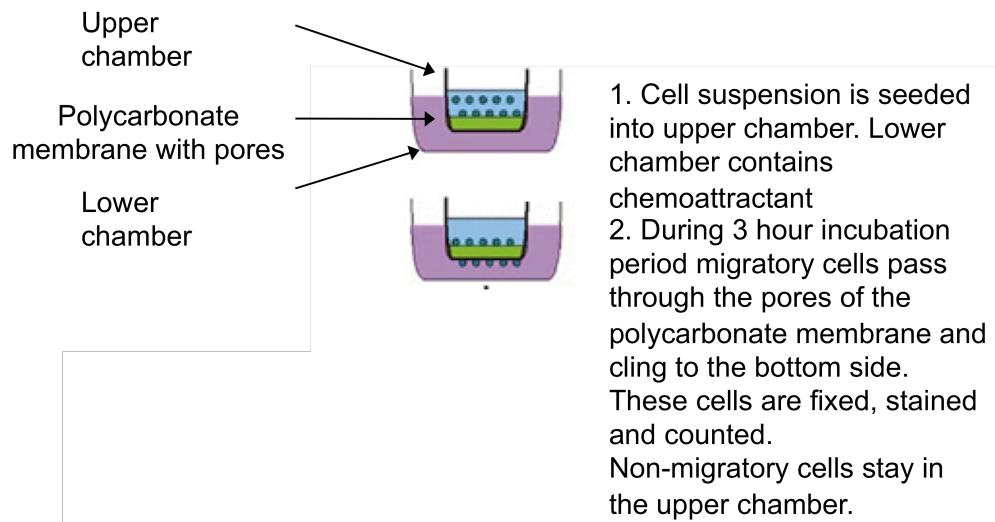


Figure 10. A diagram depicting the transwell chemotaxis assay

2.7 Real time microscopy

2.7.1 Chemotaxis pipette assay analysed by real time microscopy

RBL-CCR1 cells were sensitised with or without 25 ng/ml anti-DNP IgE SPE 7 MAb (Sigma) and 2×10^4 cells were plated onto the centre of a Matek dish (with a glass cover slip insert) (Matek Corporation) overnight at 37°C with 5% CO₂. Cells were washed three times with x1 PBS and were starved in Leibovitz-15 (L15) media (Invitrogen) containing 0.35% BSA (Sigma) in a heat chamber at 37°C for 1 hour before imaging. Cells were stimulated at 37°C, from a point source of L15 media + 0.35% BSA, containing PBS or 50 ng/ml recombinant human Mip-1 α (R and D Systems) and/or 10ng/ml of antigen, DNP-HSA (Sigma) delivered with a Femotip II micropipette (Eppendorf). The Femotip II micropipette was lowered in focus into an area of the microscope's field of view with a micromanipulator (Eppendorf). The solution was dispersed from the Femotip by using a microinjection device (Eppendorf) at an optimized constant pressure of 15 hectopascal (hPA). When necessary, air bubbles were pushed out of the micropipette tip by applying a small pressure using a microinjection device.

Cells were viewed on a Zeiss Axiovert 100M microscope using a 20x objective (Zeiss, UK). Phase Images of living cells were taken using a CCD camera coupled to an OpenLab-driven acquisition system (Improvision/Perkin Elmer) every 60 seconds for one hour.

2.7.2 Analysis of PI(3,4,5)P3 localisation in RBL-CCR1 cells in response to a Mip-1 α gradient using real time microscopy

The PH domain of AKT tagged to GFP was used to detect PI(3,4,5)P3 localisation in RBL-CCR1 cells (GFP-AKT-RBL-CCR1). Stably expressing GFP-AKT-RBL-CCR1 cells (kindly provided by Professor R. Richardson, JLC-Biomedical/Biotechnology Research Institute, North Carolina Central University, Durham, NC, USA) were sensitised with or without 25 ng/ml anti-DNP IgE SPE 7 MAb and 2×10^4 cells were plated onto the centre of Matek dish overnight at 37°C with 5% CO₂. Cells were washed three times with x1 PBS and were starved in L15 media containing 0.35% BSA in a heat chamber at 37°C for one hour before imaging. Cells were stimulated at 37°C, from a point source of L15 media + 0.35%

BSA, containing PBS or 50ng/ml recombinant human Mip-1 α and/or 10ng/ml DNP-HSA delivered with a Femotip II micropipette (Eppendorf). Cells were viewed as previously described with the exception of a 40x and 63x oil objective (Zeiss, U.K). Fluorescent images of living GFP cells, acquired in the fluorescein isothiocyanate (FITC) channel, were taken using a CCD camera coupled to an OpenLab-driven acquisition system (Improvision/Perkin Elmer) every 60 seconds for one hour.

2.8 Staining

2.8.1 Phallotoxin

Phalloidin is well established toxin for the detection of actin filaments and was used in the present study to detect F-actin in RBL-CCR1 cells

2.8.1.1 Localisation of actin filaments in RBL-CCR1 cells

RBL-CCR1 cells were sensitised with or without 25 ng/ml anti-DNP IgE SPE 7 MAb (Sigma) and 2×10^4 cells were plated onto the centre of Matek dish overnight at 37°C with 5% CO₂. After washing three times with x1 PBS, the cells were stimulated with 10 ng/ml DNP-HSA and/or 1ng/ml of recombinant human Mip-1 α (R&D Systems) in Dulbecco's modified Eagle's medium containing 0.1% BSA at 37°C with 5% CO₂. The cells were washed three times with 1x PBS and fixed with 4% Paraformaldehyde for 20 minutes at room temperature. After three successive washes with x1 PBS, cells were permeabilized with PBS containing 0.2% Triton X-100 for 10 minutes at room temperature. Non-specific binding was blocked with PBS containing 0.5% BSA for one hour at room temperature. Thereafter, filamentous actin was detected by staining with appropriately diluted Rhodamine-conjugated phalloidin in PBS (Molecular Probes, Invitrogen) for 30 minutes at room temperature in a humidified chamber. Finally, RBL-CCR1 cells were washed three times with x1 PBS and mounted in Vectorshield (Vector Labs). For phalloidin details please see table 2 at the end of this chapter.

Cells were viewed on a Zeiss 510 confocal microscope using a 40x oil objective (Zeiss). Fluorescent images of RBL-CCR1 cells, acquired in the rhodamine channel, were taken using a Zeiss-driven acquisition system.

2.8.2 Dyes

Toluidine Blue is an aniline dye that is widely used to detect mast cells. Interaction of Toluidine Blue with mast cell granules causes the dye to undergo a metachromatic shift in colour from blue to deep purple.

2.8.2.1 Identification of mast cells by Toluidine blue staining

Frozen serial sections from allergic conjunctivitis mouse model 1 were washed three times in x1 PBS and incubated with 0.1% Toluidine Blue in 90% Ethanol for 30 minutes at room temperature. Sections were washed five times in water and placed in a humidified chamber. Sections were viewed on an Olympus BX microscope using a 4x objective (Olympus Optical, UK). For counting purposes bright field images were taken using a CCD camera coupled to an Image Pro acquisition system.

2.9. Immunocytochemistry

2.9.1 Localisation of of WASP and CCR1 in RBL-CCR1 cells in response to a Mip-1 α gradient

Chemotaxis pipette assay analysed by real time video phase microscopy was performed as described in section 2.3.1 with the exception that 1) cells were plated on Matek dishes with etched grid coverslips 2) non-sensitised CCR1-RBL cells were stimulated at 37°C from a point source of LI5 media + 0.35% BSA, containing PBS or 50ng/ml recombinant human Mip-1 α delivered with a Femotip II micropipette and 3) phase images of living cells were taken with a 20x objective every 60 seconds for 20 minutes using a CCD camera coupled to an OpenLab-driven acquisition system (Improvision/Perkin Elmer) .

Thereafter the cells were washed three times with x1 PBS and fixed with 4% PFA (Sigma) for 20 minutes at room temperature. To remove any excess PFA, RBL-CCR1 cells were washed three times with x1 PBS and then permeabilized with PBS containing 0.2% Triton X-100 for 10 minutes at room temperature. Non-specific staining was blocked and F-actin staining was carried out simultaneously by incubating the cells with PBS containing 0.5% BSA and Alexa 647 conjugated

phalloidin (Molecular probes, Invitrogen) respectively, for one hour at room temperature in a humidified chamber. CCR1 and WASP staining were conducted simultaneously as follows. Cells were incubated with primary antibodies mouse anti CCR1 (R and D systems) and rabbit anti WASP (Sigma) appropriately diluted in blocking agent at room temperature for 1 hour. In each experiment a parallel secondary antibody staining (no primary antibody) was included to control for background staining of the antibody. After 3 successive washes with x1 PBS, specific binding of primary antibodies appropriately diluted in PBS was detected by incubating with secondary antibodies, mouse anti rabbit Alexa 545 (Molecular probes, Invitrogen) and goat anti rabbit Alexa 488 (Molecular probes, Invitrogen) respectively for 1 hour at room temperature in a humidified chamber. Cells were washed three times in x1 PBS and mounted in 3.7% glycerol. For phalloidin and antibody details please see table 2 at the end of this chapter.

Cells were viewed on a Zeiss Axiovert 100M microscope using a 40x oil objective (Zeiss, UK). Fluorescent images of fixed cells, acquired in the FITC, rhodamine and Cy 5 channel, were taken using a CCD camera coupled to an OpenLab-driven acquisition system (Improvision/Perkin Elmer).

2.10 Immunohistochemistry

2.10.1 Staining of murine conjunctival paraffin sections: Detection of mMCP-5 and CCR1

Dr. Mark Obayashi provided paraffin sections 5µm thick of conjunctival tissue (enucleated eyes cut longitudinally) from allergic conjunctivitis murine model 2 using BALB/c mice. Prior to immunohistochemical staining, these sections were deparaffinised with a series of xylene and ethanol washes as follows. Each section was placed in 4 containers, 5 minutes each in 100% xylene followed by 5 minutes each in 4 containers of 100% ethanol. Thereafter the sections were dipped 10 times each in 95%, 90%, 80%, 70% and 50% ethanol. Finally the sections were dipped 10 times in water. This was repeated once more before the immunostaining procedure.

Primary antibody anti mMCP-5, kindly provided by Dr. Rick Stevens, Harvard University, Boston, MA, USA, detects conjunctival mast cells characterised by the expression of mMCP-5. The use of this antibody required an antigen retrieval

procedure that was conducted prior to immunostaining as follows. Slides were placed in a beaker containing x1 Cytomation retrieval (Dako) solution at room temperature for 5 minutes. The beaker was then placed in a water bath at 95°C for 20 minutes, after which point was removed and allowed to reach room temperature. This procedure aims to improve staining by modifying the molecular conformation of 'target' proteins through an exposure of slide-mounted specimen material to a heated buffer solution.

The slides were washed three times in x1 PBS and the section circled with a wax pen (Dako). To reduce background auto-fluorescence the sections were then treated with Image T (Dako) for 30 minutes in a humidified chamber. Non-specific staining was blocked with PBS containing 5% normal goat serum and 1% BSA for 1 hour at room temperature in a humidified chamber. Mast cells were detected by incubating with anti-mMCP-5 antibody appropriately diluted in blocking agent overnight at 4°C in a humidified chamber. After three successive washes with x1 PBS the sections were incubated with secondary antibody goat anti rabbit Alexa 555 (Molecular probes, Invitrogen) appropriately dilute in 1x PBS for 1 hour at room temperature in a humidified chamber. After washing three times with x1 PBS sections were incubated with primary antibody mouse anti CCR1 appropriately diluted in blocking solution for 1 hour at room temperature in a humidified chamber. Thereafter sections were washed three times with x1 PBS and incubated with secondary antibody goat anti mouse Alexa 488 appropriately diluted in PBS for 1 hour at room temperature in a humidified chamber. Sections were washed three times with x1 PBS and mounted in Vectorshield mounting agent (Vector Labs). In each experiment a parallel secondary antibody staining (no primary antibody) was included to control for background staining of the antibody. For antibody details please see table 2 at the end of this chapter.

For counting purposes sections were viewed on an Olympus BX microscope using a 40x oil objective (Olympus Optical, UK). Fluorescent images acquired in the FITC and rhodamine channel, were taken using a CDD camera coupled to an Image Pro acquisition system.

2.10.2 Staining of conjunctival frozen sections: Detection of WASP and actin

Frozen sections from allergic conjunctivitis mouse model 1 were washed three times in x1 PBS and then treated with sodium borohydride (Sigma) to reduce

background autofluorescence. Non-specific staining was blocked and F-actin detection was carried out simultaneously by incubating with PBS containing 0.5% BSA and rhodamine-conjugated phalloidin respectively, for one hour at room temperature in a humidified chamber. WASP staining was detected by incubating the sections with a primary antibody, rabbit anti WASP (Sigma) diluted in blocking agent overnight at 4°C in a humidified chamber. Thereafter the sections were washed three times in x1 PBS and incubated with secondary antibody goat anti rabbit Alexa 488 (Molecular probes, Invitrogen) appropriately diluted in PBS for 1 hour at room temperature. Sections were washed three times with x1 PBS and mounted in Vectorshield mounting agent (Vector Labs). In each experiment a parallel secondary antibody staining (no primary antibody) was included to control for background staining of the antibody. For phalloidin and antibody details please see table 2 at the end of this chapter.

Sections were viewed on a Leica confocal SP2 microscope using a 63x oil objective. Fluorescent images acquired in the FITC, rhodamine channel, were taken using a Leica-driven acquisition system.

2.11 Analysis of Microscopy

2.11.1 Quantification of Migration

On completion of real time movies, the outline of each cell was manually traced for each time point using Open Labs Software. This software automatically generated a centre point or centroid for each cell (Figure 11).

The centroid is the average of the x and y coordinates of all of the pixels in the trace. These coordinates were converted into micro metres at the beginning of each manual trace, and imported into Image J chemotaxis and migration tool software, where a migration plot was generated. From this migration plot several parameters were calculated, including accumulated distance, Euclidean distance, velocity and directionality (Figure 12).

The accumulated distance is the cell path from the initial time point (t_i) to the final time point (t_f), where as the Euclidean distance is the straight line distance from t_i to t_f (Figure 13). The directionality of the cell was calculated by the formula: Euclidean distance/ accumulated distance.

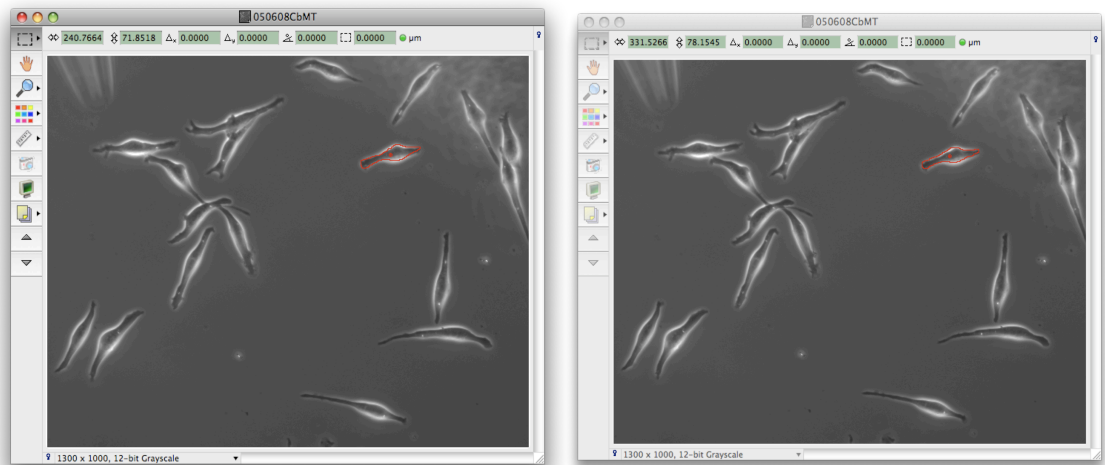


Figure 11. Open Lab snapshots showing the outline of each cell at timepoints t1 (A) and t2 (B) with its corresponding centroid x.

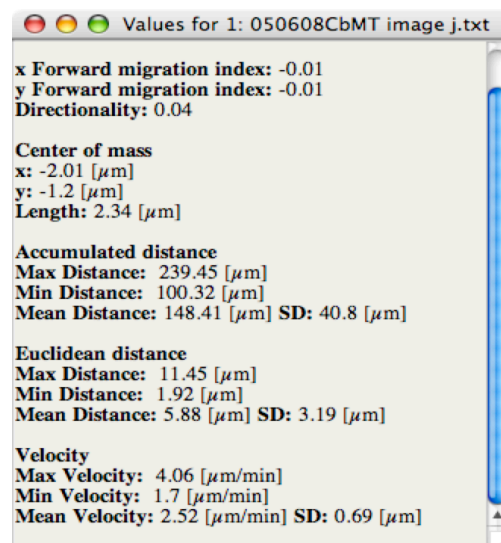
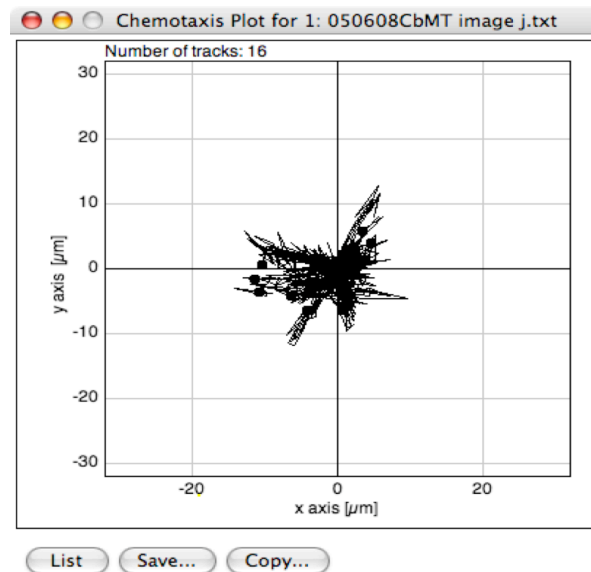


Figure 12. Image J snapshots showing a migration plot with its corresponding parameters. Cell traces were arranged to show their origins at $x=y=0$.

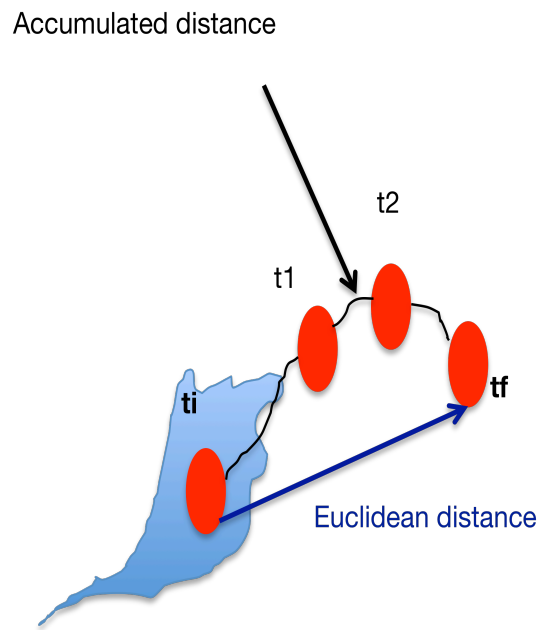


Figure 13. Accumulated and Euclidean distance, where t_i represents initial time and t_f , final time.

2.11.2 Quantification of Toluidine Blue positive murine conjunctival mast cells

Following Toluidine Blue staining of mast cells, all images were analyzed by the Image J program. Toluidine Blue positive mast cells were counted in the forniceal region of the conjunctiva marked G and AG (Figure 14) to a stromal depth of 200 μ m and 500 μ m respectively parallel to the basement membrane of the surface epithelium. Regions, G and AG, were of an equal size and this was determined using the Image J program. The results were expressed as the mean count of cells \pm standard error mean (SEM) per mm².

2.11.3 Quantification of mMCP5 and CCR1 positive murine conjunctival mast cells

Following immunohistochemistry staining of mMCP-5 and CCR1, all images were analyzed by Image Pro acquisition software system using a FITC channel to detect mMCP-5 and a TRTCI channel to detect CCR1. Thereafter, mMCP-5 and CCR1 positive mast cells were counted using a grid (0.1 mm²). The grid was placed 100 μ m parallel to the basement membrane of the surface epithelium in the area marked G. (Figure 15). The number of immunopositive cells were determined and results were expressed as the mean count of cells \pm SEM per 0.1 mm².

Figure 14. Schematic representation of the conjunctiva showing the location of the chemokine gradient, G, and the location away from the chemokine gradient, AG, the areas in which mast cells were counted.

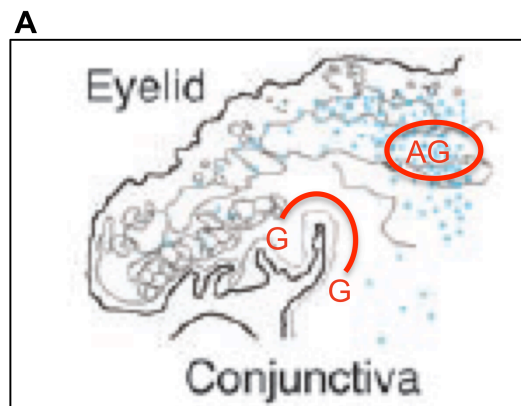
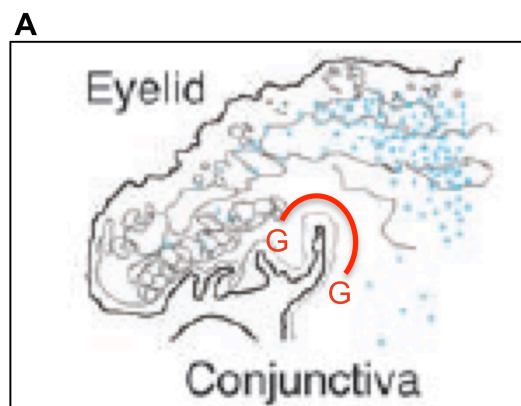


Figure 15. Schematic representation of the conjunctiva showing the location of the chemokine gradient, G, the area in which mast cells were counted.



2.12 RT-PCR

2.12.1 RNA isolation

Total RNA was extracted from cells using the RNeasy kit (Qiagen cat.74104) as per the manufacturer's instructions. Briefly, cells grown on 6- well plates ($< 1 \times 10^7$) were lysed directly by adding 350ul lysis buffer containing β mercapto-ethanol (10 μ l/ml, Sigma-Aldrich). The resulting suspension was vortexed for 1 minute and immediately stored at -80°C for future use or subjected to RNA isolation. The samples were then applied to the RNeasy Mini spin column, contaminants washed away, and RNA eluted in 20-30 μ l of RNase free water. The concentration of RNA was determined using a spectrophotometer. RNA samples were stored at -80°C and thawed on ice before use.

2.12.2 Reverse Transcription (RT)

RNA was reverse transcribed into cDNA using the QuantiTect Reverse Transcription Kit (Qiagen cat 205311), which comprises elimination of genomic DNA and reverse transcription. Briefly, 1 μ g of purified RNA sample was incubated in gDNA Wipeout buffer for 2 minutes at 42°C to eliminate any genomic DNA contamination. Thereafter, the reverse transcription reaction was performed (as per kit instructions) in a final volume of 20 μ l containing a master mix of RNA, Quantiscript Reverse Transcriptase, RNase inhibitor, dNTPs and Mg^{2+} mix, oligo-dT and RNase free water. The mixture was incubated at 42°C for 15 minutes, 95°C for 5 minutes (to inactivate the Quantiscript Reverse Transcriptase) and 4°C for 5 minutes in a thermalcycler. Following first strand synthesis reaction, a portion of the reverse transcription reaction was immediately transferred into another tube for the 3 Real Time Quantitative PCR (qPCR) reaction.

2.12.3 qPCR

Real time quantification of DNA was carried out using the QuantiTect SYBR green PCR kit (Qiagen cat 204143) as per manufacturers instructions. Primer sequences were obtained from Applied Biosystems and reconstituted to a concentration of 50 μ M in buffer. Briefly, the amplification and detection was performed in a final reaction volume of 25 μ l containing 2x SYBR Green master mix, (master mix

contained intercalating SYBR Green I dye that fluoresces when bound to ds DNA, Taq DNA polymerase, KCL, $(\text{NH}_4)_2\text{SO}_4$ and ROX dye), 0.5 μM of primer, 50ng copy DNA (cDNA) and RNase water. The mixture was incubated at 94°C for 15 seconds, 55°C for 30 seconds, 72°C for 30 seconds for 40 cycles and for 95°C for 15 seconds, 60°C for 30 seconds and 95°C for 15 seconds for 1 cycle. An annealing temperature of 52°C was used for all primers. All data were normalized to Glyceraldehyde 3-phosphate dehydrogenase (GAPDH) expression (Applied Biosystems).

2.12.4 Analysis of qPCR

Cycle threshold (C_t) values were recorded and the data was normalised by running each sample against GAPDH, as a housekeeping gene, with the relative gene expression calculated using the $\Delta\Delta C_t$ method as described below:

Δ = change

$\Delta C_t = C_t \text{ target gene} - C_t \text{ housekeeping gene}$

$\Delta\Delta C_t = \Delta C_t \text{ sample} - \Delta C_t \text{ unstimulated}$

2.13 Western Blotting

2.13.1 Protein Isolation

Following experimental conditions, cytoplasmic and nuclear proteins were extracted from cells by using Mammalian Protein Extraction Reagent (M-PER) (Thermo Scientific) as follows. Adherent cells were washed three times with x1 cold PBS. 50 μl of cold M-PER containing a protease inhibitor cocktail (Cat no: P8340, Sigma-Aldrich)-10 μl per ml of lysis buffer, Dithiothreitol (DTT) 0.5 mM, Phenyl Methyl Sulfonyl Fluoride (PMSF) 1mM and Sodium Orthovanadate 3mM was added to adherent cells and scraped rapidly. The resulting cell lysate was pipetted thoroughly and transferred to a microfuge tube. The samples were centrifuged twice at 14,000rpm for 10 minutes to pellet the cell debris and the supernatant containing the proteins of interest was collected.

Protein concentration was estimated using a Pierce bicinchoninic acid (BCA) Protein Assay Kit (Thermo Scientific). This method relies the reduction of Cu^{2+} to

Cu¹⁺ by protein in an alkaline medium. The resulting purple-colored reaction product is detected by a reagent containing BCA.

In a 96 well plate 10ul of protein or standard sample (diluted 1:4 in PBS) was added to 200ul of BCA reagent. The samples were mixed thoroughly on a plate shaker for 30 seconds and incubated at 37°C for 15 minutes. The absorbance of the resulting purple solution was then measured at 562nm using a spectrophotometer. To ensure equal loading of protein onto the electrophoresis gel protein volumes were adjusted according to relative absorbance readings. To ensure for further normalisation of amount of protein loaded, a loading control of β -actin (Abcam) was also used in each experiment. All protein samples were stored at -80°C for future use.

2.13.2 Protein Gel Electrophoresis and transfer

The NuPAGE gels and buffer systems from Invitrogen were used for protein gel electrophoresis. In this study 10% Bis-Tris gels (NP0315, Invitrogen) were used in combination with the MOPS SDS running buffer (NP0001, Invitrogen, UK) for resolution of proteins with a molecular weight between 20 and 60 kDa. All gels were of 1.5mm thickness containing 15 wells, capable of holding 30ul of solution and prepared as follows.

30 μ l of loading sample was prepared with 9 μ l of loading buffer (LDS 4X), 3 μ l of reducing agent (10X), and a maximum of 18 μ l of protein sample. As previously mentioned, in order to load equal amounts of protein, this volume of 18 μ l was adjusted based on the absorption readings (from BCA assay) and the remaining volume made up with water. To denature the protein the loading samples were boiled at 80°C for 10 minutes. The pre-casted gels were washed in distilled water and fitted into the XCell *SureLock*TM Mini-Cell mini vertical electrophoresis system (Invitrogen). Thereafter, the chamber was locked to generate a watertight compartment for the gel and the electrodes. Into this compartment, working concentration running buffer and working concentration MOPS running buffer (for bis-tris gels Cat no: NP0001 with antioxidant (500 μ l/ 200mls buffer) was added. The protein ladder and samples were loaded into the gels and were run at 180V for 50 minutes.

Before protein transfer, Poly Vinylidene Fluoride (PVDF) membranes (Hybond-P) were pre-treated with methanol for 5 minutes, washed in distilled water and

equilibrated in working concentration transfer buffer (Invitrogen). Protein transfer was conducted at 35V for 90 minutes using the XCell *SureLock*™ Mini-Cell mini transfer set up (Invitrogen).

2.13.3 Immunoblotting

Membranes were blocked in tris-buffered saline (TBS) +0.1% Tween-20 with 5% BSA at room temperature for 1 hour. Primary antibodies were diluted in blocking buffer and incubated overnight at 4°C. The membrane was washed 3 times in TBS + 0.1% Tween-20 for 15 minutes at room temperature and incubated with secondary antibody conjugated to HRP (Jackson Laboratories) for 1 hour at room temperature. After three successive washes in TBS + 0.1% Tween-20 for 15 minutes and twice with TBS, the blot was visualised with enhanced luminol-based chemiluminescent (ECL) advanced detection kit (Thermo scientific). For antibody details please see table 2 at the end of this chapter.

2.14 Statistical analysis of results

For the present study all statistics were determined using the student T-test, which assesses whether the means of two groups are statistically different from each other when measuring one variable.

Details of primary antibody or stain and applications	Target/antigen	Concentration/ dilution of primary antibody or stain	Details of secondary antibody	Concentration/ dilution of secondary antibody
Alexa 543 or Alexa 647 conjugated phalloidin (Molecular probes) Applications: immunocytochemistry and immunohistochemistry	Actin	300 units- use 1:500	N/A	N/A
Rabbit anti WASP (Sigma) Applications: immunohistochemistry frozen sections	WASP	1mg/ml-use 1:200	goat anti rabbit Alexa 488 (Molecular probes)	2ug/ml-use 1:1000
Rabbit anti WASP (Sigma) Applications: immunocytochemistry	WASP	1mg/ml-use 1:500	goat anti rabbit Alexa 488 (Molecular probes)	2ug/ml-use 1:1000
Mouse anti CCR1, Clone 53504 (R&D systems) Applications: immunocytochemistry	CCR1	500ug/ml-use 1:200	goat anti mouse Alexa 545 (Molecular probes)	2ug/ml-use 1:1000
Rabbit anti mMCP-5 (Kind gift from Dr. Rick Stevens, Harvard university, US) Applications: immunohistochemistry- paraffin sections	Conjunctival mast cells characterised by expression of mMCP-5. (see section 1.1 for further details)	250ug/ml-use 1:300	goat anti rabbit Alexa 555 (Molecular probes)	2ug/ml-use 1:1000
Mouse anti CCR1, Clone 53504 (R&D systems) Applications: immunohistochemistry paraffin sections	CCR1	500ug/ml-use 1:200	goat anti mouse Alexa 488 (Molecular probes)	2ug/ml-use 1:1000
Rabbit anti TRB3 Clone M-165 (Santa Cruz) Applications: western blotting	TRB3	200ug/ml- use 1:1000	Goat anti rabbit IgG HRP (Santa Cruz)	200ug/0.5ml- use 1:5000
Rabbit anti RGS1, Clone H-70 (Santa Cruz) Applications: western blotting	RGS1	200ug/ml- use 1:1000	Goat anti rabbit IgG HRP (Santa Cruz)	200ug/0.5ml- use 1:5000

Table 2. A table to show concentrations of stains, primary and secondary antibodies for each target antigen used in this study.

Chapter 3.

The effect of $Fc\epsilon RI$ and CCR1 co-engagement on RBL-CCR1 cell motility

3. The effect of FcεRI and CCR1 co-engagement on RBL-CCR1 cell motility

3.1 Introduction and hypothesis

Mip-1α was first observed as a histamine releasing factor in mouse peritoneal mast cells (Alam et al., 1992), though these *in vitro* experiments showed that Mip-1α was a markedly less effective histamine releasing factor than IgE/antigen. The role of Mip-1α in mast cell physiology *in vivo* is less well defined having been implicated in various mast cell functions including activation, differentiation and homing (Ono et al., 2003). Miyazaki and co-workers (2005) observed the rapid expression of Mip-1α in resident mononuclear cells following allergen challenge in a murine allergic conjunctivitis model. Subsequent studies by Toda and co-workers (2004) demonstrated that co-stimulation of RBL-CCR1 cells *in vitro* by Mip-1α and IgE/antigen synergistically enhanced degranulation and inhibited Mip-1α mediated chemotaxis. This data suggests that while CCR1 and FcεRI engagement is essential for optimal activation and degranulation of mast cells, it also affects other mast cell events such as chemotaxis.

As displayed by several cell types, the migration of cells towards chemoattractants during biological processes requires the reorganisation of the actin cytoskeleton, along with defined localisation patterns for cell motility components such as PI(3,4,5)P3 and chemokine receptors. Mast cells accumulate at sites of inflammation during an allergic response, however, at present, the mechanisms underlying mast cell migration *in vitro and in vivo* are poorly understood. A continued effort to further elucidate the mechanisms involved during mast cell migration will help identify alternative anti-inflammatory therapies.

Based on current knowledge, I hypothesise that CCR1 engagement by Mip-1α and simultaneous engagement of CCR1 and FcεRI by Mip-1α and IgE/antigen respectively, in RBL-CCR1 cells *in vitro*, can alter cell morphology, actin cytoskeleton reorganisation and the localisation of cell motility components *pertinent* for cell migration.

To address this hypothesis, the specific aims of this chapter were as follows: -

1. To analyse actin reorganisation in RBL-CCR1 cells following co-stimulation with Mip-1 α and IgE/antigen.
2. To analyse by real time microscopy the behaviour and morphology of RBL-CCR1 cells migrating towards a Mip-1 α gradient and test the effects of IgE receptor cross-linking.
3. To analyse the localisation of PI(3,4,5)P₃, CCR1 and actin in RBL-CCR1 cells migrating towards Mip-1 α gradient.

3.2 Results

3.2.1 Actin reorganisation in RBL-CCR1 cells induced by homogeneous co-stimulation by Mip-1 α and IgE/antigen

The actin cytoskeleton is a highly dynamic network, and rearrangement of the actin cytoskeleton is a crucial component of cell motility. Membrane ruffling and lamellipodia formation as a result of actin polymerisation are fundamental components of the cytoskeleton rearrangements required for cell movement. In a previous study, Toda et al (2004) showed that Fc ϵ RI engagement has an inhibitory effect on Mip-1 α -induced chemotaxis, suggesting that co-stimulation with antigen and Mip-1 α affect reorganisation of actin cytoskeleton of RBL-CCR1 cells. In order to examine the effects of co-stimulation of CCR1 and Fc ϵ RI by Mip-1 α and IgE/antigen respectively on actin reorganisation in RBL-CCR1 cells, RBL-CCR1 cells were stimulated with 1ng/ml of Mip-1 α (optimal condition for chemotaxis established by Toda et al., 2004) and 10ng/ml of DNP-HSA (antigen), thereafter actin filaments were visualized with TRITC-conjugated phalloidin. The data are representative of 4 separate experiments with more than 40 cells analysed in each.

Unstimulated RBL-CCR1 cells are pod shaped elongated cells with strong, evenly distributed actin expression (Figure 16A). RBL-CCR1 cells homogeneously stimulated with 1ng/ml of Mip-1 α dramatically induced actin rich membrane ruffles within one minute (Figure 16B). Moreover, cells stimulated with 1 ng/ml of Mip-1 α for five minutes showed further large distinct actin rich membrane ruffles (as indicated by white arrow), a flattened morphology adopting a polarized phenotype with actin rich lamellipodia (as indicated by yellow arrow) at the leading edge of the cell (Figure 16C). Interestingly, cells sensitized with IgE mAb and co-stimulated with Mip-1 α and IgE/antigen for one minute and five minutes exhibited few or no membrane ruffles (Figures 16D and 16E respectively) compared with Mip-1 α stimulated cells. Cells sensitized with IgE alone for five minutes exhibited intense cortical actin and few membrane ruffles compared with Mip-1 α stimulated cells (Figure 16F).

These results indicate that Fc ϵ RI engagement alters actin cytoskeleton reorganisation of RBL-2H3 cells. It inhibits pronounced Mip-1 α induced membrane ruffling response and thereby contributes to the inhibition of Mip-1 α induced

chemotaxis of RBL-CCR1 cells.

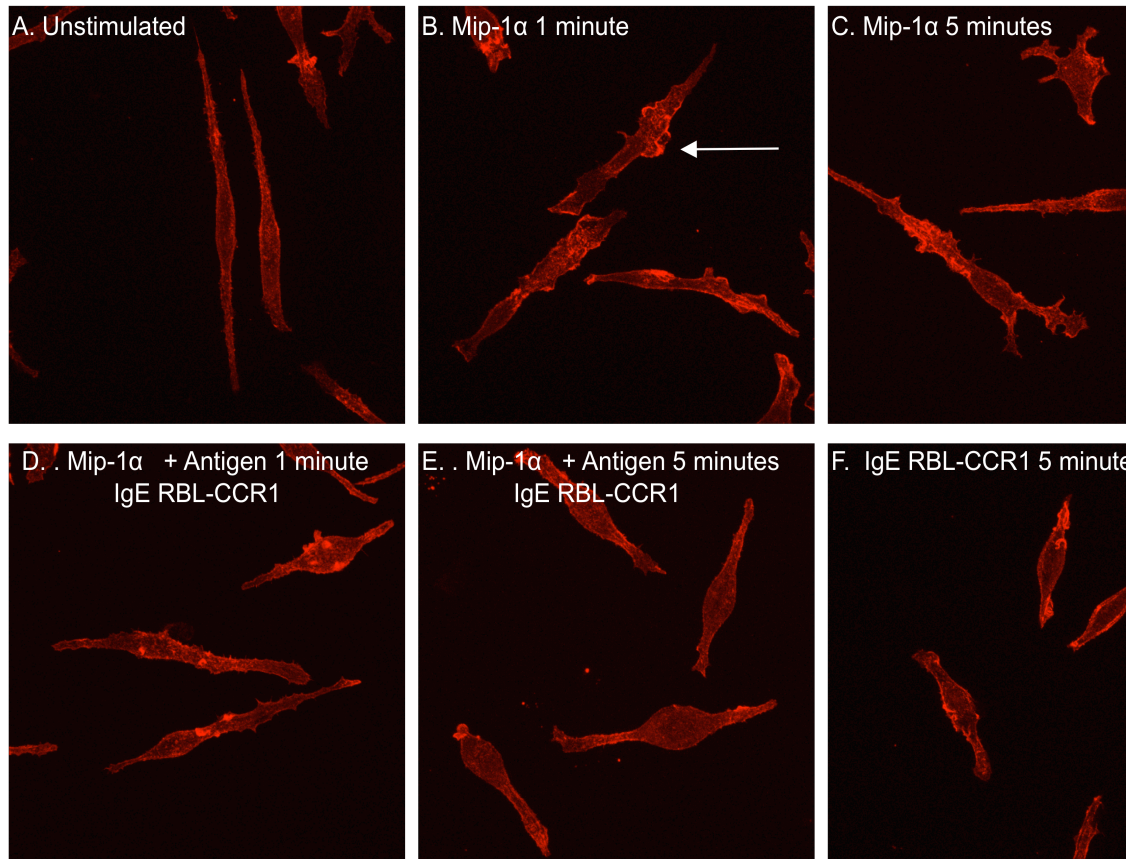


Figure 16. Rhodamine phalloidin-stained RBL-CCR1 cells showing F-actin distribution (red) and decreased membrane ruffling following stimulation with Mip-1 α and co-stimulation with Mip-1 α + IgE/Antigen. (A) Unstimulated RBL-CCR1. RBL-CCR1 cells were stimulated with Mip1a for (B) 1 minute or (C) 5 minutes; or Mip-1 α + IgE/antigen (D) 1 minute or (E) 5 minutes; and (F) IgE for 5 minutes. Mip-1 α stimulated RBL-CCR1 cells exhibit extensive membrane ruffling (as indicated by white arrow) and lamellipodia (as indicated by yellow arrow) as compared to co-stimulated cells. The data are representative of 4 separate experiments with more than 40 cells analysed in each experiment.

3.2.2 Behavioural responses of RBL-CCR1 Cells to gradients of Mip-1 α and IgE/antigen co-stimulation using real time microscopy

Chemotaxis is the directional movement of cells within a chemokine gradient. Actin polymerisation and membrane ruffling occur at the leading edge of chemotactic cells, resulting in cell polarisation and facilitating appropriate directional movement up a chemotactic gradient. In order to acquire a detailed understanding of the mechanisms involved in mast cell chemotaxis, the initial starting point for many investigations of cell motility is to characterise the behaviour of cells.

Toda et al., (2004) demonstrated using a chemotaxis transwell system (standard Boyden chamber) that Mip-1 α induced RBL-CCR1 chemotaxis and inhibition of Mip-1 α induced chemotaxis was a result of Fc ϵ R1 and CCR1 co-engagement. However, the standard Boyden chamber only determines an end point of cell motility and does not allow for the observation of cell movement to characterize the motility pattern. Therefore, a series of experiments were conducted to characterise the behaviour of RBL- CCR1 cells towards a micropipette (creating a gradient), containing either DMEM media supplemented with PBS; Mip-1 α ; both Mip-1 α and antigen (in this case RBL-CCR1 cells were sensitized with IgE MAb); antigen; Mip-1 α and antigen and Mip-1 α (however in this case RBL-CCR1 cells were sensitized with IgE MAb). For each experiment 10-15 cells per condition were recorded every minute for one hour using real time microscopy. Following this recording, the results were analysed in Image J using the chemotaxis tool that give migrational plot, directionality, Euclidean distance, accumulated distance and velocity for each condition. The data are representative of five separate movies for each condition with at least 10-15 cells analysed in each movie.

In the experiment shown in Figure 17, a micropipette (as indicated by a yellow *) filled with DMEM plus PBS (DMEM/PBS) is positioned within a field of RBL-CCR1 cells. Figures 17A-E are representative of 5 independent time-lapse videos where the red arrow shows the movement of a representative cell towards DMEM/PBS over a period of 1 hour Figure 17A shows at the onset of the experiment RBL-CCR1 cells are elongated pod shaped cells. Cells exposed to the micropipette gradient for five minutes (Figure 17B), ten minutes (Figure 17C), 30 minutes (Figure 17D) and 60 minutes (Figure 17E) were unresponsive, displaying no membrane ruffling or cell polarization. Figure 17F shows a migrational plot

representing the pathway undertaken by each RBL-2H3 cell in response to the micropipette gradient in one hour, where the x and y axis represent the distance in μm . The plot indicates the cells remain stationary, the cells seem to 'wobble' on the spot in response to DMEM/PBS gradient and their endpoint surrounding the x-y intercept, thereby inferring limited motility. A movie of the experiment described in this figure is available on CD1 movie file name, DMEMMedia.

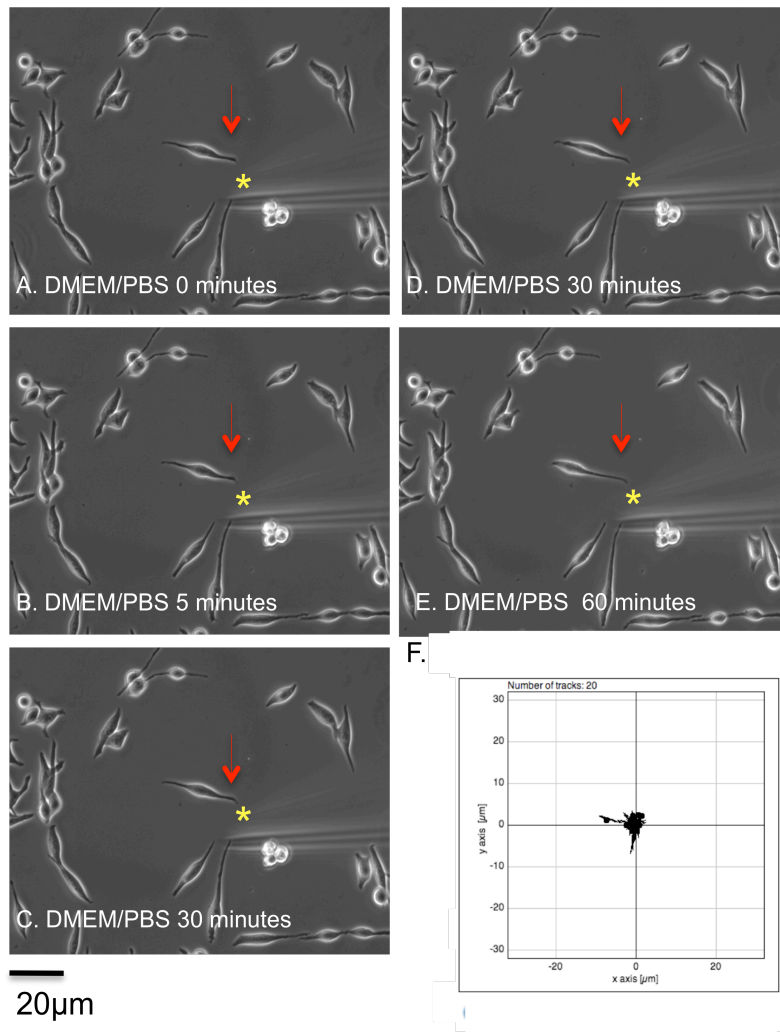


Figure 17. RBL-CCR1 cells do not migrate towards PBS/DMEM.

Time-lapse video microscopy frames of RBL-CCR1 motility towards a micropipette tip (*) containing PBS/DMEM media alone at timepoints (A) 0, (B) 5 minutes, (C) 10 minutes, (D) 30 minutes, (E) 60 minutes. Figures 2A-E are representative of 5 independent time-lapse videos where the red arrow shows the movement of a representative cell towards PBS/DMEM over a period of 1 hour. (F) RBL-CCR1 cell migrational plot depicting the path of each cell every minute for a period of 1 hour towards a micropipette tip containing media alone. Cell traces were arranged to show their origins at $x=y=0$. Migration plot shown in Figure 2F is representative of 5 independent experiments

In the experiment shown in Figure 18, a micropipette (as indicated by a yellow *) filled with 50ng/ml of Mip-1 α is positioned within a field of RBL-2H3 cells. Figures 18A-E are representative of 5 independent time-lapse videos where the red arrow shows the movement of a representative cell towards Mip-1 α over a period of 1 hour. The cells appeared unresponsive and elongated in shape at the onset (Figure 18A), however within five minutes RBL-2H3 cells showed intense membrane ruffling (Figure 18B) when exposed to the micropipette Mip-1 α gradient. By ten minutes, RBL-CCR1 cells displayed large membrane ruffles at their leading edge, formed lamellipodia and were polarised (Figure 18C). By 30 minutes (Figure 18D) and 60 minutes (Figure 18E) RBL-2H3 cells maintained a polarized phenotype and were able to chemotax toward the micropipette Mip-1 α gradient. The migrational plot in Figure 18F indicates RBL-CCR1 cells moved from 0-20+ μ m in response to a Mip-1 α gradient for one hour. A movie of the experiment described in this figure is available on CD1 movie file name, Mip1a.

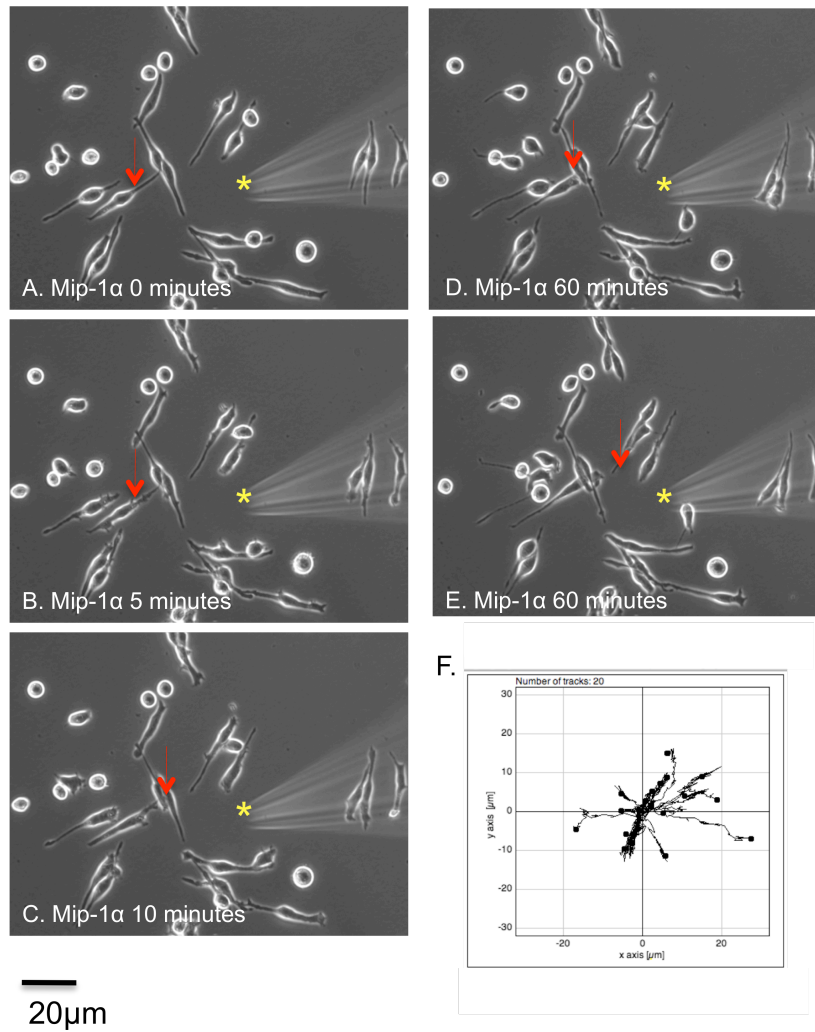


Figure 18. RBL-CCR1 cells chemotax towards Mip-1α.

Time-lapse video microscopy frames of RBL-CCR1 motility towards a micropipette tip (*) containing Mip-1α at timepoints (A) 0, (B) 5 minutes, (C) 10 minutes, (D) 30 minutes, (E) 60 minutes. Figures 2A-E are representative of 5 independent time-lapse videos where the red arrow shows the movement of a representative cell towards Mip-1α over a period of 1 hour. (F) RBL-CCR1 cell migration plot depicting the path of each cell every minute for a period of 1 hour towards a micropipette tip containing Mip-1α alone. Cell traces were arranged to show their origins at $x=y=0$. Migration plot shown in Figure 2F is representative of 5 independent experiments

In the experiment shown in Figure 19, a micropipette (as indicated by a yellow *) filled with 50ng/ml of Mip-1 α and 10ng/ml of antigen is positioned within a field of RBL-CCR1 cells sensitized with IgE MAb. Figures 19A-E are representative of 5 independent time-lapse videos where the red arrow shows the movement of a representative IgE sensitised cell towards Mip-1 α and antigen over a period of 1 hour. The cells appeared unresponsive and elongated in shape at the onset (Figure 19A). By five minutes, RBL-CCR1 cells remained unresponsive towards the Mip-1 α and antigen micropipette gradient (Figure 19B). Moreover, further exposure at ten minutes (Figure 19C), 30 minutes (Figure 19D) and 60 minutes (Figure 19E) rendered the cells inactive, with no obvious morphological changes, cell polarization or chemotaxis. Figure 19F shows a migrational plot representing the pathway undertaken by each RBL-CCR1 cell sensitized with IgE MAb in response to the micropipette Mip-1 α and antigen gradient in one hour. The pathway of the cells end mostly at the intercept of the x and y-axis thereby showing limited movement. A movie of the experiment described in this figure is available on CD1 movie file name, Mip1a and IgEAntigen.

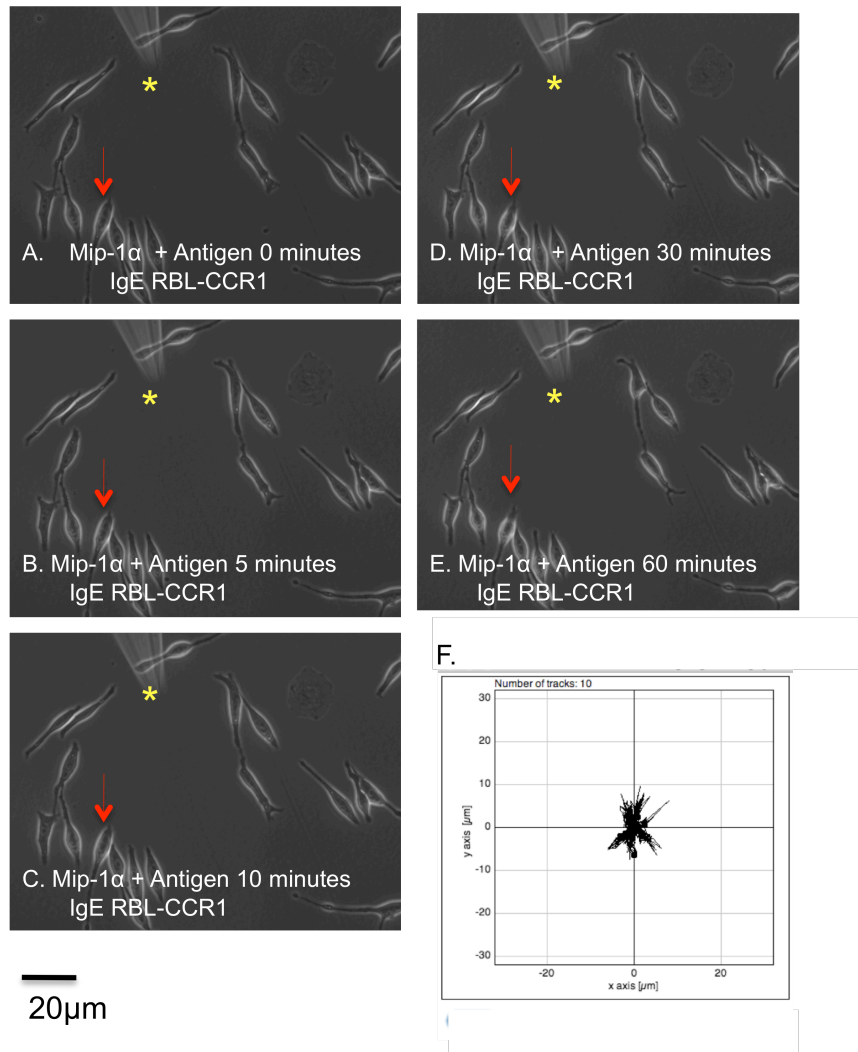


Figure 19. RBL-CCR1 cells pre-sensitised with IgE do not chemotax towards Mip-1α and antigen.

Time-lapse video microscopy frames of IgE sensitised RBL-CCR1 motility towards a micropipette tip (*) containing Mip-1α and antigen at timepoints (A) 0, (B) 5 minutes, (C) 10 minutes, (D) 30 minutes, (E) 60 minutes. Figures 2A-E are representative of 5 independent time-lapse videos where the red arrow shows the movement of a representative IgE pre-sensitized cell towards Mip-1α and antigen over a period of 1 hour. (F) RBL-CCR1 cell migration plot depicting the path of each cell every minute for a period of 1 hour towards a micropipette tip containing Mip-1α and antigen alone. Cell traces were arranged to show their origins at x=y=0. Migration plot shown in Figure 2F is representative of 5 independent experiments

In the experiment shown in Figure 20, a micropipette (*) filled with 10ng/ml of antigen is positioned within a field of RBL-CCR1 cells. The cells appeared unresponsive and elongated in shape at the onset (Figure 20A). At five minutes exposure RBL-CCR1 cells showed no obvious morphological changes towards the micropipette antigen gradient (Figure 20B). Further exposure to the micropipette antigen gradient at ten minutes (Figure 20C), 30 minutes (Figure 20D) and 60 minutes (Figure 20E) did not induce membrane ruffles or cell polarization. Figure 20F shows a migrational plot representing the pathway undertaken by each RBL-CCR1 cell in response to the micropipette antigen gradient in one hour. RBL-CCR1 cells endpoints surround the x-y intercept, thereby showing limited motility towards the micropipette antigen gradient. A movie of the experiment described in this figure is available on CD1 movie file name, Antigen.

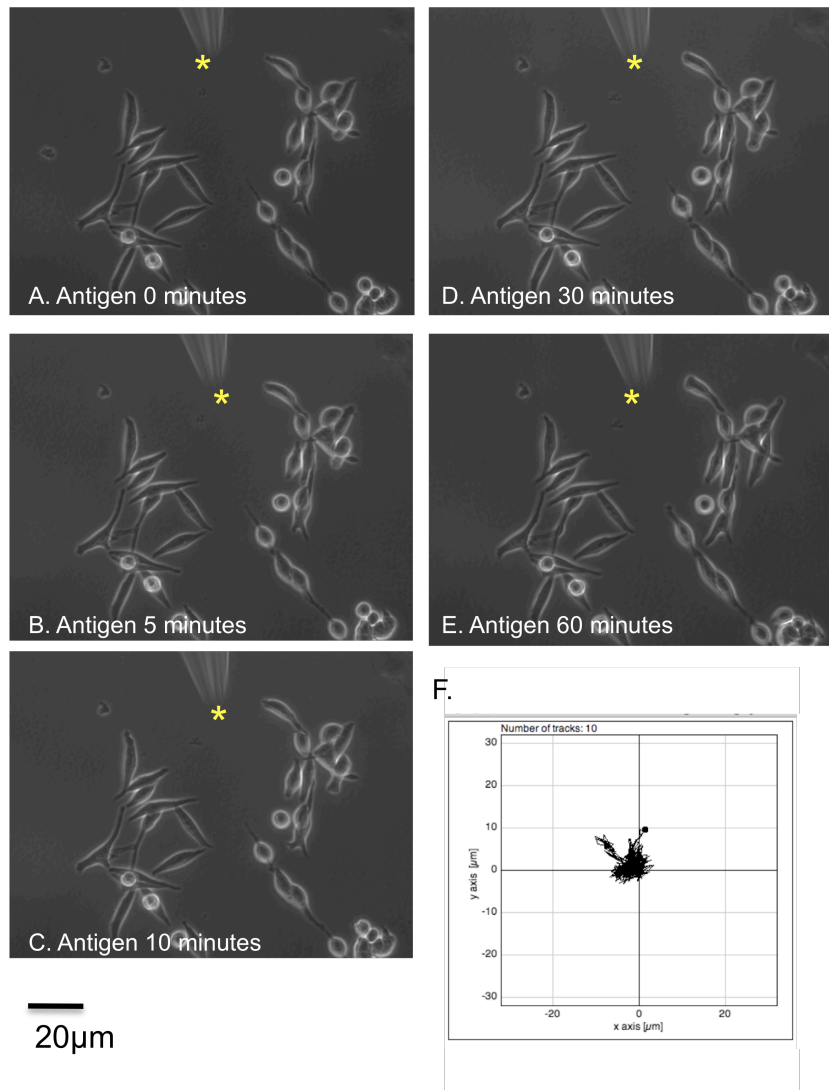


Figure 20. RBL-CCR1 cells do not migrate towards antigen.

Time-lapse video microscopy frames of RBL-CCR1 motility towards a micropipette tip (*) containing antigen at timepoints (A) 0, (B) 5 minutes, (C) 10 minutes, (D) 30 minutes, (E) 60 minutes. (F) RBL-CCR1 cell migration plot depicting the path of each cell every minute for a period of 1 hour towards a micropipette tip containing antigen alone. Cell traces were arranged to show their origins at $x=y=0$. Migration plot shown in Figure 2F is representative of 5 independent experiments

In the experiment shown in Figure 21, a micropipette (as indicated by a yellow *) filled with 50ng/ml of Mip-1 α and 10ng/ml of antigen is positioned within a field of RBL-CCR1 cells. The cells appeared unresponsive and elongated in shape at the onset (Figure 21A). However, within five minutes exposure to the micropipette Mip-1 α and antigen gradient the cells dramatically induced large membrane ruffles (Figure 21B). Further exposure to the micropipette Mip-1 α and antigen gradient at ten minutes (Figure 21C), 30 minutes (Figure 21D) and 60 minutes (Figure 21E) induced large distinct membrane ruffles, lamellipodia formation, cell polarization and chemotaxis of these cells towards the gradient. Figure 21F shows a migrational plot representing the pathway undertaken by each RBL-CCR1 cell in response to the micropipette Mip-1 α and antigen gradient in one hour. The cells are able to chemotax upto 40 μ m towards the Mip-1 α and antigen gradient. A movie of the experiment described in this figure is available on CD1 movie file name, Mip-1a and antigen.

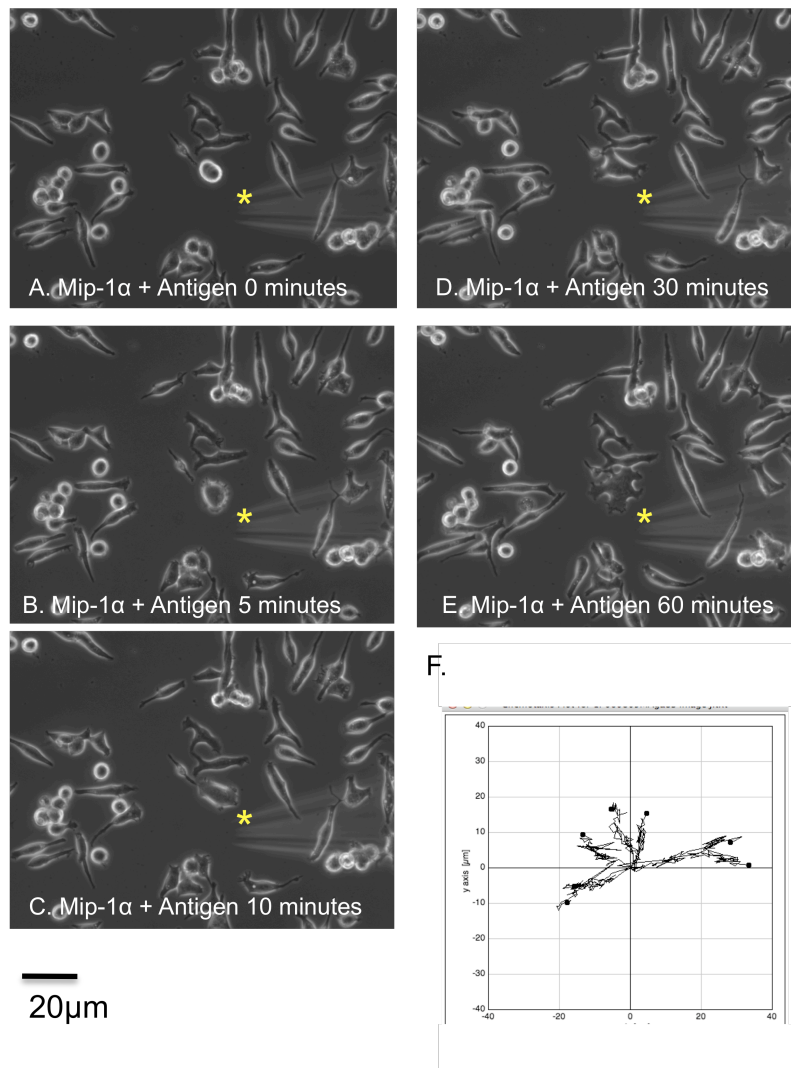


Figure 21. RBL-CCR1 chemotax towards Mip-1α and antigen.

Time-lapse video microscopy frames of RBL-CCR1 motility towards a micropipette tip (*) containing Mip-1α and antigen at timepoints (A) 0, (B) 5 minutes, (C) 10 minutes, (D) 30 minutes, (E) 60 minutes. (F) RBL-CCR1 cell migration plot depicting the path of each cell every minute for a period of 1 hour towards a micropipette tip containing Mip-1α and antigen alone. Cell traces were arranged to show their origins at x=y=0. Migration plot shown in Figure 2F is representative of 5 independent experiments

In the experiment shown in Figure 22, a micropipette (as indicated by a yellow *) filled with 50ng/ml of Mip-1 α is positioned within a field of RBL-CCR1 cells sensitised with IgE MAb. The cells appeared unresponsive and elongated in shape at the onset (Figure 22A). However, within five minutes RBL-CCR1 cells showed a varied membrane ruffling response (Figure 22B) when exposed to the micropipette Mip-1 α gradient. At ten minutes (Figure 22C) 30 minutes (Figure 22D) and 60 minutes (Figure 22E) exposure to the micropipette Mip-1 α gradient most, but not all cells were able to form lamellipodia and chemotax towards the gradient. Figure 22F shows a migrational plot representing the pathway undertaken by each RBL-CCR1 cell sensitised with IgE MAb in response to the micropipette Mip-1 α gradient in one hour. RBL-CCR1 cells were able to chemotax towards the Mip-1 α gradient, however their motility and morphological response was variable. A movie of the experiment described in this figure is available on CD1 movie file name, Mip-1a plus IgE.

These results indicate that RBL-CCR1 cells induce large membrane ruffles and are able to chemotax towards a Mip-1 α gradient. However, co-engagement of Fc ϵ R1 and CCR1 have profound effects on cell morphology and inhibit chemotaxis.

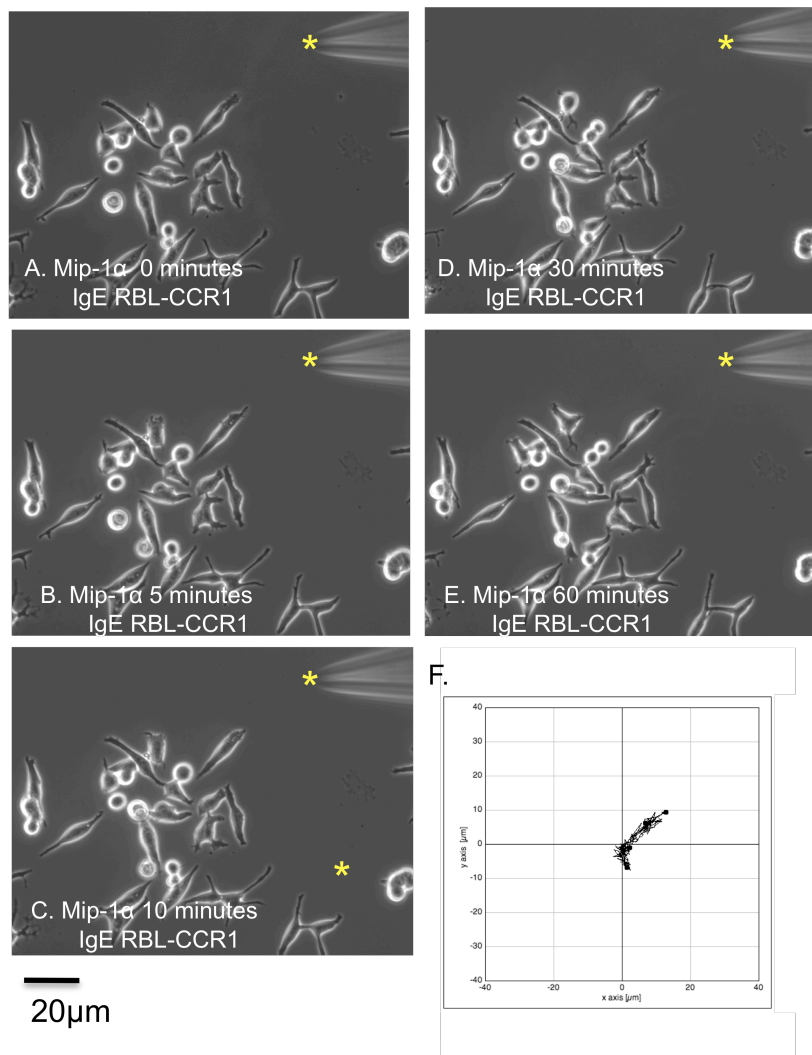


Figure 22. RBL-CCR1 sensitised with IgE chemotax towards Mip-1α.

Time-lapse video microscopy frames of RBL-CCR1 motility towards a micropipette tip (*) containing Mip-1α at timepoints (A) 0, (B) 5 minutes, (C) 10 minutes, (D) 30 minutes, (E) 60 minutes. (F) RBL-CCR1 cell migration plot depicting the path of each cell every minute for a period of 1 hour towards a micropipette tip containing Mip-1α. Cell traces were arranged to show their origins at x=y=0. Migration plot shown in Figure 2F is representative of 5 independent experiments

Figures 23A-E and table 3 show the analysis of cell motility parameters by Image J following each movie. The parameters analysed were:

1) Directionality- a value for the directionality of motion and is calculated using the following equation

$$\text{Directionality} = \text{Euclidean distance} / \text{accumulated distance}$$

2) Euclidean distance- the distance travelled from initial time (ti) to final time (tf). Figure 12 in chapter 2 materials and methods .

3) Accumulated distance- the straight line distance from initial time (ti) to final time (tf). See Figure 12 in chapter 2 materials and methods .

4) Velocity - speed

In Figure 23A, in the presence of a Mip-1 α gradient the directionality of RBL-CCR1 cells was significantly up-regulated in comparison to DMEM/PBS gradient. Interestingly, there was a significant decrease in directionality of IgE sensitised RBL-CCR1 cells in response to a Mip-1 α and antigen gradient in comparison to RBL-CCR1 cells exposed to a DMEM /PBS gradient. In Figure 23B the Euclidean distance of RBL-CCR1 cells in response to a Mip-1 α was significantly greater than that observed by DMEM /PBS gradient. However, there was a significant decrease in directionality of IgE sensitised RBL-CCR1 cells in response to a Mip-1 α and antigen gradient in comparison to RBL-CCR1 cells exposed to a DMEM/PBS gradient. In Figure 23C and 23D the accumulated distance and velocity respectively of RBL-CCR1 cells were not affected by a Mip-1 α gradient or any other conditions applied. These results indicate that a Mip-1 α gradient stimulates RBL-CCR1 cell polarisation (directionality) and this effect is not inhibited by antigen or IgE alone, but by the combination of Mip-1 α and IgE plus antigen. Although, Mip-1 α or any other combinations do not affect cell speed, Mip-1 α polarises RBL-CCR1 cells which is the reason why it increases chemotaxis.

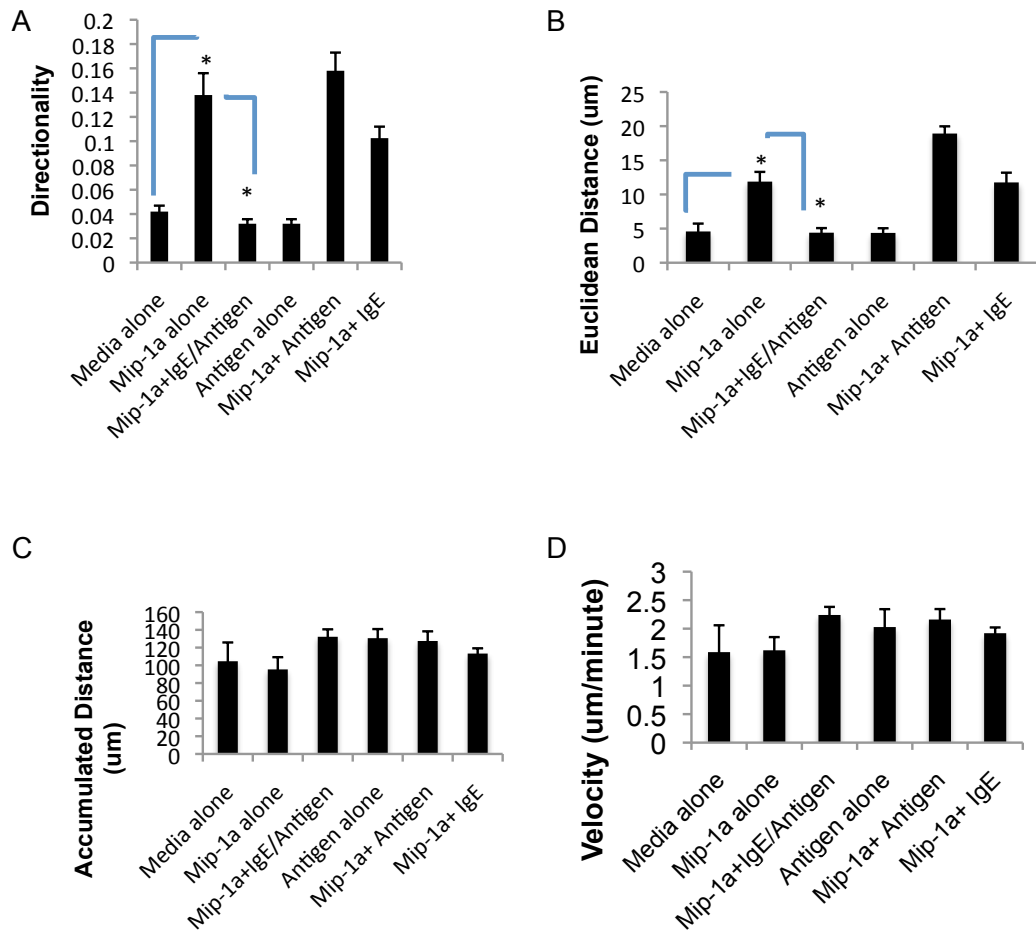


Figure 23. Motility parameters of RBL-CCR1 cells.

Motility parameters were determined using Image J. Figures 8A-D show the (A) Directionality, (B) Euclidean distance, (C) Accumulated distance and (D) velocity of RBL-CCR1 cells. The data represent the Mean +/- standard error mean (SEM) of five experiments where *, $p < 0.001$, using the student T-test.

	Media alone	Mip-1 α alone	Mip1 α +IgE/Antigen	Antigen alone	Mip-1 α + Antigen	Mip-1 α + IgE
Directionality	0.042 +/- 0.004 SEM	0.138 +/- 0.018 SEM	0.032 +/- 0.003 SEM	0.032 +/- 0.003 SEM	0.158 +/- 0.014 SEM	0.1025 +/- 0.009 SEM
Euclidean distance (um)	4.578 +/- 1.153 SEM	11.878 +/- 1.423 SEM	4.398 +/- 0.673 SEM	4.366 +/- 0.684 SEM	18.916 +/- 1.057 SEM	11.757 +/- 1.428 SEM
Accumulated distance (um)	104.584 +/- 21.199 SEM	95.37 +/- 13.792 SEM	132.186 +/- 8.411 SEM	130.6 +/- 10.279 SEM	127.424 +/- 10.909 SEM	113.252 +/- 5.940 SEM
Velocity (um/minute)	1.588 +/- 0.471 SEM	1.62 +/- 0.231 SEM	2.24 +/- 0.142 SEM	2.028 +/- 0.313 SEM	2.16 +/- 0.183 SEM	1.92 +/- 0.101 SEM

Table 3. Summary of cellular effects (motility parameters) from the pipette assays of RBL-CCR1 cells

3.2.3 Localisation of PI(3,4,5)P3 in RBL-CCR1 cells in response to a Mip-1 α gradient

The lipid product PI(3,4,5)P3, is a well known candidate for establishing cell polarity. The PH-AKT-GFP probe accumulates within seconds at the leading edge of polarised neutrophils responding to a chemoattractant (Servant et al., 2000). This asymmetric localisation activates Rho GTPases, which ultimately drives actin polymerization inducing subcellular processes such as lamellipodia, pseudopods, filopodia, membrane ruffling, and subsequently chemotaxis. Although the asymmetric localization of PI(3,4,5)P3 at the leading edge has been reported in many cells types, it is not known whether PI(3,4,5)P3 plays a role in mast cell polarization and chemotaxis.

The objective of these experiments was to examine the localisation of PI(3,4,5)P3 in RBL-CCR1 cells in response to a Mip-1 α gradient, and thereby determine whether directed cell movement in mast cells is via a PI(3,4,5)P3 mediated pathway. RBL-CCR1 cells stably expressing PH-AKT-GFP probe were exposed to a micropipette containing 50ng/ml of Mip-1 α . For each experiment a minimum of three cells were recorded every five seconds for ten minutes using real time fluorescent microscopy. The data are representative of two separate experiments with at least two cells analysed in each movie.

As shown in Figure 24A, unstimulated RBL-CCR1 are pod shaped elongated cells, in which PI(3,4,5)P3 was localised throughout the cytoplasm and nucleus. Cell a stimulated with 50ng/ml of Mip-1 α for five seconds showed a flattened morphology with PI(3,4,5)P3 localised around the cell membrane(as indicated by the white arrow) (Figure 24B) and further stimulation with Mip-1 α for ten seconds showed increased PI(3,4,5)P3 localisation around the cell membrane (Figure 24C). By one minute, cell a continued to show a flattened morphology with intense membrane ruffles, PI(3,4,5)P3 localised to, and was highly concentrated on the membrane ruffles at the leading edge (as indicated by the red arrow) (Figure 24D). By two minutes cells began to polarise, PI(3,4,5)P3 remained localised around the cell membrane (Figure 24E). At five minutes stimulation RBL-CCR1 cells showed a polarised phenotype, with a large distinct membrane ruffle and lamellipodia. Interestingly PI(3,4,5)P3 re-localised to the edge of the lamellipodia nearest the Mip-1 α gradient (Figure 24F). Moreover, at seven minutes stimulation PI(3,4,5)P3

expression was no longer observed within the large lamellipodia, but was now observed at the cell membrane (Figure 24G).

Unfortunately, as RBL-CCR1 cells no longer stably expressed the PH-AKT-GFP probe it was not possible to quantitate the localisation of PI(3,4,5)P3 in these experiments, nor examine how the localisation of PI(3,4,5)P3 was affected by co-stimulation of CCR1 and FcεR1 by Mip-1α and IgE/Ag respectively. As it was not possible to detect PI(3,4,5)P3 in RBL-CCR1 Cells using a specific PI(3,4,5)P3 antibody it was decided that the role of WASP, also a mediator of cell polarisation would be examined instead of PI(3,4,5)P3 for subsequent experiments.

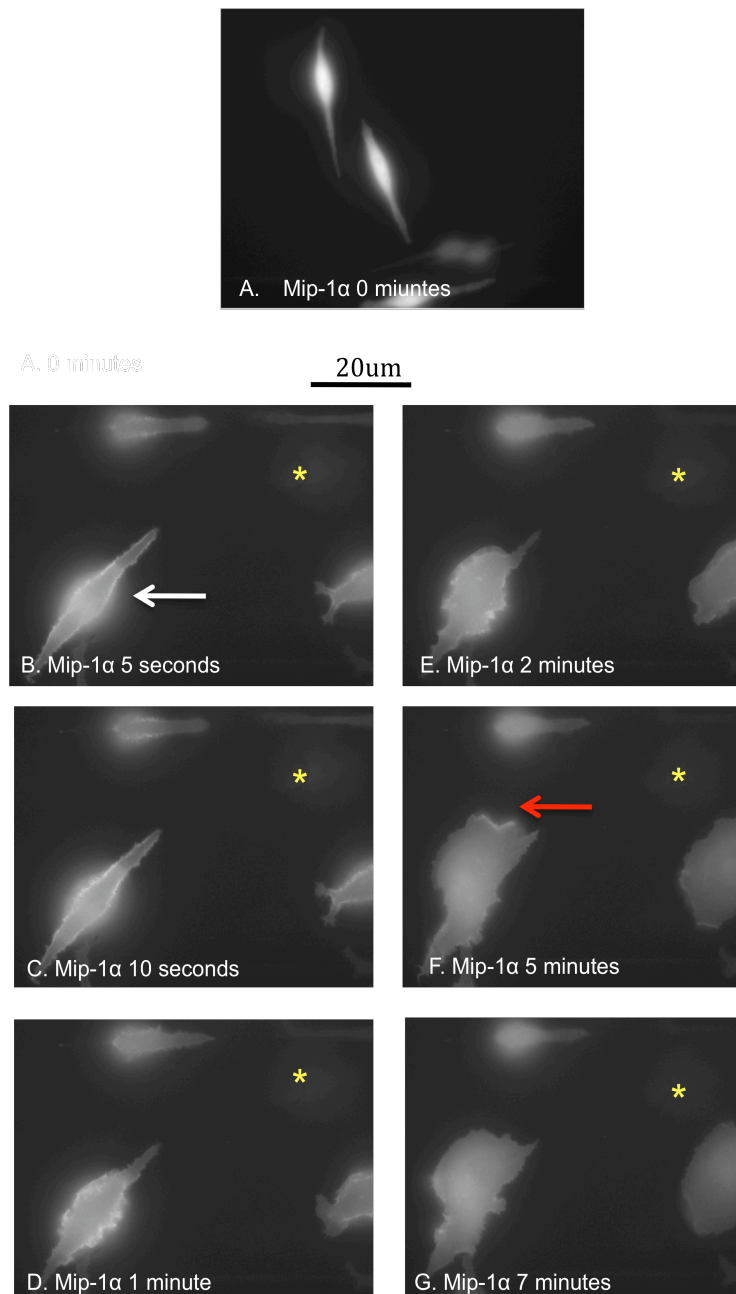


Figure 24. Localisation of PI(3,4,5)P3 at the leading edge of RBL-CCR1 cells in response to a Mip-1 α gradient. The PH domain of AKT tagged to GFP was used to detect PIP3 localisation in RBL-CCR1 cells. Stably expressing GFP-AKT-RBL-CCR1 cells were exposed to a micropipette (*) containing Mip-1 α at time points (A) 0 (B) 5 seconds (C) 10 seconds (D) 1 minute (E) 2 minutes (F) 5 minutes (G) 7 minutes. The white arrow shows localisation of PIP3 at the cell membrane at 5 seconds, while the red arrow shows the localisation of PIP3 at the leading edge at 5 minutes in one RBL-CCR1 cell in response to Mip-1 α . Figures 23A-H are representative of two independent experiments.

3.2.4 Localisation of CCR1, actin and WASP in RBL-CCR1 cells in response to a Mip-1 α gradient

A mechanism for the spatial organisation of chemokine receptors on the leukocyte cell surface following chemokine stimulation that would allow for the detection of, and subsequent chemotaxis towards a chemokine gradient remains unclear. Both symmetrical and asymmetrical distributions of chemokine receptors have been observed on the cell surface following chemokine receptor stimulation (Servant et al., 1999; Gomez-Mouton et al., 2004). Moreover, distinct localisation of CCR1 on membrane ruffles in RBL-2H3 cells following stimulation with Mip-1 α has been reported (Beer et al., 2007). WASP has been implicated in several biological processes that involve actin cytoskeletal organisation. Myers et al., (2005) previously showed localization of WASP at the leading edge of chemotaxing *Dictyostelium* cells, however to date, the localisation of WASP at the leading edge of chemotaxing mast cells responding to Mip-1 α is yet to be elucidated.

The objective of these experiments was to examine the localisation of CCR1, actin and WASP in response to a Mip-1 α gradient in RBL-CCR1 cells. RBL-CCR1 cells were exposed to a micropipette containing either 50ng/ml of Mip-1 α for 5, 10 and 20 minutes, or with DMEM/PBS for 20 minutes. RBL-CCR1 cells were fixed with PFA and stained for CCR1, actin and WASP. For each experiment a minimum of 10-15 cells were recorded every minute for 20 minutes using real time microscopy. The data are representative of five separate experiments with at least 10-15 cells analysed in each.

In the experiment shown in Figure 25, a micropipette (as indicated by a yellow *) filled with DMEM media plus PBS was positioned within a field of RBL-CCR1 cells for a the duration of 20 minutes. Figure 25A shows RBL-CCR1 cells are elongated pod shaped cells at the onset of the experiment. Cells exposed to DMEM/PBS micropipette showed a flattened morphology and were unresponsive, displaying no membrane ruffling or cell polarization (Figure 25B-E). Cells displayed CCR1 expression at the cell membrane (Figure 25B) and diffuse actin expression (Figure 25C). WASP was expressed throughout the cytoplasm and cell surface of the cells (Figure 25D). Figure 25E shows the co-localisation of CCR1 (red), actin (blue) and WASP (green), where the periphery of the cells were yellow (co-localisation of CCR1 and actin) and the cell body aqua (co-localisation of actin and WASP).

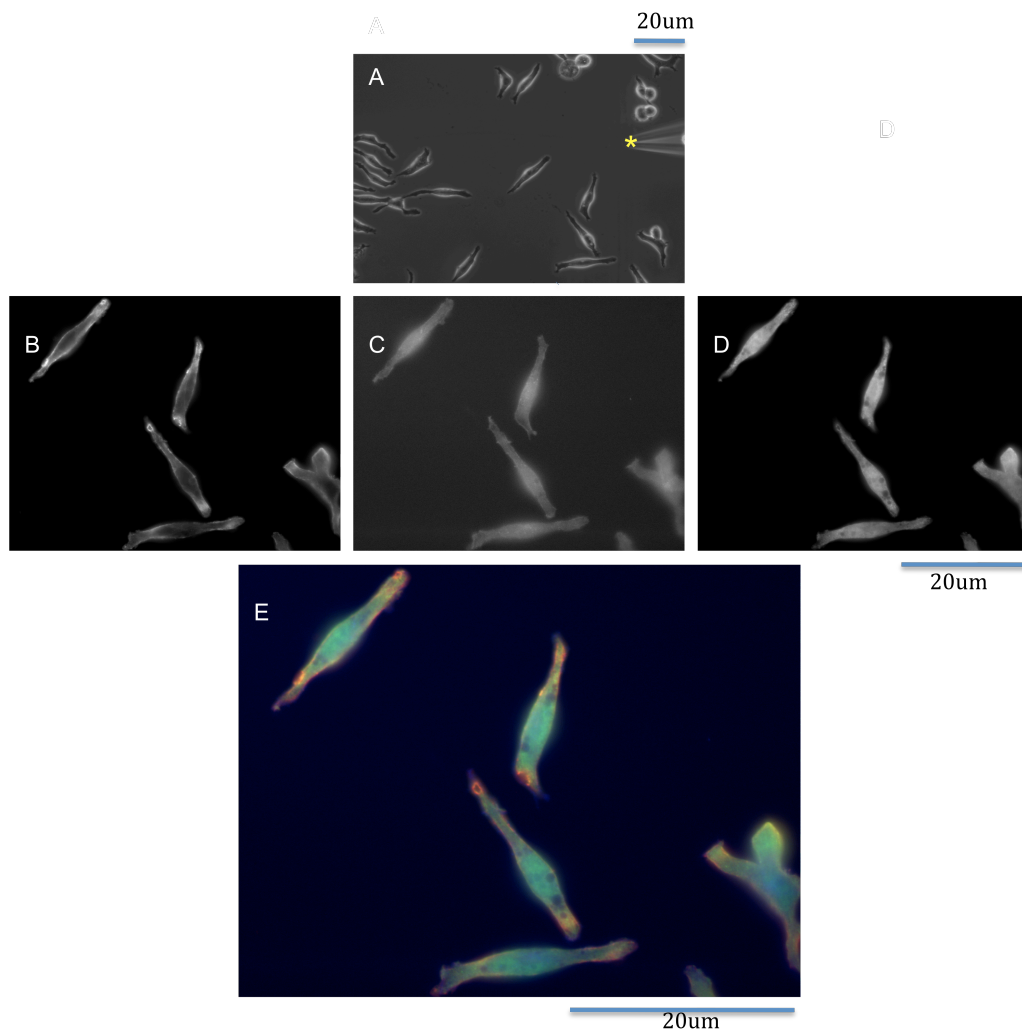


Figure 25. In response to a pipette of PBS/DMEM for 20 minutes CCR1 localises at the cell membrane, whilst actin and WASP remain throughout the cytoplasm of RBL-CCR1 cells. (A) Time-lapse video microscopy frames of RBL-CCR1 motility towards a micropipette tip (*) containing PBS/DMEM media. Images were recorded every minute for 20 minutes, cells were then fixed and stained for (B) CCR1, (C) Actin and (D) WASP. (E) co-localisation of CCR1(red), actin(blue), WASP (green). The figures shown are representative of five independent experiments.

In the experiment shown in Figure 26, a micropipette (as indicated by a yellow *) filled with 50ng/ml of Mip-1 α is positioned within a field of RBL-CCR1 cells for the duration of 5 minutes. Figure 26A shows at the onset of the experiment RBL-CCR1 cells are elongated pod shaped cells. Cells exposed to the Mip-1 α gradient displayed distinct polarised membrane ruffles and lamellipodia (Figure 25B-E). CCR1 (Figure 26B), actin (Figure 26C) and WASP (Figure 26D) were localised and enriched in the polarised membrane ruffles and lamellipodia that occurred on the side of the pipette. In addition, WASP localised to the nucleus. Figure 26E shows the co-localisation of CCR1 (red), actin (blue) and WASP (green).

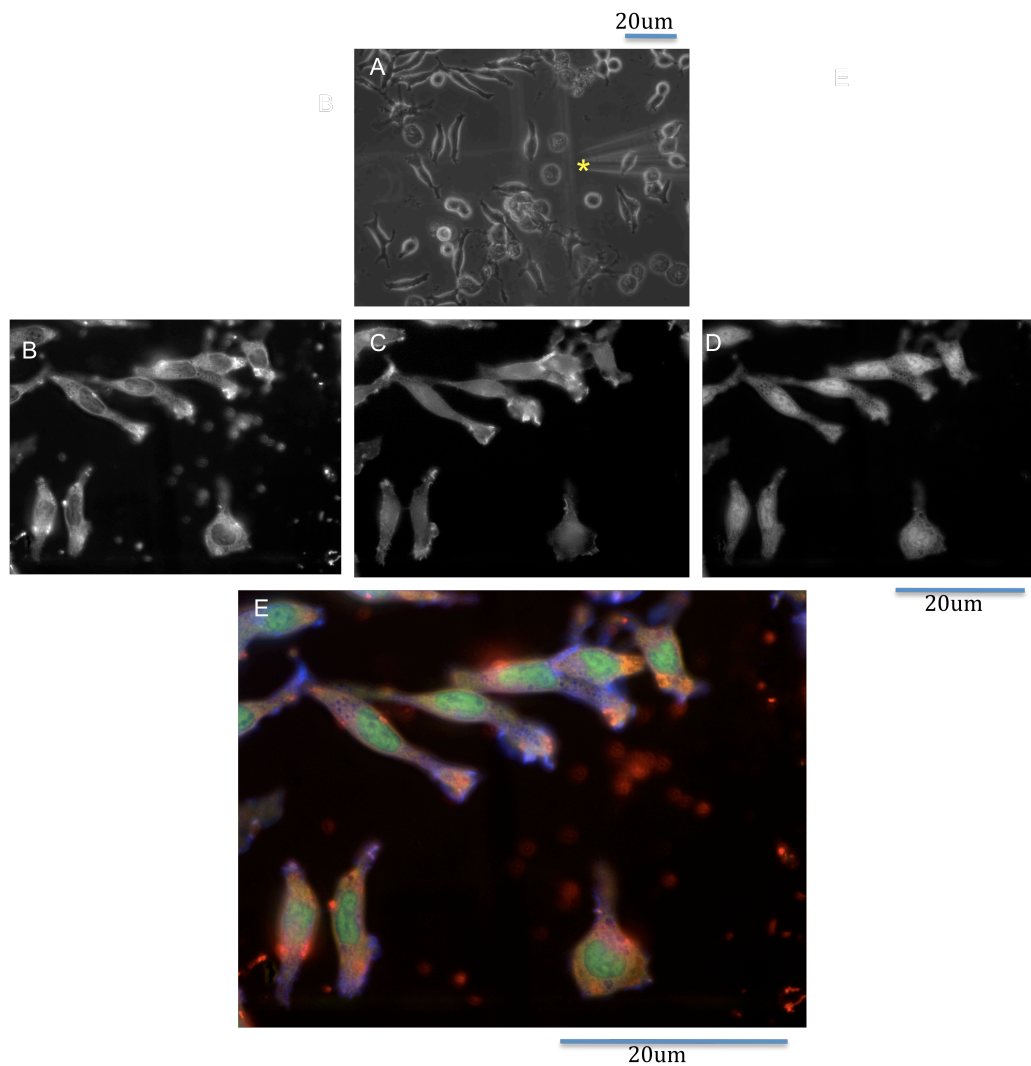


Figure 26. In response to a pipette of Mip-1 α for 5 minutes. CCR1, actin and WASP localise in the polarised membrane ruffles and lamellipodia of RBL-CCR1 cells. (A) Time-lapse video microscopy frames of RBL-CCR1 motility towards a micropipette tip (*) containing Mip-1 α . Images were recorded every minute for 5 minutes, cells were then fixed and stained for (B) CCR1, (C) Actin and (D) WASP. (E) co-localisation of CCR1(red), actin(blue), WASP (green).The figures shown are representative of five independent experiments.

In the experiment shown in Figure 27, a micropipette (as indicated by a yellow *) filled with 50ng/ml of Mip-1 α is positioned within a field of RBL-CCR1 cells for the duration of 10 minutes. Figure 27A shows at the onset of the experiment RBL-CCR1 cells are elongated pod shaped cells. Cells exposed to the Mip-1 α gradient for ten minutes displayed intense polarised membrane ruffles and lamellipodia (Figure 27B-E). CCR1 began to internalise (Figure 27B), actin continued to localise in the polarised membrane ruffles (Figure 27C) and WASP was no longer concentrated at the polarized membrane ruffles but remained in the nucleus (Figure 27D). Figure 27E shows the co-localisation of CCR1 (red), actin (blue) and WASP (green).

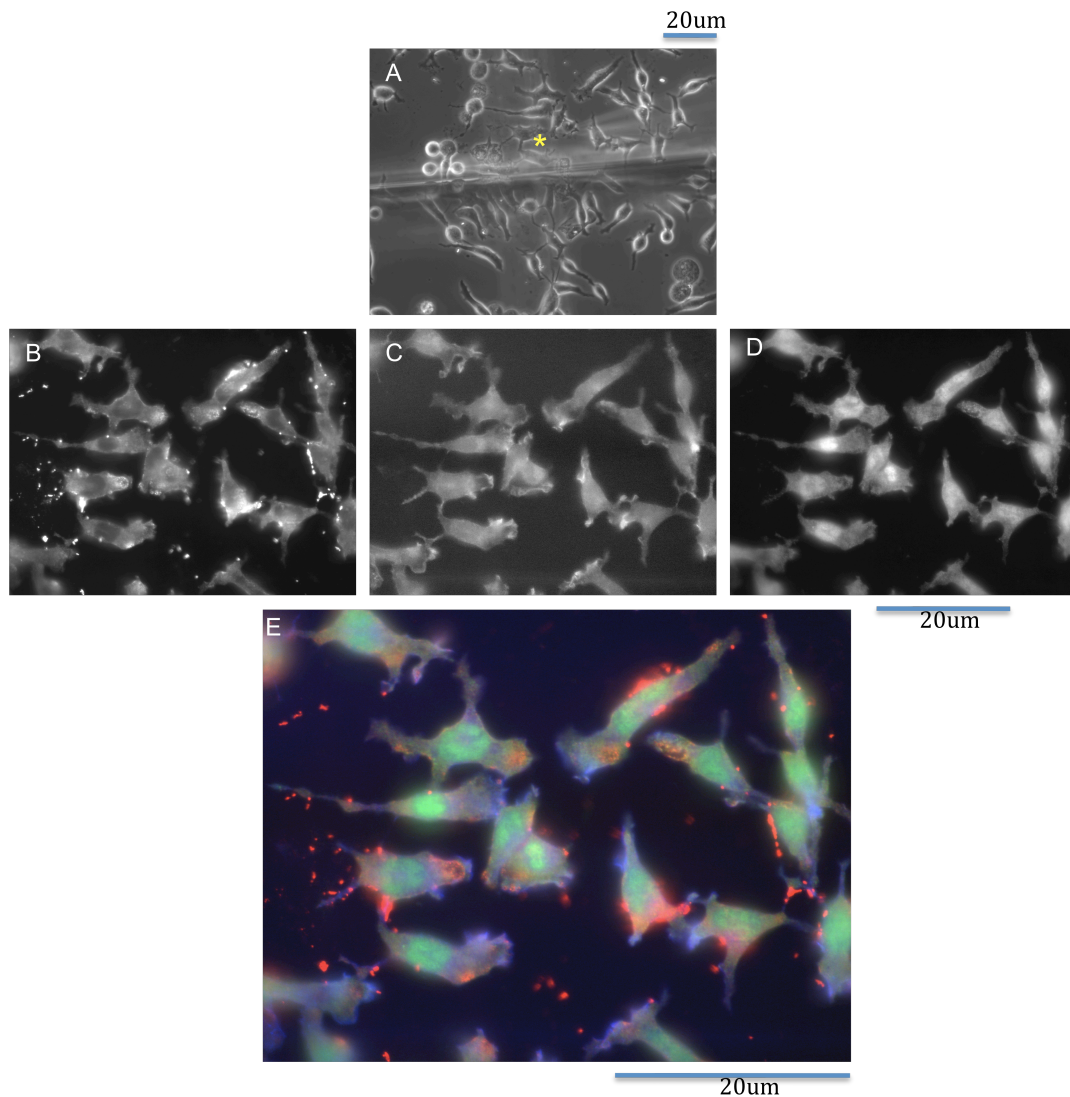


Figure 27. In response to a pipette of Mip-1 α for 10 minutes, CCR1 begins to internalise. Actin remains localised in the polarised membrane ruffles and lamellipodia, whilst WASP now re locates from the polarised membrane ruffles to the cytoplasm and nucleus of RBL-CCR1 cells.

(A) Time-lapse video microscopy frames of RBL-CCR1 motility towards a micropipette tip (*) containing Mip-1 α . Images were recorded every minute for 10 minutes, cells were then fixed and stained for (B) CCR1, (C) Actin and (D) WASP. (E) Co-localisation of CCR1(red), actin(blue), WASP (green).

The figures shown are representative of five independent experiments.

In the experiment shown in Figure 28, a micropipette (as indicated by a yellow *) filled with 50ng/ml of Mip-1 α is positioned within a field of RBL-CCR1 cells for the duration of 20 minutes. Figure 28A shows at the onset of the experiment RBL-CCR1 cells are elongated pod shaped cells. Cells exposed to the Mip-1 α gradient for 20 minutes showed a flattened morphology with reduced membrane ruffles (Figure 28B-E). CCR1 expression was no longer internalised but was now at the cell membrane (Figure 28B) while actin expression was diffuse throughout the cytoplasm (Figure 28C). WASP was no longer concentrated at the polarized membrane ruffles, but was localised within the nucleus (Figure 28D). Figure 28E shows the co-localisation of CCR1 (red), actin (blue) and WASP (green), in which CCR1, actin and WASP expression was comparable to that observed in response to a DMEM/PBS gradient.

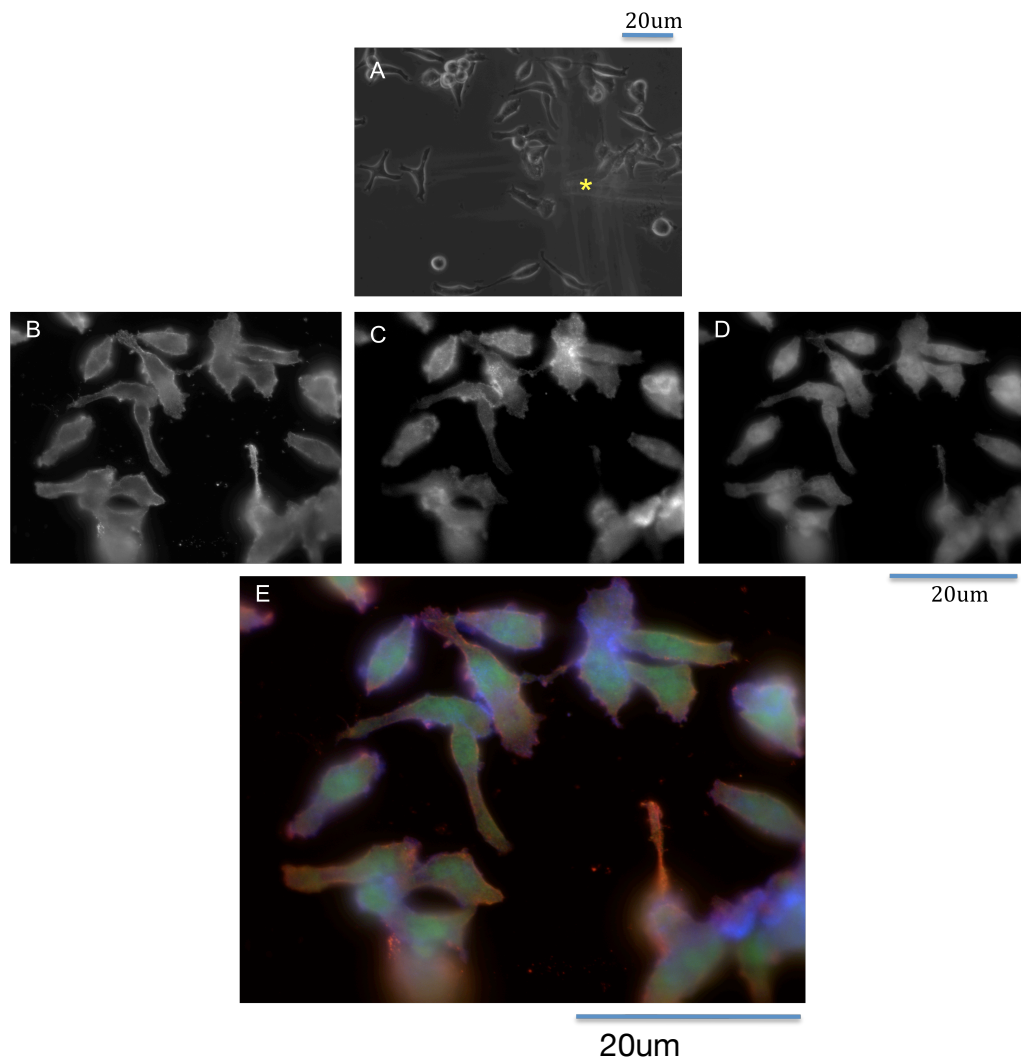


Figure 28. In response to a pipette of Mip-1 α for 20 minutes. CCR1 localises at the cell membrane. Actin begins to re-localise from the polarised membranes to the cytoplasm, whilst WASP localises throughout the cytoplasm and nucleus of RBL-CCR1 cells. (A) Time-lapse video microscopy frames of RBL-CCR1 motility towards a micropipette tip (*) containing Mip-1 α . Images were recorded every minute for 20 minutes, cells were then fixed and stained for (B) CCR1, (C) Actin and (D) WASP. (E) Co-localisation of CCR1(red), actin(blue), WASP (green). The figures shown are representative of five independent experiments.

3.3 Discussion

The ability of mast cells to chemotax towards sites of inflammation and parasitic infection, and the subsequent release of pro-inflammatory mediators is crucial process in allergic inflammation. A former study by Toda et al., (2004), demonstrated that engagement of Fc ϵ R1 and CCR1 receptor synergistically enhanced degranulation in mast cells and also exhibited profound effects on chemotaxis and cell morphology, indicating cross-talk between Fc ϵ R1 and CCR1 signalling pathways. In addition, the PI3K inhibitor, Wortmannin significantly inhibited synergistic degranulation of RBL-CCR1 cells suggesting that this pathway is mediated via PI3K. In this light the aim of this chapter was to further define the effects of Fc ϵ R1 and CCR1 engagement on cell motility.

Actin reorganisation in RBL-CCR1 cells induced by homogeneous co-stimulation by Mip-1 α and IgE/antigen

A crucial component of cell motility towards chemoattractants requires the reorganisation of the actin cytoskeleton, induction of membrane ruffling and cell polarisation. Fc ϵ RI engagement has an inhibitory effect on Mip-1 α -induced chemotaxis (Toda et al., 2004), indicating that co-stimulation with Mip-1 α and IgE/antigen affect reorganisation of actin cytoskeleton of RBL-CCR1 cells. Therefore, on this basis the first objective was to analyse the effects of co-stimulation by Mip-1 α and IgE/antigen on actin reorganisation in RBL-CCR1 cells. The data from this study demonstrates that Mip-1 α stimulation rapidly induced profound membrane ruffles and cell polarisation. However, co-stimulation with Mip-1 α and IgE/antigen decreased the membrane ruffling response of RBL-CCR1 cells. This data suggests that engagement by Fc ϵ R1 inhibits the reorganisation of the actin cytoskeleton. Moreover, this may also explain the inhibitory effect on Mip-1 α induced chemotaxis of RBL-CCR1 cells in response to co-stimulation. Toda et al.,(2004) demonstrated that Mip-1 α -mediated chemotaxis of RBL-CCR1 cells requires activation of the Rho pathway. Moreover they showed that costimulation with Mip-1 α and IgE/antigen enhanced Rac and Cdc42 activation but decreased ROCK activation in RBL-CCR1 cells. Decreased ROCK activation may also be a mechanism by which Fc ϵ R1 engagement inhibits actin reorganisation and hence Mip-1 α -mediated chemotaxis of RBL-CCR1 cells.

Behavioural responses of RBL-CCR1 Cells to gradients of Mip-1 α and IgE/antigen co-stimulation using real time microscopy

Since the beginning of the 21st century it has been possible to characterise the dynamic behaviour of immune cells using time lapse video microscopy (Cantrell et al., 2002; Mempel et al., 2004; Looney et al., 2011; Sergé et al., 2011). However, how RBL-CCR1 cell shape changes relate to actual motility is at present poorly understood. In order to analyse the effects of co-stimulation on RBL-CCR1 morphology and motility, a series of experiments using time-lapse video microscopy were conducted to observe the behaviour and other cell motility parameters such as: directionality, Euclidean distance, accumulated distance and velocity of RBL- CCR1 cells in response to Mip-1 α and IgE/antigen or Mip-1 α alone.

The current model of cell motility is frequently described as a multistep process, in which, F-actin polymerization at the front of the cell pushes out a membrane protrusion such as lamellipodia that subsequently becomes anchored to an extracellular substrate by transmembrane receptors of the integrin family. Integrins are dynamically coupled to the actin cytoskeleton and translate the internal force that is generated when myosin II contracts the actin network. The data from my study demonstrates that RBL-CCR1 cells, induce actin polymerization and chemotax towards a Mip-1 α gradient and this response is inhibited by CCR1 and Fc ϵ R1 co-stimulation. Although the leading edges of RBL-CCR1 cells remained dynamic and protruded with normal speed towards Mip-1 α gradient, RBL-CCR1 cells were unable to move their trailing edges, nevertheless, Mip-1 α gradient was still able to polarize the RBL-CCR1 cell population. Does the trailing edge contraction contribute to overall RBL-CCR1 cell body locomotion? This functional dissociation between front and back of Mip-1 α stimulated RBL-CCR1 cells demonstrates that the leading edge migrates independently and without a need for receptor-mediated coupling of contractile forces to the extracellular matrix. However, to further validate this explanation future studies should analyse the response of RBL-CCR1 cells towards a Mip-1 α gradient and CCR1 and Fc ϵ R1 co-stimulation in the presence of extracellular matrix proteins such as Collagen Type1 and Type IV, and the role of integrins during this process. Previous studies using fibroblasts and leukocytes moving on 2D substrates, demonstrate that myosin contraction at the back of the cell is required to disassemble receptor binding-sites and subsequently retract the membrane (Palecek et al., 1996; Lauffenburger and

Horwitz, 1996; Hogg et al., 2003; Morin et al., 2008). However, contrary to this, Lammermann et al., (2008) did not observe membrane tethers in myosin II-inhibited leukocytes migrating in 3D gels. Moreover, chemotactic dendritic cells mechanically adapt to the adhesive properties of their substrate by switching between integrin-mediated and integrin-independent locomotion (Renkawitz et al., 2009). Another explanation for the lack of moving distance displayed by RBL-CCR1 cells (in real time microscopy) possibly relates to the functional role and biology of mast cells, in that within an inflamed tissue, maybe it is not necessary for mast cells to move large distances to function, it could be that mast cells only need to chemotax short distances before exhibiting effector function. This data would fit in with findings by Toda and co-workers (2004), where we show that although RBL-CCR1 cells are able to chemotax towards Mip-1 α using a Boyden chamber assay, these cells transmigrate through a very thin porous membrane, thereby moving very small distances.

Leukocytes are dispersed throughout the body and have the potential to infiltrate any type of tissue. They frequently exhibit cell migration velocities that are up to 100 times faster than mesenchymal and epithelial cell types (Friedl, P. et al., 2004; Pittet & Mempel, 2008). At present there is no data indicating the relative velocity of mast cells during an allergic response, however, it would be expected, that mast cells would move extremely quickly as the first line of defence towards a chemokine gradient and a roaming pathogen or allergen, and then stop and accumulate. The data in this study shows that RBL-CCR1 cells respond within seconds to a Mip-1 α gradient, however, surprisingly, there were no significant changes in velocity when Mip-1 α mediated chemotaxis was inhibited by Mip-1 α and IgE/antigen. This data indicates that while Mip-1 α does not affect cell speed, Mip-1 α polarises RBL-CCR1 cells, which is the reason why it increases chemotaxis. Renkawitz et al., (2009) demonstrated that dendritic cells that lacked all integrin heterodimers induced velocities of up to 20 $\mu\text{m min}^{-1}$ in 100% of cells, whereas only 8% of wild-type cells had maximum flow rates of 5 $\mu\text{m min}^{-1}$. They showed that accelerated velocities was balanced by an increased actin polymerization rate, therefore, cell shape and velocity remained constant on alternating substrates. With this information at hand, it is not known at present, whether integrin depletion would affect RBL-CCR1 velocity in the presence of Mip-1 α or co-stimulation by Mip-1 α and IgE/antigen.

Localisation of PI(3,4,5)P3 in RBL-CCR1 cells in response to a Mip-1 α gradient

The accumulation of PI(3,4,5)P3, as a result of PI3K activity, along the leading edge of a chemotaxing cell (Funamoto et al., 2001; Huang et al., 2003; Merlot and Firtel, 2003; Sasaki et al., 2004) has been proposed to be an indispensable signaling event that is required for cells to undergo chemotaxis towards chemoattractants. Although PI(3,4,5)P3 has been demonstrated to be a central component in the chemotaxis of some cell types, it is not clear whether PI(3,4,5)P3 accumulation, and hence the PI3K pathway is a universal pathway for chemotaxis, or a pathway only used by certain cell types and chemoattractants. On this basis, the aim of these experiments was to examine the localisation of PI(3,4,5)P3 in RBL-CCR1 cells (using RBL-CCR1 cells stably expressing PH-AKT-GFP probe) in response to a Mip-1 α gradient, and thereby determine whether directed cell movement in mast cells is PI(3,4,5)P3 dependent. This study shows that PI(3,4,5)P3 is rapidly localized along the leading edge of RBL-CCR1 cells in response to a Mip-1 α gradient. Unfortunately, as RBL-CCR1 cells no longer stably expressed the PH-AKT-GFP probe it was not possible to quantitate PI(3,4,5)P3 accumulation at the leading edge, nor examine the localisation of PI(3,4,5)P3 by co-stimulation of CCR1 and Fc ϵ R1 engagement, and hence this data needs to be interpreted with caution. Nevertheless, PI(3,4,5)P3 accumulation along the leading edge of RBL-CCR1 cells indicates one potential mechanism of mast cell polarization and Mip-1 α -mediated chemotaxis. In addition, previous data showing inhibition of RBL-CCR1 degranulation by the non-specific PI3K inhibitor, Wortmannin, indicates that this effect is PI3K mediated.

Localisation of CCR1, actin and WASP in RBL-CCR1 cells in response to a Mip-1 α gradient

The formation of membrane ruffles and lamellipodia as a result of actin polymerisation are fundamental components of the cytoskeleton rearrangements required for cell motility and chemotaxis. Following chemokine stimulation, at present there are two chemokine receptor localisation patterns, an asymmetrical and symmetrical distribution observed on the cell surface (Servant et al., 1999; Gomez-Mouton et al., 2004). Our finding that CCR1 localises on the membrane ruffles of RBL-CCR1 stimulated with chemotactic concentrations of Mip-1 α (Beer et al., 2007) suggests the possibility by which RBL-CCR1 might localise or up

regulate their chemokine receptors on the surface of membrane ruffles in order to detect a chemokine gradient. WASP family members function as scaffold proteins, transducing a wide range of signals from proteins or membranes to mediate dynamic changes in the actin cytoskeleton. Cdc42 appears to control actin polymerization through the interaction with WASP, (Aspenstrom et al., 1996; Symons et al., 1996; Insall and Machesky, 2009; Monypenny et al., 2011), an activator of the actin nucleating Arp2/3 complex (Machesky and Gould, 1999).

Given the unstable nature of the GFP-AKT-RBL-CCR1 cell line it was not possible to conduct further analysis of PI(3,4,5)P3 localisation in response to a Mip-1 α gradient in these cells. Hence, the next question to ask was whether WASP was targeted to sites of new actin polymerization and the leading edge of chemotaxing RBL-CCR1 cells in response to a Mip-1 α gradient. In light of this information the objective of these experiments was to investigate CCR1, WASP and actin localisation in cells fixed at varying time points following stimulation with a Mip-1 α gradient. This would allow one to investigate the spatiotemporal distribution of the receptor over the course of initial stimulation, polarisation and chemotaxis. My findings show that upon stimulation by a gradient of Mip-1 α , CCR1 co-localised to sites of new actin polymerisation- the polarised membrane ruffles and lamellipodia that occurred on the side of the pipette. Interestingly, WASP localisation was also observed, along with CCR1 at the polarized membrane ruffles. With regards to this data, actin polymerisation of RBL-CCR1 cells in the presence of a Mip-1 α gradient is mediated by WASP and the localisation of CCR1 on membrane ruffles at the leading edge of RBL-CCR1 may facilitate the accurate detection of a chemokine gradient and allow for subsequent chemotaxis along it. Prolonged exposure of Mip-1 α gradient to RBL-CCR1 induces CCR1 internalisation and exclusion of WASP from the polarised actin rich ruffles and nucleus, suggesting a transient role of WASP during this process.

Chapter 4.

The effect of Fc ϵ RI and chemokine co-engagement on mast cell motility in murine allergic conjunctivitis

4. The effect of Fc ϵ RI and chemokine co-engagement on mast cell motility in murine allergic conjunctivitis

4.1 Introduction and hypothesis

During an allergic response directed migration is essential at several stages such as: mast cell progenitor movement from the bone marrow, recruitment through venules into the tissue and migration within the tissue. Reduction of mast cell accumulation at sites of inflammation would subsequently reduce mast cell activation at these sites. At present, how mast cells migrate *in vitro* and *in vivo* is very poorly understood compared to other cell types. Nevertheless, compiling together *in vitro* and *in vivo* observations will contribute to our understanding of mast cell migration, and thereby identify potential therapeutic agents. Chapter 3 of this thesis demonstrated that *in vitro*, RBL-CCR1 cells chemotax towards Mip-1 α , exhibiting profound membrane ruffles and actin cytoskeleton re-organisation. In addition, Mip-1 α mediated RBL-CCR1 chemotaxis demonstrated specific localisation of actin, CCR1 and WASP at the leading edge (edge nearest to chemokine gradient) of polarised cells, correlating with the localisation dynamics and morphological changes demonstrated in other chemotaxing cell types.

Based on current knowledge, I hypothesise that *in vivo* conjunctival murine mast cells can chemotax towards chemokine, with morphological changes and localisation of actin, CCR1 and WASP at the leading edge of polarised mast cells following allergen challenge.

To address this hypothesis, the specific aims of this chapter are as follows: -

1. To establish a model of murine allergic conjunctivitis so as to mimic ocular allergic diseases.
2. To analyse the morphology of mast cells in an inflamed (chemokine gradient present) and non-inflamed (no chemokine gradient present) murine conjunctiva.
3. To determine the kinetics of mast cell accumulation in an inflamed (chemokine gradient present) and non-inflamed (no chemokine gradient present) murine conjunctiva.

4. To investigate the localisation of WASP, CCR1 and actin in mast cells in an inflamed conjunctiva (chemokine gradient present) and non-inflamed conjunctiva (no chemokine gradient present).

4.2 Results

4.2.1 Murine models of allergic conjunctivitis

In the present study A/J and BALB/c mice were used to induce models of allergic conjunctivitis as these strains readily induce Th2 responses and are routinely used to mimic ocular allergic disease in man.

With the aid of an ophthalmologist, Mr. Tom Flynn (London), it was possible to establish a murine model of allergic conjunctivitis using A/J mice. In brief, the mouse was sensitised over a 15-day period with SRW and Alum. This was followed by experimental allergen challenge with SRW pollen by eye drops thereby inducing an inflammatory response (which would include a chemokine gradient and the release of pro-inflammatory mediators) and subsequent allergic conjunctivitis. The SRW sensitised-challenged mice showed the following symptoms; conjunctival oedema; lid oedema; redness; tearing; squinting, which reflect distinctive characteristics of the inflammatory response, and are employed as the evaluation criteria when scoring murine allergic conjunctivitis. In comparison, the sensitised non-challenged and non-sensitised, non-challenged mice did not display any of the above symptoms. (Figure 29).

Thereafter, eyes were enucleated from A/J mice and processed as either resin sections to analyse morphological changes in conjunctival mast cells by electron microscopy or cryostat serial sections to analyse kinetics of conjunctival mast cell accumulation and the localisation of actin, CCR1 and WASP in these cells. Unfortunately these experiments using A/J mice could not be completed at UCL (London), due to my extended 1.5 year absence for medical reasons and my supervisor Professor Ono leaving for the United States of America (U.S). Therefore all animal work had to be terminated. As a result, I completed the remaining aims of this chapter in Professor Ono's new laboratory in the U.S, where Dr. Obayashi (Professor Ono's post-doctoral scientist) established a murine model of allergic conjunctivitis, using BALB/c mice instead of A/J mice. Thereafter, the eyes were enucleated from BALB/c mice and processed as paraffin sections, which were used in subsequent experiments to address the same aims as those implemented for A/J mice.

Please note that although two different models were used in this study both successfully induced allergic conjunctivitis. In addition, other differences between these models were the time points of final SRW challenge and the method utilised for mast cell identification.

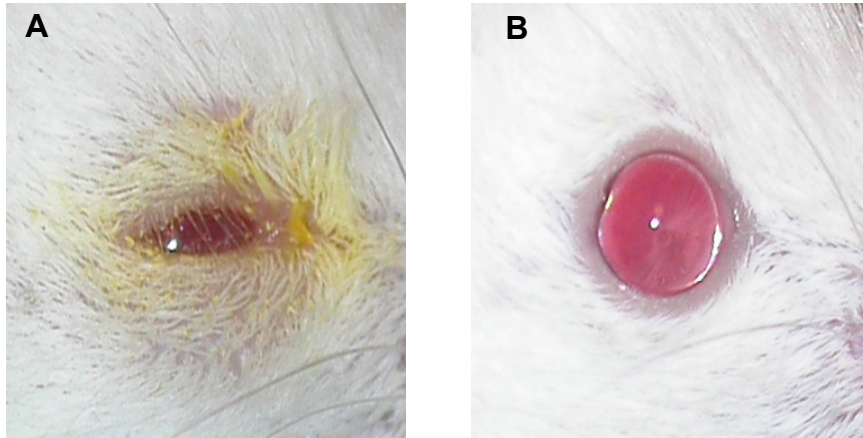


Figure 29. Symptoms of murine allergic conjunctivitis. A/J mice indicating (A) severe allergic conjunctivitis with short ragweed pollen (B) non-diseased eye with control PBS. The diseased eyes in comparison to non-diseased eyes displayed the following symptoms; conjunctival edema; lid edema; redness; tearing; squinting,

4.2.2 Behavioural and morphological responses of murine conjunctival mast cells in inflamed conjunctiva.

In order to fully understand the mechanisms of mast cell chemotaxis, the initial starting point is to characterise the behaviour and morphology of the cells *in vitro*. Chapter 3 of this thesis examined the morphological responses of RBL-CCR1 cells in response to Mip-1 α and IgE/antigen co-stimulation *in vitro* using real time microscopy. In light of this the objective of these experiments was to characterise by electron microscopy the morphological responses of mast cells in SRW sensitised-challenged, sensitised non-challenged or non-sensitised non-challenged conjunctiva *in vivo* using an A/J murine model of allergic conjunctivitis. The figures are representative of five separate experiments with at least 3-5 eyes analysed in each.

Figure 30A shows an electron micrograph representing mast cells from sensitised non-challenged or non-sensitised non-challenged conjunctiva of A/J mice. The mast cells are pod shaped elongated cells comprising numerous tightly packed black histamine containing granules. In contrast, conjunctival mast cells from the A/J murine model of allergic conjunctivitis three hours post sensitised-challenged with SRW, appeared stretched in shape with numerous branching filopodia extending from the cell membrane. The black histamine containing granules were no longer tightly packed within the cell cytoplasm. Some granules were clearly being exuded from the cell, a recognised feature indicating activation and degranulation, which is characteristic of the early phase response. (Figure 30B). At nine hours post sensitised-challenged with SRW, conjunctival mast cells were comparable in morphology to that observed at three hours post sensitised-challenged. However, in addition other inflammatory cells were also present such as neutrophils, which would be characteristic of the late phase response (Figure 30C).

Unfortunately, it was not possible to examine by electron microscopy the morphological responses of conjunctival mast cells from the BALB/c murine model of allergic conjunctivitis (model established in the U.S.A) as the eyes from these mice were processed as paraffin sections for immunohistochemistry analysis alone.

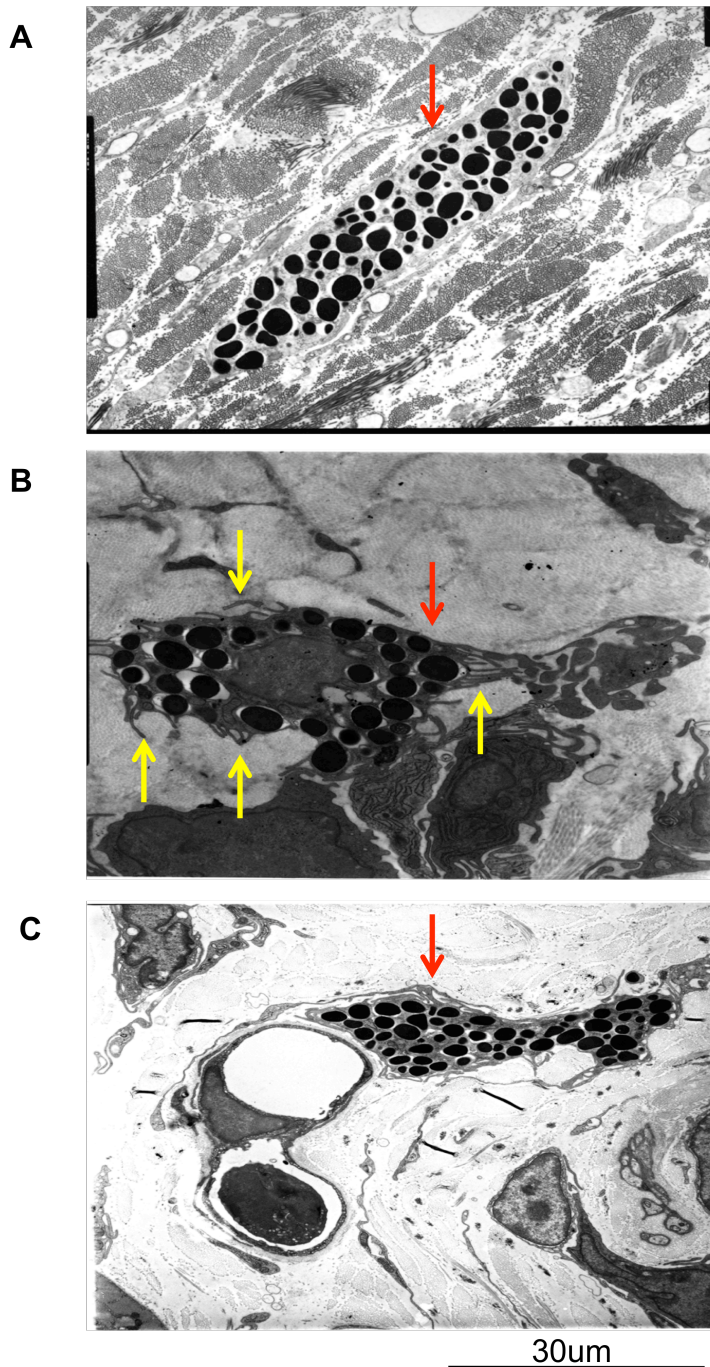


Figure 30. Morphology of murine conjunctival mast cells in naïve and post allergen challenged conjunctiva. Electron micrographs displaying images of representative mast cells (red arrow) from the conjunctiva (A) of a naïve mouse (B) 3 hours post allergen challenge indicative of the early phase response, where yellow arrows indicates filapodia (C) 9 hours post allergen challenge indicative of the late-phase response. The figures are representative of five separate experiments with at least 3-5 eyes analysed in each experiment.

4.2.3 Kinetic analysis of murine conjunctival mast cells accumulation within an inflamed conjunctiva.

Numerous studies have demonstrated that mast cells chemotax towards chemokines, accumulating at sites of inflammation during an inflammatory response. Miyazaki and co-workers (2005) previously demonstrated that a gradient of Mip-1 α was localized mainly to mononuclear cells within the forniceal area of an inflamed murine conjunctiva following allergen challenge with SRW. In light of this information a series of experiments were conducted to determine at various time points the number of mast cells in SRW sensitised-challenged, sensitised non-challenged or non-sensitised non challenged conjunctiva *in vivo* using an A/J murine model of allergic conjunctivitis. The data are representative of five separate experiments per condition with at least 3-5 eyes analysed in each condition.

Following treatment eyes were enucleated from A/J mice and processed as cryostat serial sections. Thereafter each section was stained with Toluidine Blue to identify mast cells which appeared purple in colour. Mast cells were counted: 1) in the forniceal region of the conjunctiva, a potential area of a chemokine gradient, this area was represented by the letter G and 2) and a region of similar size away from the forniceal area and no potential gradient, this area was represented by the letter AG. (Figure 31A).

In Figure 31B, an up-regulation in conjunctival mast cell accumulation was observed in areas away from the gradient in non-sensitised non-challenged mice as compared to those conjunctival mast cells observed in areas near the gradient, and those in areas near and away from the gradient in sensitised non-challenged mice. However, three hours post SRW sensitised-challenged mice exhibited a dramatic increase in conjunctival mast cell accumulation in areas near and away from the gradient when compared with conjunctival mast cells from non-sensitised non-challenged mice, respectively. Six hours post SRW, sensitised-challenged mice exhibited a downregulation in conjunctival mast cell accumulation in areas near the gradient. In addition, a further downregulation of conjunctival mast cells was observed in areas away from the gradient. At 24 hours post SRW sensitised-challenged mice, the number of conjunctival mast cells accumulated in areas near and away from the gradient was comparable to that observed in areas near and away from the gradient respectively in six hours post SRW sensitised- challenged mice.

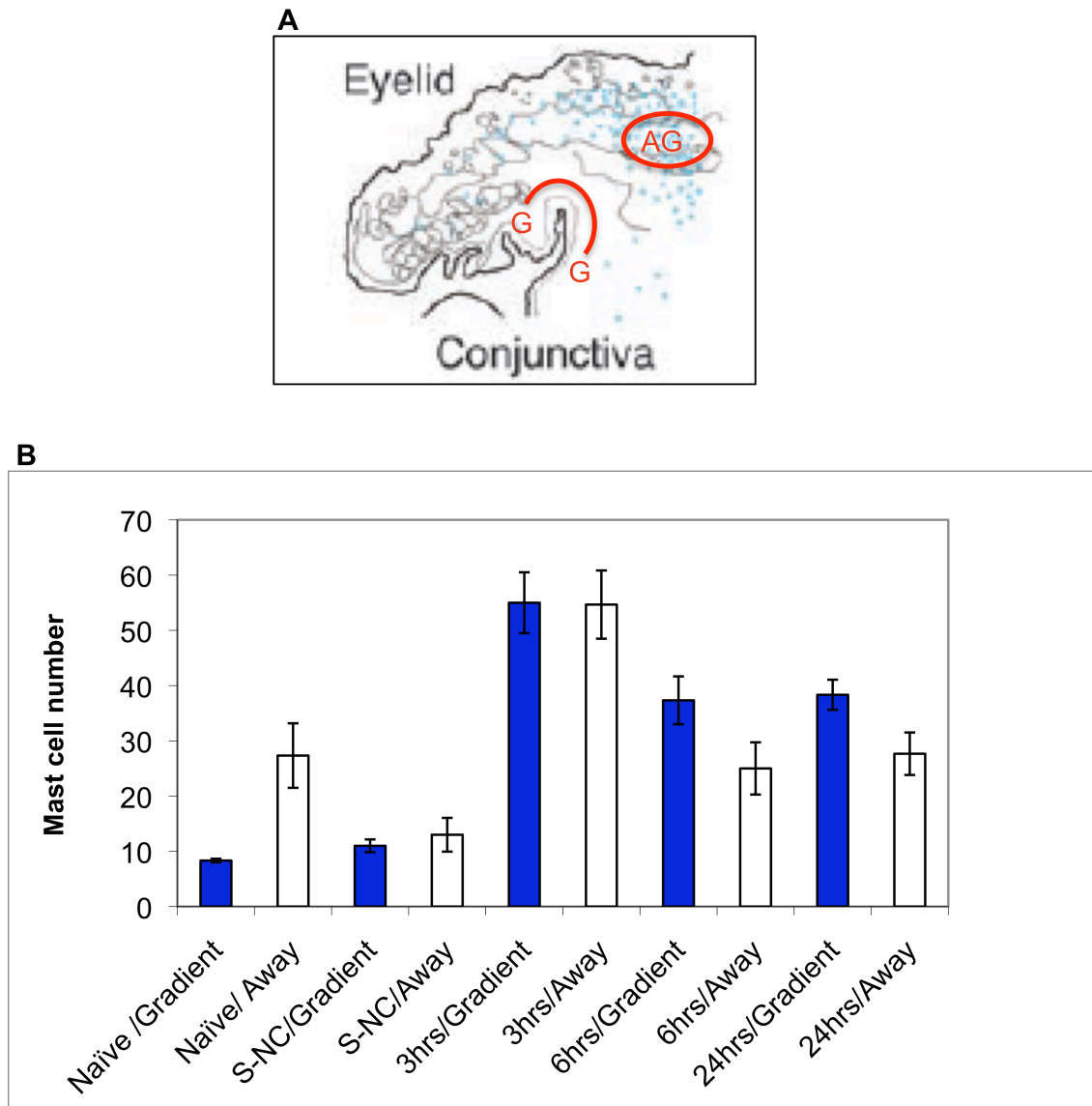


Figure 31. Kinetic analysis of mast cell accumulation within the inflamed mouse conjunctiva induced by allergic conjunctivitis model 1-using A/J mice. (A) Schematic representation of the conjunctiva showing the location of the chemokine gradient, G, and the location away from the chemokine gradient, AG. (B) Mast cells were counted in equivalent size areas in the vicinity of the gradient versus away from the gradient and the data represented as a graph. The data represent the mean \pm standard error mean (SEM) of five experiments per condition with at least 3-5 eyes analysed in each. Figure A is adapted from Miyazaki et al., 2005
Key: S-NC= Sensitized non-challenged mice

Paraffin sections from the BALB/c murine model of allergic conjunctivitis were stained with anti-mMCP-5 antibody to identify conjunctival mast cells (characterized by the expression of the chymase mMCP-5) and counter stained with anti-CCR1 antibody to identify CCR1 positive mast cells. CCR1 positive mast cells were counted in the forniceal area, a potential area of a chemokine gradient (Figure 32A). Unfortunately due to the compromised architecture of processed tissue it was not possible to identify and count conjunctival mast cells away from the forniceal area, a potential area of no chemokine gradient.

Figure 32B shows an upregulation in CCR1 positive conjunctival mast cells in the forniceal region in 30 minutes post SRW sensitised-challenged mice as compared to conjunctival mast cell accumulation observed at 30 minutes in non-sensitised non-challenged mice. In addition, a decrease in conjunctival mast cell accumulation was observed in the forniceal region of 24 hours post SRW sensitised-challenged mice compared to mast cell accumulation observed 30 minutes post SRW sensitised-challenged mice. Please note that unfortunately, as this model was induced in the U.S. the time points employed post SRW allergen challenge were different to those in the A/J murine model of allergic conjunctivitis.

Although two different models were used to analyse mast cell accumulation within an inflamed conjunctiva both models showed the same effect in that following SRW challenge in sensitised mice, an increase in mast cells can be seen in the forniceal region of the conjunctiva.

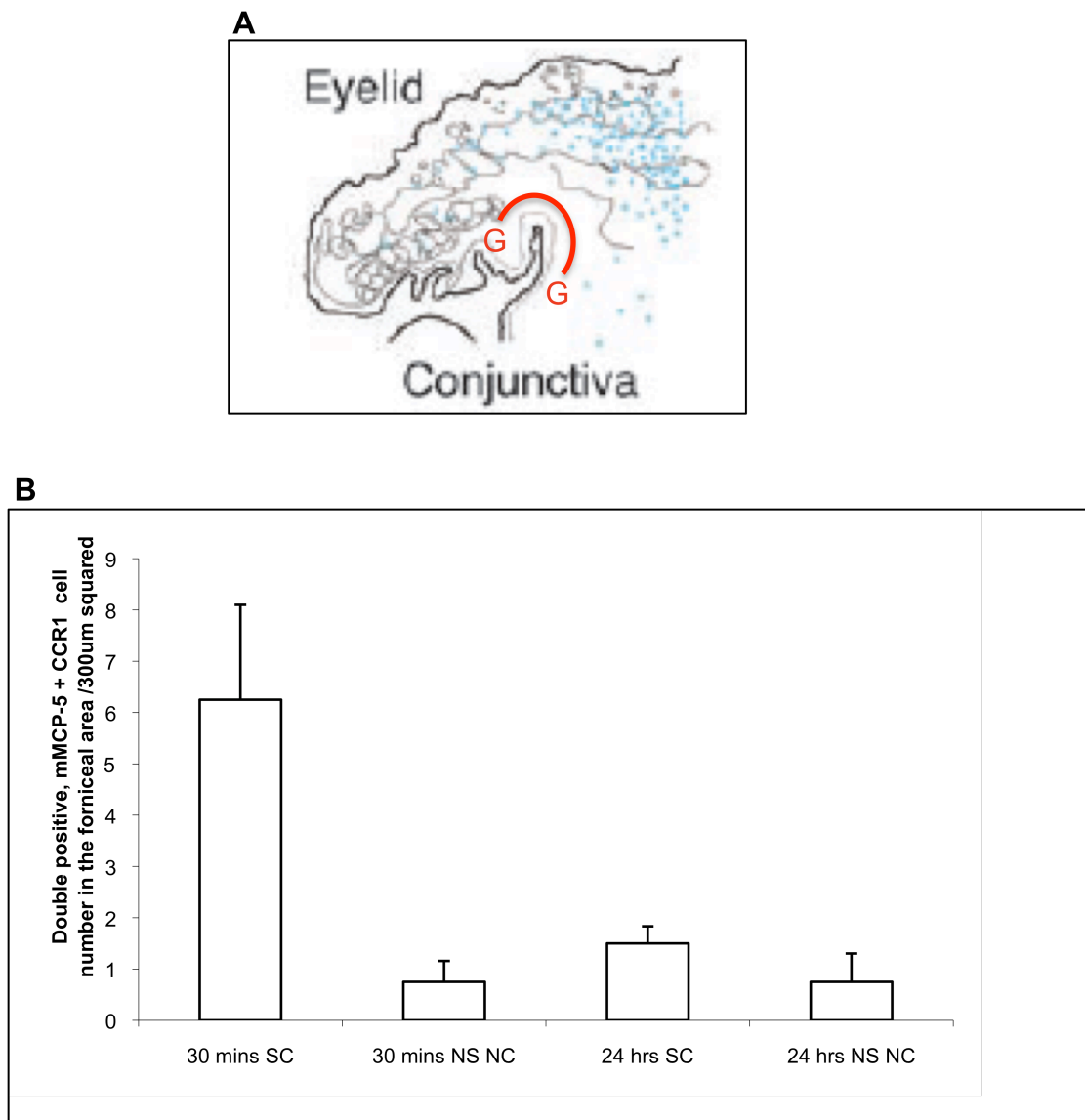


Figure 32. Kinetic analysis of mast cell accumulation within the inflamed mouse conjunctiva induced by allergic conjunctivitis model 2- using BALB/c mice. (A) Schematic representation of the conjunctiva showing the location of the chemokine gradient, G, in the forniceal region. (B) Mast cells were counted by using a grid in the vicinity of the gradient, and the data represented as a graph. The data represent the Mean \pm standard error mean (SEM) of five experiments per condition with at least 3-5 eyes analysed in each. Figure A is adapted from Miyazaki et al., 2005.

Key: SC= Sensitized challenged mice, NS-NC=Non-sensitized, non-challenged mice.

4.2.4 Localisation of CCR1, actin and WASP in conjunctival mast cells within an inflamed murine conjunctiva.

Previous reports have demonstrated that actin, CCR1 and WASP have individually and in concert shown an important role in cytoskeletal re-organisation, cell polarity and chemotaxis. Chapter 3 of this thesis analysed the localisation of actin, CCR1 and WASP in RBL-CCR1 cells in response to a Mip-1 α gradient, and showed that these components were enriched at the leading edge of these cells *in vitro*, which would be indicative of chemotaxing cells. In light of this information, the objective of these experiments by using a model of allergic conjunctivitis was to examine the morphology and localisation of actin, CCR1 and WASP following SRW allergen in sensitised mice, and thereby determine whether these observations correlate with the observations for RBL-CCR1 cells and other migrating cell types.

Cryostat serial sections from the eyes of an allergic conjunctivitis model using A/J mice were stained with Toluidine Blue to identify the mast cells and their location, whilst the serial section was stained for actin and WASP. Thereafter purple positive mast cells were numbered and were co-localised to those mast cells in the serial section, which was stained for actin and WASP.

Figure 33 shows the presence of purple positive mast cells in a SRW sensitised-challenged conjunctiva of A/J mice. In the SRW sensitised-challenged conjunctiva of A/J mice, actin localises throughout the cytoplasm of mast cell number 1 with increased actin expression observed at only one end of the cell (Figure 34A), whilst WASP also displays an asymmetric localisation within the cell (Figure 34B). Mast cell number 2 also shows actin and WASP expression within the cell, however it is difficult to see the exact distribution at this magnification of x 63 (Figure 34A and 34B). Figure 34C shows the co-localisation of actin and WASP in mast cells 1 and 2.

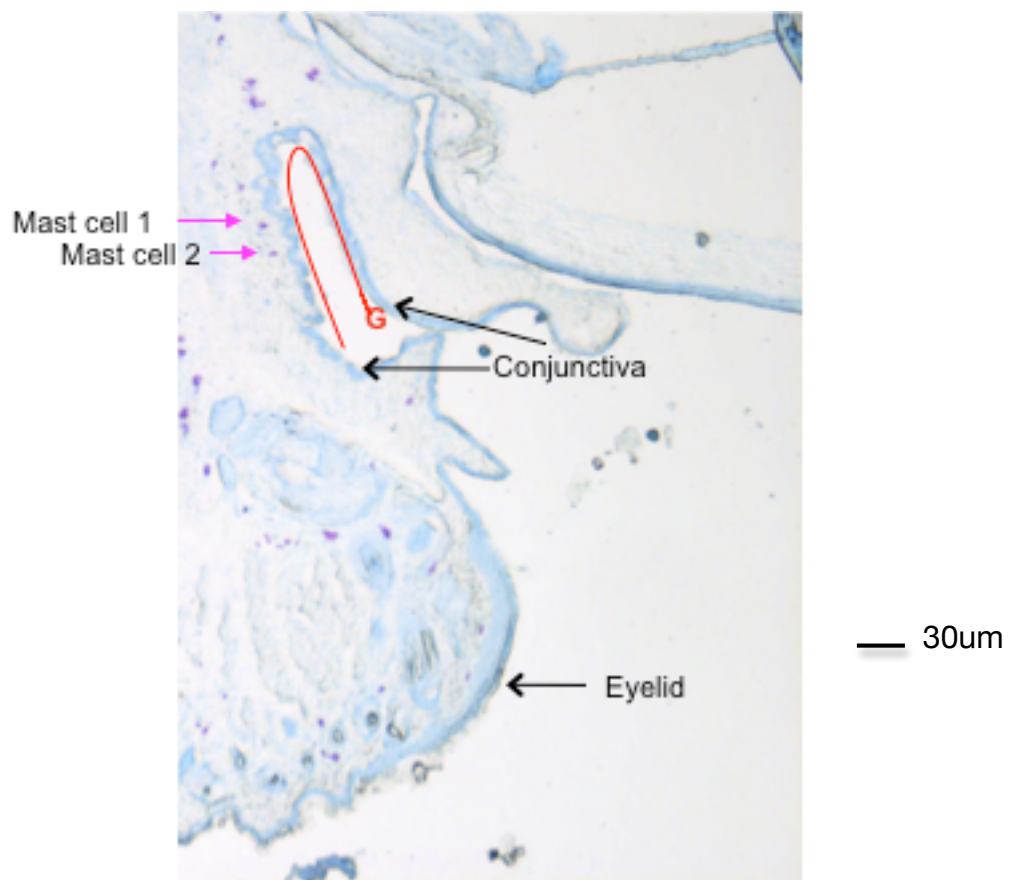
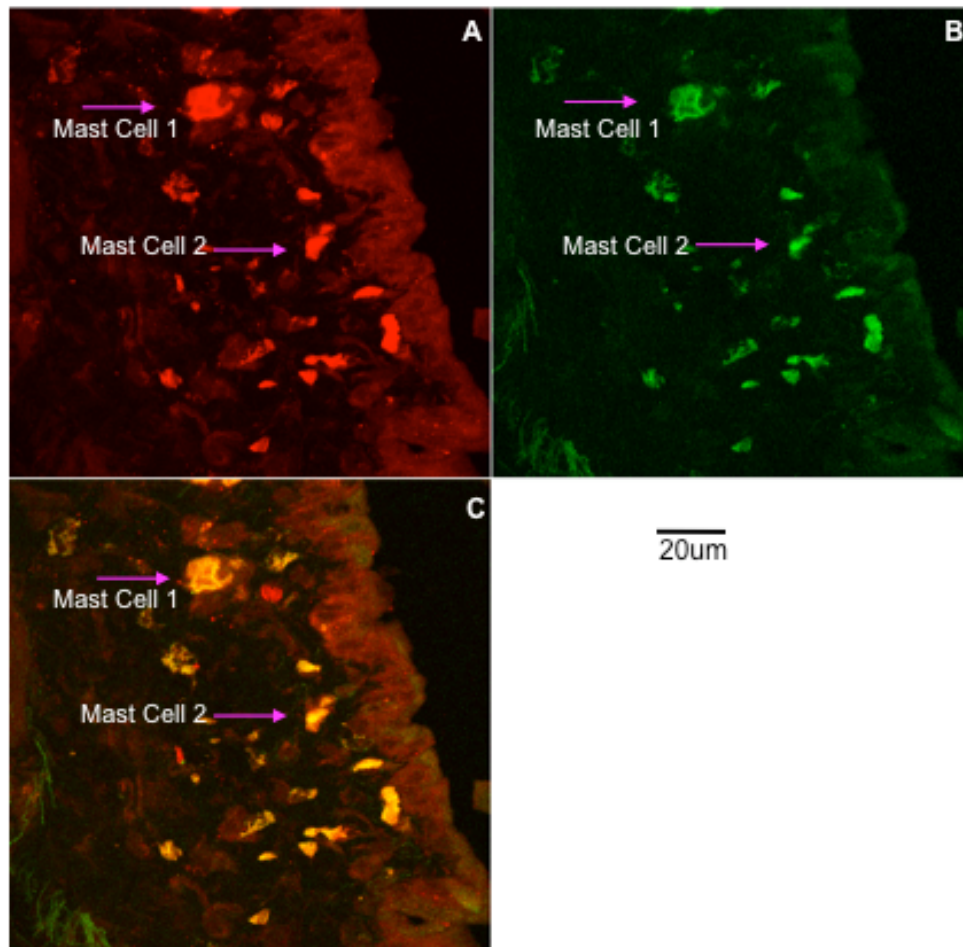


Figure 33. Conjunctival mast cells (purple) 1 and 2 (pink arrows) in the vicinity of a chemokine gradient, G, in SRW sensitised-challenged mice.



34. (A) Actin (red) and (B) WASP (green) localisation in murine conjunctival mast cells 1 and 2 (indicated by purple arrows) in the vicinity of a chemokine gradient, from a serial section of tissue shown in figure 33 in SRW sensitised-challenged mice. (C) Co-localisation (yellow) of actin (red) and WASP (green) in murine conjunctival mast cells in SRW sensitised-challenged mice.

Allergic conjunctivitis models using BALB/c mice established in the US were processed in paraffin which allowed identification of mast cells by anti-mMCP-5 antibody and CCR1 by anti-CCR1 antibody. It was possible to identify CCR1 positive mast cells by epi-fluorescence.

CCR1 positive cells present in non-sensitised non- challenged conjunctiva at 30 minutes were identified with anti-CCR1 antibody (Figure 35A) and mast cells by anti-mMCP-5 antibody (Figure 35B). Figure 35C shows the co-localisation of positive CCR1 mast cells in yellow/orange present in non-sensitised non-challenged conjunctiva at 30 minutes. In SRW sensitized-challenged conjunctiva at 30 minutes anti –CCR1 antibody identified CCR1 positive cells (Figure 36A), whilst mast cells were identified by anti-mMCP-5 antibody (Figure 36B). Figure 36C shows the co-localisation of positive CCR1 mast cells in yellow/orange in SRW sensitised-challenged conjunctiva at 30 minutes.

Although it was possible to identify CCR1 positive mast cells by epi-fluorescence microscopy, unfortunately due to time constraints in the US it was not possible to examine the localisation of CCR1 and actin within these cells using confocal microscopy. Also, it was not possible to bring the tissue sections to UCL to be analysed by confocal microscopy.

In addition to CCR1 and mast cell staining, after many attempts it was not possible to identify a source of WASP antibody, which could be used in paraffin sections.

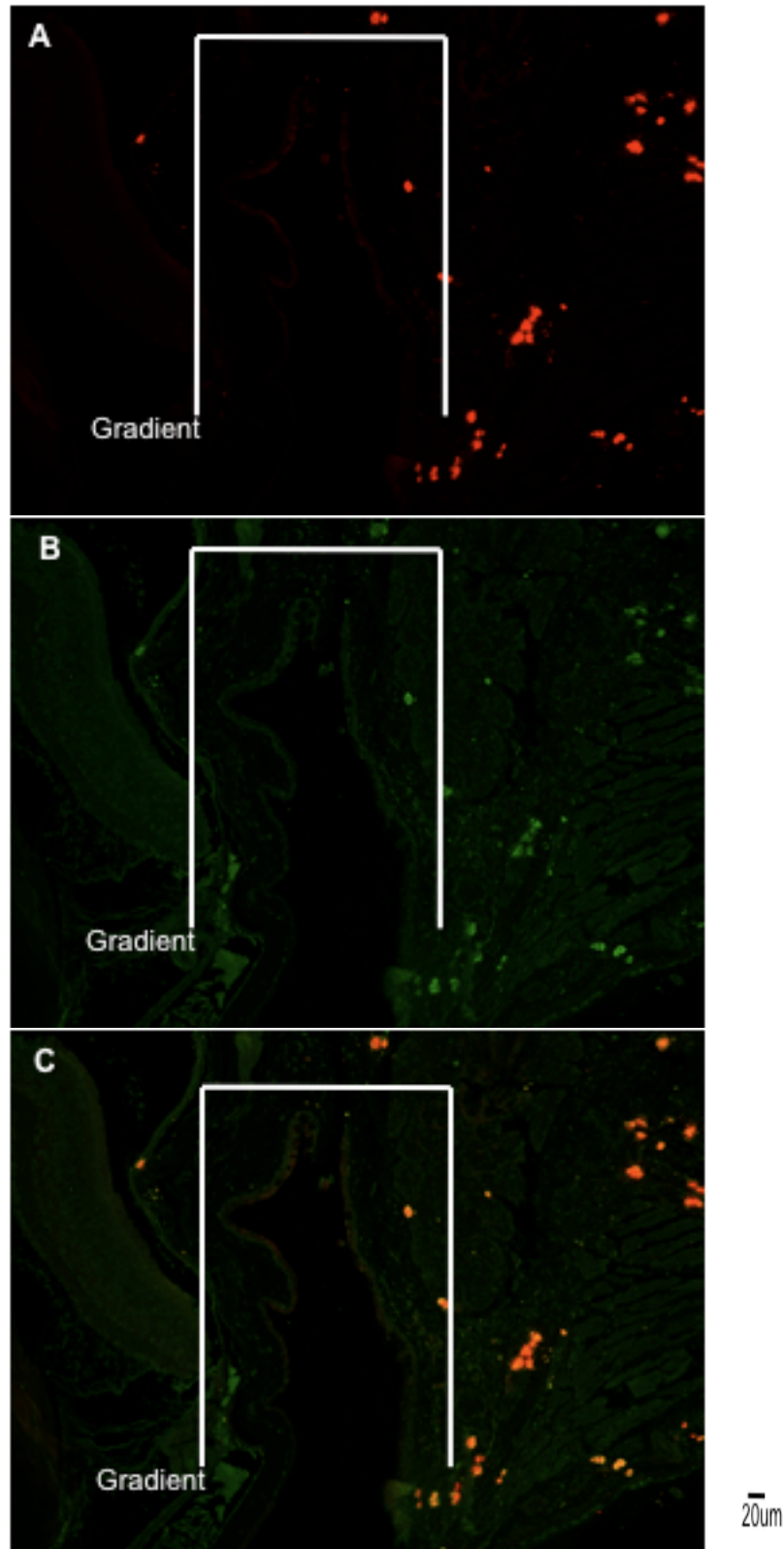


Figure 35. (A) CCR1 (green) and (B) positive mast cell (red) expression in the vicinity of a chemokine gradient (forniceal region), in non-sensitised non-challenged murine conjunctiva. (E) co-localisation (yellow/orange) of CCR1 (green) positive mast cells (red) in the vicinity of a chemokine gradient (forniceal region), in non-sensitised non-challenged murine conjunctiva. This figure is representative of five separate experiments with at least 3-5 eyes analysed in each.

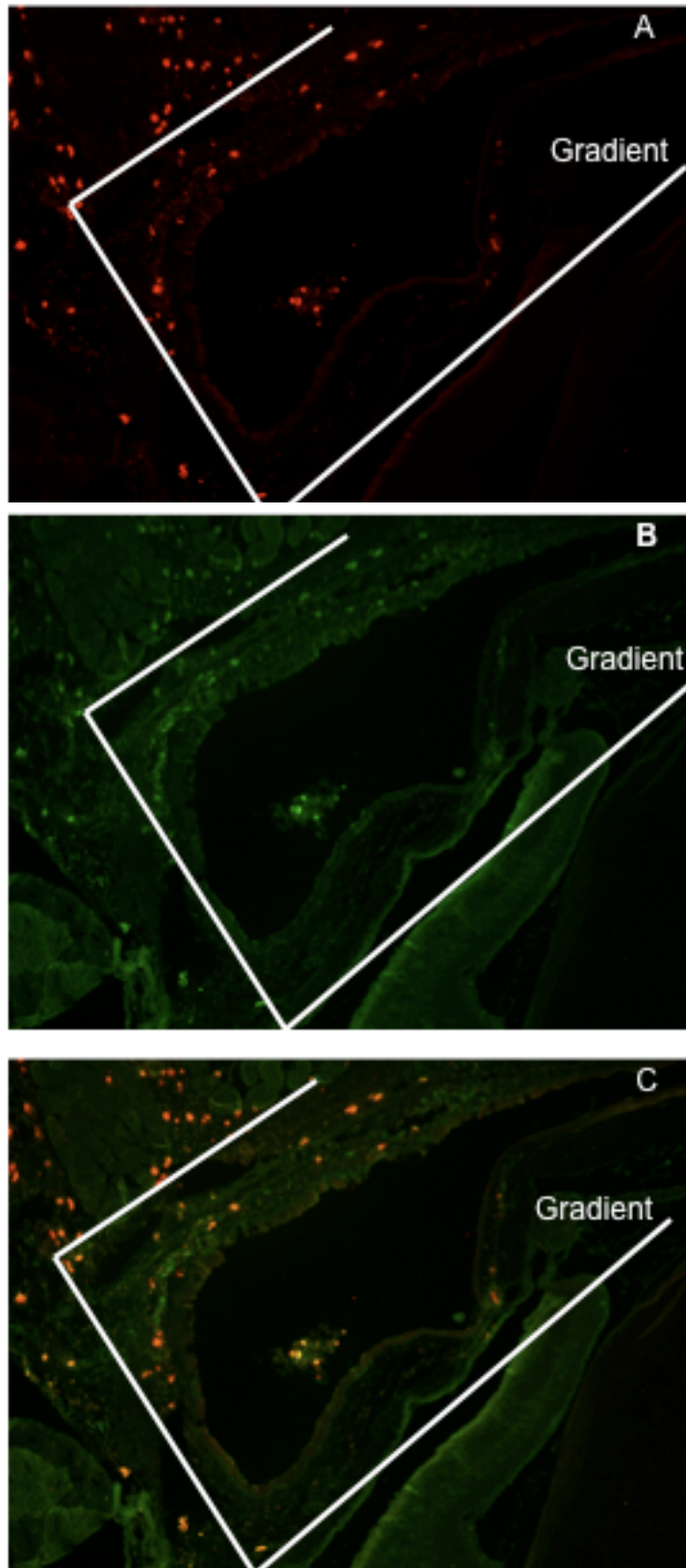


Figure 36. (A) CCR1 (green) and (B) positive mast cell (red) expression in the vicinity of a chemokine gradient (forniceal region), in sensitised-challenged murine conjunctiva. (C) co-localisation (yellow/orange) of CCR1 (green) positive mast cells (red) in the vicinity of a chemokine gradient (forniceal region), in sensitised-challenged murine conjunctiva. This figure is representative of five separate experiments with at least 3-5 eyes analysed in each.

4.3 Discussion

The eye is among the first organs to encounter environmental allergens, and as a result is a common target of inflammatory responses. Allergic eye diseases are often concomitant with other allergic diseases such as atopic dermatitis and asthma. Present drug treatment for ocular allergy targets the key mechanisms involved in the development of disease, however most of these agents are associated with significant adverse side effects. In order to establish new therapeutic approaches further investigations into the molecular basis are required.

Many eukaryotic cells undergo directed cell movement, otherwise known as chemotaxis towards a soluble ligand. This process is necessary for many biological functions, including the migration of macrophages during wound healing (Devreotes and Zigmond, 1988; Martinez-Quiles *et al.*, 2001) and the aggregation of *Dictyostelium* cells to form a multicellular organism (Parent and Devreotes, 1999; Chung *et al.*, 2001). Chemotaxis requires a defined cell polarity in which components of the cytoskeleton such as actin, WASP and CCR are differentially localized at the leading edge of a migrating cell as well as its retracting posterior (Firtel and Chung, 2000; Chung *et al.*, 2000).

Chapter 3 of this thesis demonstrated that during Mip-1 α -induced RBL-CCR1 chemotaxis, specific localisation of actin, CCR1 and WASP was enriched in polarised cells, which has been corroborated by other studies of other cell types. In addition, the morphology and chemotaxis of these cells were dramatically inhibited upon Mip-1 α and IgE/antigen co-stimulation. In light of this information, the aim of this chapter was to examine the morphology and localisation of actin, CCR1 and WASP in conjunctival murine mast cells following SRW allergen challenge.

Murine models of allergic conjunctivitis

Allergic conjunctivitis is IgE-mediated hypersensitivity reaction to aeroallergens such as short ragweed or grass pollen after they come into contact with the conjunctival surface. Many different animal models of ocular allergy have been established thus far, however it is vital to recognise that within ocular allergies, different disease entities exist and that only some of these can be mimicked by animal models. In the present study a murine model of allergic conjunctivitis was used to mimic ocular allergic disease in man. Both A/J and BALB/c mice

successfully induced allergic conjunctivitis displaying symptoms commonly present such as: conjunctival edema; lid edema; redness; tearing; and squinting. These symptoms reflect the distinctive categories of the inflammatory response and are employed as the evaluation criteria when scoring murine allergic conjunctivitis.

Behavioural and morphological responses of murine conjunctival mast cells in inflamed conjunctiva.

In chapter 3 of this thesis, RBL-CCR1 cells *in vitro* demonstrated profound morphological changes, including extensive membrane ruffling in response to a gradient of Mip-1 α alone and abolished membrane ruffling upon of Mip-1 α and IgE/antigen stimulation. In light of this, the objective of the experiments in this chapter was to characterise the morphological responses of mast cells in SRW sensitised-challenged conjunctiva.

Reports have shown chemokine stimulation induces actin polymerisation and the formation of filopodia and lamellipodia at the edge of the cell membrane closest to the chemokine gradient and that these are essential steps during chemotaxis (Berzat et al., 2010; Van Haastert et al., 2010; Roussos et al., 2011; Wang et al., 2011). In the present study, three and nine hours in post SRW sensitised-challenged mice, conjunctival mast cells appeared polarised and displayed numerous filopodia from the cell membrane compared to sensitised non-challenged or non-sensitised non-challenged mice, in which, mast cells remain elongated in shape and displayed no processes from the cell membrane. This would fit in with data from chapter 3, which showed that RBL-CCR1 cells exposed to a Mip-1 α gradient, induced extensive membrane ruffling and also adopted a polarised cell phenotype. RBL-CCR1 cells pre-treated with IgE and exposed to a gradient of Mip-1 α and antigen inhibited membrane ruffling (Chapter 3), hence, we can assume that in the presence of allergen and chemokine in the murine allergic conjunctivitis model, mast cells should not display any membrane ruffling. However, this is not the case *in vivo*, and a likely explanation is that morphological changes of RBL-CCR1 cells in the presence of chemokine and antigen is transient and rapid *in vitro*.

Kinetic analysis of murine conjunctival mast cells accumulation within an inflamed conjunctiva.

In the present study a series of experiments were conducted to analyse mast cell accumulation within the inflamed conjunctiva in two different models of murine allergic conjunctivitis. In the present study the A/J murine model of allergic conjunctivitis showed an increase in Toluidine Blue stained mast cells in the forniceal area in three hours post SRW sensitized-challenged mice compared to a non-sensitised non-challenged and sensitized non-challenged mice, thereby suggesting that the increase in conjunctival mast cells is in response to a chemokine gradient generated in the forniceal region. However, six hours post SRW, sensitized-challenged mice, exhibit a decrease in conjunctival mast cell numbers compared to three hours post SRW, suggesting that the chemokine gradient no longer exists.

In the present study, mast cells from the BALB/c murine model of allergic conjunctivitis were identified by anti-mMCP-5 antibody and counter stained with anti-CCR1 antibody to identify CCR1. The chemokine receptor CCR1 can bind several chemokines including Mip-1 α , RANTES, MCP-2 and MCP-3 (Ochi et al., 1999; Humbles et al., 2002). Using the BALB/c murine model of allergic conjunctivitis an increase in CCR1 positive mast cells were observed in the forniceal region of 30 minutes post SRW sensitised-challenged mice compared to non-sensitised non-challenged mice. This data suggests that the increased CCR1 positive mast cell number could be in response to a Mip-1 α chemokine gradient generated in the forniceal region. This would also correlate with a previous study by Miyazaki and co-workers (2005) who demonstrated that a gradient of Mip-1 α was localized mainly to mononuclear cells within the forniceal region of an inflamed murine conjunctiva. In addition, this observation would also correlate with data from chapter 3 and studies by Toda et al (2004) demonstrating that RBL-CCR1 mast cells can chemotax towards a Mip-1 α chemokine gradient within a time frame of 30 minutes (real time microscopy pipette assay) to three hours (transwell chamber assay). However, in 24 hours post SRW sensitised-challenged mice there is a decrease in mast cell number in the forniceal region compared to non-sensitised non-challenged mice. An explanation for this is that the chemokine gradient no longer exists within the forniceal region as this time point could be representative of the late phase response. To validate whether this time point is representative of the

late phase, one could stain for immune cells which are characteristic of the late phase response, such as T cells or eosinophils. However, it is important to note that both models showed the same effect in that following SRW challenge in sensitised mice, an increase in mast cells can be seen in the forniceal region of the conjunctiva.

Reports have shown that progenitor mast cells are capable of homing from the circulation into the tissue (Abonia et al., 2006; Hallgren et al., 2007). Although, there is an increase in mast cell number in the forniceal area of an inflamed conjunctiva it is not possible to establish whether resident mast cells have migrated within the tissue towards the chemokine gradient, or whether these are progenitor mast cells homing into the tissue from circulation. Future studies should validate this by analysing the number of progenitor mast cells versus mature mast cells in the forniceal region. In addition, this data fits with previous clinical findings that demonstrated during the pollen season, the median mast cell numbers in the conjunctiva increased by 61% in seasonal allergic conjunctivitis patients compared to normal patients and remained increased in allergic patients out of season (Kumagai et al., 2006). In addition, murine models of antigen induced Th2 pulmonary inflammation demonstrate a significant increase in airway mast cells, in comparison to non-sensitised non-challenged mice which have few mast cells (Ikeda et al., 2003)

Localisation of actin, WASP and CCR1 in conjunctival mast cells within an inflamed murine conjunctiva.

Local mast cell hyperplasia, a prominent feature of the allergic response, is likely to involve mast cell progenitor recruitment and migration of mature mast cells within the inflamed tissue. Therefore, the therapeutic targeting of the mechanisms that regulate mast cell migration during inflammation may possibly reduce the mast cell accumulation to the affected tissues and ease the subsequent effect of mast cell activation in these locations. At present there are no therapeutic agents that specifically target mast cell migration. However, a reduction of tissue resident mast cells has been demonstrated in murine allergic models that are genetically deficient in PI3K (Ali et al., 2004; Koyasu et al., 2005)

The objective of these experiments was to examine the specific localisation of actin, CCR1 and WASP in murine conjunctival mast cells using an A/J and BALB/c

murine models of allergic conjunctivitis and thereby determine whether these observations mimic RBL-CCR1 cells and other chemotaxing cell types.

Myers and co-workers (2005) reported that WASP played an essential role in organizing polarized F-actin assembly in chemotaxing cells *in vitro*, and was preferentially localized at the leading edge and uropod of chemotaxing cells *in vitro*. Recently, a WASP biosensor was constructed to report WASP activation and localisation *in vivo*, demonstrating localization of WASP in actin protrusions at the cell periphery of macrophages and neutrophils following CSF-1 stimulation (Cammer et al., 2009). In addition, actin displays an asymmetric localization pattern in chemotaxing neutrophils and monocytes *in vivo* following Mip-1 α stimulation (Khandoga et al., 2009). Although there are reports demonstrating the expression and potential roles of actin and WASP in several cell types during migration *in vivo* and *in vitro* (Tharp et al., 2006; Colditz et al., 2007; Lammermann et al., 2008;), at present there are no studies examining the localisation of WASP, actin or CCR1 in chemotaxing mast cells *in vivo*. Consistent with *hematopoietic* cells, conjunctival mast cells observed in this study express WASP (Guinamard et al., 1998; Mani et al., 2009). In SRW sensitized-challenged mice, it was possible to see an asymmetric distribution of WASP and actin in conjunctival A/J murine mast cells at a x63 magnification, however more cells need to be analysed to validate this. Unfortunately it was not possible to compare the localisation of WASP and actin in sensitised non-challenged and non-sensitised non-challenged conjunctivas as it was technically difficult to co-localise Toluidine Blue positive mast cells with the corresponding actin and Wasp stained serial sections. However, this can be overcome if a suitable WASP antibody can be identified for use in paraffin sections. Future experiments could use this antibody along with mMCP-5, which successfully identified mast cells in paraffin sections. In light of current knowledge *in vivo* and observations for actin and WASP in RBL-CCR1 cells *in vitro*, it is possible that mast cells *in vivo* may show the same localization patterns during chemotaxis.

Both asymmetrical and symmetrical CCR localisation patterns have been demonstrated on the cell surface *in vitro* (Servant et al., 1999; Gomez-Moulton et al., 2004; Schröppel et al., 2004; Fifadara et al., 2010). Although differential expression of chemokine receptors has been observed in monocyte subpopulations *in vivo* (Saederup et al., 2010), to date, there are no reports demonstrating chemokine receptor localisation patterns on the cell surface *in vivo*. Although using paraffin sections it was possible to observe CCR1 positive

conjunctival mast cells in SRW sensitised challenged and non-challenged non-sensitised BALB/c mice, unfortunately at this magnification it was not possible to examine the exact localisation of CCR1 within these cells. To validate the exact localisation of WASP, actin and CCR1, future experiments must analyse WASP, actin and CCR1 stained tissue, and observe cells using a x63 magnification along with X, Y and Z –stacks at 0.5 um step size use generate a 3-dimensional image of these cells. This would enable the whole cell to be visualised and possibly the exact location of each component within the cell.

Chapter 5.

The role of RGS1 in mast cell degranulation, mediator release and chemotaxis

5. The role of RGS1 in mast cell degranulation, mediator release and chemotaxis

5.1 Introduction and hypothesis

Previous studies demonstrate signaling from the Fc ϵ R1 receptor following allergen mediated cross-linking results in two phenomena: 1) arrested chemotaxis towards a chemokine gradient (Toda et al., 2004) and 2) enhanced production of pro-inflammatory molecules when CCR1 and Fc ϵ R1 receptors are dually engaged (Nifidra et al., 2010). Moreover, in a recent study by Aye and Ono (unpublished data) the gene expression for several genes including RGS1 and TRB 3, were up-regulated after stimulating IgE sensitised RBL-CCR1 cells with Mip1- α . Further expression of RGS1 and TRB3 were observed by co-stimulation by Mip1- α and IgE/antigen respectively. The possibility that RGS1 and TRB3 might also function as signaling molecules in mast cell processes requires further elucidation.

Based on current knowledge, I hypothesise that the signaling molecule RGS1, downstream of Fc ϵ R1 signaling, can regulate mast cell degranulation, chemotaxis and mediator release.

To address this hypothesis, the specific aims of this chapter were as follows:

1. Using RNA interference to characterise how RGS1 affects RBL-CCR1 degranulation, in which RBL-CCR1 cells are co-stimulated with Mip1- α and IgE/antigen and appropriate controls. In addition, examine the functionality of CCR1 on RBL-CCR1 degranulation by using the CCR1 antagonist met-RANTES.
2. Using RNA interference analyse how RGS1 affects cytokine and chemokine release from RBL-CCR1 cells following degranulation, in which RBL-CCR1 cells are co-stimulated with Mip1- α and IgE/antigen and appropriate controls.
3. Using RNA interference analyse how RGS1 affects gene expression of IL-6, IL-13 and CCL7

4. Using RNA interference analyse how RGS1 affects RBL-CCR1 chemotaxis, in which RBL-CCR1 cells are co-stimulated with Mip1- α and IgE/antigen and appropriate controls.

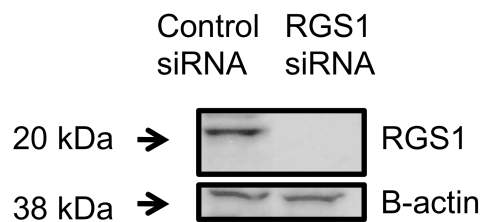
5.2 Results

5.2.1 Depletion of endogenous RGS1 in RBL-CCR1 cells by RNA interference.

In the first instance, RNA interference was used to deplete RGS1 content in RBL-CCR1 cells and thereby determine how RGS1 controls RBL-CCR1 degranulation, mediator release and chemotaxis. Western Blotting in Figure 37 confirmed that RGS1 protein was reduced in RBL-CCR1 cells expressing RGS1 siRNA compared with cells expressing the control RGS1 siRNA. The data are representative of more than 10 separate experiments.

Figure 37. Reduction of endogenous RGS1 in RBL-CCR1 cells by RNA interference.

RBL-CCR1 cells were transfected with either RGS1 siRNA or control siRNA. Lysates were prepared and RGS1 expression was evaluated by western blot using anti-RGS1 Ab. Anti-actin was used to further assess protein loading. Data are representative of 10 experiments.



5.2.2. Effect of RGS1 on RBL-CCR1 degranulation

The objective of these experiments was to initially examine the effect of RGS1 on RBL-CCR1 degranulation, in which RBL-CCR1 cells were co-stimulated with Mip1- α and IgE/antigen. Simultaneously, the functionality of CCR1 on RBL-CCR1 degranulation and its interaction with RGS1 during this response was also examined using the CCR1 antagonist met-RANTES. Degranulation of RBL-CCR1 was determined by measuring the release of the granule protein beta-hexosaminidase. The data are representative of 3 separate experiments, in which each condition was analysed in triplicate per experiment.

As shown in Figure 38, Mip1- α stimulated RBL-CCR1 cells treated with control siRNA caused a significant increase in degranulation compared to non-sensitised RBL-CCR1 cells treated with control siRNA. However, Mip1- α stimulated RBL-CCR1 cells treated with RGS1 siRNA induced a significant increase in degranulation in comparison to Mip1- α stimulated RBL-CCR1 cells treated with control siRNA. Interestingly, co-stimulation with Mip1- α and IgE/antigen induced a significant increase in degranulation in RBL-CCR1 cells treated with RGS1 siRNA compared to co-stimulated RBL-CCR1 cells treated with control siRNA, and RGS1 siRNA treated cells stimulated with either Mip1- α or IgE/antigen. However, by using met-RANTES on RGS1 and control siRNA treated cells under co-stimulation conditions degranulation observed was significantly decreased.

These results suggest that CCR1 and Fc ϵ RI cooperatively mediate optimal degranulation and this event can be significantly increased when RBL-CCR1 cells are treated with RGS1 siRNA. Moreover, by using the CCR1 antagonist met-RANTES, degranulation levels are significantly reduced in RGS1 siRNA treated cells thereby indicating CCR1 mediated functions.

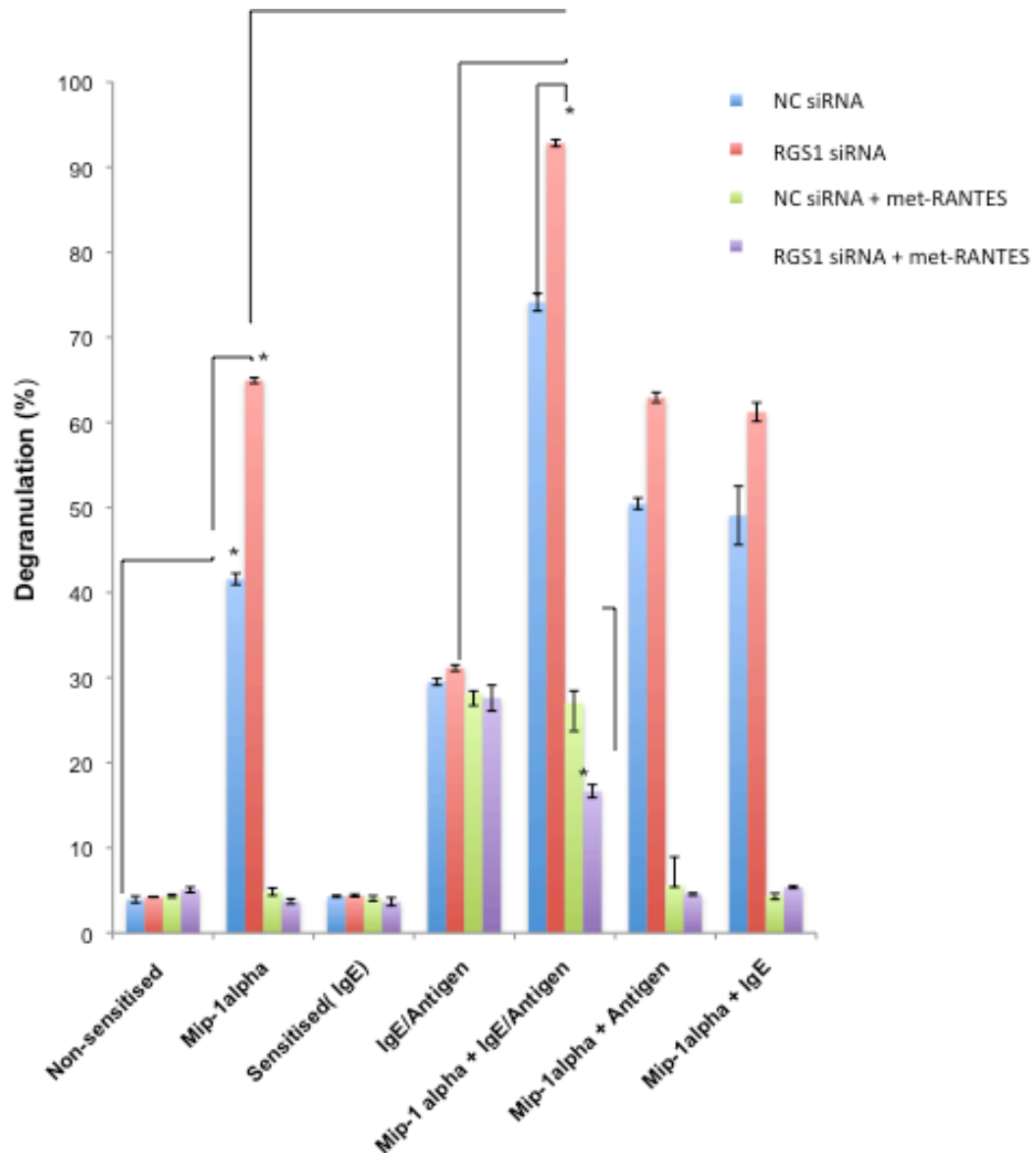


Figure 38. Co-stimulation by Mip1- α and IgE/antigen enhanced degranulation of RGS1 siRNA treated RBL-CCR1 cells. After sensitization with IgE, RBL-CCR1 cells were stimulated with antigen and Mip1- α or with Mip1- α alone with or without CCR1 antagonist met-RANTES. The data represent the Mean \pm standard error mean (SEM) of five experiments where *, $p < 0.001$, using the student T-test. KEY: Rgs1 siRNA= RGS1siRNA. NC siRNA= control siRNA.

5.2.3 Effect of RGS1 on RBL-CCR1 mediator release of cytokines and chemokines

The objective of these experiments was to examine the effect of RGS1 on mediator release from RBL-CCR1 cells co-stimulated with Mip1- α and IgE/antigen 24 hours post degranulation. The mediators that were analysed from each cell supernatant were IL-4, IL-6, IL-10, MCP-1 and Mip1- α . The data are representative of 3 separate experiments, in which each condition was analysed in triplicate per experiment

Figure 39 shows the secretion levels of chemokines and cytokines in response to co-stimulation by Mip1- α and IgE/antigen respectively, compared with stimulation by IgE/antigen alone. IL-4, IL-6 and MCP-1 were all secreted at significantly higher levels from co-stimulated RBL-CCR1 cells treated with RGS1 siRNA compared to co-stimulated cells treated with control siRNA. No significant changes were observed in IL-10 and Mip1- α secretion under these conditions.

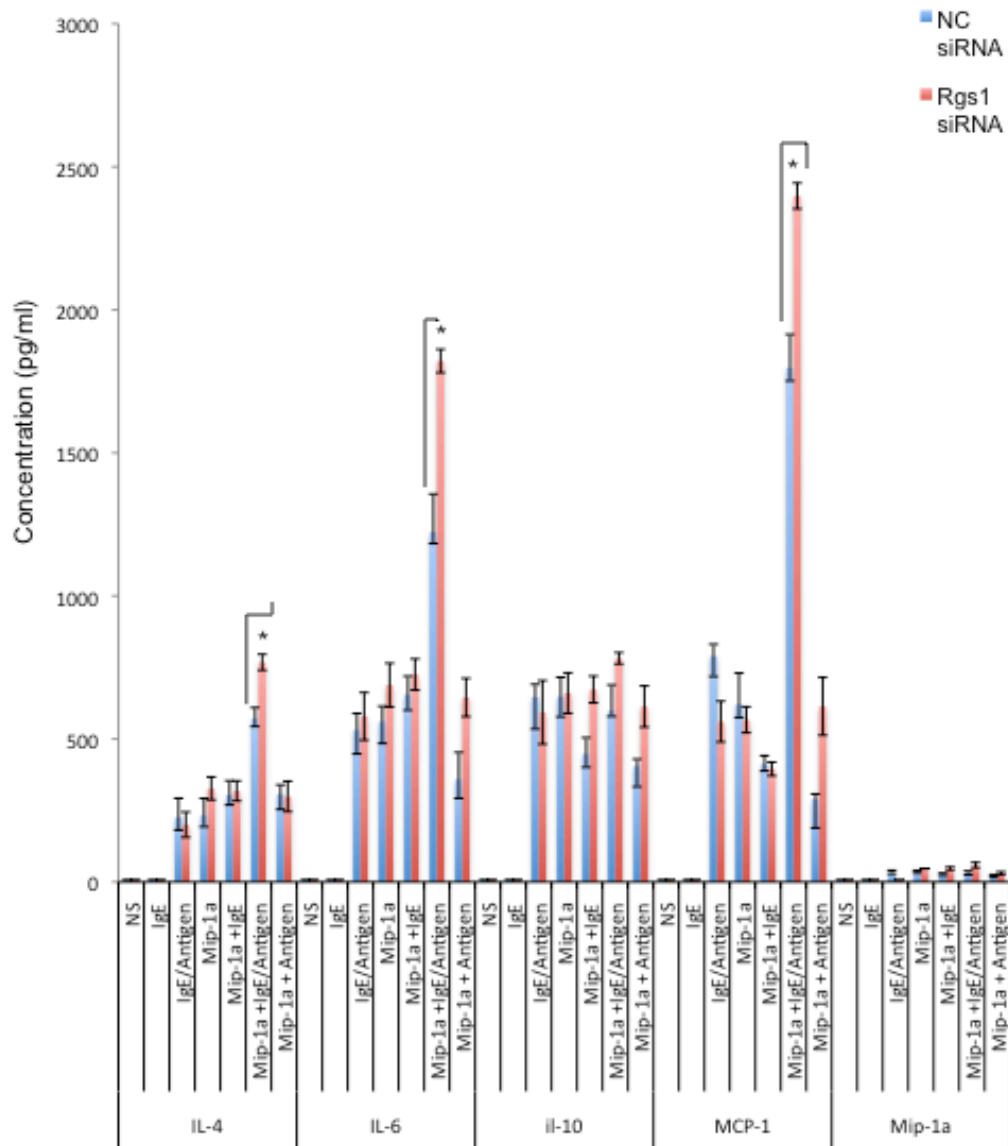


Figure 39. Co-stimulation by Mip-1 α and IgE/antigen enhanced mediator release of IL-4, IL-6 and MCP-1 from RGS1 siRNA treated RBL-CCR1 cells.

After sensitization with IgE, RBL-CCR1 cells were co-stimulated with antigen and Mip1- α or with Mip1- α alone. 24 hours post degranulation, supernatants were collected and analysed for chemokines and cytokine secretion. The data represent the Mean \pm standard error mean (SEM) of five experiments where *, $p < 0.001$, using the student T-test.

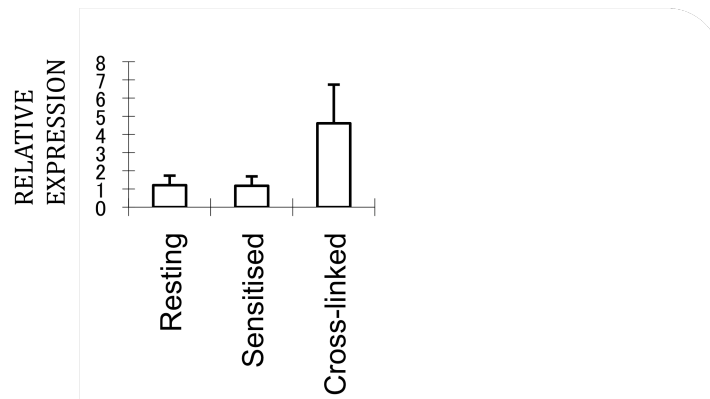
KEY: Rgs1 siRNA= RGS1siRNA. NC siRNA= control siRNA.

5.2.4 Gene expression of Inflammatory mediators IL-6, IL-13 and CCL7 in RBL-CCR1 cells

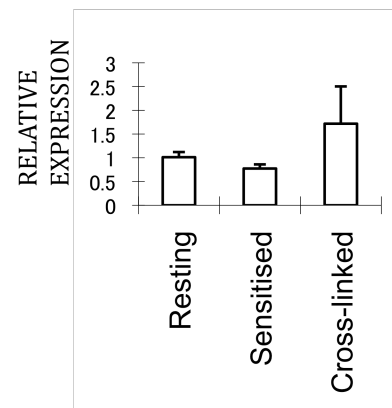
The objective of these experiments was to examine gene expression of IL-6, IL-13 and CCL7. The data are representative of 3 separate experiments, in which each condition was analysed in triplicate per experiment.

Figure 40 shows the relative gene expression of (A) IL-6 (B) IL-13 and (C) CCL7. Cross-linking with IgE and antigen showed no statistically significant differences in IL-6, IL-13 and CCL7 gene expression compared to non-sensitized and IgE sensitized RBL-CCR1 cells

A



B



C

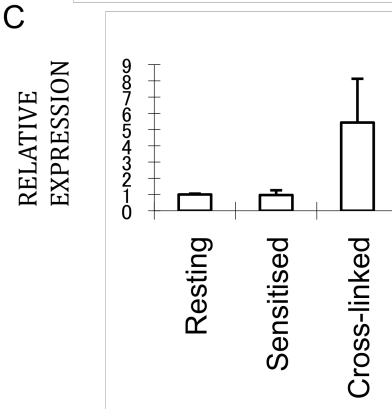


Figure 40. Gene expression of inflammatory mediators following IgE/Antigen stimulation of RBL-CCR1 cells.

(A) IL-6, (B) IL-13 and (C) CCL7 mRNA are expressed by RBL-CCR1 cells, and the levels vary with stimulation. Triplicate samples were collected from unstimulated cells or from cells stimulated with or without IgE for 30 min at 37°C. Realtime mRNA detection was performed using an Applied Bioscience thermocycler 7500. Expression was quantified using the Delta-delta CT calculation method and represented relative expression. Expression levels were normalized to that of GAPDH. The data are representative of three independent experiments.

5.2.5 Effect of RGS1 on the gene expression of inflammatory mediators IL-6, IL-13 and CCL7 in RBL-CCR1 cells

Figure 41 shows effect of RGS1 on (A) IL-6, (B) IL-13 and (C) CCL7 gene expression. This data is derived from one experiment, in which each condition was analysed in triplicate. Upon cross-linking, IL-6, IL-13 and CCL7 gene expression seem to be up-regulated in RBL-CCR1 cells, however, as the error bars are large and data is from 1 experiment only it should be viewed with caution.

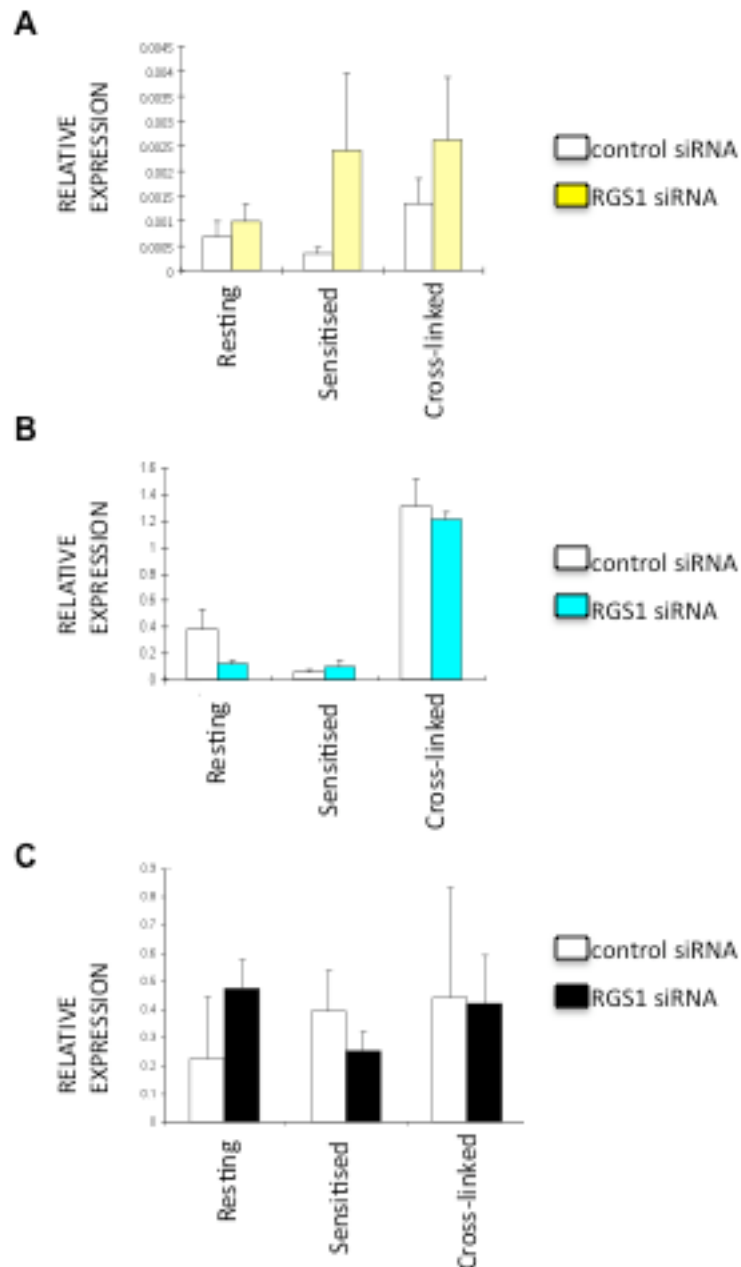


Figure 41. Effect of RGS1 on gene expression of inflammatory mediators following IgE/Antigen stimulation of RBL-CCR1 cells. (A) IL-6, (B) IL-13 and (C) CCL7 mRNA are expressed by RBL-CCR1 cells, and the levels vary with stimulation. Triplicate samples were collected from resting cells or from cells stimulated with or without IgE for 30 min at 37°C. Real time mRNA detection was performed using an Applied Bioscience thermocycler 7500. Expression was quantified using the Delta-delta CT calculation method and represented relative expression. Expression levels were normalized to that of GAPDH. The data shown is from one experiment only.

5.2.6 Effect of RGS1 on RBL-CCR1 chemotaxis

The objective of these experiments by using a transwell chemotaxis system was to examine the effect of RGS1 on RBL-CCR1 chemotaxis, in which RBL-CCR1 cells were co-stimulated with Mip1- α and IgE/antigen. The data are representative of 3 separate experiments, in which each condition was analysed in triplicate per experiment.

Figure 42 shows the chemotaxis of RBL-CCR1 cells in response to co-stimulation of CCR1 and Fc ϵ R1 by Mip1- α and IgE/antigen respectively, compared with stimulation by Mip1- α alone. RGS1 siRNA treated RBL-CCR1 cells demonstrated a significant increase in chemotaxis upon Mip1- α stimulation compared to control siRNA treated cells stimulated by Mip1- α . Interestingly, upon RGS1 siRNA treatment co-stimulated RBL-CCR1 cells showed a significant increase in chemotaxis as compared to co-stimulated control siRNA treated cells.

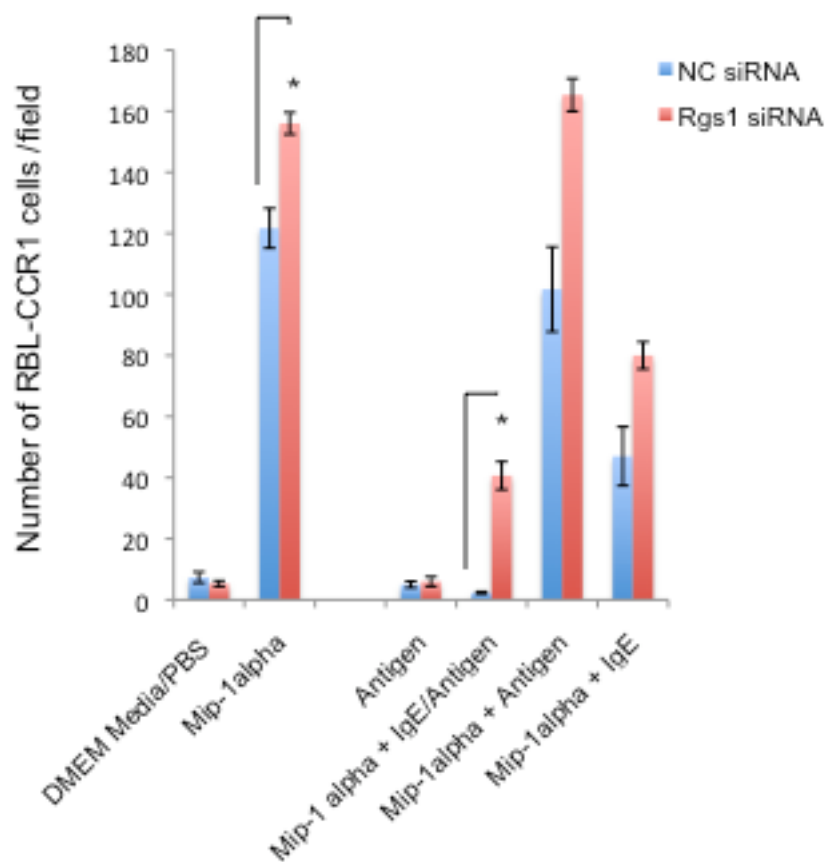


Figure 42. Co-stimulation by Mip1- α and IgE/antigen enhanced chemotaxis of RGS1 siRNA treated RBL-CCR1 cells.

After sensitization with IgE, RBL-CCR1 cells were co-stimulated with Mip1- α and antigen or with Mip1- α . The data represent the Mean \pm standard error mean (SEM) of three experiments where *, $p < 0.01$, using the student T-test.

KEY: Rgs1 siRNA= RGS1siRNA. NC siRNA= control siRNA.

5.3 Discussion

Previous reports demonstrate that cross-talk between CCR1 and FcεR1 signaling pathways in RBL-CCR1 cells results in two phenomena: enhanced degranulation and arrested chemotaxis towards a chemokine gradient (Toda et al., 2004). Unpublished data by Aye and Ono showed that RGS1 was up-regulated after stimulating IgE sensitised RBL-CCR1 cells with Mip1-α. Interestingly further up-regulation of RGS1 was observed by co-stimulation by Mip-1α. Therefore, the overall objective of this study was to establish whether RGS1 might also function as a signaling molecule in degranulation, mediator release and chemotaxis of RBL-CCR1 cells, in which RBL-CCR1 cells were co-stimulated with Mip1-α and IgE/antigen. The findings from my work are the first to show that RGS1 negatively regulates biological responses such as degranulation, mediator release and chemotaxis of RBL-CCR1 cells in response to CCR1 and FcεR1 co-stimulation.

The first aim of this study was to analyse the role of RGS1 in RBL-CCR1 degranulation, in which RBL-CCR1 cells were co-stimulated with Mip1-α and IgE/antigen. In addition to these experiments, the CCR1 antagonist met-RANTES was employed to examine the functionality of CCR1 on RBL-CCR1 degranulation. Upon co-stimulation with Mip1-α and IgE/antigen, RGS1 siRNA cells significantly enhanced degranulation as compared to co-stimulated control RBL-CCR1 cells. RGS proteins mediate binding to Gα subunits and GAP activity. RGS GAP activity accelerates the transformation of Gα to its inactive form, thereby promoting termination of GPCR signaling pathways.

Previous data showed that synergistic degranulation by CCR1 and FcεR1 is mediated by a PI3K pathway. In the present study, siRNA treatment of RGS1 would further promote CCR1 chemokine signaling, and along with FcεR1 engagement this would explain the increased degranulation levels observed in RGS1 siRNA RBL-CCR1 cells. Recent studies demonstrate that another member of the RGS family, RGS13, was up-regulated after FcεR1 aggregation in human and murine mast cells. Moreover, and surprisingly, RGS13^{-/-} mice induced increased IgE-mediated anaphylactic responses due to increased mast cell degranulation (Bansal et al., 2008). Thus, together these data suggest that RGS1 may regulate the intrinsic response of mast cells to environmental allergens through its inhibition of IgE/antigen mediated PI3K activity. Abnormalities in RGS1

expression could contribute to the pathogenesis of diseases, such as anaphylaxis and mastocytosis, associated with increased mast cell responsiveness. In the present study CCR1 activity was blocked by using the CCR1 antagonist met-RANTES, this resulted in decreased RBL-CCR1 degranulation. Thus, it would be appropriate to hypothesize that a certain level of signaling from CCR1 is important for RBL-CCR1 activation.

Having analysed the effect of RGS1 on RBL-CCR1 degranulation, subsequent experiments from this study aimed to analyse the effect of RGS1 on chemokine and cytokine secretion from RBL-CCR1 following degranulation, in which RBL-CCR1 cells are co-stimulated with Mip1- α and IgE/antigen. The panel of chemokines and cytokines analysed were IL-4, IL-6, IL-10, MCP-1 and Mip1- α . The work from this study demonstrated that IL-4, IL-6 and MCP-1 were secreted at significantly higher levels from RGS1 siRNA treated RBL-CCR1 cells following co-stimulation of CCR1 and Fc ϵ R1 compared with Fc ϵ R1 alone or control cells. This data is consistent with other reports demonstrating that activation of mast cells can release several cytokines including IL-4, IL-6, which have significant effects in the mucosa, including the induction of adhesion molecules and chemokines that contribute the recruitment of inflammatory cells characteristic of the late-phase response (Anderson, 2001; Cook et al., 1998; Fifadara et al., 2009). MCP-1 is secreted in the ocular allergic disease VKC and produced by mast cells, epithelial cells, fibroblasts and macrophages (Kumagai et al., 2006; Leonardi et al., 2006; Leonardi et al., 2003). The data from the present study shows an increase in secreted levels of MCP-1 from Mip1- α and IgE/antigen co-stimulated RBL-CCR1 cells treated with RGS1 siRNA. Together, this data suggests that RGS1 regulates chemokine and cytokine secretion, most probably by driving the GPCR-CCR1 signaling pathway forward. However, the exact mechanism by which RGS1 plays a role in chemokine and cytokine secretion, and other events such as mast cell differentiation, homing, survival and ability to recruit other inflammatory cells requires further elucidation.

To date several members of the RGS family have been implicated in regulating immune cell migration; chemotaxis induced by CXCL12 was greater in short hairpin RGS13-HMC-1 cells compared with control (Bansal et al., 2008 a); RGS 2 and RGS16 overexpression inhibits chemotactic responses of lymphocyte cell lines *in vitro* (Bowman et al., 1998); RGS1 deficient B-cells chemotaxed to a greater extent after exposure to the chemokines CXCL13 and CXCL12 (Shi et al., 2002).

However, the role of RGS1 on mast cell motility is yet to be reported. Hence, the next aim of this study was to analyse whether RGS1 affects RBL-CCR1 chemotaxis, in which RBL-CCR1 cells were co-stimulated with Mip1- α and IgE/antigen. Data from the present study shows that RGS1 siRNA RBL-CCR1 cells pre-sensitised with IgE induced significantly greater levels of chemotaxis towards a gradient of Mip1- α and antigen as compared to co-stimulated control IgE pre-sensitised cells. This data suggests that 1) RGS 1 is a negative regulator of RBL-CCR1 chemotaxis and 2) by depleting RGS1, CCR1-GPCR pathway is accelerated thereby further increasing Mip1- α mediated chemotaxis.

Chapter 6

The role of TRB 3 in mast cell degranulation, mediator release and chemotaxis

6. The role of TRB 3 in mast cell degranulation, mediator release and chemotaxis

6.1 Introduction and hypothesis

Tribbles have been described as a family of proteins with potent signaling regulatory functions. They have been shown to interact with and modulate the activity of several MAPK activator MAPKK proteins (Kiss-Toth et al, 2004; Kiss-Toth et al, 2006). This suggests that TRB3 may also stimulate pro-inflammatory cytokines to activate a MAPK response when gene expression levels are high as well as play an important role in the allergic response. In addition, as previously described in Chapter 5, Aye and Ono (unpublished data) demonstrated the gene expression of TRB3 was further up-regulated after stimulating IgE sensitised RBL-CCR1 cells with Mip1- α and IgE/antigen.

Based on current knowledge, I hypothesise that TRB3, downstream of Fc ϵ R1 signaling, can regulate mast cell degranulation, chemotaxis and mediator release.

To address this hypothesis, the specific aims of this chapter were as follows: -

1. Using RNA interference to characterise how TRB3 affects RBL-CCR1 degranulation, in which RBL-CCR1 cells are co-stimulated with Mip1- α and IgE/antigen and appropriate controls.
2. Using RNA interference analyse how TRB3 affects cytokine and chemokine release from RBL-CCR1 cells following degranulation, in which RBL-CCR1 cells are co-stimulated with Mip1- α and IgE/antigen and appropriate controls.
3. Using RNA interference analyse how TRB3 affects RBL-CCR1 chemotaxis, in which RBL-CCR1 cells are co-stimulated with Mip1- α and IgE/antigen and appropriate controls.

6.2 Results

6.2.1 Depletion of endogenous TRB3 in RBL-CCR1 cells by RNA interference.

RNA interference was employed to deplete TRB3 content in RBL-CCR1 cells and therefore determine how TRB3 may affect RBL-CCR1 in processes such as degranulation, mediator release and chemotaxis. Western Blotting in Figure 43 confirmed that TRB3 protein was reduced in RBL-CCR1 cells expressing TRB3 siRNA compared with cells expressing the control TRB3 siRNA. The data are representative of more than 10 separate experiments.

Figure 43. Reduction of endogenous TRB3 in RBL-CCR1 cells by RNA interference.

RBL-CCR1 cells were transfected with either TRB3 siRNA or control siRNA. Lysates were prepared and TRB3 expression was evaluated by western blot with anti-TRB3 Ab. Anti-actin was used to further assess protein loading. Data are representative of 10 experiments.



6.2.2 Effect of TRB3 on RBL-CCR1 degranulation

The objective of these experiments was to examine the effect of TRB3 on RBL-CCR1 degranulation, in which RBL-CCR1 cells were co-stimulated with Mip1- α and IgE/antigen and appropriate controls. Degranulation of RBL-CCR1 was determined by measuring the release of the granule protein beta-hexosaminidase. The data are representative of 3 separate experiments, in which each condition was analysed in triplicate per experiment.

As shown in Figure 44, TRB3 siRNA treated RBL-CCR1 cells co-stimulated with Mip1- α and IgE/antigen displayed a significant increase in degranulation compared to co-stimulated cells treated with either control siRNA; IgE/antigen stimulated cells treated with TRB3 siRNA or; TRB3 siRNA treated cells stimulated with Mip1- α .

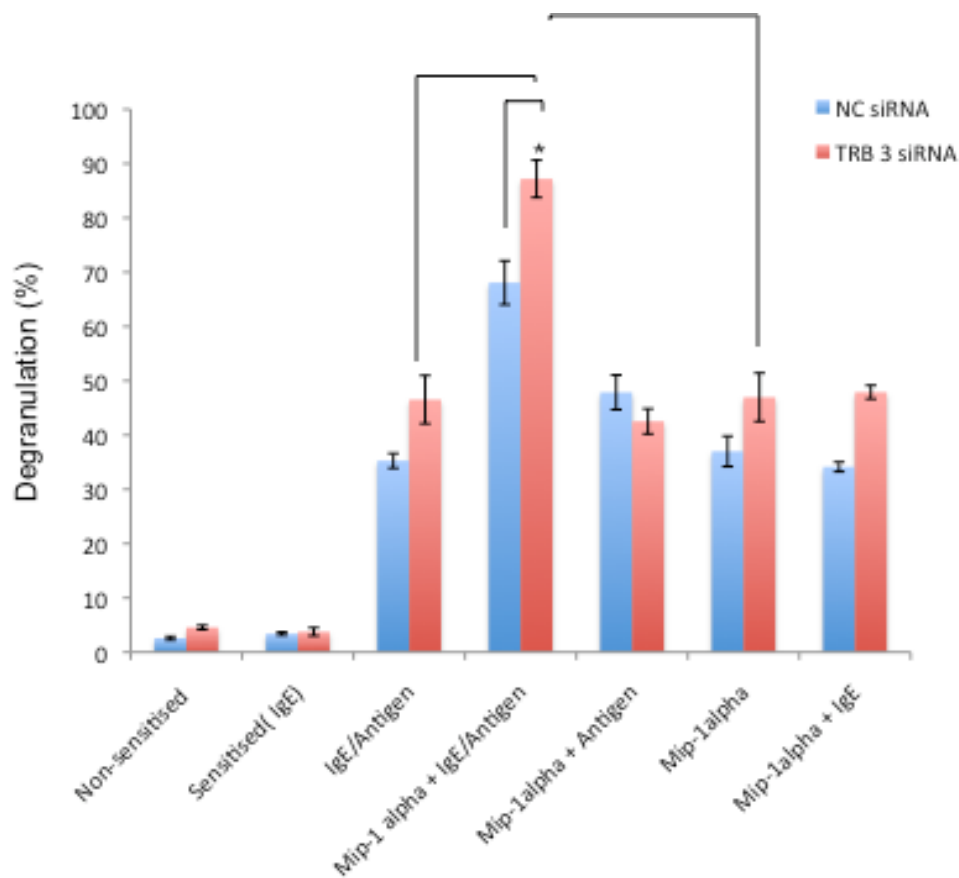


Figure 44. Co-stimulation by Mip1- α and IgE/antigen enhanced degranulation of TRB3 siRNA treated RBL-CCR1 cells.

After sensitization with IgE, RBL-CCR1 cells were stimulated with antigen and Mip1- α or with Mip1- α alone. The data represent the Mean \pm standard error mean (SEM) of three experiments where *, $p < 0.01$, using the student T-test.

KEY: TRB 3 siRNA= TRB3 siRNA. NC siRNA= control siRNA.

6.2.3 Effect of TRB3 on RBL-CCR1 mediator release of cytokines and chemokines

The objective of these experiments was to examine the effect of TRB3 on mediator release from RBL-CCR1 cells co-stimulated with Mip1- α and IgE/antigen 24 hours post degranulation. The chemokines and cytokines that were analysed from each cell supernatant were 1L-4, IL-6, IL-10, MCP-1 and Mip1- α . The data are representative of 3 separate experiments, in which each condition was analysed in triplicate per experiment.

As shown Figure 45, the expression of 1L-4, IL-6, IL-10, MCP-1 and Mip1- α in response to co-stimulation of CCR1 and Fc ϵ RI by Mip1- α and IgE/antigen respectively, compared with stimulation by IgE/antigen alone. Co-stimulated RBL-CCR1 cells treated with TRB3 siRNA secreted significantly high levels of IL-10 and MCP-1 compared to control siRNA treated co-stimulated RBL-CCR1 cells. In addition, RBL-CCR1 cells treated with TRB3 siRNA secreted significantly low levels of IL-4 and IL-6 in response to co-stimulation by Mip1- α and IgE/antigen compared to co-stimulated control siRNA treated cells.

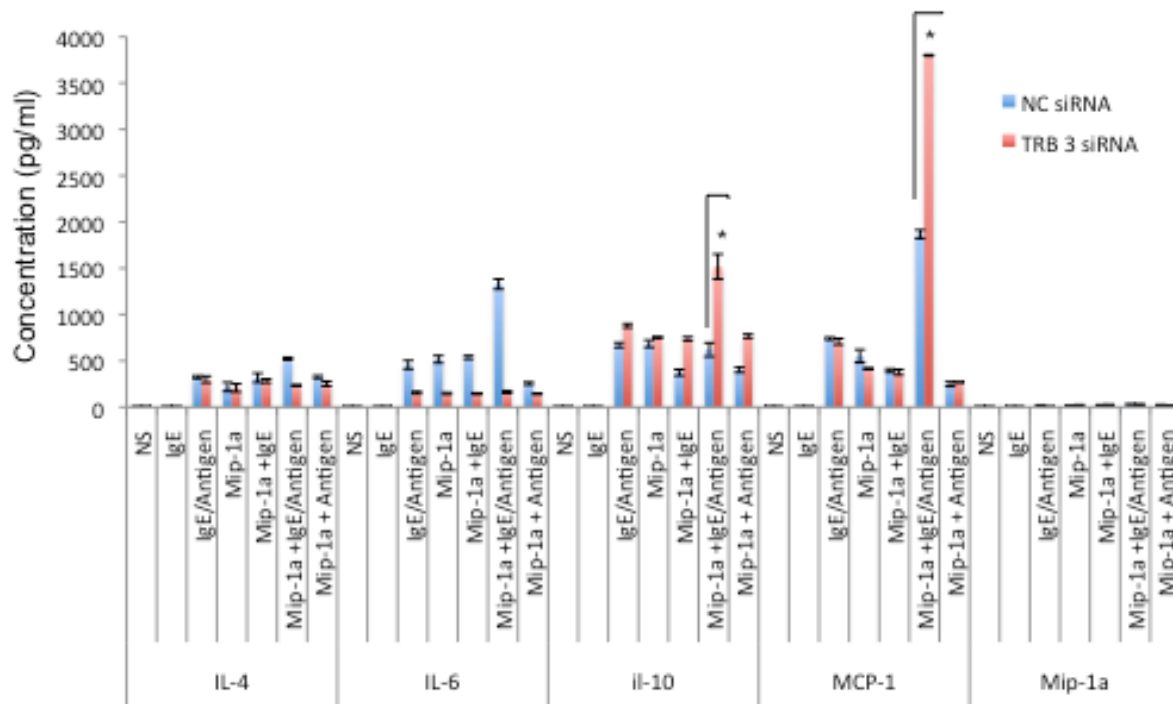


Figure 45. Co-stimulation with Mip-1 α and IgE/antigen enhanced mediator release of IL-10, and MCP-1 from TRB 3 siRNA treated RBL-CCR1 cells.

RBL-CCR1 cells were stimulated with Mip1- α and antigen (cells sensitised with IgE) or with Mip1- α alone. 24 hours post degranulation, supernatants were collected and analysed for chemokines and cytokine secretion. The data represent the Mean \pm standard error mean (SEM) of three experiments where *, $p < 0.01$, using the student T-test.

KEY: Rgs1 siRNA= RGS1siRNA. NC siRNA= control siRNA.

6.2.4 Effect of TRB3 on RBL-CCR1 chemotaxis

The objective of these experiments by using a transwell chemotaxis system was to examine the effect of TRB3 on RBL-CCR1 chemotaxis, in which RBL-CCR1 cells were co-stimulated with Mip-a and IgE/antigen. The data are representative of 3 separate experiments, in which each condition was analysed in triplicate per experiment.

As shown In Figure 46, shows the chemotaxis of RBL-CCR1 cells in response to co-stimulation by Mip1- α and IgE/antigen compared to stimulation by Mip1- α alone. Interestingly TRB3 siRNA treated RBL-CCR1 cells co-stimulated with Mip1a and IgE/antigen showed a significant increase in chemotaxis compared to co-stimulated control siRNA treated cells.

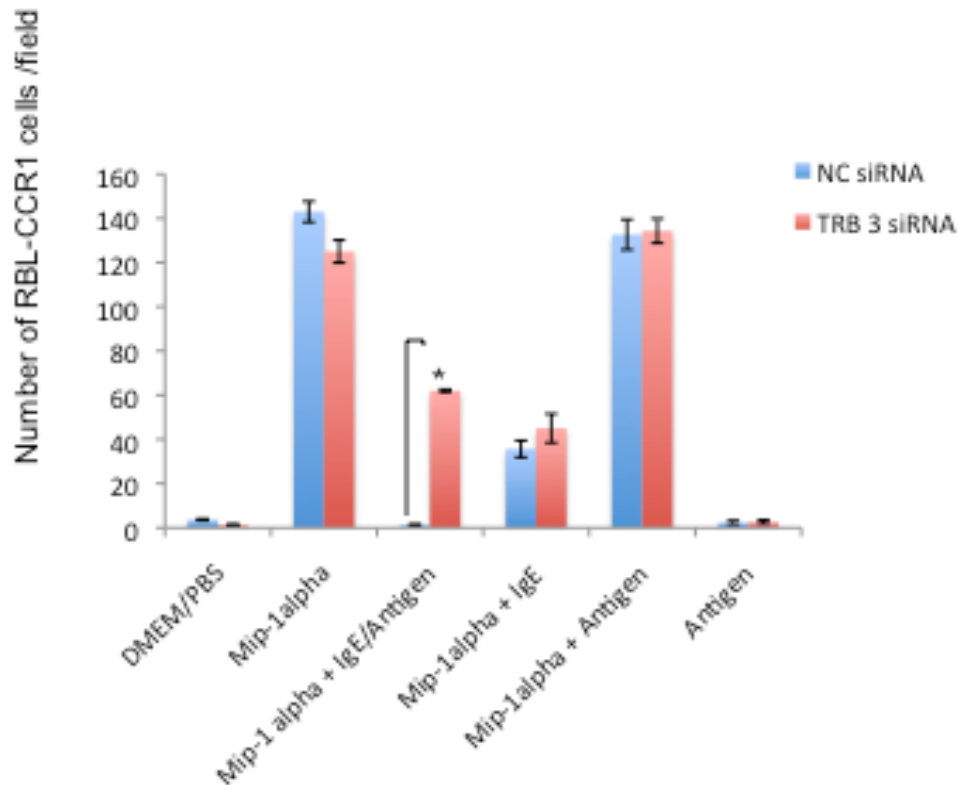


Figure 46. Co-stimulation by Mip1- α and IgE/antigen enhanced chemotaxis of TRB3 siRNA treated RBL-CCR1 cells.

RBL-CCR1 cells were stimulated with Mip1- α and antigen (cells sensitised with IgE) or with Mip1- α . The data represent the Mean \pm standard error mean (SEM) of three experiments where *, $p < 0.001$, using the student T-test.

KEY: TRB 3 siRNA= TRB 3 siRNA. NC siRNA= control siRNA.

6.3 Discussion

As previously mentioned, the gene expression of two genes, RGS1 and TRB3 were up-regulated after co-stimulation by Mip1- α and IgE/antigen (Aye and Ono, unpublished data). Tribbles have been described as a family of proteins with potent signaling regulatory functions, in which they interact with and modulate the activity of signal transduction pathways, including the PI3K (Ilyedjian, 2005; Du et al., 2003) and MAPK (Kiss-Toth et al., 2004; Hegedus et al., 2007) systems. On this basis, the overall aim of the present study was to analyse whether TRB3 may regulate degranulation, mediator release and chemotaxis of RBL-CCR1 cells, in which RBL-CCR1 cells are co-stimulated with Mip1- α and IgE/antigen. The findings from this study are the first to demonstrate that TRB3 indeed plays a negative regulatory role on RBL-CCR1 degranulation, mediator release and chemotaxis in response to CCR1 and Fc ϵ RI co-stimulation.

Co-stimulation by Mip1- α and IgE/antigen synergistically enhances degranulation of RBL-CCR1 cells, and this effect is mediated via a PI3K pathway (Toda et al., 2004). The signal transduction molecule, AKT, is transported to the cell membrane upon PI3K activation and is a fundamental component in cytoskeletal re-organisation, intracellular signaling and cell survival (Lemmon et al., 2002; Costello et al., 2002). Du et al., (2003) demonstrated in hepatic cells that TRB3 is a pseudokinase that binds AKT and inhibits phosphorylation of AKT, which is required for AKT to be active. This has been confirmed by other similar cell types (Naiki et al., 2007; Matsushima et al., 2006), including chondrocytes (Cravero et al., 2009). The first objective of this study was to determine whether TRB3 affects RBL-CCR1 degranulation, in which RBL-CCR1 cells were co-stimulated with Mip1- α and IgE/antigen. My findings demonstrated that upon co-stimulation with Mip1- α and IgE/antigen TRB3 siRNA RBL-CCR1 cells induced a significant increase in degranulation compared to co-stimulated cells treated with either control or IgE/antigen stimulated cells treated with TRB3 siRNA. This data suggests that TRB3 is a negative regulator of RBL-CCR1 degranulation, and moreover, through co-stimulation by CCR1 and Fc ϵ RI, TRB3 drives a signal cascade, possibly by inhibiting AKT that regulates the level of degranulation that is important in the allergic response. Future studies could analyse the interaction of TRB3 and AKT phosphorylation during CCR1 and Fc ϵ RI engagement on RBL-CCR1 cells.

TRB3 plays an important role in the regulation of several cytokines and

chemokines. It has been documented that TRB3 acts as a negative regulator of NF- κ B, a known regulator of IL-6 production (Grogan et al., 2001). Down regulation of TRB2 enhances IL-8 production both in THP-1 cells and in human primary monocytes via a MAPK signalling pathway (Eder et al., 2008). In addition, Smith et al., (2011) demonstrated that knockdown of TRIB3 by siRNA interference up-regulated TLR2-mediated NF- κ B activation and chemokine induction in response to *Helicobacter pylori* (H. pylori) LPS. IL-4 has also been associated with the allergic response by promoting the production of IgE, and chemokine and mucus production at the site of allergic inflammation (Kelly-Welch et al., 2003; Ownby, D.R. et al., 2001).

Following on from the regulatory role of TRB3 on RBL-CCR1 degranulation, subsequent experiments from this study aimed to investigate the effects of TRB3 on other mast cell processes such as mediator release following RBL-CCR1 degranulation, in which RBL-CCR1 cells were co-stimulated with Mip1- α and IgE/antigen. The findings from the present study demonstrated that upon co-stimulation by Mip1- α and IgE/antigen, RBL-CCR1 cells treated with TRB3 siRNA secreted significantly high levels of IL-10 and MCP-1 but significantly low levels of IL-4 and IL-6 compared to TRB3 siRNA treated cells stimulated with IgE/antigen alone. Surprisingly, the findings from this investigation demonstrate that a lack of TRB3 in RBL-CCR1 cells decreases levels of IL-4 and IL-6 (which does not correlate with previous reports for IL-6), thereby indicating that TRB3 does not serve as a negative regulator for these particular cytokines. It is possible that TRB3 is a positive regulator of NF- κ B, hence, future studies should validate this by analysing the interaction of TRB3 and NF- κ B following CCR1 and Fc ϵ RI engagement of RBL-CCR1 cells. MCP-1 is considered an important chemokine in immune interactions because it recruits monocytes to an area where it will promote an inflammatory response. However, MCP-1 is not a very potent chemoattractant for mast cells and is associated with the recruitment of lymphocytes and eosinophils (Taub et al., 1995). Data obtained from the present study demonstrated that MCP-1 was significantly increased through TRB3 siRNA treatment following CCR1 and Fc ϵ RI engagement, which indicates that TRB3 is a negative regulator for this chemokine. Hence, the negative regulatory effect of TRB3 on MCP-1 could potentially affect the recruitment of various immune cells such as monocytes and lymphocytes during an inflammatory response. Anti-inflammatory mediators, such as IL-10 antagonise the activities of Th1 cytokines (Lester et al., 1995; Romagnani

et al., 2000). The data from my study demonstrated that IL-10 secretion was also significantly increased through TRB3 siRNA treatment following CCR1 and FcεRI engagement of RBL-CCR1 cells. This data indicates that TRB3 is not only a negative regulator of MCP-1, but also for the anti-inflammatory cytokine IL-10.

The chemotaxis of cells to sites of inflammation in response to pathogenic stimuli or cytokines/chemokines is regulated via a PI3K signalling pathway. This study, along with the findings of Toda et al., (2004) demonstrated that co-stimulation by Mip1-α and IgE/antigen exhibited profound effects on RBL-CCR1 actin cytoskeleton and thereby, inhibited Mip1-α induced chemotaxis. As previously mentioned TRB3 inhibits AKT phosphorylation in many cell types (Du et al., 2003; Cravero et al., 2009), which in turn could potentially effect downstream signalling of the PI3K pathway and the chemotaxis process. Therefore it is of crucial importance to the physiological resolution of inflammation to have effective control mechanisms in place, which control mast cell responses. To date there are no reports demonstrating a regulatory role of TRB3 on mast cell chemotaxis. The final aim of the present study was to examine the effect of TRB3 on RBL-CCR1 chemotaxis, in which RBL-CCR1 cells were co-stimulated with Mip1-α and IgE/antigen. The findings from this study demonstrate that TRB3 siRNA treated RBL-CCR1 cells co-stimulated with Mip1α and IgE/antigen showed a significant increase in chemotaxis compared to co-stimulated control siRNA treated cells, but a significant decrease in chemotaxis compared to Mip1-α stimulated TRB3 siRNA treated cells. The results from this investigation indicate that while TRB3 is a negative regulator of IgE sensitized RBL-CCR1 chemotaxis towards Mip1-α and antigen, it serves as a positive regulator of RBL-CCR1 chemotaxis towards Mip1-α. It was not possible in the present study to further elucidate the exact molecular signalling components involved in this process following Mip1-α and FcεRI engagement, however, it is possible that TRB3 mediates its effects on chemotaxis by either modulating PI3K activation/AKT phosphorylation and/or MAPK systems, hence future studies should aim to test this.

Chapter 7
General discussion and future work

7. General discussion and future work

Allergic diseases affect 25% of the general population and costs associated with these diseases dominate public health budgets. At present therapeutic approaches target key mechanisms involved in the development of the clinical disease, these include: histamine with histamine receptor antagonists, mast cells with mast cell stabilisers, inflammation with corticosteroids, and finally severe inflammation with immuno-modulators (Verhagen et al., 2005; Leonardi et al., 2008, Frew, 2011). However, all of these agents pose side effects, whilst some such as corticosteroids give rise to adverse side effects such as glaucoma and cataracts. Hence, to establish novel therapeutic strategies, further insights to better understand the molecular basis of the allergic response are required.

Previous studies demonstrated that CCR1 and Fc ϵ R1 engagement following allergen mediated cross-linking resulted in three phenomena 1) enhanced synergistic degranulation in RBL-CCR1 cells and *ex vivo* murine conjunctival cells, 2) arrest of Mip-1 α induced chemotaxis of RBL-CCR1 cells (Toda et al., 2004; Miyazaki et al., 2005) and 3) gene expression up-regulation of RGS1 and TRB3 in RBL-CCR1 cells (Aye and Ono, unpublished data). Considering the role of mast cells in allergic inflammation the previous findings I have just discussed are consistent with the biology of the response. In that mast cells would migrate toward a chemoattractant gradient at sites of inflammation, but stop and accumulate where the concentration of allergen is high. Meanwhile the degranulation of mast cells at sites of inflammation is enhanced by co-stimulation with Mip-1 α and allergen at the sites where cells accumulate thereby focusing the inflammatory response.

The chemotaxis of mast cells to sites of inflammation and the subsequent release of mediators such as histamine and cytokines/chemokines upon degranulation are crucial to eliciting allergic inflammation. Unlike many other cell types such as neutrophils, fibroblasts, T-cells and *Dictyostelium* there is as yet very little evidence to understand mast cell chemotaxis at this level. The data presented in this study illuminate the role of WASP, CCR1 and actin polymerisation as mechanisms underlying Mip-1 α induced RBL-CCR1 chemotaxis. Moreover, CCR1 and Fc ϵ R1 engagement inhibits RBL-CCR1 actin reorganisation and other cell motility parameters such as directionality, which are required for Mip-1 α induced chemotaxis. In addition, by using siRNA the present study is the first to show that

RGS1 and TRB3 serve as negative regulators of RBL-CCR1 chemotaxis upon CCR1 and FcεR1 engagement.

Immune cells such as neutrophils and dendritic cells are highly motile. They can detect the presence of chemoattractant signals, and guide their movement in the direction of the concentration gradient of these signals. This process known as chemotaxis, has a role in diverse functions such as immune surveillance, wound healing and tissue homeostasis (Baggiolini, 1998; Norman and Hickey, 2005; Thelen and Stein, 2008; Zinselmeyer et al., 2008; Beltman et al., 2009; Velazquez and Teran, 2010). The mechanisms involved in cell motility have been extensively studied *in vitro* and *in vivo*, using a variety of different model systems and cell types. Chemotaxis can be divided into discrete stages. First, cells must adhere to their surrounding environment. When the cell response is chemotactic, chemotaxis requires that cells sense the direction of the chemical gradient in order to establish polarity. Polarization might improve chemotaxis by enhancing the persistence of movement towards the source. Once directionality is established, forward movement is driven by protrusion of a leading edge composed of lamellipodia which is periodically induced at points on the cell membrane. This is accompanied by simultaneous cell retraction, actin reorganization and detachment of adhesions at the cell rear. An array of proteins are required for efficient cell chemotaxis, ranging from actin-binding proteins, such as the Arp2/3 complex which are activated by adaptor proteins such as WASP; PI3Ks; PI(3,4,5)P₃ and GTP-binding proteins of the Rho family, Rac, Cdc42, and Rho (Machesky & Insall, 1998; Vanhaesebroeck et al., 2005; Villalonga and Ridley, 2006; Oak et al., 2007; Costa et al., 2007; Cain and Ridley, 2009).

The data presented here are the first to show by real time microscopy that CCR1 and FcεR1 engagement exhibits profound effects on RBL-CCR1 morphology: decreased membrane ruffling and inhibition of Mip-1α induced chemotaxis of RBL-CCR1 cells. The Rho family, Rac, Cdc42, and Rho control chemotaxis by mediating the reorganization of the actin cytoskeleton. Toda et al., (2004) demonstrated that Mip-1α-mediated chemotaxis of RBL-CCR1 cells was inhibited by Rho kinase (ROCK) inhibitor, Y-27632. Meanwhile, co-stimulation by Mip-1α and IgE/antigen enhanced Rac and Cdc42 activation but decreased ROCK activation in RBL-CCR1 cells compared with cells stimulated with Mip-1α alone. In addition to these findings, this study has demonstrated that Mip-1α induced

chemotaxis of RBL-CCR1 cells stimulates new sites of actin polymerization at the leading edge of polarized cells, along with WASP and CCR1 co-localisation at these sites, indicating that these events are necessary for the detection of, and subsequent chemotaxis of RBL-CCR1 towards a Mip-1 α gradient. *In vitro* studies demonstrate the Arp2/3 complex, which binds to the sides of pre-existing filaments and induces the formation of branches, thereby mediates actin polymerization. Activation of Arp2/3 is induced by the WASP/ Cdc42 pathway (Millard et al., 2004). Cdc42 seems to function as a master regulator of polarity in eukaryotic cells, and *in vitro* assays have shown that Cdc42 is active towards the front of migrating neutrophils (Etienne-Manneville, 2006; Van Keymeulen et al., 2006). This data corroborates with the present study in which WASP localization at the leading edge of polarised RBL-CCR1 cells would be an indication of Cdc42 activation at these new sites of actin polymerisation. Since Arp2/3 is a nucleator of actin polymerization (via WASP/Cdc42), future studies should analyse the role of Arp2/3 on RBL-CCR1 cell motility upon CCR1 and Fc ϵ R1 engagement. In addition, the key event that determines where actin polymerization occurs in polarized RBL-CCR1 cells is potentially determined by the localization of active Rac in the cell. This is probably achieved by locally produced PI(3,4,5)P3 as previously reported by Welch et al., 2003.

Chemoattractant receptors in both neutrophils and *Dictyostelium* signal through similar G proteins. Most systems contain a $\beta\gamma$ subunit, in which the $\beta\gamma$ -complex is a critical mediator for chemotaxis. The chemoattractant receptors in *Dictyostelium* and neutrophils are uniformly distributed along the cell perimeter during chemotaxis (Xiao et al., 1997; Servant et al., 1999). Surprisingly, in the present study CCR1 was localized at the leading edge of polarized RBL-CCR1 cells suggesting that these upstream components of the GPCR signal pathways shows a specific localization in chemotaxing or polarized RBL-CCR1 cells. Asymmetric CCR1 receptor localisation is consistent with Gomez-Mouton et al., 2004, who demonstrated asymmetrical distributions of chemokine receptors on the cell surface in response to a chemoattractant gradient. Future studies should analyse the spatial and temporal organisation of CCR1 and WASP in RBL-CCR1 cells following CCR1 and Fc ϵ R1 engagement so as to further define the molecular basis of arrested mast cell chemotaxis during the allergic response. This data collectively suggests that mast cells may use an ARP 2/3/WASP and GPCR -mediated pathways to facilitate chemotaxis during an allergic response, whereby co-

stimulation by CCR1 and FcεR1 engagement would enhance degranulation and mediator release from stationary mast cells, potentially affecting the late phase response and recruitment of other immune cells.

Numerous reports implicate PI3K isoforms and PI(3,4,5)P3 link early chemoattractant signals with downstream components of the chemotaxis response (Devreotes and Janetopoulos, 2003; Sadhu et al., 2003; Iglesias, 2009; Vanhaesebroeck et al., 2010). PI(3,4,5)P3 is generated from PtdIns(4,5)P2 by PI3Ks in *Dicytostelium* and in neutrophils and mediates cell polarization, and hence chemotaxis. Several studies have reported that the GFP—PH domain probe is recruited selectively to the membrane at the leading edge of *Dicytostelium*, fibroblasts, and neutrophils after exposure of to different chemoattractant stimuli (Merlot and Firtel, 2003). This is consistent with the present study which showed PI(3,4,5)P3 accumulation (using a GFP—PH domain probe) at the leading edge of polarized RBL-CCR1 cells in response to a Mip-1α gradient, suggesting a potential mechanism of RBL-CCR1 polarity and Mip-1α mediated chemotaxis. As it was not possible to reproduce these experiments more than twice, the indication that chemotaxis of RBL-CCR1 towards the chemokine Mip-1α cells might be mediated via a PI(3,4,5)P3 mediated pathway must be interpreted with caution.

To establish novel therapeutic approaches for allergic diseases and elucidate immunological mechanisms, animal models of ocular allergies have been developed over the past decade (Merayo-Llodes et al., 1996 ; Izushi et al., 2002; Groneberg et al., 2003; Miyazaki et al., 2005). Conjunctival mast cells are well-established targets for evaluating potential pharmaceutical interventions in ocular disease. The accumulation of mast cells into sites of inflammation occur by two mechanisms: 1) migration of progenitor mast cells from the blood and 2) re-localisation of mature mast cells within the tissue (Abonia et al., 2005; Gurish et al., 2001). Following on from analysing the effects of CCR1 and FcεR1 engagement on RBL-CCR1 motility *in vitro*, subsequent experiments analysed mast cell motility in murine allergic conjunctivitis. The findings from this study showed an increase in conjunctival mast cells in the inflamed conjunctiva compared to non-diseased eyes for both models of murine allergic conjunctivitis. Previous reports have indicated that increased numbers of mast cell progenitors at sites of inflammation may contribute to the accumulation of mature mast cells (Mwamtemi et al., 2001; Gurish and Boyce, 2006). However, from the present study, whether the increase in mast cell number in the inflamed conjunctiva is a

result of mast cell progenitor infiltration from circulation or resident mast cell re-localisation within the tissue is yet to be determined. CCR1⁺ mast cells were observed in the bronchial epithelium of patients with asthma (Amin et al., 2005). The level of Mip-1 α is increased in the asthmatic lung (Bisset and Schmid-Grendelmeier, 2005; Alam et al., 1996).

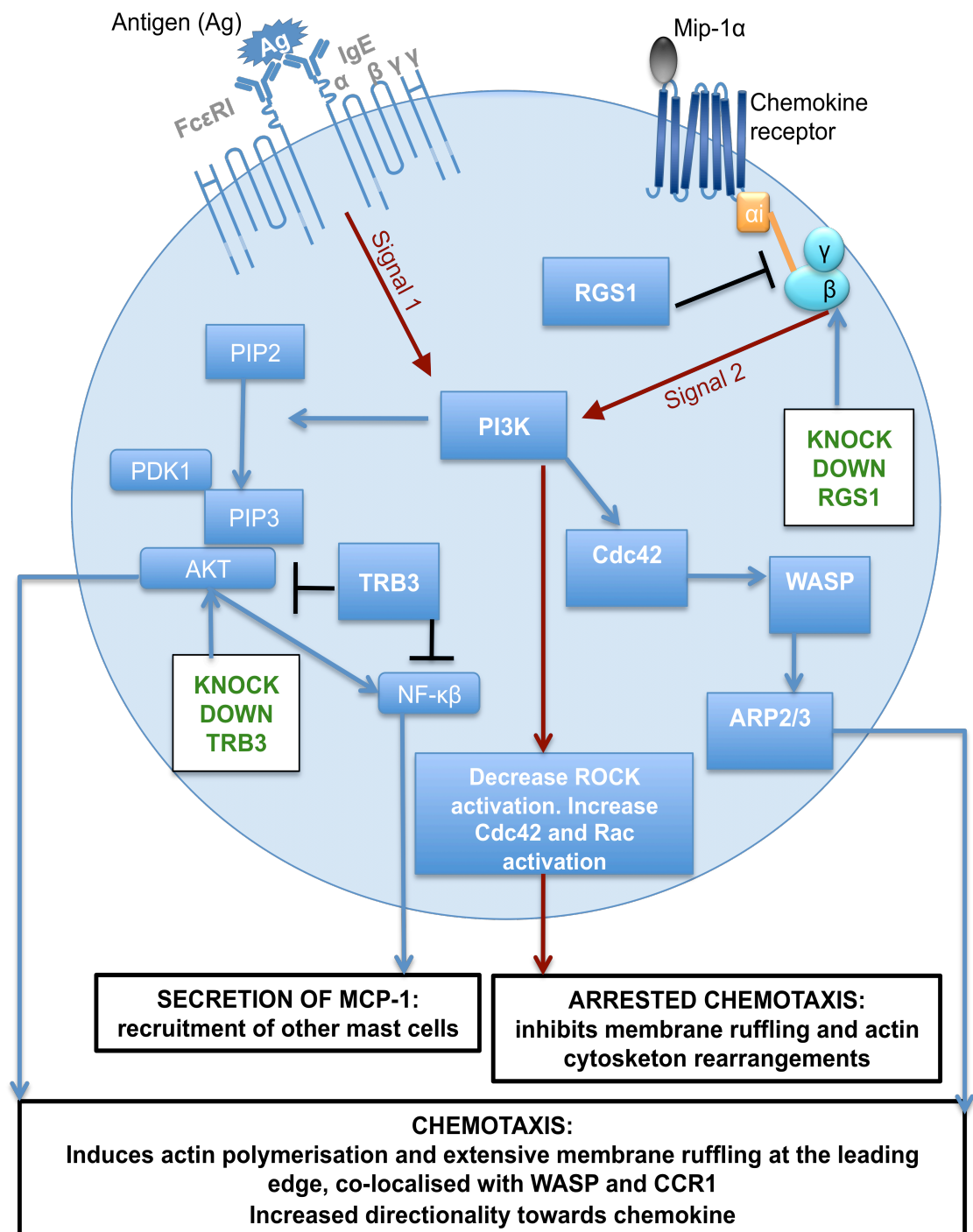
In addition to WASP and CCR1 posing potential mechanisms for mast cell polarisation and chemotaxis, the data presented in this study is the first to show that RGS1 and TRB3 regulate chemotaxis of RBL-CCR1 cells following CCR1 and Fc ϵ R1 engagement. The primary transducer used by GPCRs is the heterotrimeric G protein, which consists of α , β and γ subunits. In the absence of receptor stimulation, these subunits co-exist as one complex, in which the α subunit is bound to GDP. Upon GPCR stimulation by chemokine, G α exchanges GTP for GDP and temporarily dissociates from the $\beta\gamma$ subunit, in which the $\beta\gamma$ subunit is essential for chemotaxis via PI3K signalling pathway at the cell membrane. RGS proteins accelerate the return of G α to its inactive GDP-form thereby facilitating the re-formation of the G α -GDP- $\beta\gamma$ subunit and promoting more rapid termination of G-protein signalling pathways (Watson et al., 1996). In the present study, RGS1 siRNA treated RBL-CCR1 cells co-stimulated with Mip-1 α and IgE/antigen significantly up-regulated chemotaxis of RBL-CCR1 cells, indicating that RGS1 is a negative regulator of RBL-CCR1 chemotaxis. It is possible that this response is mediated by the inhibition of RGS activity, which would result in the dissociation of the $\beta\gamma$ subunit from G α subunit thereby further promoting PI3K down stream signalling and chemotaxis. This mechanism would potentially corroborate with a recent study by Bansal et al., 2008 who showed that phosphorylation, and chemotaxis induced by CXCL12 were greater in short hairpin RGS13-HMC-1 cells compared with control. In addition, RGS13 over-expression inhibited CXCL12-evoked phosphorylation and chemotaxis. Unlike RGS1, TRB3 modulates several cellular processes such as mediator release by interacting with NF- κ B or MAPKs (Du et al., 2003; Koo et al., 2004; Hegedus et al., 2007), which would otherwise induce cell polarization/chemotaxis and cytokine/chemokine release. The data presented here is the first to demonstrate that TRB3 is negative regulator of RBL-CCR1 chemotaxis, following CCR1 and Fc ϵ R1 engagement. Upon CCR1 and Fc ϵ R1 engagement TRB3 siRNA treated RBL-CCR1 cells significantly upregulated chemotaxis, and it is possible that these affects are mediated via a PI3K/ pathway.

However, a previous study by Sung et al., 2007 demonstrated that depletion of TRB1 (using siRNA) led to an increase in transmigrated smooth muscle cells in response to PDGF. Inhibition of the JNK pathway demolished the effect of siRNA TRB1 treatment, suggesting that TRB1 may be a negative regulator of smooth muscle chemotaxis via inhibitory activity of the JNK pathway. It is very possible that the basic molecular mechanisms responsible for tribbles action are similar for TRB3 to those reported for TRB1 previously. Future experiments should further define the role of TRB3 on RBL-CCR1 chemotaxis and its interaction with PI3K and JNK signaling pathways upon CCR1 and FcεR1 engagement.

Mast cell activation requires co-ordinated events that result in degranulation and mediator release when encountering a given antigen (Furumoto et al., 2004; Gilfillan and Tkaczyk, 2006). Mast cells express CCR1, CCR2, CCR3 and CCR5 (Ono et al., 2003) on their cell surface, where MCP-1 is the respective ligand for CCR2. In addition, MCP-1 directly activates mast cells in murine models of airway inflammation, and up-regulated levels of MCP-1 have been identified in bronchoalveolar lavage fluid and bronchial tissue in patients with asthma (Alam et al., 1996). The present study demonstrated that upon CCR1 and FcεR1 engagement, depletion of RGS1 and TRB3 significantly upregulated the secretion of several cytokines and chemokines, which included MCP-1. This data suggests that RGS1 and TRB3 are negative regulators of MCP-1 secretion, by possibly promoting NF-κβ activation, and hence gene transcription of MCP-1. Regulation of MCP-1 by TRB3 and RGS1 would potentially determine the level of mediator release from degranulating mast cells, which are important in the recruitment of other mast cells, and hence the allergic inflammatory response.

In conclusion, the mechanisms underlying mast cell accumulation and arrest at sites of inflammation are a therapeutic target for allergic diseases. The discovery that chemokines control the movement and activation of immune cells, has provided attractive new targets for anti-inflammatory drug design. A CCR1 antagonist has been shown to decrease the number of clinical symptoms related to asthmatic type inflammation in murine models of asthma (Carpenter et al., 2005). Although a CCR1 antagonist could potentially treat allergic diseases, a disadvantage regarding CCR antagonists is that many chemokines are promiscuous ligands. RGS proteins expressed in mast cells and lymphocytes (Druey et al, 1996; Reif and Cyster et al., 2000; Oliveira-Dos-Santos et al., 2000;

Bansal et al., 2008) represent a vital regulatory component of the signalling pathways induced by GPCRs in allergic inflammation. Hence, inhibition of RGS activity may potentially exhibit profound effects on the specificity and potency of GPCR-targeted drugs. A compound that specifically inhibits RGS4 activity *in vitro* has recently shown promise (Roman et al., 2007). In view of the present study, RGS1 regulates degranulation, mediator release and chemotaxis in RBL-CCR1 cells, suggesting that RGS1 might represent a useful target for therapeutic intervention for the treatment of allergic diseases. In addition, the findings from this study provide evidence that TRB3 can act as a regulator of mast cell chemotaxis. Manipulation of TRB3 may be particularly attractive to the pharmaceutical industry as the predicted prevention of down-regulation would be to reduce the allergic inflammatory response.



A schematic model to describe the molecular basis of mast cell motility in allergic inflammation based on the findings from this study.

FcεR1 engagement by antigen (signal 1) and CCR1 engagement by Mip-1α (signal 2) independently induce degranulation of mast cells via PI3K. Mip-1α (signal 2) induced mast cell chemotaxis is mediated via PI3K, WASP, CCR1 and actin polymerisation at the leading edge of the cell. However, co-stimulation by Mip-1α and IgE/antigen (signal 1 plus 2) results in inhibition of membrane ruffling and arrested chemotaxis. Depletion of RGS1 and TRB3 induce increased chemotaxis in the presence of signal 1 and 2.

KEY: Signal 1= FcεR1 engagement by antigen. Signal 2=CCR1 engagement by Mip-1α

Chapter 8. References

Abe, M., Kurosawa, M., Igarashi, Y., Ishikawa, O. and Miyachi, Y. (2000) Influence of IgE-mediated activation of cultured human mast cells on proliferation and type I collagen production by human dermal fibroblasts. *J. Allergy Clin. Immunol.* 106, S72–S77

Abonia JP, Austen KF, Rollins BJ, Joshi SK, Flavell RA, Kuziel WA, Koni PA, Gurish MF. Constitutive homing of mast cell progenitors to the intestine depends on autologous expression of the chemokine receptor CXCR2. *Blood.* 2005 Jun 1;105(11):4308-13.

Abonia JP, Hallgren J, Jones T, Shi T, Xu Y, Koni P, Flavell RA, Boyce JA, Austen KF, Gurish MF. Alpha-4 integrins and VCAM-1, but not MAdCAM-1, are essential for recruitment of mast cell progenitors to the inflamed lung. *Blood.* 2006 Sep 1;108(5):1588-94.

Akbari O, Faul JL, Hoyte EG, et al. CD4₊ invariant T-cell receptor+natural killer T cells in bronchial asthma. *N Engl J Med* 354:1117–1129, 2006.

Alam R, Forsythe PA, Stafford S, Lett-Brown MA, Grant JA. Macrophage inflammatory protein-1 alpha activates basophils and mast cells. *J Exp Med.* 1992 Sep 1;176(3):781-6.

Alam R, York J, Boyars M, Stafford S, Grant JA, Lee J, Forsythe P, Sim T, Ida N. Increased MCP-1, RANTES, and MIP-1alpha in bronchoalveolar lavage fluid of allergic asthmatic patients. *Am J Respir Crit Care Med.* 1996 Apr;153(4 Pt 1):1398-404.

Alcami A. Viral mimicry of cytokines, chemokines and their receptors. *Nat Rev Immunol.* 2003 Jan;3(1):36-50

Alexander JM, Nelson CA, van Berkel V, Lau EK, Studts JM, Brett TJ, Speck SH, Handel TM, Virgin HW, Fremont DH. Structural basis of chemokine sequestration by a herpesvirus decoy receptor. *Cell.* 2002 Nov 1;111(3):343-56.

Alexandrakis M, Letourneau R, Kempuraj D, Kandere-Grzybowska K, Huang M, Christodoulou S, Boucher W, Seretakis D, Theoharides TC. Flavones inhibit proliferation and increase mediator content in human leukemic mast cells (HMC-1). *Eur J Haematol*. 2003 Dec;71(6):448-54.

Ali K, Bilancio A, Thomas M, Pearce W, Gilfillan AM, Tkaczyk C, Kuehn N, Gray A, Giddings J, Peskett E, Fox R, Bruce I, Walker C, Sawyer C, Okkenhaug K, Finan P, Vanhaesebroeck B. Essential role for the p110delta phosphoinositide 3-kinase in the allergic response. *Nature*. 2004 Oct 21;431(7011):1007-11.

Amin K, Janson C, Harvima I, Venge P, Nilsson G. CC chemokine receptors CCR1 and CCR4 are expressed on airway mast cells in allergic asthma. *J Allergy Clin Immunol*. 2005 Dec;116(6):1383-6.

Anderson DW. Cytokines as drug targets. *IDrugs*. 2001 Apr;4(4):375-7.

Anfossi N, Lucas M, Diefenbach A, Bühring HJ, Raulet D, Tomasello E, Vivier E. Contrasting roles of DAP10 and KARAP/DAP12 signaling adaptors in activation of the RBL-2H3 leukemic mast cell line. *Eur J Immunol*. 2003 Dec;33(12):3514-22.

Anthony, R. M., Rutitzky, L. I., Urban, J. F., Jr., Stadecker, M. J. and Gause, W. C. Protective immune mechanisms in helminth infection. *Nat. Rev. Immunol*. 7, 975–987. (2007)

Apostolou I, Verginis P, Kretschmer K, et al. Peripherally induced Treg: Mode, stability, and role in specific tolerance. *J Clin Immunol* 28:619–624, 2008.

Applequist, S. E., Wallin, R. P. and Ljunggren, H. G. Variable expression of Toll-like receptor in murine innate and adaptive immune cell lines. *Int. Immunol*. 14, 1065–1074. (2002)

Aragay AM, Mellado M, Frade JM, Martin AM, Jimenez-Sainz MC, Martinez-A C, Mayor F Jr. Monocyte chemoattractant protein-1-induced CCR2B receptor desensitization mediated by the G protein-coupled receptor kinase 2. *Proc Natl Acad Sci U S A*. 1998 Mar 17;95(6):2985-90.

Asai K, Kitaura J, Kawakami Y, Yamagata N, Tsai M, Carbone DP, Liu FT, Galli SJ, Kawakami T. Regulation of mast cell survival by IgE. *Immunity*. 2001 Jun;14(6):791-800.

Aspenström P, Lindberg U, Hall A. Two GTPases, Cdc42 and Rac, bind directly to a protein implicated in the immunodeficiency disorder Wiskott-Aldrich syndrome. *Curr Biol*. 1996 Jan 1;6(1):70-5.

Baecher-Allan C, Brown JA, Freeman GJ, and Hafler DA. CD4⁺CD25^{high} regulatory cells in human peripheral blood. *J Immunol* 167:1245–1253, 2001.

Baeuerle, P.A. I κ B-NF- κ B structures: at the interface of inflammation control. *Cell* 1998, 95, 729-731.

Baggiolini M. Chemokines and leukocyte traffic. *Nature*. 1998 Apr 9;392(6676):565-8.

Baldwin, A.S. Control of oncogenesis and cancer therapy resistance by the transcription factor NF- κ B. *J. Clin. Investig.* 2001, 107, 241-246.

Bansal G, DiVietro JA, Kuehn HS, Rao S, Nocka KH, Gilfillan AM, Druey KM. RGS13 controls G protein-coupled receptor-evoked responses of human mast cells. *J Immunol*. 2008 Dec 1;181(11):7882-90.

Bansal G, Xie Z, Rao S, Nocka KH, Druey KM. Suppression of immunoglobulin E-mediated allergic responses by regulator of G protein signaling 13. *Nat Immunol*. 2008 Jan;9(1):73-80.

Barlic J, Khandaker MH, Mahon E, Andrews J, DeVries ME, Mitchell GB, Rahimpour R, Tan CM, Ferguson SS, Kelvin DJ. β -arrestins regulate interleukin-8-induced CXCR1 internalization. *J Biol Chem*. 1999 Jun 4;274(23):16287-94.

Bear JE, Rawls JF, Saxe CL 3rd. SCAR, a WASP-related protein, isolated as a suppressor of receptor defects in late *Dictyostelium* development. *J Cell Biol*. 1998 Sep 7;142(5):1325-35.

Beaven MA. Our perception of the mast cell from Paul Ehrlich to now. *Eur J Immunol*. 2009 Jan;39(1):11-25.

Beer F, Kuo CH, Morohoshi K, Goodliffe J, Munro P, Aye CC, Dawson M, Richardson RM, Jones LH, Ikeda Y, Nakamura T, Toda M, Flynn T, Ohbayashi M, Miyazaki D, Ono SJ. Role of beta-chemokines in mast cell activation and type I hypersensitivity reactions in the conjunctiva: in vivo and in vitro studies. *Immunol Rev*. 2007 Jun;217:96-104

Beltman JB, Marée AF, de Boer RJ. Analysing immune cell migration. *Nat Rev Immunol*. 2009 Nov;9(11):789-98. Epub 2009 Oct 16.

Bernards A. GAPs galore! A survey of putative Ras superfamily GTPase activating proteins in man and Drosophila. *Biochim Biophys Acta*. 2003 Mar 17;1603(2):47-82.

Berzat A, Hall A. Cellular responses to extracellular guidance cues. *EMBO J*. 2010 Aug 18;29(16):2734-45.

Bilenki L, Yang J, Fan Y, et al. Natural killer T cells contribute to airway eosinophilic inflammation induced by ragweed through enhanced IL-4 and eotaxin production. *Eur J Immunol* 34:345–354, 2004

Bishop AL, Hall A. Rho GTPases and their effector proteins. *Biochem J*. 2000 Jun 1;348 Pt 2:241-55.

Bisset LR, Schmid-Grendelmeier P. Chemokines and their receptors in the pathogenesis of allergic asthma: progress and perspective. *Curr Opin Pulm Med*. 2005 Jan;11(1):35-42.

Bissonnette EY, Enciso JA, Befus AD. TGF-beta1 inhibits the release of histamine and tumor necrosis factor-alpha from mast cells through an autocrine pathway. *Am J Respir Cell Mol Biol*. 1997 Mar;16(3):275-82.

Borish LC, Steinke JW. Cytokines and chemokines. *J Allergy Clin Immunol*. 2003 Feb;111(2 Suppl):S460-75.

Bousso P, Bhakta NR, Lewis RS, Robey E. Science. 2002 Jun 7;296(5574):1876-80. Dynamics of thymocyte-stromal cell interactions visualized by two-photon microscopy.

Bowers, A.J.; Scully, S.; Boylan, J.F. SKIP3, a novel Drosophila tribbles ortholog, is overexpressed in human tumors and is regulated by hypoxia. Oncogene 2003, 18, 2823.

Bowman EP, Campbell JJ, Druey KM, Scheschonka A, Kehrl JH, Butcher EC. Regulation of chemotactic and proadhesive responses to chemoattractant receptors by RGS (regulator of G-protein signaling) family members. J Biol Chem. 1998 Oct 23;273(43):28040-8.

Byrne, S. N., Limon-Flores, A. Y. and Ullrich, S. E. (2008) Mast cell migration from the skin to the draining lymph nodes upon ultraviolet irradiation represents a key step in the induction of immune suppression. J. Immunol. 180, 4648–4655

Campellone KG, Webb NJ, Znameroski EA, Welch MD. WHAMM is an Arp2/3 complex activator that binds microtubules and functions in ER to Golgi transport. Cell. 2008 Jul 11;134(1):148-61.

Cammer M, Gevrey JC, Lorenz M, Dovas A, Condeelis J, Cox D. The mechanism of CSF-1-induced Wiskott-Aldrich syndrome protein activation in vivo: a role for phosphatidylinositol 3-kinase and Cdc42. J Biol Chem. 2009 Aug 28;284(35):23302-11.

Campbell DJ, and Ziegler SF. FOXP3 modifies the phenotypic and functional properties of regulatory T cells. Nat Rev Immunol 7:305–310, 2007.

Cantrell DA. Phosphoinositide 3-kinase signalling pathways. J Cell Sci. 2001 Apr;114 (Pt 8):1439-45

Carpenter KJ, Ewing JL, Schuh JM, Ness TL, Kunkel SL, Aparici M, Miralpeix M, Hogaboam CM. Therapeutic targeting of CCR1 attenuates established chronic fungal asthma in mice. Br J Pharmacol. 2005 Aug;145(8):1160-72.

Castellani ML, Vecchiet J, Salini V, Conti P, Theoharides TC, Caraffa A, Antinolfi P, Teté S, Ciampoli C, Cuccurullo C, Cerulli G, Felaco M, Boscolo P. Stimulation of CCL2 (MCP-1) and CCL2 mRNA by substance P in LAD2 human mast cells. *Transl Res.* 2009 Jul;154(1):27-33.

Chadborn NH, Ahmed AI, Holt MR, Prinjha R, Dunn GA, Jones GE, Eickholt BJ. PTEN couples Sema3A signalling to growth cone collapse. *J Cell Sci.* 2006 Mar 1;119(Pt 5):951-7.

Chahdi, A., Sorokin, A., Dunn, M. J. and Landry, Y. The Rac/Cdc42 guanine nucleotide exchange factor beta1Pix enhances mastoparan-activated Gi-dependent pathway in mast cells. *Biochem. Biophys. Res. Commun.* 317, 384–389. (2004)

Chen L, Janetopoulos C, Huang YE, Iijima M, Borleis J, Devreotes PN. Two phases of actin polymerization display different dependencies on PI(3,4,5)P₃ accumulation and have unique roles during chemotaxis. *Mol Biol Cell.* 2003 Dec;14(12):5028-37.

Chung CY, Funamoto S, Firtel RA. Signaling pathways controlling cell polarity and chemotaxis. *Trends Biochem Sci.* 2001 Sep;26(9):557-66.

Chung CY, Lee S, Briscoe C, Ellsworth C, Firtel RA. Role of Rac in controlling the actin cytoskeleton and chemotaxis in motile cells. *Proc Natl Acad Sci U S A.* 2000 May 9;97(10):5225-30.

Chung CY, Potikyan G, Firtel RA. Control of cell polarity and chemotaxis by Akt/PKB and PI3 kinase through the regulation of PAKα. *Mol Cell.* 2001 May;7(5):937-47.

Chung MJ, Park JK, Park YI. Anti-inflammatory effects of low-molecular weight chitosan oligosaccharides in IgE-antigen complex-stimulated RBL-2H3 cells and asthma model mice. *Int Immunopharmacol.* 2012 Feb;12(2):453-9.

Cocchi F, DeVico AL, Garzino-Demo A, Arya SK, Gallo RC, Lusso P. Identification of RANTES, MIP-1 α, and MIP-1 β as the major HIV-suppressive factors produced by CD8⁺ T cells. *Science.* 1995 Dec 15;270(5243):1811-5.

Colditz IG, Schneider MA, Pruenster M, Rot A. Chemokines at large: in-vivo mechanisms of their transport, presentation and clearance. *Thromb Haemost.* 2007 May;97(5):688-93.

Colgan JD, Hankel IL. Signaling pathways critical for allergic airway inflammation. *Curr Opin Allergy Clin Immunol.* 2010 Feb;10(1):42-7.

Cook EB, Stahl JL, Lilly CM, Haley KJ, Sanchez H, Luster AD, Graziano FM, Rothenberg ME. Epithelial cells are a major cellular source of the chemokine eotaxin in the guinea pig lung. *Allergy Asthma Proc.* 1998 Jan-Feb;19(1):15-22.

Coombes JL, Robinson NJ, Maloy KJ, et al. Regulatory T cells and intestinal homeostasis. *Immunol Rev* 204:184 –194, 2005.

Cory GO, Cramer R, Blanchoin L, Ridley AJ. Phosphorylation of the WASP-VCA domain increases its affinity for the Arp2/3 complex and enhances actin polymerization by WASP. *Mol Cell.* 2003 May;11(5):1229-39.

Costello PS, Gallagher M, Cantrell DA. Sustained and dynamic inositol lipid metabolism inside and outside the immunological synapse. *Nat Immunol.* 2002 Nov;3(11):1082-9.

Cravero JD, Carlson CS, Im HJ, Yammani RR, Long D, Loeser RF. Increased expression of the Akt/PKB inhibitor TRB3 in osteoarthritic chondrocytes inhibits insulin-like growth factor 1-mediated cell survival and proteoglycan synthesis. *Arthritis Rheum.* 2009 Feb;60(2):492-500.

Curnock AP, Ward SG. Development and characterisation of tetracycline-regulated phosphoinositide 3-kinase mutants: assessing the role of multiple phosphoinositide 3-kinases in chemokine signaling. *J Immunol Methods.* 2003 Feb;273(1-2):29-41

Dahl ME, Dabbagh K, Liggitt D, Kim S, Lewis DB. Viral-induced T helper type 1 responses enhance allergic disease by effects on lung dendritic cells. *Nat Immunol.* 2004 Mar;5(3):337-43.

Dardalhon V, Awasthi A, Kwon H, et al. IL-4 inhibits TGF- β -induced Foxp3⁺ T cells and, together with TGF- β , generates IL-9⁺ IL-10⁺ Foxp3⁻ effector T cells. *Nat Immunol* 2008; 9:1347-1355.

DerMardirossian C, Bokoch GM. GDIs: central regulatory molecules in Rho GTPase activation. *Trends Cell Biol.* 2005 Jul;15(7):356-63.

Derry JM, Ochs HD, Francke U. Isolation of a novel gene mutated in Wiskott-Aldrich syndrome. *Cell.* 1994 Aug 26;78(4):635-44.

Devreotes P, Janetopoulos C. Eukaryotic chemotaxis: distinctions between directional sensing and polarization. *J Biol Chem.* 2003 Jun 6;278(23):20445-8.

Devreotes PN, Zigmond SH. Chemotaxis in eukaryotic cells: a focus on leukocytes and Dictyostelium. *Annu Rev Cell Biol.* 1988;4:649-86.

Droese J, Mokros T, Hermosilla R, Schüle R, Lipp M, Höpken UE, Rehm A. HCMV-encoded chemokine receptor US28 employs multiple routes for internalization. *Biochem Biophys Res Commun.* 2004 Sep 10;322(1):42-9.

Druey KM, Blumer KJ, Kang VH, Kehrl JH. Inhibition of G-protein-mediated MAP kinase activation by a new mammalian gene family. *Nature.* 1996 Feb 22;379(6567):742-6.

Du, K.; Herzig, S.; Kulkarni, R.N.; Montminy, M. TRB3: a tribbles homolog that inhibits Akt/PKB activation by insulin in liver. *Science* 2003, 300, 1574-1577.

Du, K.; Tsichlis, P.N. Regulation of the Akt kinase by interacting proteins. *Oncogene* 2005, 24, 7401-7409.

Duhen T, Geiger R, Jarrossay D, et al. Production of interleukin 22 but not interleukin 17 by a subset of human. *Nat Immunol.* 2009 Aug;10(8):857-63.

Echtenacher B, Männel DN, Hültner L. Critical protective role of mast cells in a model of acute septic peritonitis. *Nature.* 1996 May 2;381(6577):75-7.

Eder K, Guan H, Sung HY, Ward J, Angyal A, Janas M, Sarmay G, Duda E, Turner M, Dower SK, Francis SE, Crossman DC, Kiss-Toth E. Tribbles-2 is a novel regulator of inflammatory activation of monocytes. *Int Immunol*. 2008 Dec;20(12):1543-50.

Eiseman E, Bolen JB. Engagement of the high-affinity IgE receptor activates src protein-related tyrosine kinases. *Nature*. 1992 Jan 2;355(6355):78-80

Eisenbarth SC, Piggott DA, Huleatt JW, Visintin I, Herrick CA, Bottomly K. Lipopolysaccharide-enhanced, toll-like receptor 4-dependent T helper cell type 2 responses to inhaled antigen. *J Exp Med*. 2002 Dec 16;196(12):1645-51.

Etienne-Manneville S, Hall A. Rho GTPases in cell biology. *Nature*. 2002 Dec 12;420(6916):629-35.

Etienne-Manneville S. In vitro assay of primary astrocyte migration as a tool to study Rho GTPase function in cell polarization. *Methods Enzymol*. 2006;406:565-78.

Eyerich S, Eyerich K, Pennino D, et al. Th22 cells represent a distinct human T cell subset involved in epidermal immunity and remodeling. *J Clin Invest* 119:3573–3585, 2009.

Fan J, Malik AB. Toll-like receptor-4 (TLR4) signaling augments chemokine-induced neutrophil migration by modulating cell surface expression of chemokine receptors. *Nat Med*. 2003 Mar;9(3):315-21.

Ferguson GJ, Milne L, Kulkarni S, Sasaki T, Walker S, Andrews S, Crabbe T, Finan P, Jones G, Jackson S, Camps M, Rommel C, Wymann M, Hirsch E, Hawkins P, Stephens L. PI(3)Kgamma has an important context-dependent role in neutrophil chemokinesis. *Nat Cell Biol*. 2007 Jan;9(1):86-91.

Ferguson SS, Zhang J, Barak LS, Caron MG. Molecular mechanisms of G protein-coupled receptor desensitization and resensitization. *Life Sci*. 1998;62(17-18):1561-5.

Ferry, X., Brehin, S., Kamel, R. and Landry, Y. G protein-dependent activation of mast cell by peptides and basic secretagogues. *Peptides* 23, 1507–1515. (2002)

Fifadara NH, Aye CC, Raghuwanshi SK, Richardson RM, Ono SJ. CCR1 expression and signal transduction by murine BMMC results in secretion of TNF- α , TGF β -1 and IL-6. *Int Immunol*. 2009 Aug;21(8):991-1001.

Fifadara NH, Beer F, Ono S, Ono SJ. Interaction between activated chemokine receptor 1 and Fc ϵ RI at membrane rafts promotes communication and F-actin-rich cytoneme extensions between mast cells. *Int Immunol*. 2010 Feb;22(2):113-28.

Firtel RA, Chung CY. The molecular genetics of chemotaxis: sensing and responding to chemoattractant gradients. *Bioessays*. 2000 Jul;22(7):603-15.

Franchi, L., Park, J. H., Shaw, M. H., Marina-Garcia, N., Chen, G., Kim, Y. G. and Nunez, G. Intracellular NOD-like receptors in innate immunity, infection and disease. *Cell Microbiol*. 10, 1–8 (2008)

Fredriksson R, Lagerström MC, Lundin LG, Schiöth HB. The G-protein-coupled receptors in the human genome form five main families. Phylogenetic analysis, paralogon groups, and fingerprints. *Mol Pharmacol*. 2003 Jun;63(6):1256-72.

Friedl, P. Prespecification and plasticity: Shifting mechanisms of cell migration. *Curr. Opin. Cell Biol*. 16, 14–23 (2004).

Fruman DA, Cantley LC. Phosphoinositide 3-kinase in immunological systems. *Semin Immunol*. 2002 Feb;14(1):7-18.

Fukao T, Yamada T, Tanabe M, Terauchi Y, Ota T, Takayama T, Asano T, Takeuchi T, Kadowaki T, Hata Ji J, Koyasu S. Selective loss of gastrointestinal mast cells and impaired immunity in PI3K-deficient mice. *Nat Immunol*. 2002 Mar;3(3):295-304.

Funamoto S, Milan K, Meili R, Firtel RA. Role of phosphatidylinositol 3' kinase and a downstream pleckstrin homology domain-containing protein in controlling chemotaxis in dictyostelium. *J Cell Biol*. 2001 May 14;153(4):795-810.

Furumoto Y, Brooks S, Olivera A, Takagi Y, Miyagishi M, Taira K, Casellas R, Beaven MA, Gilfillan AM, Rivera J. J Immunol. Cutting Edge: Lentiviral short hairpin RNA silencing of PTEN in human mast cells reveals constitutive signals that promote cytokine secretion and cell survival. 2006 May 1;176(9):5167-71.

Furumoto Y, Gonzalez-Espinosa C, Gomez G, Kovarova M, Odom S, Parravicini V, Ryana JJ, Rivera J. Rethinking the role of Src family protein tyrosine kinases in the allergic response: new insights on the functional coupling of the high affinity IgE receptor. Immunol Res. 2004;30(2):241-53

Galli S.J., S. Nakae, M. Tsai. Mast cells in the development of adaptive immune responses. Nat Immunol, 6 (2) (2005), pp. 135–142

Galli SJ, Grimaldeston M, Tsai M. Immunomodulatory mast cells: negative, as well as positive, regulators of immunity. Nat Rev Immunol. 2008 Jun;8(6):478-86

Garbuzenko E, Nagler A, Pickholtz D, Gillery P, Reich R, Maquart FX, Levi-Schaffer F. Human mast cells stimulate fibroblast proliferation, collagen synthesis and lattice contraction: a direct role for mast cells in skin fibrosis. Clin Exp Allergy. 2002 Feb;32(2):237-46.

Garman SC, Kinet JP, Jardetzky TS. Crystal structure of the human high-affinity IgE receptor. Cell. 1998 Dec 23;95(7):951-61.

Ghosh, S.; Karin, M. Missing pieces in NF- κ B puzzle. 2002, 109, S81-S96.

Gilfillan AM, Tkaczyk C. Integrated signalling pathways for mast-cell activation. Nat Rev Immunol. 2006 Mar;6(3):218-30.

Gilman AG. G proteins: transducers of receptor-generated signals. Annu Rev Biochem. 1987;56:615-49.

Goldschmidt, M.E.; McLeod, K.J.; Taylor, W.R. (2001). Integrin-mediated mechanotransduction in vascular smooth muscle cells: frequency and force response characteristics. Circ. Res. 2001, 88, 674-680.

Gómez-Moutón C, Lacalle RA, Mira E, Jiménez-Baranda S, Barber DF, Carrera AC, Martínez-A C, Mañes S. Dynamic redistribution of raft domains as an organizing platform for signaling during cell chemotaxis. *J Cell Biol.* 2004 Mar 1;164(5):759-68.

Gonzalo JA, Qiu Y, Lora JM, Al-Garawi A, Villeval JL, Boyce JA, Martinez-A C, Marquez G, Goya I, Hamid Q, Fraser CC, Picarella D, Cote-Sierra J, Hodge MR, Gutierrez-Ramos JC, Kolbeck R, Coyle AJ. Coordinated involvement of mast cells and T cells in allergic mucosal inflammation: critical role of the CC chemokine ligand 1:CCR8 axis.

Gordon JR, Galli SJ. Release of both preformed and newly synthesized tumor necrosis factor alpha (TNF-alpha)/cachectin by mouse mast cells stimulated via the Fc epsilon RI. A mechanism for the sustained action of mast cell-derived TNF-alpha during IgE-dependent biological responses. *J Exp Med.* 1991 Jul 1;174(1):103-7.

Gordon JR, Galli SJ. Mast cells as a source of both preformed and immunologically inducible TNF-alpha/cachectin. *Nature.* 1990 Jul 19;346(6281):274-6.

Gould HJ, Sutton BJ. IgE in allergy and asthma today. *Nat Rev Immunol.* 2008 Mar;8(3):205-17.

Grogan JL, Mohrs M, Harmon B, Lacy DA, Sedat JW, Locksley RM. Early transcription and silencing of cytokine genes underlie polarization of T helper cell subsets. *Immunity.* 2001 Mar;14(3):205-15.

Groneberg DA, Bielory L, Fischer A, Bonini S, Wahn U. Animal models of allergic and inflammatory conjunctivitis. *Allergy.* 2003 Nov;58(11):1101-13.

Grosshans, J.; Wieschaus, E. A genetic link between morphogenesis and cell division during formation of the ventral furrow in *Drosophila*. *Cell* 2000, 101, 523-531.

Guinamard R, Aspenström P, Fougereau M, Chavrier P, Guillemot JC. Tyrosine phosphorylation of the Wiskott-Aldrich syndrome protein by Lyn and Btk is regulated by CDC42. *FEBS Lett.* 1998 Sep 4;434(3):431-6.

Gurish MF, Bryce PJ, Tao H, Kisselgof AB, Thornton EM, Miller HR, Friend DS, Oettgen HC. IgE enhances parasite clearance and regulates mast cell responses in mice infected with *Trichinella spiralis*. *J Immunol.* 2004 Jan 15;172(2):1139-45.

Gurish MF, Tao H, Abonia JP, Arya A, Friend DS, Parker CM, Austen KF. Intestinal mast cell progenitors require CD49 β 7 (alpha4beta7 integrin) for tissue-specific homing. *J Exp Med.* 2001 Nov 5;194(9):1243-52.

Gurish MF, Boyce JA. Mast cells: ontogeny, homing, and recruitment of a unique innate effector cell. *J Allergy Clin Immunol.* 2006 Jun;117(6):1285-91.

Gutkind JS. The pathways connecting G protein-coupled receptors to the nucleus through divergent mitogen-activated protein kinase cascades. *J Biol Chem.* 1998 Jan 23;273(4):1839-42.

Haidl, I. D., McAlpine, S. M. and Marshall, J. S. Enhancement of mast cell IL-6 production by combined Toll-like and nucleotide-binding oligomerization domain-like receptor activation. *Int. Arch. Allergy Immunol.* 154, 227–235 (2010)

Hallgren J, Jones TG, Abonia JP, Xing W, Humbles A, Austen KF, Gurish MF. Pulmonary CXCR2 regulates VCAM-1 and antigen-induced recruitment of mast cell progenitors. *Proc Natl Acad Sci U S A.* 2007 Dec 18;104(51):20478-83.

Han IH, Park SJ, Ahn MH, Ryu JS. Involvement of mast cells in inflammation induced by *Trichomonas vaginalis* via crosstalk with vaginal epithelial cells. *Parasite Immunol.* 2012 Jan;34(1):8-14. doi: 10.1111/j.1365-3024.2011.01338.x.

Harriague J, Bismuth G. Imaging antigen-induced PI3K activation in T cells. *Nat Immunol.* 2002 Nov;3(11):1090-6.

Hashimoto, K., Uchikawa, R., Tegoshi, T., Takeda, K., Yamada, M. and Arizono, N. Immunity-mediated regulation of fecundity in the nematode *Heligmosomoides polygyrus* : the potential role of mast cells. *Parasitology* 137, 881–887. (2010)

He Ling; Simmen, F.A.; Mehendale, H.M.; Martin, J.J.R.; Badger, T.M. Chronic ethanol intake impairs insulin signaling in rats by disrupting Akt association with the cell membrane: role of TRB3 in inhibition of Akt/protein kinase B activation. *J. Biol. Chem.* 2006, 281, 11126-11134.

Hegedus, Z.; Czibula, A.; Kiss-Toth, E. Tribbles: a family of kinase-like proteins with potent signaling regulatory function. *Cellular Signaling* 2007, 19, 238-250.

Hegedus, Z.; Czibula, Kiss-Toth. Tribbles: novel regulators of cell function; evolutionary aspects. *Cell Mol. Life Sci.* 2006, 63, 1632-1641.

Hepworth MR, Danilowicz-Luebert E, Rausch S, Metz M, Klotz C, Maurer M, Hartmann S. Mast cells orchestrate type 2 immunity to helminths through regulation of tissue-derived cytokines. *Proc Natl Acad Sci U S A.* 2012 Apr 9.

Hewson CA, Watson JR, Liu WL, Fidock MD. A differential role for ceramide kinase in antigen/Fc ϵ RI-mediated mast cell activation and function. *Clin Exp Allergy.* 2011 Mar;41(3):389-98. doi: 10.1111/j.1365-2222.2010.03682.x.

Higgs HN, Pollard TD. Activation by Cdc42 and PIP(2) of Wiskott-Aldrich syndrome protein (WASp) stimulates actin nucleation by Arp2/3 complex. *J Cell Biol.* 2000 Sep 18;150(6):1311-20.

Higgs HN, Pollard TD. Regulation of actin polymerization by Arp2/3 complex and WASp/Scar proteins. *J Biol Chem.* 1999 Nov 12;274(46):32531-4.

Hoffmann HJ, Frandsen PM, Christensen LH, Schiøtz PO, Dahl R. Cultured human mast cells are heterogeneous for expression of the high-affinity IgE receptor Fc ϵ RI. *Int Arch Allergy Immunol.* 2012;157(3):246-50.

Hogg, N., Laschinger, M., Giles, K. & McDowall, A. T-cell integrins: More than just sticking points. *J. Cell Sci.* 116, 4695–4705 (2003).

Hoth M, Penner R. Depletion of intracellular calcium stores activates a calcium current in mast cells. *Nature*. 1992 Jan 23;355(6358):353-6.

Hsu, C. L., Neilsen, C. V. and Bryce, P. J. IL-33 is produced by mast cells and regulates IgE-dependent inflammation. *PLoS ONE* 5, e11944. (2010)

Huang E, Nocka K, Beier DR, Chu TY, Buck J, Lahm HW, Wellner D, Leder P, Besmer P. The hematopoietic growth factor KL is encoded by the Sl locus and is the ligand of the c-kit receptor, the gene product of the W locus. *Cell*. 1990 Oct 5;63(1):225-33.

Huang YE, Iijima M, Parent CA, Funamoto S, Firtel RA, Devreotes P. Receptor-mediated regulation of PI3Ks confines PI(3,4,5)P₃ to the leading edge of chemotaxing cells. *Mol Biol Cell*. 2003 May;14(5):1913-22.

Hültner L, Druez C, Moeller J, Uyttenhove C, Schmitt E, Rüde E, Dörmer P, Van Snick J. Mast cell growth-enhancing activity (MEA) is structurally related and functionally identical to the novel mouse T cell growth factor P40/TCGFIII (interleukin 9). *Eur J Immunol*. 1990 Jun;20(6):1413-6.

Hültner L, Moeller J. Mast cell growth-enhancing activity (MEA) stimulates interleukin 6 production in a mouse bone marrow-derived mast cell line and a malignant subline. *Exp Hematol*. 1990 Sep;18(8):873-7.

Humbles AA, Lu B, Friend DS, Okinaga S, Lora J, Al-Garawi A, Martin TR, Gerard NP, Gerard C. The murine CCR3 receptor regulates both the role of eosinophils and mast cells in allergen-induced airway inflammation and hyperresponsiveness. *Proc Natl Acad Sci U S A*. 2002 Feb 5;99(3):1479-84.

Hur EM, Kim KT. *Cell Signal*. G protein-coupled receptor signalling and cross-talk: achieving rapidity and specificity. 2002 May;14(5):397-405.

Ibarra N, Blagg SL, Vazquez F, Insall RH. Nap1 regulates Dictyostelium cell motility and adhesion through SCAR-dependent and -independent pathways. *Curr Biol*. 2006 Apr 4;16(7):717-22.

Ikeda RK, Nayar J, Cho JY, Miller M, Rodriguez M, Raz E, Broide DH. Resolution of airway inflammation following ovalbumin inhalation: comparison of ISS DNA and corticosteroids. *Am J Respir Cell Mol Biol*. 2003 Jun;28(6):655-63.

Ikeuchi H, Kuroiwa T, Hiramatsu N, Kaneko Y, Hiromura K, Ueki K, Nojima Y. Expression of interleukin-22 in rheumatoid arthritis: potential role as a proinflammatory cytokine. *Arthritis Rheum*. 2005 Apr;52(4):1037-46.

Insall RH, Machesky LM. Actin dynamics at the leading edge: from simple machinery to complex networks. *Dev Cell*. 2009 Sep;17(3):310-22.

Irani AM, Nilsson G, Miettinen U, Craig SS, Ashman LK, Ishizaka T, Zsebo KM, Schwartz LB. Recombinant human stem cell factor stimulates differentiation of mast cells from dispersed human fetal liver cells. *Blood*. 1992 Dec 15;80(12):3009-21.

Ishizaka K, Tomioka H, Ishizaka T. Mechanisms of passive sensitization. I. Presence of IgE and IgG molecules on human leukocytes. *J Immunol*. 1970 Dec;105(6):1459-67.

Itoh M, Takahashi T, Sakaguchi N, et al. Thymus and autoimmunity: Production of CD25+CD4+naturally anergic and suppressive T cells as a key function of the thymus in maintaining immunologic self-tolerance. *J Immunol* 162:5317–5326,

Iwaki S, Tkaczyk C, Metcalfe DD, Gilfillan AM. Roles of adaptor molecules in mast cell activation. *Chem Immunol Allergy*. 2005;87:43-58.

Iwakura Y, and Ishigame H. The IL-23/IL-17 axis in inflammation. *J Clin Invest* 116:1218 –1222, 2006.

Ilyedjian PB. Lack of evidence for a role of TRB3/NIPK as an inhibitor of PKB-mediated insulin signalling in primary hepatocytes. *Biochem J*. 2005 Feb 15;386(Pt 1):113-8.

Ilyedjian, P.B. Lack of evidence for a role of TRB3/NIPK as inhibitor of PKB-mediated insulin signaling in primary hepatocytes. *Biochem. J*. 2004, 386,113-118.

Izushi K, Nakahara H, Tai N, Mio M, Watanabe T, Kamei C. The role of histamine H(1)receptors in late-phase reaction of allergic conjunctivitis. *Eur J Pharmacol* 2002;440:79–82.

Jabril-Cuenod B, Zhang C, Scharenberg AM, Paolini R, Numerof R, Beaven MA, Kinet JP. Syk-dependent phosphorylation of Shc. A potential link between FcepsilonRI and the Ras/mitogen-activated protein kinase signaling pathway through SOS and Grb2. *J Biol Chem*. 1996 Jul 5;271(27):16268-72.

Jamur MC, Moreno AN, Mello LF, Souza Júnior DA, Campos MR, Pastor MV, Grodzki AC, Silva DC, Oliver C. Mast cell repopulation of the peritoneal cavity: contribution of mast cell progenitors versus bone marrow derived committed mast cell precursors. *BMC Immunol*. 2010 Jun 24;11:32.

Jones, P.L.; Jones, F.S.; Zhou, B.; Rabinovitch, M. Induction of vascular smooth muscle cell tenascin-C gene expression by denatured type I collagen is dependent upon a beta3 integrin-mediated nitrogen-activated protein kinase pathway and 122-base pair promoter element. *J. Cell Sci*. 1999, 12, 435-445.

Kalesnikoff J, Huber M, Lam V, Damen JE, Zhang J, Siraganian RP, Krystal G. Monomeric IgE stimulates signaling pathways in mast cells that lead to cytokine production and cell survival. *Immunity*. 2001 Jun;14(6):801-11.

Karin, M.; Ben-Neriah, Y. Phosphorylation meets ubiquitination: the control of NF- κ B activity. *Annu. Rev. Immunol*. 2000, 18, 621-663.

Karin, M.; Lin, A. NF- κ B at the crossroads of life and death. *Nat. Immunol*. 2002, 3, 221-222.

Katz HR, Raizman MB, Gartner CS, Scott HC, Benson AC, Austen KF. Secretory granule mediator release and generation of oxidative metabolites of arachidonic acid via Fc-IgG receptor bridging in mouse mast cells. *J Immunol*. 1992 Feb 1;148(3):868-71.

Kawakami T, Galli SJ. Regulation of mast-cell and basophil function and survival by IgE. *Nat Rev Immunol*. 2002 Oct;2(10):773-86.

Kawamoto K, Aoki J, Tanaka A, Itakura A, Hosono H, Arai H, Kiso Y, Matsuda H. Nerve growth factor activates mast cells through the collaborative interaction with lysophosphatidylserine expressed on the membrane surface of activated platelets. *J Immunol*. 2002 Jun 15;168(12):6412-9.

Kelly-Welch AE, Hanson EM, Boothby MR, Keegan AD. Interleukin-4 and interleukin-13 signaling connections maps. *Science*. 2003 Jun 6;300(5625):1527-8.

Khandoga AG, Khandoga A, Reichel CA, Bihari P, Rehberg M, Krombach F. In vivo imaging and quantitative analysis of leukocyte directional migration and polarization in inflamed tissue. *PLoS One*. 2009;4(3):e4693.

Kim AS, Kakalis LT, Abdul-Manan N, Liu GA, Rosen MK. Autoinhibition and activation mechanisms of the Wiskott-Aldrich syndrome protein. *Nature*. 2000 Mar 9;404(6774):151-8.

Kinet JP, Blank U, Brini A, Jouvin MH, Küster H, Mejan O, Ra C. The high-affinity receptor for immunoglobulin E: a target for therapy of allergic diseases. *Int Arch Allergy Appl Immunol*. 1991;94(1-4):51-5.

Kinet JP. The high-affinity IgE receptor (Fc epsilon RI): from physiology to pathology. *Annu Rev Immunol*. 1999;17:931-72.

Kirshenbaum AS, Akin C, Wu Y, Rottem M, Goff JP, Beaven MA, Rao VK, Metcalfe DD. Characterization of novel stem cell factor responsive human mast cell lines LAD 1 and 2 established from a patient with mast cell sarcoma/leukemia; activation following aggregation of Fc epsilon RI or Fc gamma RI. *Leuk Res*. 2003 Aug;27(8):677-82.

Kiss-Toth E, Bagstaff SM, Sung HY, Jozsa V, Dempsey C, Caunt JC, Oxley KM, Wyllie DH, Polgar T, Harte M, O'Neill LA, Qwarnstrom EE, Dower SK. Human tribbles, a protein family controlling mitogen-activated protein kinase cascades. *J Biol Chem*. 2004 Oct 8;279(41):42703-8.

Kiss-Toth, E.; Wyllie, D.H.; Holland, K.; Marsden, L.; Jozsa, V.; Oxley, K.M.; Polgar, T.; Qvarnstrom, E.E.; Dower, S.K. Functional mapping and identification of novel regulators for the Toll/Interleukin-1 signaling network by transcription cloning. *Cellular Signaling* 2006, 18 (2), 202-214.

Kitamura Y, Shimada M, Hatanaka K, Miyano Y. Development of mast cells from grafted bone marrow cells in irradiated mice. *Nature*. 1977 Aug 4;268(5619):442-3.

Kochan T, Singla A, Tosi J, Kumar A. TLR2 ligand pretreatment attenuates retinal microglial inflammatory response but enhances their phagocytic activity towards *Staphylococcus aureus*. *Infect Immun*. 2012 Mar 19.

Koo, S.H.; Satoh, H.; Herzig, S.; Lee, C; Hedrick, S; Kulkarni, R; Evans, R.M.; Olefsky, J.; Montminy, M. PGC-1 promotes insulin resistance in liver through PPAR-alpha-dependent induction of TRB3. *Nat. Med*. 2004, 10, 530-534.

Kool M, Hammad H, Lambrecht BN. Cellular networks controlling Th2 polarization in allergy and immunity. *F1000 Biol Rep*. 2012;4:6.

Koyasu S, Minowa A, Terauchi Y, Kadowaki T, Matsuda S. (2005) The role of phosphoinositide-3-kinase in mast cell homing to the gastrointestinal tract. *Novartis Found. Symp*. 271, 152–161 (discussion 161–165, 198–199)

Krupnick JG, Santini F, Gagnon AW, Keen JH, Benovic JL. Modulation of the arrestin-clathrin interaction in cells. Characterization of beta-arrestin dominant-negative mutants. *J Biol Chem*. 1997 Dec 19;272(51):32507-12.

Kulczycki A Jr, Metzger H. The interaction of IgE with rat basophilic leukemia cells. II. Quantitative aspects of the binding reaction. *J Exp Med*. 1974 Dec 1;140(6):1676-95.

Kulka M, Alexopoulou L, Flavell RA, Metcalfe DD. Activation of mast cells by double-stranded RNA: evidence for activation through Toll-like receptor 3. *J Allergy Clin Immunol*. 2004 Jul;114(1):174-82.

Kumagai N, Fukuda K, Fujitsu Y, Yamamoto K, Nishida T. Role of structural cells of the cornea and conjunctiva in the pathogenesis of vernal keratoconjunctivitis. *Prog Retin Eye Res.* 2006 Mar;25(2):165-87.

Laffargue M, Calvez R, Finan P, Trifilieff A, Barbier M, Altruda F, Hirsch E, Wymann MP. Phosphoinositide 3-kinase gamma is an essential amplifier of mast cell function. *Immunity.* 2002 Mar;16(3):441-51.

Lämmermann T, Bader BL, Monkley SJ, Worbs T, Wedlich-Söldner R, Hirsch K, Keller M, Förster R, Critchley DR, Fässler R, Sixt M. Rapid leukocyte migration by integrin-independent flowing and squeezing. *Nature.* 2008 May 1;453(7191):51-5.

Lauffenburger DA, Horwitz AF. Cell migration: a physically integrated molecular process. *Cell.* 1996 Feb 9;84(3):359-69.

Lemmon MA, Ferguson KM, Abrams CS. Pleckstrin homology domains and the cytoskeleton. *FEBS Lett.* 2002 Feb 20;513(1):71-6.

Leonardi A, Cortivo R, Fregona I, Plebani M, Secchi AG, Abatangelo G. Effects of Th2 cytokines on expression of collagen, MMP-1, and TIMP-1 in conjunctival fibroblasts. *Invest Ophthalmol Vis Sci.* 2003 Jan;44(1):183-9.

Leonardi A, Curnow SJ, Zhan H, Calder VL. Multiple cytokines in human tear specimens in seasonal and chronic allergic eye disease and in conjunctival fibroblast cultures. *Clin Exp Allergy.* 2006 Jun;36(6):777-84.

Leonardi A, Motterle L, Bortolotti M. Allergy and the eye. *Clin Exp Immunol.* 2008 Sep;153 Suppl 1:17-21.

Lester MR, Hofer MF, Gately M, Trumble A, Leung DY. Down-regulating effects of IL-4 and IL-10 on the IFN-gamma response in atopic dermatitis. *J Immunol.* 1995 Jun 1;154(11):6174-81.

Lewis RA, Soter NA, Diamond PT, Austen KF, Oates JA, Roberts LJ 2nd. Prostaglandin D2 generation after activation of rat and human mast cells with anti-IgE. *J Immunol.* 1982 Oct;129(4):1627-31.

Li ,C.; Xu, Q. Mechanical stress – initiated signal transductions in vascular smooth muscle cells. *Cell Signal* 2000, 12, 435-445.

Linardopoulou EV, Parghi SS, Friedman C, Osborn GE, Parkhurst SM, Trask BJ. Human subtelomeric WASH genes encode a new subclass of the WASP family. *PLoS Genet.* 2007 Dec;3(12):e237.

Littlepage LE, Egeblad M, Werb Z. Coevolution of cancer and stromal cellular responses. *Cancer Cell.* 2005 Jun;7(6):499-500.

Locksley, R.M.; Killeen, N.; Lenardo, M.J. The TNF and TNF receptor super families: integrating mammalian biology. *Cell* 2001, 104, 487-501.

Loetscher P, Seitz M, Baggiolini M, Moser B. Interleukin-2 regulates CC chemokine receptor expression and chemotactic responsiveness in T lymphocytes. *J Exp Med.* 1996 Aug 1;184(2):569-77.

Looney MR, Thornton EE, Sen D, Lamm WJ, Glenn RW, Krummel MF. Stabilized imaging of immune surveillance in the mouse lung. *Nat Methods.* 2011 Jan;8(1):91-6.

Lorentz A, Schuppan D, Gebert A, Manns MP, Bischoff SC. Regulatory effects of stem cell factor and interleukin-4 on adhesion of human mast cells to extracellular matrix proteins. *Blood.* 2002 Feb 1;99(3):966-72.

Ma W, Bryce PJ, Humbles AA, Laouini D, Yalcindag A, Alenius H, Friend DS, Oettgen HC, Gerard C, Geha RS. CCR3 is essential for skin eosinophilia and airway hyperresponsiveness in a murine model of allergic skin inflammation. *J Clin Invest.* 2002 Mar;109(5):621-8.

Machesky LM, Gould KL. The Arp2/3 complex: a multifunctional actin organizer. *Curr Opin Cell Biol.* 1999 Feb;11(1):117-21.

Machesky LM, Mullins RD, Higgs HN, Kaiser DA, Blanchoin L, May RC, Hall ME, Pollard TD. Scar, a WASp-related protein, activates nucleation of actin filaments by the Arp2/3 complex. *Proc Natl Acad Sci U S A.* 1999 Mar 30;96(7):3739-44.

Malaviya R, Ikeda T, Ross E, Abraham SN. Mast cell modulation of neutrophil influx and bacterial clearance at sites of infection through TNF- α . *Nature*. 1996 May 2;381(6577):77-80.

Malaviya, R., Ikeda, T., Ross, E. and Abraham, S. N., Mast cell modulation of neutrophil influx and bacterial clearance at sites of infection through TNF- α . *Nature* 1996. 381: 77–80.

Manetti R, Parronchi P, Giudizi MG, et al. Natural killer cell stimulatory factor (interleukin 12 [IL-12]) induces T helper type 1 (Th1)-specific immune responses and inhibits the development of IL-4-producing Th cells. *J Exp Med* 177:1199–1204, 1993.

Manetz TS, Gonzalez-Espinosa C, Arudchandran R, Xirasagar S, Tybulewicz V, Rivera J. *Mol Cell Biol*. 2001 Jun;21(11):3763-74.

Mani M, Venkatasubrahmanyam S, Sanyal M, Levy S, Butte A, Weinberg K, Jahn T. Wiskott-Aldrich syndrome protein is an effector of Kit signaling. *Blood*. 2009 Oct 1;114(14):2900-8.

Marinissen MJ, Chiariello M, Gutkind JS. Regulation of gene expression by the small GTPase Rho through the ERK6 (p38 gamma) MAP kinase pathway. *Genes Dev*. 2001 Mar 1;15(5):535-53.

Marinissen MJ, Gutkind JS. G-protein-coupled receptors and signaling networks: emerging paradigms. *Trends Pharmacol Sci*. 2001 Jul;22(7):368-76.

Marquardt DL, Walker LL. Dependence of mast cell IgE-mediated cytokine production on nuclear factor-kappaB activity. *J Allergy Clin Immunol*. 2000 Mar;105(3):500-5.

Marshall JG, Booth JW, Stambolic V, Mak T, Balla T, Schreiber AD, Meyer T, Grinstein S. Restricted accumulation of phosphatidylinositol 3-kinase products in a plasmalemmal subdomain during Fc gamma receptor-mediated phagocytosis. *J Cell Biol*. 2001 Jun 25;153(7):1369-80

Martinez-Quiles N, Rohatgi R, Antón IM, Medina M, Saville SP, Miki H, Yamaguchi H, Takenawa T, Hartwig JH, Geha RS, Ramesh N. WIP regulates N-WASP-mediated actin polymerization and filopodium formation. *Nat Cell Biol.* 2001 May;3(5):484-91.

Matsuda K, Piliponsky AM, Iikura M, Nakae S, Wang EW, Dutta SM, Kawakami T, Tsai M, Galli SJ. Monomeric IgE enhances human mast cell chemokine production: IL-4 augments and dexamethasone suppresses the response. *J Allergy Clin Immunol.* 2005 Dec;116(6):1357-63.

Matsushima H, Yamada N, Matsue H, Shimada S. TLR3-, TLR7-, and TLR9-mediated production of proinflammatory cytokines and chemokines from murine connective tissue type skin-derived mast cells but not from bone marrow-derived mast cells. *J Immunol.* 2004 Jul 1;173(1):531-41.

Maurer, M., Lopez, K. S., Siebenhaar, F., Moelle, K., Metz, M., Knop, J. and von, S. E. Skin mast cells control T cell-dependent host defense in *Leishmania major* infections. *FASEB J.* 20, 2460–2467. (2006)

Maurer, M., Paus, R. and Czarnecki, B. M. (1995) Mast cells as modulators of hair follicle cycling. *Exp. Dermatol.* 4, 266–271

Maurer, M., Wedemeyer, J., Metz, M., Piliponsky, A. M., Weller, K., Chatterjea, D., Clouthier, D. E. et al., Mast cells promote homeostasis by limiting endothelin-1-induced toxicity. *Nature* 2004. 432: 512–516.

Mayumi-Matsuda. K.; Kojima, S.; Suzuki, H.; Sakata, T. Identification of a novel kinase-like gene induced during neuronal cell death. *Biochem. Biophys. Res. Commun.* 1999, 258,260-264.

McAlpine SM, Issekutz TB, Marshall JS. Virus stimulation of human mast cells results in the recruitment of CD56⁺ T cells by a mechanism dependent on CCR5 ligands. *FASEB J.* 2012 Mar;26(3):1280-9.

McLachlan JB, Hart JP, Pizzo SV, Shelburne CP, Staats HF, Gunn MD, Abraham SN. Mast cell-derived tumor necrosis factor induces hypertrophy of draining lymph nodes during infection. *Nat Immunol*. 2003 Dec;4(12):1199-205.

McLachlan, C.P. Shelburne, J.P. Hart, S.V. Pizzo, R. Goyal, R. Brooking-Dixon, H.F. Staats, S.N. Abraham. Mast cell activators: a new class of highly effective vaccine adjuvants. *Nat Med*, 14 (5) (2008), pp. 536–541

McLane MP, Haczku A, van de Rijn M, Weiss C, Ferrante V, MacDonald D, Renauld JC, Nicolaides NC, Holroyd KJ, Levitt RC. Interleukin-9 promotes allergen-induced eosinophilic inflammation and airway hyperresponsiveness in transgenic mice. *Am J Respir Cell Mol Biol*. 1998 Nov;19(5):713-20.

Mellor EA, Austen KF, Boyce JA. Cysteinyl leukotrienes and uridine diphosphate induce cytokine generation by human mast cells through an interleukin 4-regulated pathway that is inhibited by leukotriene receptor antagonists. *J Exp Med*. 2002 Mar 4;195(5):583-92.

Mempel, T. R., Henrickson, S. E. & Von Andrian, U. H. T-cell priming by dendritic cells in lymph nodes occurs in three distinct phases. *Nature* 427, 154–159 (2004).

Menon AK, Holowka D, Webb WW, Baird B. Cross-linking of receptor-bound IgE to aggregates larger than dimers leads to rapid immobilization. *J Cell Biol*. 1986 Feb;102(2):541-50.

Merayo-Llodes J, Zhao TZ, Dutt JE, Foster CS. A new murine model of allergic conjunctivitis and effectiveness of nedocromil sodium. *J Allergy Clin Immunol* 1996;97:1129–1140.

Merlot S, Firtel RA. Leading the way: Directional sensing through phosphatidylinositol 3-kinase and other signaling pathways. *J Cell Sci*. 2003 Sep 1;116(Pt 17):3471-8.

Metcalf DD, Baram D, Mekori YA. Mast cells. *Physiol Rev*. 1997 Oct;77(4):1033-79.

Metcalf DD, Peavy RD, Gilfillan AM. Mechanisms of mast cell signaling in anaphylaxis. *J Allergy Clin Immunol*. 2009 Oct;124(4):639-46

Metz M, Magerl M, Köhl NF, Valeva A, Bhakdi S, Maurer M. Mast cells determine the magnitude of bacterial toxin-induced skin inflammation. *Exp Dermatol*. 2009 Feb;18(2):160-6.

Micheau, O.; Lens, S.; Gaide, O.; Alevizopoulos, K.; Tschopp, J. NF- κ B signals induce the expression of c-FLIP. *Mol.Cell Biol*. 2001, 21, 5299-5305.

Miki H, Miura K, Takenawa T. N-WASP, a novel actin-depolymerizing protein, regulates the cortical cytoskeletal rearrangement in a PIP2-dependent manner downstream of tyrosine kinases. *EMBO J*. 1996 Oct 1;15(19):5326-35.

Miki H, Suetsugu S, Takenawa T. WAVE, a novel WASP-family protein involved in actin reorganization induced by Rac. *EMBO J*. 1998 Dec 1;17(23):6932-41.

Millard TH, Sharp SJ, Machesky LM. Signalling to actin assembly via the WASP (Wiskott-Aldrich syndrome protein)-family proteins and the Arp2/3 complex. *Biochem J*. 2004 May 15;380(Pt 1):1-17.

Miller MJ, Wei SH, Parker I, Cahalan MD. Two-photon imaging of lymphocyte motility and antigen response in intact lymph node. *Science*. 2002 Jun 7;296(5574):1869-73.

Miller, H.R. and Pemberton, A.D. (2002) Tissue-specific expression of mast cell granule serine proteinases and their role in inflammation in the lung and gut. *Immunology* 105, 375–390

Milner JD, Brechley JM, Laurence A, et al. Impaired T(H)17 cell differentiation in subjects with autosomal dominant hyper-IgE syndrome. *Nature* 452:773–776, 2008.

Miyazaki D, Nakamura T, Toda M, Cheung-Chau KW, Richardson RM, Ono SJ. Macrophage inflammatory protein-1 α as a costimulatory signal for mast cell-mediated immediate hypersensitivity reactions. *J Clin Invest*. 2005 Feb;115(2):434-42.

Molet S, Hamid Q, Davoine F, et al. IL-17 is increased in asthmatic airways and induces human bronchial fibroblasts to produce cytokines. *J Allergy Clin Immunol* 108:430–438, 2001.

Monypenny J, Chou HC, Bañón-Rodríguez I, Thrasher AJ, Antón IM, Jones GE, Calle Y. Role of WASP in cell polarity and podosome dynamics of myeloid cells. *Eur J Cell Biol*. 2011 Feb-Mar;90(2-3):198-204.

Morin NA, Oakes PW, Hyun YM, Lee D, Chin YE, King MR, Springer TA, Shimaoka M, Tang JX, Reichner JS, Kim M. Nonmuscle myosin heavy chain IIA mediates integrin LFA-1 de-adhesion during T lymphocyte migration. *J Exp Med*. 2008 Jan 21;205(1):195-205.

Moritz, D. R., Rodewald, H. R., Gheyselinck, J. and Klemenz, R. The IL-1 receptor-related T1 antigen is expressed on immature and mature mast cells and on fetal blood mast cell progenitors. *J. Immunol*. 161, 4866–4874. (1998)

Mosmann TR, Cherwinski H, Bond MW, Giedlin MA, Coffman RL. Two types of murine helper T cell clone. I. Definition according to profiles of lymphokine activities and secreted proteins. *J Immunol* 1986; 136:2348-2357.

Mota I, Vugman I. Effects of anaphylactic shock and compound 48/80 on the mast cells of the guinea pig lung. *Nature*. 1956 Mar 3;177(4505):427-9.

Mueller A, Kelly E, Strange PG. Pathways for internalization and recycling of the chemokine receptor CCR5. *Blood*. 2002 Feb 1;99(3):785-91.

Muller-Eberhard, H.J. 1988. Molecular organization and function of the complement system. *Annu.Rev. Biochem*. 57: 321–347.

Mullins RD, Heuser JA, Pollard TD. The interaction of Arp2/3 complex with actin: nucleation, high affinity pointed end capping, and formation of branching networks of filaments. *Proc Natl Acad Sci U S A*. 1998 May 26;95(11):6181-6.

Mwamtemi HH, Koike K, Kinoshita T, Ito S, Ishida S, Nakazawa Y, Kurokawa Y, Shinozaki K, Sakashita K, Takeuchi K, Shiohara M, Kamijo T, Yasui Y, Ishiguro A, Kawano Y, Kitano K, Miyazaki H, Kato T, Sakuma S, Komiyama A. An increase in circulating mast cell colony-forming cells in asthma. *J Immunol.* 2001 Apr 1;166(7):4672-7.

Myers SA, Han JW, Lee Y, Firtel RA, Chung CY. A Dictyostelium homologue of WASP is required for polarized F-actin assembly during chemotaxis. *Mol Biol Cell.* 2005 May;16(5):2191-206.

Nadler MJ, Matthews SA, Turner H, Kinet JP. Signal transduction by the high-affinity immunoglobulin E receptor Fc epsilon RI: coupling form to function. *Adv Immunol.* 2000;76:325-55.

Nagasaka, A., Matsue, H., Matsushima, H., Aoki, R., Nakamura, Y., Kambe, N., Kon, S., Uede, T. and Shimada, S. (2008) Osteopontin is produced by mast cells and affects IgE-mediated degranulation and migration of mast cells. *Eur. J. Immunol.* 38, 489–499

Naiki T, Saijou E, Miyaoka Y, Sekine K, Miyajima A. TRB2, a mouse Tribbles ortholog, suppresses adipocyte differentiation by inhibiting AKT and C/EBPbeta. *J Biol Chem.* 2007 Aug 17;282(33):24075-82.

Nakae S, Suto H, Kakurai M, Sedgwick JD, Tsai M, Galli SJ. Mast cells enhance T cell activation: Importance of mast cell-derived TNF. *Proc Natl Acad Sci U S A.* 2005 May 3;102(18):6467-72.

Nakano, C. Nishiyama, H. Yagita, A. Koyanagi, H. Akiba, S. Chiba, H. Ogawa, K. Okumura. Notch signaling confers antigen-presenting cell functions on mast cells. *J Allergy Clin Immunol*, 123 (1) (2009), pp. 74–81

Naveen B, Shankar BS, Subrahmanyam G. Fc epsilon RI cross-linking activates a type II phosphatidylinositol 4-kinase in RBL 2H3 cells. *Mol Immunol.* 2005 Aug;42(12):1541-9.

Neill DR, Wong SH, Bellosi A, et al. Nuocytes represent a new innate effector leukocyte that mediates type-2 immunity. *Nature* 464:1367–1370, 2010.

Nilsson G, Blom T, Kusche-Gullberg M, Kjellén L, Butterfield JH, Sundström C, Nilsson K, Hellman L. Phenotypic characterization of the human mast-cell line HMC-1. *Scand J Immunol.* 1994 May;39(5):489-98.

Nilsson G, Butterfield JH, Nilsson K, Siegbahn A. Stem cell factor is a chemotactic factor for human mast cells. *J Immunol.* 1994 Oct 15;153(8):3717-23.

Nilsson G, Johnell M, Hammer CH, Tiffany HL, Nilsson K, Metcalfe DD, Siegbahn A, Murphy PM. C3a and C5a are chemotaxins for human mast cells and act through distinct receptors via a pertussis toxin-sensitive signal transduction pathway. *J Immunol.* 1996 Aug 15;157(4):1693-8.

Norman MU, Hickey MJ. Mechanisms of lymphocyte migration in autoimmune disease. *Tissue Antigens.* 2005 Sep;66(3):163-72.

Oak JS, Matheu MP, Parker I, Cahalan MD, Fruman DA. Lymphocyte cell motility: the twisting, turning tale of phosphoinositide 3-kinase. *Biochem Soc Trans.* 2007 Nov;35(Pt 5):1109-13.

Ochi H, Hirani WM, Yuan Q, Friend DS, Austen KF, Boyce JA. T helper cell type 2 cytokine-mediated comitogenic responses and CCR3 expression during differentiation of human mast cells in vitro. *J Exp Med.* 1999 Jul 19;190(2):267-80.

Odom S, Gomez G, Kovarova M, Furumoto Y, Ryan JJ, Wright HV, Gonzalez-Espinosa C, Hibbs ML, Harder KW, Rivera J. Negative regulation of immunoglobulin E-dependent allergic responses by Lyn kinase. *J Exp Med.* 2004 Jun 7;199(11):1491-502.

Ohoka, N.; Yoshii, S.; Hattori, T.; Onozaki, K.; Hayashi, H. TRB3, a novel ER stress-inducible gene, is induced via ATF4-CHOP pathway and is involved in cell death. *EMBO J.* 2005, 24, 1243-1255.

Okayama Y, Hagaman DD, Metcalfe DD. A comparison of mediators released or generated by IFN-gamma-treated human mast cells following aggregation of Fc gamma RI or Fc epsilon RI. *J Immunol.* 2001 Apr 1;166(7):4705-12.

Okayama Y, Tkaczyk C, Metcalfe DD, Gilfillan AM. Comparison of Fc epsilon RI- and Fc gamma RI-mediated degranulation and TNF-alpha synthesis in human mast cells: selective utilization of phosphatidylinositol-3-kinase for Fc gamma RI-induced degranulation. *Eur J Immunol.* 2003 May;33(5):1450-9.

Okumura S, Kashiwakura J, Tomita H, Matsumoto K, Nakajima T, Saito H, Okayama Y. Identification of specific gene expression profiles in human mast cells mediated by Toll-like receptor 4 and Fc epsilon RI. *Blood.* 2003 Oct 1;102(7):2547-54.

Oliveira SH, Lukacs NW. Stem cell factor and IgE-stimulated murine mast cells produce chemokines (CCL2, CCL17, CCL22) and express chemokine receptors. *Inflamm Res.* 2001 Mar;50(3):168-74.

Oliveira-Dos-Santos AJ, Matsumoto G, Snow BE, Bai D, Houston FP, Whishaw IQ, Mariathasan S, Sasaki T, Wakeham A, Ohashi PS, Roder JC, Barnes CA, Siderovski DP, Penninger JM. Regulation of T cell activation, anxiety, and male aggression by RGS2. *Proc Natl Acad Sci U S A.* 2000 Oct 24;97(22):12272-7.

Ono SJ, Nakamura T, Miyazaki D, Ohbayashi M, Dawson M, Toda M. Chemokines: roles in leukocyte development, trafficking, and effector function. *J Allergy Clin Immunol.* 2003 Jun;111(6):1185-99;

Ord, D.; Ord, T. Characterization of human NIPK (TRB3, SKIP3) gene activation in stressful conditions. *Biochem. Biophys. Res. Commun.* 2005, 330, 210-218.

Ord, D.; Ord T. Mouse NIPK interacts with ATF4 and affects its transcriptional activity. *Exp. Cell Res.* 2003, 286, 308-320.

Orsini MJ, Benovic JL. Characterization of dominant negative arrestins that inhibit beta2-adrenergic receptor internalization by distinct mechanisms. *J Biol Chem.* 1998 Dec 18;273(51):34616-22.

Ownby DR. Pediatric asthma and development of atopy. *Curr Opin Allergy Clin Immunol.* 2001 Apr;1(2):125-6.

Palecek SP, Schmidt CE, Lauffenburger DA, Horwitz AF. Integrin dynamics on the tail region of migrating fibroblasts. *J Cell Sci.* 1996 May;109 (Pt 5):941-52.

Papakonstanti EA, Ridley AJ, Vanhaesebroeck B. The p110delta isoform of PI 3-kinase negatively controls RhoA and PTEN. *EMBO J.* 2007 Jul 11;26(13):3050-61.

Parent CA, Devreotes PN. A cell's sense of direction. *Science.* 1999 Apr 30;284(5415):765-70.

Park H, Li Z, Yang XO, et al. A distinct lineage of CD4 T cells regulates tissue inflammation by producing interleukin 17. *Nat Immunol* 2005; 6:1133-1141.

Parker LC, Whyte MK, Vogel SN, Dower SK, Sabroe I. Toll-like receptor (TLR)2 and TLR4 agonists regulate CCR expression in human monocytic cells. *J Immunol.* 2004 Apr 15;172(8):4977-86.

Parravicini V, Gadina M, Kovarova M, Odom S, Gonzalez-Espinosa C, Furumoto Y, Saitoh S, Samelson LE, O'Shea JJ, Rivera J. Fyn kinase initiates complementary signals required for IgE-dependent mast cell degranulation. *Nat Immunol.* 2002 Aug;3(8):741-8.

Parronchi P, De Carli M, Manetti R, Simonelli C, Sampognaro S, Piccinni MP, Macchia D, Maggi E, Del Prete G, Romagnani S. IL-4 and IFN (alpha and gamma) exert opposite regulatory effects on the development of cytolytic potential by Th1 or Th2 human T cell clones. *J Immunol.* 1992 Nov 1;149(9):2977-83.

Pejler, G. et al. (2010) Mast cell proteases: multifaceted regulators of inflammatory disease. *Blood* 115, 4981–4990

Pelletier C, Guérin-Marchand C, Iannascoli B, Marchand F, David B, Weyer A, Blank U. Specific signaling pathways in the regulation of TNF-alpha mRNA synthesis and TNF-alpha secretion in RBL-2H3 mast cells stimulated through the high affinity IgE receptor. *Inflamm Res.* 1998 Dec;47(12):493-500.

Pierce KL, Maudsley S, Daaka Y, Luttrell LM, Lefkowitz RJ. Role of endocytosis in the activation of the extracellular signal-regulated kinase cascade by sequestering and nonsequestering G protein-coupled receptors. *Proc Natl Acad Sci U S A*. 2000 Feb 15;97(4):1489-94.

Pierce KL, Premont RT, Lefkowitz RJ. Seven-transmembrane receptors. *Nat Rev Mol Cell Biol*. 2002 Sep;3(9):639-50.

Piliponsky, A. M., Chen, C. C., Grimbaldston, M. A., Burns-Guydish, S. M., Hardy, J., Kalesnikoff, J., Contag, C. H. et al., Mast cell-derived TNF can exacerbate mortality during severe bacterial infections in C57BL/6-KitW-sh/W-sh mice. *Am. J. Pathol*. 2010. 176: 926–938.

Piliponsky, A. M., Chen, C.-C., Nishimura, T., Metz, M., Rios, E. J., Dobner, P. R., Wada, E. et al., Neurotensin increases mortality and mast cells reduce neurotensin levels in a mouse model of sepsis. *Nat. Med*. 2008. 14:392–398.

Pitchford SC, Furze RC, Jones CP, Wengner AM, Rankin SM. Differential mobilization of subsets of progenitor cells from the bone marrow. *Cell Stem Cell*. 2009 Jan 9;4(1):62-72.

Pittet, M. J. & Mempel, T. R. Regulation of T-cell migration and effector functions: Insights from in vivo imaging studies. *Immunol. Rev*. 221, 107–129 (2008).

Plaut M, Pierce JH, Watson CJ, Hanley-Hyde J, Nordan RP, Paul WE. Mast cell lines produce lymphokines in response to cross-linkage of Fc epsilon RI or to calcium ionophores. *Nature*. 1989 May 4;339(6219):64-7.

Pollard TD. Regulation of actin filament assembly by Arp2/3 complex and formins. *Annu Rev Biophys Biomol Struct*. 2007;36:451-77.

Pollitt AY, Insall RH. Abi mutants in Dictyostelium reveal specific roles for the SCAR/WAVE complex in cytokinesis. *Curr Biol*. 2008 Feb 12;18(3):203-10.

Posner BA, Mukhopadhyay S, Tesmer JJ, Gilman AG, Ross EM. Modulation of the affinity and selectivity of RGS protein interaction with G alpha subunits by a conserved asparagine/serine residue. *Biochemistry*. 1999 Jun 15;38(24):7773-9.

Price KS, Friend DS, Mellor EA, De Jesus N, Watts GF, Boyce JA. CC chemokine receptor 3 mobilizes to the surface of human mast cells and potentiates immunoglobulin E-dependent generation of interleukin 13. *Am J Respir Cell Mol Biol*. 2003 Apr;28(4):420-7.

Prodeus AP, Zhou X, Maurer M, Galli SJ, Carroll MC. Impaired mast cell-dependent natural immunity in complement C3-deficient mice. *Nature*. 1997 Nov 13;390(6656):172-5

Prudente S, Morini E, Trischitta V. The emerging role of TRIB3 as a gene affecting human insulin resistance and related clinical outcomes. *Acta Diabetol*. 2009 Jun;46(2):79-84.

Prudente, S.; Hribal, M.L.; Flex. E.; Turchi, F.; Morini, E.; De Cosmo, S.; Bacci,S.; Tassi, V.; Cardellini, M.; Lauro, R.; Sesti, G.; Dallapiccola, B.; Trischitta,V. The functional Q84R polymorphism of mammalian tribbles homolog TRB3 is associated with insulin resistance and related cardiovascular risk in Caucasians from Italy. *Diabetes* 2005, 54, 2807-2811.

Pushparaj, P. N., Tay, H. K., H'ng, S. C., Pitman, N., Xu, D., McKenzie, A., Liew, F. Y. and Melendez, A. J. The cytokine interleukin-33 mediates anaphylactic shock. *Proc. Natl. Acad. Sci. U.S.A.* 106, 9773–9778. (2009)

Raja, Sivamani K, Garcia MS, Isseroff RR.Wound re-epithelialization: modulating keratinocyte migration in wound healing. *Front Biosci*. 2007 May 1;12:2849-68

Ramesh N, Antón IM, Hartwig JH, Geha RS. WIP, a protein associated with wiskott-aldrich syndrome protein, induces actin polymerization and redistribution in lymphoid cells. *Proc Natl Acad Sci U S A*. 1997 Dec 23;94(26):14671-6.

Ramji, D.P.; Foka, P. CCAAT/enhancer-binding proteins: structure function and regulation. *Biochem. J*. 2002, 365, 561-575.

Reif K, Cyster JG. RGS molecule expression in murine B lymphocytes and ability to down-regulate chemotaxis to lymphoid chemokines. *J Immunol*. 2000 May 1;164(9):4720-9.

Renkawitz J, Schumann K, Weber M, Lämmermann T, Pflücke H, Piel M, Polleux J, Spatz JP, Sixt M. Adaptive force transmission in amoeboid cell migration. *Nat Cell Biol.* 2009 Dec;11(12):1438-43

Rickert P, Weiner OD, Wang F, Bourne HR, Servant G. Leukocytes navigate by compass: roles of PI3Kgamma and its lipid products. *Trends Cell Biol.* 2000 Nov;10(11):466-73.

Ridley AJ, Hall A. The small GTP-binding protein rho regulates the assembly of focal adhesions and actin stress fibers in response to growth factors. *Cell.* 1992 Aug 7;70(3):389-99.

Ridley AJ, Paterson HF, Johnston CL, Diekmann D, Hall A. The small GTP-binding protein rac regulates growth factor-induced membrane ruffling. *Cell.* 1992 Aug 7;70(3):401-10.

Ridley AJ. Rho GTPases and actin dynamics in membrane protrusions and vesicle trafficking. *Trends Cell Biol.* 2006 Oct;16(10):522-9.

Ritter U, A. Meissner, J. Ott, H. Körner. Analysis of the maturation process of dendritic cells deficient for TNF and lymphotoxin- α reveals an essential role for TNF. *J Leukoc Biol*, 74 (2003), pp. 216–222

Rivera J, Fierro NA, Olivera A, Suzuki R. New insights on mast cell activation via the high affinity receptor for IgE. *Adv Immunol.* 2008;98:85-120

Rivera J, Gilfillan AM. Molecular regulation of mast cell activation. *J Allergy Clin Immunol.* 2006 Jun;117(6):1214-25

Rivera J. Molecular adapters in Fc(ϵ)RI signaling and the allergic response. *Curr Opin Immunol.* 2002 Dec;14(6):688-93.

Roberts LJ 2nd, Lewis RA, Oates JA, Austen KF. Prostaglandin thromboxane, and 12-hydroxy-5,8,10,14-eicosatetraenoic acid production by ionophore-stimulated rat serosal mast cells. *Biochim Biophys Acta.* 1979 Nov 21;575(2):185-92.

Robinson RC, Turbedsky K, Kaiser DA, Marchand JB, Higgs HN, Choe S, Pollard TD. Crystal structure of Arp2/3 complex. *Science*. 2001 Nov 23;294(5547):1679-84.

Rohatgi R, Ma L, Miki H, Lopez M, Kirchhausen T, Takenawa T, Kirschner MW. The interaction between N-WASP and the Arp2/3 complex links Cdc42-dependent signals to actin assembly. *Cell*. 1999 Apr 16;97(2):221-31.

Roitt I, Peter J. Delves, Seamus J. Martin, Dennis R. Burton and Ivan M. . Roitt's Essential Immunology (Essentials). 2010.

Romagnani P, Annunziato F, Piccinni MP, Maggi E, Romagnani S. Th1/Th2 cells, their associated molecules and role in pathophysiology. *Eur Cytokine Netw*. 2000 Sep;11(3):510-1.

Roman DL, Talbot JN, Roof RA, Sunahara RK, Traynor JR, Neubig RR. Identification of small-molecule inhibitors of RGS4 using a high-throughput flow cytometry protein interaction assay. *Mol Pharmacol*. 2007 Jan;71(1):169-75.

Roos J, DiGregorio PJ, Yeromin AV, Ohlsen K, Lioudyno M, Zhang S, Safrina O, Kozak JA, Wagner SL, Cahalan MD, Veliçelebi G, Stauderman KA. STIM1, an essential and conserved component of store-operated Ca²⁺ channel function. *J Cell Biol*. 2005 May 9;169(3):435-45

Rottem M, Goff JP, Albert JP, Metcalfe DD. The effects of stem cell factor on the ultrastructure of Fc epsilon RI+ cells developing in IL-3-dependent murine bone marrow-derived cell cultures. *J Immunol*. 1993 Nov 1;151(9):4950-63.

Roussos ET, Condeelis JS, Patsialou A. Chemotaxis in cancer. *Nat Rev Cancer*. 2011 Jul 22;11(8):573-87.

Roy AA, Baragli A, Bernstein LS, Hepler JR, Hébert TE, Chidiac P. RGS2 interacts with Gs and adenylyl cyclase in living cells. *Cell Signal*. 2006 Mar;18(3):336-48.

Rubtsov YP, Rasmussen JP, Chi EY, et al. Regulatory T cell derived interleukin-10 limits inflammation at environmental interfaces. *Immunity* 2008; 28:546-558.

Ruitenbergh EJ, Elgersma A. Absence of intestinal mast cell response in congenitally athymic mice during *Trichinella spiralis* infection. *Nature*. 1976 Nov 18;264(5583):258-60.

Sadhu C, Masinovsky B, Dick K, Sowell CG, Staunton DE. Essential role of phosphoinositide 3-kinase delta in neutrophil directional movement. *J Immunol*. 2003 Mar 1;170(5):2647-54.

Saederup N, Cardona AE, Croft K, Mizutani M, Cottle AC, Tsou CL, Ransohoff RM, Charo IF. Selective chemokine receptor usage by central nervous system myeloid cells in CCR2-red fluorescent protein knock-in mice. *PLoS One*. 2010 Oct 27;5(10):e13693.

Sahai E. Illuminating the metastatic process. *Nat Rev Cancer*. 2007 Oct;7(10):737-49.

Sakaguchi S. Regulatory T cells: Key controllers of immunologic self-tolerance. *Cell* 101:455– 458, 2000.

Sallusto F, Baggiolini M. Chemokines and leukocyte traffic. *Nat Immunol*. 2008 Sep;9(9):949-52.

Sallusto, F., Lenig, D., Mackay, C.R. & Lanzavecchia, A. Flexible programs of chemokine receptor expression on human polarized T helper 1 and 2 lymphocytes. *J. Exp. Med.* 187, 875–883 (1998).

Sallusto, F., Mackay, C.R. & Lanzavecchia, A. Selective expression of the eotaxin receptor CCR3 by human T helper 2 cells. *Science* 277, 2005–2007 (1997).

Sanderson MP, Gelling SJ, Rippmann JF, Schnapp A. Comparison of the anti-allergic activity of Syk inhibitors with optimized Syk siRNAs in FcεRI-activated RBL-2H3 basophilic cells. *Cell Immunol*. 2010;262(1):28-34.

Sasaki AT, Chun C, Takeda K, Firtel RA. Localized Ras signaling at the leading edge regulates PI3K, cell polarity, and directional cell movement. *J Cell Biol*. 2004 Nov 8;167(3):505-18.

Sasaki T, Irie-Sasaki J, Jones RG, Oliveira-dos-Santos AJ, Stanford WL, Bolon B, Wakeham A, Itie A, Bouchard D, Kozieradzki I, Joza N, Mak TW, Ohashi PS,

Suzuki A, Penninger JM. Function of PI3Kgamma in thymocyte development, T cell activation, and neutrophil migration. *Science*. 2000 Feb 11;287(5455):1040-6.

Schmidt A, Hall A. Guanine nucleotide exchange factors for Rho GTPases: turning on the switch. *Genes Dev*. 2002 Jul 1;16(13):1587-609.

Schoeber JP, Topala CN, Wang X, Diepens RJ, Lambers TT, Hoenderop JG, Bindels RJ. RGS2 inhibits the epithelial Ca²⁺ channel TRPV6. *J Biol Chem*. 2006 Oct 6;281(40):29669-74.

Schröppel B, Zhang N, Chen P, Zang W, Chen D, Hudkins KL, Kuziel WA, Sung R, Bromberg JS, Murphy B. Differential expression of chemokines and chemokine receptors in murine islet allografts: the role of CCR2 and CCR5 signaling pathways. *J Am Soc Nephrol*. 2004 Jul;15(7):1853-61.

Schulman ES, Kagey-Sobotka A, MacGlashan DW Jr, Adkinson NF Jr, Peters SP, Schleimer RP, Lichtenstein LM. Heterogeneity of human mast cells. *J Immunol*. 1983 Oct;131(4):1936-41.

Schwarzer, R.; Dames, S.; Tondera, D.; Kippel, A. Kaufmann, J. TRB3 is a PI3-kinase dependent indicator for nutrient starvation. *Cell Signal* 2005, 18, 899-909.

Seagrave J, Pfeiffer JR, Wofsy C, Oliver JM. Relationship of IgE receptor topography to secretion in RBL-2H3 mast cells. *J Cell Physiol*. 1991 Jul;148(1):139-51.

Seder RA, Paul WE, Davis MM, and Fazekas de St. Groth B. The presence of interleukin 4 during in vitro priming determines the lymphokine-producing potential of CD4₊ T cells from T cell receptor transgenic mice. *J. Exp. Med*. 176:1091–1098, 1992.

Segal DM, Taurog JD, Metzger H. Dimeric immunoglobulin E serves as a unit signal for mast cell degranulation. *Proc Natl Acad Sci U S A*. 1977 Jul;74(7):2993-7.

Selim, E.; Frkanec, J.T.; Cunard, R. Fibrates upregulate TRB3 in lymphocytes independent of PPAR α by augmenting CCAAT/enhancer-binding protein β (C/EBP β) expression. *Molec. Immunol.* 2007, 44, 1218-1229.

Sepich DS, Solnica-Krezel L (2005) Analysis of cell movements in zebrafish embryos: morphometrics and measuring movement of labeled cell populations in vivo. *Methods Mol Biol* 294: 211–233

Sergé A, de Keijzer S, Van Hemert F, Hickman MR, Hereld D, Spaink HP, Schmidt T, Snaar-Jagalska BE. Quantification of GPCR internalization by single-molecule microscopy in living cells. *Integr Biol (Camb)*. 2011 May 3.

Servant G, Weiner OD, Herzmark P, Balla T, Sedat JW, Bourne HR. Polarization of chemoattractant receptor signaling during neutrophil chemotaxis. *Science*. 2000 Feb 11;287(5455):1037-40.

Servant G, Weiner OD, Neptune ER, Sedat JW, Bourne HR. Dynamics of a chemoattractant receptor in living neutrophils during chemotaxis. *Mol Biol Cell*. 1999 Apr;10(4):1163-78.

Shevach EM. Mechanisms of foxp3₊ T regulatory cell-mediated suppression. *Immunity* 30:636–645, 2009.

Shi GX, Harrison K, Wilson GL, Moratz C, Kehrl JH. RGS13 regulates germinal center B lymphocytes responsiveness to CXC chemokine ligand (CXCL)12 and CXCL13. *J Immunol*. 2002 Sep 1;169(5):2507-15.

Silberstein, R., Melnick, M., Greenberg, G. and Minkin, C. (1991) Bone remodeling in W/W^v mast cell deficient mice. *Bone* 12, 227–236

Smith SM, Moran AP, Duggan SP, Ahmed SE, Mohamed AS, Windle HJ, O'Neill LA, Kelleher DP. Tribbles 3: a novel regulator of TLR2-mediated signaling in response to *Helicobacter pylori* lipopolysaccharide. *J Immunol*. 2011 Feb 15;186(4):2462-71.

Soll DR, Wessels D, Heid PJ, Voss E (2003) Computer-assisted reconstruction and motion analysis of the three-dimensional cell. *Scientific World J* 3: 827–841

Sozanni S. , P. Allavena, G. D'Amico, W. Luini, G. Bianchi, M. Kataura, T. Imai, O. Yoshie, R. Bonecchi, A. Mantovani. Differential regulation of chemokine receptors during dendritic cell maturation: a model for their trafficking properties. *J Immunol*, 161 (3) (1998), pp. 1083–1086

Stelekati, Z. Orinska, S. Bulfone-Paus. Mast cells in allergy: innate instructors of adaptive responses. *Immunobiology*, 212 (6) (2007), pp. 505–519

Stephens LR, Hughes KT, Irvine RF. Pathway of phosphatidylinositol(3,4,5)-trisphosphate synthesis in activated neutrophils. *Nature*. 1991 May 2;351(6321):33-9.

Sullivan KE, Mullen CA, Blaese RM, Winkelstein JA. A multiinstitutional survey of the Wiskott-Aldrich syndrome. *J Pediatr*. 1994 Dec;125(6 Pt 1):876-85.

Sung HY, Guan H, Czibula A, King AR, Eder K, Heath E, Suvarna SK, Dower SK, Wilson AG, Francis SE, Crossman DC, Kiss-Toth E. Human tribbles-1 controls proliferation and chemotaxis of smooth muscle cells via MAPK signaling pathways. *J Biol Chem*. 2007 Jun 22;282(25):18379-87.

Supajatura V, Ushio H, Nakao A, Okumura K, Ra C, Ogawa H. Protective roles of mast cells against enterobacterial infection are mediated by Toll-like receptor 4. *J Immunol*. 2001 Aug 15;167(4):2250-6

Supajatura, V., Ushio, H., Nakao, A. et al. Differential responses of mast cell Toll-like receptors 2 and 4 in allergy and innate immunity. *J. Clin. Invest* 109,1351–1359. (2002)

Suto, S. Nakae, M. Kakurai, J.D. Sedgwick, M. Tsai, S.J. Galli. Mast cell-associated TNF promotes dendritic cell migration. *J Immunol*, 176 (7) (2006), pp. 4102–4112

Svitkina TM, Borisy GG. Correlative light and electron microscopy of the cytoskeleton of cultured cells. *Methods Enzymol*. 1998;298:570-92.

Symons M, Derry JM, Karlak B, Jiang S, Lemahieu V, McCormick F, Francke U, Abo A. Wiskott-Aldrich syndrome protein, a novel effector for the GTPase CDC42Hs, is implicated in actin polymerization. *Cell*. 1996 Mar 8;84(5):723-34.

Takenawa T, Suetsugu S. The WASP-WAVE protein network: connecting the membrane to the cytoskeleton. *Nat Rev Mol Cell Biol*. 2007 Jan;8(1):37-48.

Taub DD, Proost P, Murphy WJ, Anver M, Longo DL, van Damme J, Oppenheim JJ. Monocyte chemotactic protein-1 (MCP-1), -2, and -3 are chemotactic for human T lymphocytes. *J Clin Invest*. 1995 Mar;95(3):1370-6.

Temann UA, Ray P, Flavell RA. Pulmonary overexpression of IL-9 induces Th2 cytokine expression, leading to immune pathology. *J Clin Invest*. 2002 Jan;109(1):29-39.

Thakurdas, S. M., Melicoff, E., Sansores-Garcia, L., Moreira, D. C., Petrova, Y., Stevens, R. L. and Adachi, R., The mast cell-restricted tryptase mMCP-6 has a critical immunoprotective role in bacterial infections. *J. Biol. Chem*. 2007. 282: 20809–20815.

Tharp WG, Yadav R, Irimia D, Upadhyaya A, Samadani A, Hurtado O, Liu SY, Munisamy S, Brainard DM, Mahon MJ, Nourshargh S, van Oudenaarden A, Toner MG, Poznansky MC. Neutrophil chemorepulsion in defined interleukin-8 gradients in vitro and in vivo. *J Leukoc Biol*. 2006 Mar;79(3):539-54.

Thelen M, Peveri P, Kern P, von Tscharner V, Walz A, Baggiolini M. Mechanism of neutrophil activation by NAF, a novel monocyte-derived peptide agonist. *FASEB J*. 1988 Aug;2(11):2702-6.

Thelen M, Stein JV. How chemokines invite leukocytes to dance. *Nat Immunol*. 2008 Sep;9(9):953-9.

Tkaczyk C, Gilfillan AM. Fc(epsilon)R1-dependent signaling pathways in human mast cells. *Clin Immunol*. 2001 May;99(2):198-210.

Tkaczyk C, Okayama Y, Metcalfe DD, Gilfillan AM. Fcγ receptors on mast cells: activatory and inhibitory regulation of mediator release. *Int Arch Allergy Immunol*. 2004 Mar;133(3):305-15.

Toda M, Dawson M, Nakamura T, Munro PM, Richardson RM, Bailly M, Ono SJ. Impact of engagement of FcεRI and CC chemokine receptor 1 on mast cell activation and motility. *J Biol Chem*. 2004 Nov 12;279(46):48443-8.

Tsukamoto H, Fukudome K, Takao S, Tsuneyoshi N, Ihara H, Ikeda Y, Kimoto M. Multiple potential regulatory sites of TLR4 activation induced by LPS as revealed by novel inhibitory human TLR4 mAbs. *Int Immunol*. 2012 Apr 12.

Unkeless JC, Eisen HN. Binding of monomeric immunoglobulins to Fc receptors of mouse macrophages. *J Exp Med*. 1975 Dec 1;142(6):1520-33.

Van Haastert PJ. Chemotaxis: insights from the extending pseudopod. *J Cell Sci*. 2010 Sep 15;123(Pt 18):3031-7.

Van Keymeulen A, Wong K, Knight ZA, Govaerts C, Hahn KM, Shokat KM, Bourne HR. To stabilize neutrophil polarity, PIP3 and Cdc42 augment RhoA activity at the back as well as signals at the front. *J Cell Biol*. 2006 Jul 31;174(3):437-45.

Van, N. L., Adriaensen, D. and Timmermans, J. P. (2007) The bidirectional communication between neurons and mast cells within the gastrointestinal tract. *Auton. Neurosci*. 133, 91–103

Vanhaesebroeck B, Ali K, Bilancio A, Geering B, Foukas LC. Signalling by PI3K isoforms: insights from gene-targeted mice. *Trends Biochem Sci*. 2005 Apr;30(4):194-204.

Vanhaesebroeck B, Guillermet-Guibert J, Graupera M, Bilanges B. The emerging mechanisms of isoform-specific PI3K signalling. *Nat Rev Mol Cell Biol*. 2010 May;11(5):329-41.

Varadaradjalou S, Féger F, Thieblemont N, Hamouda NB, Pleau JM, Dy M, Arock M. Toll-like receptor 2 (TLR2) and TLR4 differentially activate human mast cells. *Eur J Immunol*. 2003 Apr;33(4):899-906.

Velazquez JR, Teran LM. Chemokines and Their Receptors in the Allergic Airway Inflammatory Process. *Clin Rev Allergy Immunol*. 2010 Mar 30.

Veldhoen M, Uyttenhove C, van Snick J, et al. Transforming growth factor-beta "reprograms" the differentiation of T helper 2 cells and promotes an interleukin 9-producing subset. *Nat Immunol* 9:1341–1346, 2008.

Veldhoen M, Uyttenhove C, van Snick J, et al. Transforming growth factor-beta "reprograms" the differentiation of T helper 2 cells and promotes an interleukin 9-producing subset. *Nat Immunol* 9:1341–1346, 2008.

Venkatesan S, Rose JJ, Lodge R, Murphy PM, Foley JF. Distinct mechanisms of agonist-induced endocytosis for human chemokine receptors CCR5 and CXCR4. *Mol Biol Cell*. 2003 Aug;14(8):3305-24.

Venkatesha RT, Berla Thangam E, Zaidi AK, Ali H. Distinct regulation of C3a-induced MCP-1/CCL2 and RANTES/CCL5 production in human mast cells by extracellular signal regulated kinase and PI3 kinase. *Mol Immunol*. 2005 Mar;42(5):581-7.

Verhagen J, Taylor A, Blaser K, Akdis M, Akdis CA. T regulatory cells in allergen-specific immunotherapy. *Int Rev Immunol*. 2005 Sep-Dec;24(5-6):533-48.

Vila-Coro AJ, Mellado M, Martín de Ana A, Martínez-A C, Rodríguez-Frade JM. Characterization of RANTES- and aminooxypentane-RANTES-triggered desensitization signals reveals differences in recruitment of the G protein-coupled receptor complex. *J Immunol*. 1999 Sep 15;163(6):3037-44.

Vila-Coro AJ, Rodríguez-Frade JM, Martín De Ana A, Moreno-Ortíz MC, Martínez-A C, Mellado M. The chemokine SDF-1alpha triggers CXCR4 receptor dimerization and activates the JAK/STAT pathway. *FASEB J*. 1999 Oct;13(13):1699-710.

Villalonga P, Ridley AJ. Rho GTPases and cell cycle control. *Growth Factors*. 2006 Sep;24(3):159-64.

Vines CM, Prossnitz ER. Mechanisms of G protein-coupled receptor-mediated degranulation. *FEMS Microbiol Lett*. 2004 Jul 1;236(1):1-6.

Waern, I., Jonasson, S., Hjoberg, J., Bucht, A., Abrink, M., Pejler, G. and Wernersson, S. Mouse mast cell protease 4 is the major chymase in murine airways and has a protective role in allergic airway inflammation. *J. Immunol.* 183, 6369–6376. (2009)

Wang F, Herzmark P, Weiner OD, Srinivasan S, Servant G, Bourne HR. Lipid products of PI(3)Ks maintain persistent cell polarity and directed motility in neutrophils. *Nat Cell Biol.* 2002 Jul;4(7):513-8.

Wang Y, Chen CL, Iijima M. Signaling mechanisms for chemotaxis. *Dev Growth Differ.* 2011 May;53(4):495-502.

Wang Z, Lai Y, Bernard JJ, Macleod DT, Cogen AL, Moss B, Di Nardo A. Skin mast cells protect mice against vaccinia virus by triggering mast cell receptor S1PR2 and releasing antimicrobial peptides. *J Immunol.* 2012 Jan 1;188(1):345-57.

Wang, C.Y.; Mayo, M.W.; Korneluk, R.G.; Goeddel, D.V.; Baldwin, A.S., Jr. NF-KAPPA B antipoptosis: induction of TRAF-1 and TRAF-2 and C-IAP1 and C-IAP2 to suppress caspase-8 activation. *Science* 1998, 281, 1680-1683.

Ward, S.G. (2004) Do phosphoinositide 3-kinases direct lymphocyte navigation? *Trends Immunol.* 25, 67–74

Watanabe K, Kishihara K, Hamano S, Koga M, Nomoto K, Tada I. Delayed expulsion of the nematode *Trichinella spiralis* in mice lacking the mucosal mast cell-specific granule chymase, mouse mast cell protease-1. *J Exp Med.* 2000 Dec 18;192(12):1849-56.

Watanabe K, Kishihara K, Hamano S, Koga M, Nomoto K, Tada I. *Strongyloides ratti*: implication of mast cell-mediated expulsion through FcepsilonRI-independent mechanisms. *Parasite.* 2009 Sep;16(3):209-14.

Watson N, Linder ME, Druey KM, Kehrl JH, Blumer KJ. RGS family members: GTPase-activating proteins for heterotrimeric G-protein alpha-subunits. *Nature.* 1996 Sep 12;383(6596):172-5.

Weiner OD, Neilsen PO, Prestwich GD, Kirschner MW, Cantley LC, Bourne HR. A PtdInsP(3)- and Rho GTPase-mediated positive feedback loop regulates neutrophil polarity. *Nat Cell Biol.* 2002 Jul;4(7):509-13.

Welch HC, Coadwell WJ, Stephens LR, Hawkins PT. Phosphoinositide 3-kinase-dependent activation of Rac. *FEBS Lett.* 2003 Jul 3;546(1):93-7.

Welch MD, DePace AH, Verma S, Iwamatsu A, Mitchison TJ. The human Arp2/3 complex is composed of evolutionarily conserved subunits and is localized to cellular regions of dynamic actin filament assembly. *J Cell Biol.* 1997 Jul 28;138(2):375-84.

Welle, M. (1997) Development, significance, and heterogeneity of mast cells with particular regard to the mast cell-specific proteases chymase and tryptase. *J. Leukocyte Biol.* 61, 233–245

Willard MD, Willard FS, Li X, Cappell SD, Snider WD, Siderovski DP. Selective role for RGS12 as a Ras/Raf/MEK scaffold in nerve growth factor-mediated differentiation. *EMBO J.* 2007 Apr 18;26(8):2029-40.

Wodnar-Filipowicz A, Heusser CH, Moroni C. Production of the haemopoietic growth factors GM-CSF and interleukin-3 by mast cells in response to IgE receptor-mediated activation. *Nature.* 1989 May 11;339(6220):150-2.

Wojta J, Kaun C, Zorn G, Ghannadan M, Hauswirth AW, Sperr WR, Fritsch G, Printz D, Binder BR, Schatzl G, Zwirner J, Maurer G, Huber K, Valent P. C5a stimulates production of plasminogen activator inhibitor-1 in human mast cells and basophils. *Blood.* 2002 Jul 15;100(2):517-23.

Wolk K, Witte E, Hoffmann U, Doecke WD, Endesfelder S, Asadullah K, Sterry W, Volk HD, Wittig BM, Sabat R. IL-22 induces lipopolysaccharide-binding protein in hepatocytes: a potential systemic role of IL-22 in Crohn's disease. *J Immunol.* 2007 May 1;178(9):5973-81.

Woodfolk JA. High-dose allergen exposure leads to tolerance. *Clin Rev Allergy Immunol* 28:43–58, 2005

Woodfolk JA. Cytokines as a therapeutic target for allergic diseases: a complex picture. *Curr Pharm Des.* 2006;12(19):2349-63.

Woolhiser MR, Brockow K, Metcalfe DD. Activation of human mast cells by aggregated IgG through FcγRI: additive effects of C3a. *Clin Immunol.* 2004 Feb;110(2):172-80.

Wu, M.; Liang-Guo, X.; Zhonghe, Z.; Hong-Bing, S. SINK is a p65-interacting negative regulator of NF-κB-dependent transcription. *J. Biol. Chem.* 2003, 278, 27072-27079.

Xiao Z, Zhang N, Murphy DB, Devreotes PN. Dynamic distribution of chemoattractant receptors in living cells during chemotaxis and persistent stimulation. *J Cell Biol.* 1997 Oct 20;139(2):365-74.

Xystrakis E, Boswell SE, and Hawrylowicz CM. T regulatory cells and the control of allergic disease. *Expert Opin Biol Ther* 6:121–133, 2006.

Yamazaki, H. Yokozeki, T. Satoh, I. Katayama, K. Nishioka. TNF-α, RANTES, and MCP-1 are major chemoattractants of murine langerhans cells to the regional lymph nodes. *Exp Dermatol*, 7 (1) (1998), pp. 35–41

Yang M, Kumar RK, and Foster PS. Interferon-γ and pulmonary macrophages contribute to the mechanisms underlying prolonged airway hyperresponsiveness. *Clin Exp Allergy* 40:163–173, 2010.

Yee NS, Paek I, Besmer P. Role of kit-ligand in proliferation and suppression of apoptosis in mast cells: basis for radiosensitivity of white spotting and steel mutant mice. *J Exp Med.* 1994 Jun 1;179(6):1777-87.

Yu, M., Tsai, M., Tam, S. Y., Jones, C., Zehnder, J. and Galli, S. J. Mast cells can promote the development of multiple features of chronic asthma in mice. *J. Clin. Invest* 116, 1633–1641. (2006)

Zhang Y, Foudi A, Geay JF, Berthebaud M, Buet D, Jarrier P, Jalil A, Vainchenker W, Louache F. Intracellular localization and constitutive endocytosis of CXCR4 in human CD34+ hematopoietic progenitor cells. *Stem Cells.* 2004;22(6):1015-29.

Zhong H, Wade SM, Woolf PJ, Linderman JJ, Traynor JR, Neubig RR. A spatial focusing model for G protein signals. Regulator of G protein signaling (RGS) protein-mediated kinetic scaffolding. *J Biol Chem*. 2003 Feb 28;278(9):7278-84.

Zinselmeyer BH, Lynch JN, Zhang X, Aoshi T, Miller MJ. Video-rate two-photon imaging of mouse footpad - a promising model for studying leukocyte recruitment dynamics during inflammation. *Inflamm Res*. 2008 Mar;57(3):93-6.

Zong, W.X.; Edelstein, L.C.; Chen, C.; Bash, J.; Gelinas, C. The prosurvival Bcl-2 homolog Bfl-1/A1 is a direct transcriptional target of NF- κ B that blocks TNF-induced apoptosis. *Genes Dev*. 1999, 13, 382-387.

Zuchero JB, Coutts AS, Quinlan ME, Thangue NB, Mullins RD. p53-cofactor JMY is a multifunctional actin nucleation factor. *Nat Cell Biol*. 2009 Apr;11(4):451-9.

Chapter 9. Publications